



<https://theses.gla.ac.uk/>

Theses Digitisation:

<https://www.gla.ac.uk/myglasgow/research/enlighten/theses/digitisation/>

This is a digitised version of the original print thesis.

Copyright and moral rights for this work are retained by the author

A copy can be downloaded for personal non-commercial research or study, without prior permission or charge

This work cannot be reproduced or quoted extensively from without first obtaining permission in writing from the author

The content must not be changed in any way or sold commercially in any format or medium without the formal permission of the author

When referring to this work, full bibliographic details including the author, title, awarding institution and date of the thesis must be given

Enlighten: Theses

<https://theses.gla.ac.uk/>  
[research-enlighten@glasgow.ac.uk](mailto:research-enlighten@glasgow.ac.uk)

**Excitation-contraction coupling in muscles of  
the Norway lobster *Nephrops norvegicus***

**Janet Holmes**

A thesis submitted for the degree of Doctor of Philosophy  
to the Faculty of Science of the University of Glasgow

Division of Environmental and Evolutionary Biology  
Institute of Biomedical and Life Sciences  
University of Glasgow

March 1997

ProQuest Number: 10391275

All rights reserved

INFORMATION TO ALL USERS

The quality of this reproduction is dependent upon the quality of the copy submitted.

In the unlikely event that the author did not send a complete manuscript and there are missing pages, these will be noted. Also, if material had to be removed, a note will indicate the deletion.



ProQuest 10391275

Published by ProQuest LLC (2017). Copyright of the Dissertation is held by the Author.

All rights reserved.

This work is protected against unauthorized copying under Title 17, United States Code  
Microform Edition © ProQuest LLC.

ProQuest LLC.  
789 East Eisenhower Parkway  
P.O. Box 1346  
Ann Arbor, MI 48106 – 1346

Teris  
10816  
Copy 2



## ACKNOWLEDGEMENTS

This work was carried out in the Division of Environmental and Evolutionary Biology of the University of Glasgow and in the Zoology Department at the University of Salzburg in Austria. I would like to thank Professor Felicity Huntingford for the research facilities at Glasgow and Dr. Stefan Galler for facilities in Salzburg.

I am very grateful to Dr. Douglas Neil for his supervision, endless patience, interest and enthusiasm, especially during the writing-up period.

I would also like to give great thanks to Dr. Stefan Galler for his help during the time that I was in Austria and for his suggestions regarding my thesis. In addition Karlheinz Hilber provided endless assistance, advice and suggestions on the skinned fibre work.

Considerable technical assistance was provided by Graham Adam, Kate Orr, June Freel, Cathy McLagan, Willie Orr, Alan McGregor and Nosrat Mirzai. A special thanks is due to Liz Denton for her advice on data presentation using the Mac, a skill I won't forget in a hurry, and not necessarily through choice!

While in Glasgow I have made many friends who have all provided endless support, whether it be related to my thesis work or socially. Thanks to Murray Roberts, Andrea Fiddett, Phil Cairney, Francis Neat, Vickie Heaney, Iain Barber, Svenni Valdimarsson, Fia Selmer, and Elvira Poloczanska. I would also like to thank Steve Arnott for his help and delightful pranks, which never fail to amuse me!

This project was funded by a BBSRC grant together with a CASE award from the C. S. L., Aberdeen and I am grateful for the financial backing that they provided.

Finally I would specially like to thank Dave Fraser and my parents for their continual support, consideration and patience, particularly during the writing-up period.



*Nephrops norvegicus*

|                         |                |
|-------------------------|----------------|
| <b>List of Contents</b> | <b>i-vii</b>   |
| <b>List of Tables</b>   | <b>viii-ix</b> |
| <b>List of Figures</b>  | <b>x-xiv</b>   |
| <b>Summary</b>          | <b>xv-xvii</b> |

## LIST OF CONTENTS

Page

## CHAPTER 1: General Introduction

|  |    |
|--|----|
| 1.1 Ca <sup>2+</sup> signalling in cells .....                                     | 1  |
| 1.2 Excitation-contraction coupling in muscle .....                                | 3  |
| 1.2.1 Depolarisation of the sarcolemma .....                                       | 3  |
| 1.2.2 Propagation of the inward current into the interior<br>of the cell .....     | 4  |
| 1.2.3 The dihydropyridine (DHP) receptors .....                                    | 5  |
| 1.2.4 The charge-coupled model or mechanical coupling .....                        | 6  |
| 1.2.5 CICR as an excitation-contraction (EC) coupling mechanism<br>in muscle ..... | 8  |
| 1.2.6 The ryanodine receptor .....   | 8  |
| 1.2.7 Release of Ca <sup>2+</sup> from the sarcoplasmic reticulum .....            | 9  |
| 1.2.8 Binding of Ca <sup>2+</sup> ions to the regulatory proteins .....            | 11 |
| 1.3 Muscle diversity .....   | 12 |

CHAPTER 2: EC coupling in the *Nephrops* abdominal superficial  
flexor muscle

|  |    |
|--|----|
| 2.1 INTRODUCTION .....   | 16 |
| 2.1.1 Fast muscle .....  | 16 |
| 2.1.2 Slow muscle .....  | 16 |
| 2.1.3 Morphological, biochemical and histochemical<br>properties of the SF muscle fibres ..... | 17 |
| 2.1.4 Mechanical properties of the SF muscle fibres .....                                      | 17 |
| 2.1.5 Innervation of the SF muscle fibres .....  | 17 |
| 2.1.6 Presynaptic and postsynaptic events in the SF muscle fibres .....                        | 18 |
| 2.1.7 Excitation contraction (EC) coupling in the SF muscle fibres .....                       | 19 |

|  |    |
|--|----|
| <b>2.2 MATERIALS &amp; METHODS</b> .....                       | 19 |
| <b>2.2.1 The whole SF muscle bundle preparation</b> .....      | 19 |
| 2.2.1.1 Dissection of the abdomen .....                        | 19 |
| 2.2.1.2 Solutions .....  | 20 |
| 2.2.1.3 Drug application, cooling and perfusion .....          | 20 |
| 2.2.1.4 Stimulation of the preparation .....                   | 20 |
| 2.2.1.5 Tension measurements and intracellular recording ..... | 21 |
| 2.2.1.6 Calibration of the force transducer .....              | 21 |
| 2.2.1.7 Data analysis .....                                    | 21 |
| <b>2.2.2 Single fibre experiments</b> .....                    | 22 |
| 2.2.2.1 Preparation of intact single fibres .....              | 22 |
| 2.2.2.2 Experimental set-up .....                              | 22 |
| 2.2.2.3 Mounting the fibre between the carbon needles .....    | 23 |
| 2.2.2.4 Activation of the muscle fibre .....                   | 23 |
| 2.2.2.5 Recording system .....                                 | 24 |
| <b>2.2.3 Two electrode voltage clamp technique</b> .....       | 24 |
| 2.2.3.1 Preparation of single fibres for voltage clamp .....   | 24 |
| 2.2.3.2 Voltage clamp solutions .....                          | 25 |
| 2.2.3.3 Electrodes and voltage recording .....                 | 25 |
| <b>2.3 RESULTS</b> .....                                       | 26 |
| 2.3.1 Voltage and frequency of neuronal stimulation .....      | 26 |
| 2.3.2 Membrane potential .....                                 | 27 |
| 2.3.3 Excitatory post-synaptic potentials .....                | 27 |
| 2.3.4 $Ca^{2+}$ .....  | 29 |
| 2.3.5 Electrical field stimulation .....                       | 29 |
| 2.3.6 $K^+$ contractures .....                                 | 30 |
| 2.3.7 Voltage clamping muscle fibres .....                     | 30 |
| 2.3.8 Pharmacological agents .....                             | 31 |
| 2.3.8.1 Caffeine .....   | 31 |
| 2.3.8.2 Tetracaine .....                                       | 33 |
| 2.3.8.3 Butanedione monoxime .....                             | 34 |
| <b>2.4 DISCUSSION</b> .....                                    | 34 |

|   |    |
|---|----|
| 2.4.1 Activation thresholds.....  | 34 |
| 2.4.2 Excitation contraction coupling in the SF muscle of <i>Nephrops</i> ..... | 35 |
| 2.4.3 The involvement of $Ca^{2+}$ in EC coupling .....                         | 35 |
| 2.4.4 Depolarisation using high concentration potassium saline.....             | 37 |
| 2.4.5 Caffeine .....  | 38 |
| 2.4.6 Tetracaine.....   | 40 |
| 2.4.7 Butanedione monoxime (BDM).....   | 41 |

**CHAPTER 3: The effects of  $Mn^{2+}$  on membrane-intact muscle fibres**

|  |           |
|--|-----------|
| <b>3.1 INTRODUCTION.....</b>   | <b>74</b> |
| 3.1.1 Manganese as a $Ca^{2+}$ channel blocker .....                               | 74        |
| 3.1.2 Excitation-contraction (EC) coupling.....                                    | 74        |
| 3.1.3 The passage of $Mn^{2+}$ ions through $Ca^{2+}$ channels.....                | 75        |
| 3.1.4 Theories of how $Mn^{2+}$ ions block and pass through $Ca^{2+}$ channels.... | 76        |
| 3.1.5 Muscle contraction .....   | 78        |
| 3.1.6 Effects of $Mn^{2+}$ on smooth muscle.....                                   | 78        |
| 3.1.7 The effects of $Mn^{2+}$ on the SF muscle preparation .....                  | 79        |
| <b>3.2 MATERIALS &amp; METHODS .....</b>   | <b>79</b> |
| 3.2.1 Solutions .....  | 79        |
| <b>3.3 RESULTS .....</b>   | <b>80</b> |
| <b>3.4 DISCUSSION.....</b>   | <b>81</b> |
| 3.4.1 $Mn^{2+}$ inhibits muscle force .....  | 82        |
| 3.4.2 $Mn^{2+}$ -evoked muscle force.....  | 83        |
| 3.4.3 How does $Mn^{2+}$ increase muscle force? .....                              | 85        |

**CHAPTER 4: Myofibrillar force kinetics of different fibre types  
measured in chemically skinned fibres**

|  |            |
|--|------------|
| <b>4.1 INTRODUCTION.....</b>                               | <b>100</b> |
| 4.1.1 The role of troponin (Tn) in muscle contraction..... | 100        |
| 4.1.2 Regulation of muscle contraction.....                | 101        |

|  | <i>Page</i> |
|--|-------------|
| 4.1.2.1 Steric hindrance hypothesis .....  | 101         |
| 4.1.2.2 Ca <sup>2+</sup> binding and crossbridge attachment regulation .....                 | 102         |
| 4.1.3 Skinned fibre experiments .....  | 102         |
| 4.1.4 Co-operativity .....   | 102         |
| 4.1.5 Isoforms of troponin .....   | 103         |
| 4.1.6 Stretch activation .....   | 103         |
| 4.1.7 Ca <sup>2+</sup> -sensitivity .....  | 104         |
| 4.1.8 Stiffness .....  | 104         |
| 4.1.9 Speed of muscle contraction and shortening velocity .....                              | 105         |
| 4.1.10 Sarcomere length .....  | 106         |
| 4.1.11 Fibre identification .....  | 106         |
| 4.1.12 The S <sub>1</sub> and S <sub>2</sub> fibre types of <i>Nephraps norvegicus</i> ..... | 107         |
| <b>4.2 MATERIALS &amp; METHODS</b> .....   | <b>109</b>  |
| 4.2.1 Animal preparation .....   | 109         |
| 4.2.2 The SF muscle bundle preparation .....   | 109         |
| 4.2.3 Fast extensor muscle preparation .....   | 109         |
| 4.2.4 Preparation of single fibres .....   | 110         |
| 4.2.5 Solutions .....  | 110         |
| 4.2.6 Experimental set-up .....  | 111         |
| 4.2.7 Measurements of shortening velocity .....  | 112         |
| 4.2.7.1 Manual constant load experiments .....   | 112         |
| 4.2.7.2 Force clamp ramp experiments .....   | 112         |
| 4.2.8 Force measurements .....   | 112         |
| 4.2.9 Changes in fibre length .....  | 113         |
| 4.2.10 Measurements of sarcomere length .....  | 113         |
| 4.2.11 Recording system .....  | 113         |
| 4.2.12 Experimental procedure .....  | 114         |
| 4.2.13 Activation of the muscle fibre .....  | 114         |
| 4.2.14 Kinetic measurements .....  | 115         |
| 4.2.15 Determination of the fibre types using gel electrophoresis .....                      | 115         |
| 4.2.16 Analysis of data .....  | 116         |
| <b>4.3 RESULTS</b> .....   | <b>116</b>  |

|   | <i>Page</i> |
|---|-------------|
| 4.3.1 Sarcomere length.....   | 116         |
| 4.3.2 Maximal tension.....  | 117         |
| 4.3.3 Quick stretches and releases .....                                  | 117         |
| 4.3.3.1 Stretch activation .....  | 118         |
| 4.3.3.2 Quick releases.....   | 118         |
| 4.3.4 Stiffness .....   | 119         |
| 4.3.5 Shortening velocity .....   | 120         |
| 4.3.6 Filament sliding .....  | 122         |
| <b>4.4 DISCUSSION.....</b>  | <b>122</b>  |
| 4.4.1 Shortening velocity .....   | 122         |
| 4.4.2 What determines shortening velocity .....                           | 125         |
| 4.4.3 Force transients in response to quick changes in fibre length ..... | 126         |
| 4.4.3.1 Stretch activation.....   | 126         |
| 4.4.3.2 Quick release .....   | 127         |
| 4.4.4 Muscle fibre stiffness .....  | 128         |
| 4.4.5 The fast fibre type .....   | 129         |

**CHAPTER 5: The effects of  $Mn^{2+}$  on the activation of skinned fibres**

|  |            |
|--|------------|
| <b>5.1 INTRODUCTION.....</b>   | <b>152</b> |
| 5.1.1 Activation of skinned muscle fibres with divalent cations..... | 152        |
| 5.1.2 Skinned fibre experiments with manganese .....                 | 153        |
| 5.1.3 The activation of vertebrate smooth muscle by $Mn^{2+}$ .....  | 153        |
| 5.1.4 The activation of Nephrops skinned by $Mn^{2+}$ .....          | 154        |
| <b>5.2 MATERIALS &amp; METHODS .....</b>                             | <b>155</b> |
| 5.2.1 Preparation of single fibres.....                              | 155        |
| 5.2.2 Solutions .....  | 155        |
| 5.2.3 Activation of the muscle fibre.....                            | 156        |
| 5.2.4 Experimental protocols.....                                    | 156        |
| 5.2.4.1 pCa and pMn force relationships .....                        | 156        |
| 5.2.4.2 Low ATP experiments.....                                     | 156        |
| 5.2.5 Kinetic measurements .....                                     | 157        |

|  | <i>Page</i> |
|--|-------------|
| 5.2.6 Analysis of data: pCa and pMn force curves .....                                       | 157         |
| 5.2.7 Graphical representation of results .....  | 158         |
| <b>5.3 RESULTS</b> .....   | <b>158</b>  |
| 5.3.1 Force transients induced by Mn <sup>2+</sup> .....                                     | 158         |
| 5.3.2 Relaxation after Mn <sup>2+</sup> activation .....                                     | 159         |
| 5.3.3 Comparison with maximal Ca <sup>2+</sup> activation .....                              | 159         |
| 5.3.4 pMn- and pCa-tension relationship .....  | 159         |
| 5.3.5 Hill coefficients .....  | 160         |
| 5.3.6 Ca <sup>2+</sup> contamination .....   | 160         |
| 5.3.7 EGTA .....   | 160         |
| 5.3.8 Effects of ionic strength on the Ca <sup>2+</sup> activated force .....                | 161         |
| 5.3.9 ATP control experiments .....  | 161         |
| 5.3.9.1 Muscle fibre force .....   | 161         |
| 5.3.9.2 Muscle fibre stiffness .....   | 162         |
| 5.3.9.3 Maximal shortening velocity .....  | 163         |
| 5.3.10 Stretch activation experiments .....  | 163         |
| <b>5.4 DISCUSSION</b> .....  | <b>164</b>  |
| 5.4.1 Activation of S <sub>1</sub> fibres by Mn <sup>2+</sup> .....                          | 164         |
| 5.4.2 The role of MgATP and MnATP .....  | 164         |
| 5.4.2.1 Does MgATP limit force production? .....   | 165         |
| 5.4.2.2 Does competitive inhibition between MnATP and MgATP<br>limit force production? ..... | 165         |
| 5.4.3 Kinetic measurements made under Mn <sup>2+</sup> .....                                 | 166         |
| 5.4.4 Stretch activation .....   | 167         |
| 5.4.5 Ionic concentration .....  | 167         |
| 5.4.6 Can Mn <sup>2+</sup> bind to troponin? .....   | 167         |

**CHAPTER 6: General Discussion**

|  |     |
|--|-----|
| 6.1 EC coupling properties of the SF muscle of <i>Nephrops</i> ..... | 191 |
| 6.1.1 EC properties identified using membrane-intact fibres .....    | 191 |
| 6.1.2 Sarcolemmal ion channel properties .....                       | 194 |

|  | <i>Page</i> |
|--|-------------|
| 6.1.3 Myofibrillar properties .....                            | 196         |
| 6.1.4 Acto-myosin regulation in decapod crustaceans .....      | 197         |
| 6.1.5 Fibre heterogeneity within single populations .....      | 197         |
| 6.2 Manganese .....  | 198         |
| 6.2.1 The activation properties of $Mn^{2+}$ ions .....        | 198         |
| 6.2.2 Ecological effects of $Mn^{2+}$ in the environment ..... | 200         |
| <b>REFERENCES</b> .....  | <b>202</b>  |

## LIST OF TABLES

|   | <i>Page</i> |
|---|-------------|
| <b>Chapter 2</b>  |             |
| <b>Table 2.1</b> Resting potentials recording from the S <sub>1</sub> and S <sub>2</sub> fibre types of a single SF muscle .....  | 43          |
| <b>Table 2.2</b> Total depolarisation at the 10th EPSP at different frequencies of stimulation in the S <sub>1</sub> and S <sub>2</sub> fibre types. Data from three preparations ..... | 43          |
| <b>Table 2.3</b> Ratio between the 1st and 10th EPSP at different frequencies of stimulation in the S <sub>1</sub> and S <sub>2</sub> fibre types. Data from three preparations .....   | 43          |
| <b>Chapter 4</b>  |             |
| <b>Table 4.1</b> Maximal unloaded shortening velocity at different time intervals .....   | 131         |
| <b>Chapter 5</b>  |             |
| <b>Table 5.1</b> Composition of B, A and Mn <sup>2+</sup> solutions .....   | 170         |
| <b>Table 5.2</b> Composition of low ATP solutions .....   | 170         |
| <b>Table 5.3</b> Mixing proportions of solutions A and B used for the pCa-tension experiments, and the final pCa of the mixtures. ....  | 171         |
| <b>Table 5.4</b> Hill coefficients, constants and pMn <sub>50</sub> values for the Mn <sup>2+</sup> -activation experiments .....   | 171         |
| <b>Table 5.5</b> Hill coefficients, constants and pCa <sub>50</sub> values for the Ca <sup>2+</sup> -activation experiments .....   | 172         |
| <b>Table 5.6</b> Lists the MnATP and MgATP concentrations that are in the different pMn solutions. As MnATP increased. MgATP decreases .....  | 172         |
| <b>Table 5.7</b> The stretch activation (t <sub>2</sub> ) times (ms) for 5 S <sub>1</sub> fibres when   |             |

|  |     |
|--|-----|
| exposed to different concentrations of $Mn^{2+}$ and when<br>maximally $Ca^{2+}$ -activated..... | 172 |
| <b>Table 5.8</b> Binding constants for EGTA.....   | 173 |
| <b>Table 5.9</b> Binding constants for ATP.....  | 173 |

## LIST OF FIGURES

|  | <i>Page</i> |
|--|-------------|
| <b>Chapter 2</b>   |             |
| <b>Fig. 2.1</b> Morphology of the superficial flexor (SF) muscle in<br><i>Nephrops norvegicus</i> .....  | 44          |
| <b>Fig. 2.2</b> Six motor neurones innervate the SF muscle of <i>Nephrops</i> .....  | 45          |
| <b>Fig. 2.3</b> Experimental set-up for the SF muscle bundle experiments .....   | 46          |
| <b>Fig. 2.4</b> Effect of stimulus frequency and voltage on the neuronally-<br>evoked force from the medial muscle bundle of the SF muscle .....   | 47          |
| <b>Fig. 2.5</b> Absolute neuronally-evoked force from the medial and lateral<br>bundles of a single SF muscle stimulated at different frequencies .....  | 48          |
| <b>Fig. 2.6</b> Effect of stimulus frequency on the force of the SF muscle bundles .....   | 49          |
| <b>Fig. 2.7</b> Effect of stimulus frequency on the relative force of the SF muscle<br>bundles .....   | 50          |
| <b>Fig. 2.8</b> Effect of stimulus frequency on EPSPs from the S <sub>1</sub> and S <sub>2</sub> fibre<br>types of the SF muscle .....   | 51          |
| <b>Fig. 2.9</b> Facilitation of EPSPs .....  | 52          |
| <b>Fig. 2.10</b> Effect of changes in the Ca <sup>2+</sup> concentration on muscle contraction .....   | 53          |
| <b>Fig. 2.11</b> Effect of Ca <sup>2+</sup> concentration of the force produced by the SF muscle<br>bundles .....  | 54          |
| <b>Fig. 2.12</b> Effect of Ca <sup>2+</sup> -free saline on the neuronally-evoked force and<br>the force evoked by electrical field stimulation of the medial<br>muscle bundle of the SF muscle .....          | 55          |
| <b>Fig. 2.13</b> Effect of Ca <sup>2+</sup> free saline on the force produced by neuronal<br>stimulation and EPSPs recorded from the S <sub>1</sub> and S <sub>2</sub> fibre<br>types from the SF muscle ..... | 56          |
| <b>Fig. 2.14</b> Effect of calcium-free saline on the force and EPSPs recorded<br>from the SF muscle .....   | 57          |
| <b>Fig. 2.15</b> Potassium-induced contractures in the SF muscle bundles .....   | 58          |
| <b>Fig. 2.16</b> Potassium-induced contractures in the SF muscle bundles .....   | 59          |

|  |    |
|--|----|
| <b>Fig. 2.17</b> Voltage clamp recording of fast inward $\text{Ca}^{2+}$ currents ( $I_{\text{Ca}}$ )<br>in an $\text{S}_1$ fibre.....   | 60 |
| <b>Fig. 2.18</b> Voltage clamp recordings showing outward $\text{K}^+$ currents in the<br>$\text{S}_2$ (A) and $\text{S}_1$ (B) fibre types.....                               | 61 |
| <b>Fig. 2.19</b> Caffeine contractures in the SF muscle bundles.....   | 62 |
| <b>Fig. 2.20</b> Effect of caffeine on neuronally-evoked force from the SF<br>muscle bundles.....  | 63 |
| <b>Fig. 2.21</b> Effect of caffeine on the SF muscle bundles.....  | 64 |
| <b>Fig. 2.22</b> Effect of caffeine on the force evoked by electrical field<br>stimulation of the SF muscle bundles.....   | 65 |
| <b>Fig. 2.23</b> Caffeine-induced contractures in the absence of extracellular $\text{Ca}^{2+}$ .....  | 66 |
| <b>Fig. 2.24</b> Effect of caffeine on the force produced by a single fibre in the<br>presence and absence of $\text{Ca}^{2+}$ .....   | 67 |
| <b>Fig. 2.25</b> Effects of tetracaine on the force and EPSPs from the SF<br>muscle bundles.....   | 78 |
| <b>Fig. 2.26</b> Effect of tetracaine on the force and EPSPs from the SF muscle<br>bundles.....  | 69 |
| <b>Fig. 2.27</b> Tetracaine blocks force in the SF muscle bundles and reverses<br>the effects of caffeine.....   | 70 |
| <b>Fig. 2.28</b> Caffeine and BDM have similar effects on the resting force<br>of the SF muscle bundles.....   | 71 |
| <b>Fig. 2.29</b> BDM increases the resting force in the lateral muscle bundle<br>of the SF muscle in $\text{Ca}^{2+}$ -free saline.....  | 72 |
| <b>Fig. 2.30</b> 10 mM BDM increases the resting force of the SF muscle<br>bundles and induces an oscillation in the membrane potential<br>of the $\text{S}_2$ fibre type..... | 73 |

### Chapter 3

|   |    |
|---|----|
| <b>Fig. 3.1</b> Enhancement of force by low concentrations of $\text{Mn}^{2+}$ .....                        | 88 |
| <b>Fig. 3.2</b> Effects of $\text{Mn}^{2+}$ on the neuronally-evoked force of the SF<br>muscle bundles..... | 89 |

|  |    |
|--|----|
| <b>Fig. 3.3</b> Effects of $Mn^{2+}$ on the force evoked by electrical field stimulation<br>of the SF muscle bundles ..... | 90 |
| <b>Fig. 3.4</b> Effect of $Mn^{2+}$ on force and EPSPs .....   | 91 |
| <b>Fig. 3.5</b> $Mn^{2+}$ inhibits $K^+$ -induced force. ....  | 92 |
| <b>Fig. 3.6</b> $K^+$ -induced force is blocked by 10 mM $Mn^{2+}$ in the SF<br>muscle bundles. ....                       | 93 |
| <b>Fig. 3.7</b> $Mn^{2+}$ blocks $K^+$ -induced force. ....  | 94 |
| <b>Fig. 3.8</b> Application of caffeine induces force after application of high<br>concentration $Mn^{2+}$ . ....          | 95 |
| <b>Fig. 3.9</b> Caffeine-induced contractures in the presence of $Mn^{2+}$ .....   | 96 |
| <b>Fig. 3.10</b> Long term $Mn^{2+}$ experiment. ....  | 97 |
| <b>Fig. 3.11</b> Delayed force increase induced by $Mn^{2+}$ in the presence of high $K^+$ . ....                          | 98 |
| <b>Fig. 3.12</b> The inward $Ca^{2+}$ currents are blocked by $Mn^{2+}$ .....  | 99 |

#### Chapter 4

|  |     |
|--|-----|
| <b>Fig. 4.1</b> Mechanical part of the experimental apparatus. ....  | 132 |
| <b>Fig. 4.2</b> A simplified diagram of the experimental set-up used for the<br>skinned fibre mechanical experiments (from Galler, 1994). .... | 133 |
| <b>Fig. 4.3</b> Force and length changes during constant load experiments. ....  | 134 |
| <b>Fig. 4.4</b> SDS-PAGE (10 % gel) of membrane-intact (A) and skinned<br>(B) $S_1$ , $S_2$ and fast (F) fibres. ....                          | 135 |
| <b>Fig. 4.5</b> Original traces of force and fibre length during an experiment. ....   | 136 |
| <b>Fig. 4.6</b> Length changes applied to a muscle fibre and the force response<br>during a stretch activation. ....                           | 137 |
| <b>Fig. 4.7</b> Properties of the $S_1$ , $S_2$ and fast fibre types. ....   | 138 |
| <b>Fig. 4.8</b> Stretch activation in the $S_2$ fibre type. ....   | 139 |
| <b>Fig. 4.9</b> Stretch activation in the $S_1$ fibre type. ....   | 140 |
| <b>Fig. 4.10</b> Stretch activation in the fast fibre type. ....   | 141 |
| <b>Fig. 4.11</b> Force-length relationship of the fibre types. ....  | 142 |
| <b>Fig. 4.12</b> Quick release experiment in the $S_1$ fibre type. ....  | 143 |
| <b>Fig. 4.13</b> Quick release experiment in the $S_2$ fibre type. ....  | 144 |

|   | <i>Page</i> |
|---|-------------|
| <b>Fig. 4.14</b> Quick release experiment in the fast fibre type. ....  | 145         |
| <b>Fig. 4.15</b> $T_1$ plots for the fast (A), $S_2$ (B) and $S_1$ (C) fibre types. ....  | 146         |
| <b>Fig. 4.16</b> Examples of the original force-velocity and intrapolated<br>shortening plots for the $S_1$ fibre type. ....  | 147         |
| <b>Fig. 4.17</b> Examples of the original force-velocity and intrapolated<br>shortening plots for the $S_2$ fibre type. ....  | 148         |
| <b>Fig. 4.18</b> Examples of the original force-velocity and intrapolated<br>shortening plots for the fast fibre type. ....   | 149         |
| <b>Fig. 4.19</b> Examples of force-velocity plots for the $S_1$ , $S_2$ and fast<br>fibre types. ....   | 150         |
| <b>Fig. 4.20</b> Relationship between shortening velocity measured by the<br>manual and constant load ramp methods. ....  | 151         |
| <br><b>Chapter 5</b>  |             |
| <b>Fig. 5.1</b> Relationship between the relative isometric steady-state force<br>and the free $Mn^{2+}$ concentration. ....  | 174         |
| <b>Fig. 5.2</b> Activations recorded under 5 mM $Mn^{2+}$ solution. ....  | 175         |
| <b>Fig. 5.3</b> Activations recorded under 10 mM and 30 mM $Mn^{2+}$ solutions. ....  | 176         |
| <b>Fig. 5.4</b> Relationship between the relative isometric steady-state<br>force ( $P/P_0$ ) and pCa. ....   | 177         |
| <b>Fig. 5.5</b> Relationship between the relative isometric steady-state<br>force ( $P/P_0$ ) and pMn. ....   | 178         |
| <b>Fig. 5.6</b> Relationship between the relative isometric steady-state<br>force ( $P/P_0$ ) and pCa and pMn. ....   | 179         |
| <b>Fig. 5.7</b> The relationship between MgATP and MnATP when they<br>are in solution together. ....  | 180         |
| <b>Fig. 5.8</b> Original force traces of a single $S_1$ fibre in response to<br>different $Mn^{2+}$ solutions (pMn 4.0-1.52) and their equivalent<br>low MgATP solutions (pCa 4.7) .... | 181         |
| <b>Fig. 5.9</b> Effect of MgATP on muscle fibre maximal tension. ....   | 182         |
| <b>Fig. 5.10</b> Effect of MnATP on muscle fibre maximal tension. ....  | 182         |

|   |     |
|---|-----|
| <b>Fig. 5.11</b> The effect of $Mn^{2+}$ on muscle fibre stiffness.....   | 183 |
| <b>Fig. 5.12</b> Relationship between stiffness and maximal tension. ....   | 184 |
| <b>Fig. 5.13</b> The effect of MnATP on muscle fibre stiffness at<br>different $Mn^{2+}$ concentrations. ....   | 185 |
| <b>Fig. 5.14</b> The effect of MgATP on muscle fibre stiffness. ....  | 185 |
| <b>Fig. 5.15</b> Effect of $Mn^{2+}$ on maximal shortening velocity ( $V_{max}$ ).....  | 186 |
| <b>Fig. 5.16</b> Effect of $Mn^{2+}$ on the rate of filament sliding.....   | 186 |
| <b>Fig. 5.17</b> Comparison of the $V_{max}$ of the 2 mM $Mn^{2+}$ solution which contains<br>0.72 mM MgATP with the equivalent low MgATP $Ca^{2+}$ solution. ....                  | 187 |
| <b>Fig. 5.18</b> Comparison of the rate of filament sliding of the 2 mM $Mn^{2+}$<br>solution which contains 0.72 mM MgATP with the equivalent<br>low MgATP $Ca^{2+}$ solution..... | 187 |
| <b>Fig. 5.19</b> Effect of $Mn^{2+}$ on stretch activation.....   | 188 |
| <b>Fig. 2.20</b> Effect of high and low concentrations of $Mn^{2+}$ on stretch<br>activation.....   | 189 |
| <b>Fig. 5.21</b> Effect of low MgATP on stretch activation.....   | 190 |

## SUMMARY

Crustacean muscle fibres are classified into tonic and phasic types. Within this classification a further subdivision of fibres can be made on the basis of histochemical and biochemical techniques, and electron microscopy. While some muscles are composed of fibres with uniform morphological and physiological properties (homogenous muscles), others muscles comprise mixed populations of fibres with different properties (heterogeneous muscles).

Crustacean muscles have been used extensively as a model system in the study of the excitation-contraction (EC) coupling mechanism, but few studies have related the properties of EC coupling to the differences between fibre types, mainly due to difficulties in fibre type identification following physiological measurements. Working on the heterogeneous population of  $S_1$  and  $S_2$  fibres found in the lateral and medial bundles of the superficial flexor (SF) muscle of the Norway lobster, *Nephrops norvegicus* overcomes this problem of relating structure to function since the fibre types have been identified on the basis of several criteria. This project uses the SF muscle system to investigate the EC coupling properties of two slow fibre phenotypes.

Experiments on membrane-intact fibres of the SF muscle, both as intact nerve-muscle preparations and as single fibres, demonstrate that the EC coupling mechanism in the medial and lateral bundles of the SF muscle is  $Ca^{2+}$ -induced  $Ca^{2+}$ -release (CICR) since both the flux of  $Ca^{2+}$  ions across the sarcolemma and the release of  $Ca^{2+}$  ions from the sarcoplasmic reticulum (SR) are essential for muscle contraction, and since the external  $Ca^{2+}$  ions themselves cannot directly activate the myofibrillar proteins (indicating the involvement of an intermediate step ~ release of  $Ca^{2+}$  from the SR). Evidence for this includes: (1) an inhibition of the subsequent steps of CICR on removal of external  $Ca^{2+}$  from the saline, (2) depletion of the SR of  $Ca^{2+}$  by repeated application of caffeine, and (3) the application of pharmacological agents: tetracaine blocks the release of  $Ca^{2+}$  ions from the SR, and 2,3-butanedione monoxime acts in a similar manner to caffeine to induce the release of  $Ca^{2+}$  ions from the SR in the absence of external  $Ca^{2+}$ .

Based on experiments conducted on the whole muscle bundle preparation, the medial and lateral muscle bundles express similar EC coupling properties. However, studies using

the two electrode voltage clamp technique indicate that the S<sub>1</sub> and S<sub>2</sub> fibre types express different populations of sarcolemmal ion channels. Differences were observed in both the inward Ca<sup>2+</sup> currents the outward K<sup>+</sup> currents.

The heavy metal ion Mn<sup>2+</sup> has been used as a tool to investigate the involvement of Ca<sup>2+</sup> ions in the different steps of EC coupling, both at the level of the sarcolemmal ion channels and in the activation of the myofibrillar proteins. Experiments conducted on the nerve-muscle preparation show that Mn<sup>2+</sup> at high concentrations (above 18 μM) inhibits the neuronally-evoked muscle force and the force evoked by electrical field stimulation in a dose-dependent manner, and at concentrations above 10 mM blocks the K<sup>+</sup>-induced force. It is thought that Mn<sup>2+</sup> inhibits force by blocking the sarcolemmal Ca<sup>2+</sup> channels which carry the inward current.

At low concentrations (below 18 μM) Mn<sup>2+</sup> increases the size of the evoked forces and increases the resting force produced when the fibres are depolarised by high K<sup>+</sup> solutions for 3 hours. This latter result indicates that under certain conditions Mn<sup>2+</sup> ions can penetrate through sarcolemmal ion channels, and either activate the contractile machinery directly or affect the amplification step of EC coupling at the SR. Experiments conducted on chemically-skinned S<sub>1</sub> fibres which do not possess a sarcolemma or internal Ca<sup>2+</sup> store (SR) show that Mn<sup>2+</sup> ions can activate the contractile proteins, which supports the first suggestion. These experiments indicate that the Ca<sup>2+</sup>-binding properties of the regulatory protein troponin are not specific for Ca<sup>2+</sup>, but that Mn<sup>2+</sup> ions, which have a similar ionic radius and energy of hydration, can also activate the contractile mechanism. However, from stretch activation experiments, which are thought to reflect the kinetics of the crossbridge cycle, the shorter t<sub>2</sub> times under Mn<sup>2+</sup> suggest that Mn<sup>2+</sup> does not bind in exactly the same way as Ca<sup>2+</sup> to troponin.

In contrast to the effect of Mn<sup>2+</sup> at lower concentrations higher Mn<sup>2+</sup> concentrations (5-30 mM) inhibit force in a dose-dependent manner. Since Mn<sup>2+</sup> has a higher affinity for ATP than Ca<sup>2+</sup> the levels of free MgATP may be limiting in solutions with higher concentrations of Mn<sup>2+</sup>. However, from tension and stiffness measurements made using Ca<sup>2+</sup> solutions containing low concentrations of MgATP it is apparent that the decreased MgATP levels do not appear to limit force. One other possible explanation is that

competitive inhibition occurs between the MnATP and MgATP, and that this effect is stronger at lower MgATP concentrations.

Kinetic experiments conducted on skinned fibres show that the fibre types differ in their shortening velocity, maximal power output, stretch activation, stiffness, and filament sliding. From these measurements it is possible to clarify further the roles of these fibres within the abdomen of *Nephrops*. S<sub>1</sub> fibres express higher shortening velocity, being able to shorten almost twice the distance per unit time when compared to the S<sub>2</sub> fibres, but have lower maximal power values than the S<sub>2</sub> fibres. The S<sub>2</sub> fibres have slower, long-lasting contractions which are fatigue-resistant, and thus appropriate to maintain abdominal posture, and have high maximal power values giving high energy efficiency. The S<sub>1</sub> fibres are adapted for more rapid contractions which control slow movements of the abdomen, but are less energy efficient since they are only recruited intermittently. These differences are thought to arise from variations in the kinetics of the crossbridge cycle, may relate to the expression of different myofibrillar protein isoforms (myosin heavy-chain, myosin light-chain, troponin), and probably underlie the different functional roles of the fibres within the abdomen of *Nephrops*.

**Chapter 1**  
**General Introduction**

### 1.1 $\text{Ca}^{2+}$ signalling in cells

Over the past few decades enormous progress has been made in our understanding of how cells use calcium ( $\text{Ca}^{2+}$ ) ions to regulate their activity. Early in evolution only a few basic signalling systems existed, but these have since been modified to meet the particular signalling requirements of different cells, ranging from photoreceptors detecting brief flashes of light to liver cells responding to slow changes in circulating hormone levels.

External signals mediated by the binding of growth factors, hormones or neurotransmitters to receptors on the cell surface initiate signalling pathways, and thereafter information flows from one component to the next until the final effector system is activated. In most cells the initial intracellular signal involves  $\text{Ca}^{2+}$ , and common features are the entry of external  $\text{Ca}^{2+}$  into cells and the mobilisation of internal  $\text{Ca}^{2+}$  stores. However, a number of more complex  $\text{Ca}^{2+}$  signals can also be involved, such as repetitive  $\text{Ca}^{2+}$  spikes, oscillations and regenerative  $\text{Ca}^{2+}$  waves which propagate across cells. The mechanisms underlying these complex signals still remain relatively elusive.

The intracellular membrane stores from which  $\text{Ca}^{2+}$  is released are thought to be specialised subcompartments of the endoplasmic reticulum (ER). Intracellular  $\text{Ca}^{2+}$  stores incorporate three major components: pumps to sequester  $\text{Ca}^{2+}$ , binding proteins (such as calsequestrin) which store  $\text{Ca}^{2+}$ , and specific receptors such as the inositol 3,4 triphosphate receptor ( $\text{InP}_3\text{R}$ ) and the ryanodine receptor (RyR) which release  $\text{Ca}^{2+}$  into the cytosol. These last two receptors share many structural and functional homologies, the most striking of which is a common sensitivity to  $\text{Ca}^{2+}$ , and this probably reflects a common evolutionary origin (Fadool & Ache, 1992). The distribution of RyR and  $\text{InP}_3\text{R}$  differs from cell to cell: some cells (e.g. vertebrate skeletal muscle) have only RyR, others (e.g. *Xenopus* oocytes) have only  $\text{InP}_3\text{R}$  (Parys, *et al.*, 1992) while a number (e.g. sea urchin eggs) contain both (McPherson *et al.*, 1992). The regenerative properties of the RyR and the  $\text{InP}_3\text{R}$  are thought to be fundamental to the generation of  $\text{Ca}^{2+}$  oscillations and spikes (Berridge, 1993).

Calcium-regulated pathways are important for the control of different cellular processes, many of which are still not well understood. For example, in fertilisation it is still something of a mystery how the sperm triggers the explosive release of  $\text{Ca}^{2+}$  within the egg, while in the brain the high density of  $\text{InP}_3\text{R}$  in Purkinje cells makes this one of the most well understood pathways (Walton *et al.*, 1991). Many hypotheses have been proposed to explain intracellular  $\text{Ca}^{2+}$  signalling (Berridge & Irvine, 1989; Tsien & Tsien, 1990; Berridge, 1990; Meyer & Stryer, 1991), and one of the most widely accepted theories is that  $\text{Ca}^{2+}$  can act as a diffusible messenger to enhance its own release through the process of calcium-induced-calcium-release (CICR) (Tsien & Tsien, 1990).

The generalised CICR mechanism has two main components: an entry mechanism at the plasma membrane, which regulates the supply of  $\text{Ca}^{2+}$  to the second component, and the oscillator itself which consists of  $\text{Ca}^{2+}$  stores that have either RyR or  $\text{InP}_3\text{R}$  responsible for CICR. The *Xenopus* oocyte is an example of a cell in which repetitive spiking depends upon cyclic release of  $\text{Ca}^{2+}$  from internal stores through the regenerative process of CICR (Parker & Yao, 1991). The external  $\text{Ca}^{2+}$  which influxes is taken up by the internal stores. This has two main actions: firstly it sensitises the receptors by elevating internal  $\text{Ca}^{2+}$  levels, and secondly it provides the trigger which activates CICR. In *Xenopus* oocytes, increasing doses of  $\text{InP}_3$  lead to localised elevations of  $\text{Ca}^{2+}$ , called hot spots, which are transformed into an all-or-nothing response. As the  $\text{Ca}^{2+}$  trigger reaches a critical level, regenerative waves are generated in the form of  $\text{Ca}^{2+}$  spikes. Spiking is terminated through the build up of cytosolic free  $\text{Ca}^{2+}$ , which prevents further  $\text{Ca}^{2+}$  release and switches the channel into its inactive state through an inhibitory effect on the release channel. The free  $\text{Ca}^{2+}$  is removed either by being pumped back into the internal  $\text{Ca}^{2+}$  stores, or by being pumped out of the cell, thus returning it to its resting state.

One well-researched area of calcium signalling is in muscle cells.  $\text{Ca}^{2+}$  ions play a critical role in both the activation and the regulation of muscle contraction, either through  $\text{InP}_3$ -activated  $\text{Ca}^{2+}$ -release, as in smooth muscle cells, or by various calcium release mechanisms, as in skeletal and cardiac muscle cells. This project investigates CICR as the excitation-contraction (EC) coupling mechanism in crustacean muscle.

## 1.2 Excitation-contraction coupling mechanisms in muscle

The series of events which couples the electrical events at the muscle membrane to the mechanical events of muscle contraction is known as excitation-contraction (EC) coupling (Sandow, 1952). The main features of EC coupling are considered below.

### 1.2.1 Depolarisation of the sarcolemma

The ionic mechanisms involved in the excitability of membranes and the generation of the action potential (AP) were discovered by Hodgkin and Huxley (1952) using the voltage clamp technique. They identified two major ionic fluxes, an inward  $\text{Na}^+$  current ( $I_{\text{Na}}$ ) and an outward  $\text{K}^+$  current ( $I_{\text{K}}$ ). The inward movement of  $\text{Na}^+$  ions across the cell membrane causes a build up of positive charge inside the membrane, and hence depolarisation, while the exit of  $\text{K}^+$  ions reverses this process. The inward  $\text{Na}^+$  current is crucial for the propagation of electrical signals as APs.

The arrival of an AP at the terminals of a motor nerve stimulates the release of neurotransmitter (e.g. acetylcholine, glutamate) at the neuromuscular junction. Through binding to specific receptor sites on postsynaptic ion channels, the neurotransmitter acts as the ligand to gate them open, allowing specific ions to flow along their electrochemical gradients and so depolarising the membrane.

In vertebrate skeletal muscle the major extracellular ion is  $\text{Na}^+$ , as in the nerve, and in most cases the sarcolemma is electrically excitable. Therefore, when the membrane potential of the sarcolemma reaches a certain threshold value, an AP is generated and propagates along the muscle fibre. This acts as the trigger to initiate the release of internal  $\text{Ca}^{2+}$  stores from the sarcoplasmic reticulum (SR) activating muscle contraction.

In vertebrate cardiac and smooth muscle, and in certain invertebrate muscles such as those of crustaceans,  $\text{Ca}^{2+}$  ions, in addition to or instead of  $\text{Na}^+$  ions, carry the inward current across the sarcolemma through voltage-gated  $\text{Ca}^{2+}$  channels (Hagiwara & Byerly, 1981). This causes a change in the internal free  $\text{Ca}^{2+}$  ion concentration, which in turn triggers the ultimate response of muscle contraction.

For crustacean muscle, Fatt & Katz (1953) discovered this involvement of  $\text{Ca}^{2+}$  ions while investigating neuromuscular transmission in the large diameter muscle fibres of crab legs. They found that APs were unusually small in normal crab saline, but when the  $\text{Na}^+$  ions were replaced with quaternary ammonium ions, such as choline, tetrathylammonium (TEA), or tetrabutylammonium (TBA) the AP's increased in size. The TBA-induced AP was maintained after washing with an isotonic sucrose solution containing only  $\text{Ca}^{2+}$ ,  $\text{Mg}^{2+}$  and K ions. They concluded that the inward current was carried by the influx of  $\text{Ca}^{2+}$  or  $\text{Mg}^{2+}$  ions, or the efflux of some internal ion. Working with crayfish muscle, Fatt & Ginsborg (1958) showed that the AP produced under TEA was independent of  $\text{Na}^+$  and  $\text{Mg}^{2+}$  ions, and concluded that it was produced by an increased membrane permeability for  $\text{Ca}^{2+}$  ions. Moreover, when  $\text{Ca}^{2+}$  was replaced by  $\text{Ba}^{2+}$  or  $\text{Sr}^{2+}$ , all-or-nothing APs were obtained, even without TEA. Therefore in crustacean muscle depolarisation appears to be dependent upon the inflow of  $\text{Ca}^{2+}$  ions rather than  $\text{Na}^+$  ions across the cell membrane.

Hagiwara & Naka, (1964) also observed  $\text{Ca}^{2+}$  'spikes' in crustacean muscle by lowering the intracellular free  $\text{Ca}^{2+}$  concentration. Working with muscle fibres of the giant barnacle (*Balanus nubilus*) they injected  $\text{Ca}^{2+}$ -binding anions (such as sulphate, citrate and ethylenediaminetetraacetic acid (EDTA)) into the myoplasm. This conferred the ability to make strong  $\text{Ca}^{2+}$ -dependent APs in normal extracellular solutions. The internal free  $\text{Ca}^{2+}$  concentration had to be reduced below  $1 \times 10^{-7}$  M to permit all-or-nothing APs (Hagiwara & Nakajima, 1966b). Further evidence supporting the  $\text{Ca}^{2+}$ -dependent AP hypothesis was provided by Hagiwara & Naka (1964) who measured  $\text{Ca}^{2+}$  fluxes during an AP.

### **1.2.2 Propagation of the inward current into the interior of the cell**

Two main problems concerning EC coupling had still to be addressed: firstly how was the influx of external  $\text{Ca}^{2+}$  ions responsible for activating the myofibrils? and secondly were any other intermediate steps involved? Huxley & Taylor (1955, 1958) conducted a series of local activation experiments on single frog muscle fibres using micropipettes as electrodes to depolarise small areas of muscle membrane. Under weak depolarisation a local contraction could be observed in the two half sarcomeres adjoining a stimulated 'Z' line, causing the width of the corresponding 'I' band to become smaller. When the stimulation electrode was placed at the junction of an 'I' or 'A' bands, however, no

contraction occurred. These experiments were later confirmed by Porter and Palade (1957) and Peachy (1965, 1973). Comparative experiments by Huxley and Straub (1958) showed similar results in lizard and crab muscle, although in these cases the local contractures did not occur near the 'Z' line but at the junction of the 'A' and 'I' bands. The same response was also demonstrated in the muscles of other crustaceans and fish, whereas all amphibian muscle shows local contractures at the Z disc. The actual mechanism of inward transmission of the surface excitation only became clearer when the fine structure of muscle fibres was revealed by electron microscopy. Thus the work of Huxley and Straub (1958) on lizard muscle was confirmed by the ultrastructural studies of Robertson (1956) on the lizard, *Lacerata viridis*. He discovered an invaginated tubular structure between the junction of the 'I' and 'A' band that connected the outer membrane to the interior of the muscle fibre. The transverse tubule (T) system was present in the correct position to account for the fast inward conducting mechanism found by Huxley and Straub (1958). It has subsequently become established as the mechanism by which the spread of excitation along the muscle membrane is rapidly propagated into the interior of the muscle cell (for review, see Fanzini-Armstrong & Jorgenson, 1994).

### 1.2.3 The dihydropyridine (DHP) receptors

The voltage-dependent  $\text{Ca}^{2+}$  channels which are responsible for the inward  $\text{Ca}^{2+}$  ( $I_{\text{Ca}}$ ) current across T-tubule membranes of muscle have been identified as the L-type  $\text{Ca}^{2+}$  channels on the basis of their sensitivity to blocking by the dihydropyridines (DHPs) (Hess *et al.*, 1984). The DHPs suppress the surface membrane  $I_{\text{Ca}}$  by preferentially binding to the inactivated state of the L-type  $\text{Ca}^{2+}$  channel, and thus cause an increased occupancy of the inactivated state (Bean, 1984; Hille, 1977). As well as being associated with the RyR complex, experiments with labelled [ $^3\text{H}$ ] dihydropyridine have shown that the DHP-specific binding sites are concentrated in the T-tubule membrane fraction (Fosset *et al.*, 1983). The isolated DHP receptor consists of three peptide subunits, alpha ( $\alpha$ ), beta ( $\beta$ ) and gamma ( $\gamma$ ) (Leung *et al.*, 1988). It is thought that the  $\alpha$  subunit makes up the  $\text{Ca}^{2+}$  channel (Prerez-Reyes, 1989). DHP receptors have been shown to act either as voltage-operated channels or as  $\text{Ca}^{2+}$  release channels, which underlie the two mechanisms for the control of SR  $\text{Ca}^{2+}$ -release:

1. the charge-coupled model (mechanical coupling).
2. calcium-induced-calcium-release (CICR).

#### 1.2.4 The charge-coupled model or mechanical coupling

The studies by Schneider and Chandler (1973) on frog skeletal muscle fibres led to the development of a charge-coupled model for coupling across the T-tubule membrane. By measuring charge movements in the presence of TTX, TEA and  $Rb^+$  ions to block the ionic currents it was possible to identify the components that corresponded to the movements of a possible voltage sensor. These had the following properties:

1. they flowed for a few milliseconds after depolarisation and returned after repolarisation.
2. they had a steep voltage dependence around  $-45mV$ .
3. they disappeared when the T-tubules were disrupted by osmotic shocks, and contraction then ceased (Chandler *et al.*, 1976).
4. they became refractory if the fibres were depolarised for longer than a few seconds.

On the basis of these findings, Chandler and colleagues proposed that upon depolarisation a charge component within the T-tubules serves as a voltage sensor, opening the  $Ca^{2+}$  release channels of the SR. They also suggested that mechanical linkage via the feet seen under the electron microscope might couple the two membranes together. This idea was confirmed by using the electron microscope to investigate the triadic junctions ('feet'). The DHP receptor is located next to the SR  $Ca^{2+}$ -release channel, the ryanodine receptor, which suggests that the foot is the transduction mechanism in vertebrate skeletal muscle. However, no direct link between the DHP receptor and the RyR of the SR has yet been found (Brandt *et al.*, 1990)

The first indications that DHP receptors might function not only as  $\text{Ca}^{2+}$  channels, but more significantly as voltage sensors for SR  $\text{Ca}^{2+}$  release came with the finding that the phenylalkylamine D600 (gallopamine) blocked recovery of both the contractile ability (Eisenberg *et al.*, 1983) and charge movement (Hui *et al.*, 1984) during repolarisation after prolonged depolarisation. Furthermore, during strong hyperpolarisations, fibres depolarised in D600 recovered  $\text{Ca}^{2+}$ -release and charge movements with parallel time courses (Feldmeyer *et al.*, 1990). The identification of the DHP receptor as a voltage sensor for  $\text{Ca}^{2+}$  release was finally confirmed with experiments using dysgenic muscles, which lack DHP receptors. The expression of DHP receptors in dysgenic skeletal myotubules restored mechanical activity (Tanabe *et al.*, 1987).

The possible dual, or alternative roles of the skeletal DHP receptor as a voltage sensor for  $\text{Ca}^{2+}$ -release and/or as an external membrane channel with a voltage sensor controlling its own voltage-dependent gating has given rise to the following questions:

1. what are the amounts of charge movement in relation to the two possible functions of the DHP receptor (Lamb, 1991, Schwartz *et al.*, 1985)?
2. does the charge-coupling mechanism control  $\text{Ca}^{2+}$  release in all muscle types?

Though DHP receptors are present in the T-tubular membrane of vertebrate skeletal muscle, they do not appear to function as  $\text{Ca}^{2+}$  channels (Schwartz *et al.*, 1985, Lamb, 1991). The kinetics of channel opening are very slow (Sanchez & Stefani, 1983) and the  $\text{Ca}^{2+}$  influx through these or other  $\text{Ca}^{2+}$ -conducting channels in T-tubules is not thought to be involved in activating SR  $\text{Ca}^{2+}$  release in frog skeletal muscle fibres (Brum *et al.*, 1987; Miledi *et al.*, 1984). However, in vertebrate cardiac muscle and crustacean muscle the  $\text{Ca}^{2+}$  inflow through L-type  $\text{Ca}^{2+}$  channels is faster than in vertebrate skeletal muscle, is larger in amplitude and is necessary for activating SR  $\text{Ca}^{2+}$  release (Beukelmann & Wier, 1988; Callewaert *et al.*, 1988; London & Krueger, 1986). This suggests that the 'mechanical- or charge-coupling' model is only true for SR  $\text{Ca}^{2+}$  release in vertebrate skeletal muscle.

One explanation for the presence of different SR  $\text{Ca}^{2+}$ -release mechanisms is that an evolutionary step has taken place, transforming the  $\text{Ca}^{2+}$  channel form of the primitive

DHP receptor found in invertebrate muscle into the voltage sensor form of the vertebrate skeletal muscle DHP receptor (Inoue *et al.*, 1994). Inoue and colleagues suggest that this evolutionary step took place somewhere between the cephalochordates and the agnathans.

### 1.2.5 CICR as an excitation-contraction (EC) coupling mechanism in muscle

In vertebrate cardiac and invertebrate skeletal muscle, the  $\text{Ca}^{2+}$  released from the SR is not controlled directly by voltage but by the influx of external  $\text{Ca}^{2+}$  ions (i.e. the process of CICR), through L-type  $\text{Ca}^{2+}$  channels (DHP receptors) in the T-tubules and muscle membrane. Through CICR, a concentration of free  $\text{Ca}^{2+}$  which is too low to cause tension by direct activation of the myofibrils, is able to release stored  $\text{Ca}^{2+}$  from the SR, which in turn activates muscle contraction (Ashley *et al.*, 1993; Palade & Györke, 1993).

The  $\text{Ca}^{2+}$  release channel has been shown to be the ryanodine receptor (RyR) in vertebrate skeletal muscle (Lai *et al.*, 1988; Smith *et al.*, 1988), cardiac muscle (Williams & Ashley, 1989) and invertebrate skeletal muscle (Loesser *et al.*, 1992). In the case of invertebrate and cardiac muscle, it is the depolarisation-induced inward  $\text{Ca}^{2+}$  flux into the muscle fibre which occurs at the T-tubules through the DHP receptors that is thought to be the source of the trigger for  $\text{Ca}^{2+}$  release through the RyR.

### 1.2.6 The ryanodine receptor (RyR)

Although the physiological actions of the plant alkaloid ryanodine on muscles have been known for some years (Jenden & Fairhurst, 1969), the suspicion that it acted on the SR was only confirmed when it was demonstrated that ryanodine binds specifically to the SR membrane (Pessah *et al.*, 1987; Fleischer *et al.*, 1985). Experiments using labelled [ $^3\text{H}$ ] ryanodine showed that the specific ryanodine binding site was located on the terminal cisternae of the SR, the major site of  $\text{Ca}^{2+}$  release.

The arrangement of the RyR was elucidated by Franzini-Armstrong (1970) based on electron micrographs of the triadic junction. 'Foot'-like structures are apparent in the triads, which form a close connection between the T-tubules and the terminal cisternae of

the SR. Incorporation of isolated receptor proteins into planar lipid bilayers formed  $\text{Ca}^{2+}$  channels which were identical to the 'native'  $\text{Ca}^{2+}$  channels of the terminal cisternae of the SR, thus confirming the identity of the RyR (Lai *et al.*, 1988). Studies using freeze fracture microscopy and experiments which have incorporated isolated receptors into the membranes of isolated SR, have defined the RyR complex in more detail (Smith *et al.*, 1988; Hymel *et al.*, 1988). The RyR comprises a foot-like structure, with a major cytoplasmic domain that is about 12 nm in size and extends outwards from the surface of the SR to make a connection with the transverse tubules (Inui *et al.*, 1987). On the luminal side of the terminal cisternae is an aggregation of the  $\text{Ca}^{2+}$ -binding protein calsequestrin (MacLennan & Wong, 1971). The outer side of the cisternae are the RyR, and on the T side of each complex are four tubular tetrads which have been tentatively identified as dihydropyridine (DHP) receptors. From morphological evidence there appears to be twice as many RyR as DHP receptors (Block *et al.*, 1988).

Work on crustacean muscle RyR has shown that it has a similar structure to that of vertebrate striated muscles, but does not possess the high-affinity  $\text{Ca}^{2+}$  binding site which has been identified in vertebrate skeletal and vertebrate cardiac muscle RyR (for reviews, see Lai & Meissner, 1989; Fleischer & Inui, 1989; Meissner, 1994). In addition, single channel activity has been reported from RyRs purified from crayfish and lobster muscle SR when they were incorporated into planar lipid bilayers (Formelová *et al.*, 1990; Arispe *et al.*, 1992). Seok *et al.* (1992) carried out an extensive study on lobster RyRs. They showed that lobster RyRs are sensitive to ryanodine and other agents such as caffeine and ruthenium red, but were inhibited by tetracaine. They also demonstrated that purified RyR have very similar properties to those from mammalian skeletal muscle and cardiac muscle, but were less sensitive to  $\text{Ca}^{2+}$  (for review, see Meissner, 1994). However, it is apparent from studies by Block *et al.* (1988) that the physical relationship between the RyR and the DHP receptors within the RyR complex is different in vertebrate skeletal muscle and invertebrate skeletal muscle (Block *et al.*, 1988).

### **1.2.7 Release of $\text{Ca}^{2+}$ from the sarcoplasmic reticulum (SR)**

Several lines of evidence suggest that in crustacean muscle  $\text{Ca}^{2+}$  entry alone is insufficient for EC coupling, and that  $\text{Ca}^{2+}$  release from the SR is required.

1. In crab muscle, Mounier and Goblet (1987) showed that the  $\text{Ca}^{2+}$  entry was insufficient to activate tension, and that contraction was inhibited in the presence of procaine, which blocks  $\text{Ca}^{2+}$  release from the SR, even in the presence of an inward  $\text{Ca}^{2+}$  current.
2. Mechanically-skinned fibres which possess intact SR, developed tension when bathed in saline containing a concentration of  $\text{Ca}^{2+}$  ions too low to activate the contractile proteins directly (Goblet & Mounier, 1986).
3. In cultured crayfish muscle fibres, which lack an intracellular  $\text{Ca}^{2+}$ -store, despite the presence of APs and  $\text{Ca}^{2+}$  currents of normal amplitude there is no contractile response (Uhrlik *et al.*, 1986).
4. Caffeine-induced  $\text{Ca}^{2+}$  release from the SR has been demonstrated in barnacle and lobster muscle bathed in  $\text{Ca}^{2+}$ -free saline (Rojas *et al.*, 1987).
5. Mechanically-skinned fibres which possess intact SR from lobster and crab striated muscle have ryanodine-sensitive SR stores of  $\text{Ca}^{2+}$  that can be released by both caffeine and micromolar levels of  $\text{Ca}^{2+}$  (Lea, 1996).

The SR is an internal membrane system which forms a network of tubules lying longitudinally between the myofibrils (Peachy, 1965). The tubules end in blind sacs, the terminal cisternae, which are filled with  $\text{Ca}^{2+}$  ions. The cisternae are closely associated with the contractile elements, the myofibrils, and with the transverse tubules of the T system.

Many workers have demonstrated that membrane depolarisation can be uncoupled from the later, force-generating steps of EC coupling. For example, Fatt and Katz (1953) demonstrated that it was possible to induce abnormally large AP's in crustacean muscle without producing contraction. Others showed that in many smooth muscle cells, contracture could be induced hormonally without any change in the membrane potential (Somlyoe & Somlyoe, 1968). Similarly Heilbrunn and Wiercinski, (1947) demonstrated that muscle fibres could be made to contract without a change in membrane potential by injecting  $\text{Ca}^{2+}$  salts into muscle fibres. It was also shown that skinned muscle fibres which had had their sarcolemma destroyed, either chemically, mechanically or by a freeze drying

process (Podolsky, 1968) contracted when exposed to solutions containing  $\text{Ca}^{2+}$  ions and ATP (Stephenson & Williams, 1980, 1983). Finally, experiments conducted in the absence of extracellular  $\text{Ca}^{2+}$  ions showed that caffeine could induce muscle contraction by releasing the intracellular  $\text{Ca}^{2+}$  from the SR stores (Chiarandini *et al.*, 1970a). This process was reversible if  $\text{Ca}^{2+}$  was re-introduced to the external medium, allowing the depleted SR  $\text{Ca}^{2+}$  stores to be replenished. These experiments confirmed the existence of an intermediate step, the release of  $\text{Ca}^{2+}$  ions from the SR.

Electron micrographs show that the terminal cisternae of the SR are closely apposed to the T tubules, forming the triadic T-SR junction (Franzini-Armstrong & Peachy, 1981). The existence of electron-dense bridges, 'feet' spanning the 16 nm gap within the triads, indicate that the SR and T tubules are intimately connected (Franzini-Armstrong, 1970, 1975; Franzini-Armstrong & Peachy, 1981). Franzini-Armstrong suggested that these 'feet' are involved with T system-SR coupling and that they act as a  $\text{Ca}^{2+}$  release channel. Consistent with these ideas are other findings, such as the density of 'feet' being much reduced in slow muscle where  $\text{Ca}^{2+}$  release and the activation process are much slower, and the fact that these feet were present in all muscle types from spiders to fish (Franzini-Armstrong & Nunzi 1983).

### **1.2.8 Binding of $\text{Ca}^{2+}$ ions to the regulatory proteins**

Muscle contraction is produced by the sliding of actin (thin) filaments along myosin (thick) filaments. The head regions of the myosin molecules project sideways from the filament shaft and engage in an ATP-driven cycle in which they attach to the adjacent actin molecules. In this way the projections form regular crossbridges which undergo a conformational change that pulls the myosin filaments against the actin filaments, and then detach, a process called crossbridge cycling (for review, see Woledge, 1985). Muscle contraction is discussed further in Section 4.1. In all muscle types the interaction of the actin and myosin is triggered by an increase in the intracellular free  $\text{Ca}^{2+}$  concentration. However, the regulatory proteins which detect and respond to the  $\text{Ca}^{2+}$  ions differ depending on muscle type. There are two mechanisms for  $\text{Ca}^{2+}$  regulation of actin-myosin interaction: (1) actin regulated muscle, and (2) myosin regulated muscle, although it should be noted that some muscles have been shown to have dual regulation, for example those of nematodes (Lehman & Szent-Györgyi, 1975)

In actin-regulated muscle the  $\text{Ca}^{2+}$  binding protein troponin (Tn), which is situated on the actin filament, is the intracellular switch regulating the contractile machinery (see Section 4.1). This mechanism is present in vertebrate skeletal muscle and in many types of invertebrate muscle.

In myosin-regulated muscle the myosin molecule itself acts as a  $\text{Ca}^{2+}$  receptor and is directly activated by  $\text{Ca}^{2+}$ . This mechanism is present in a number of higher invertebrate groups (annelids, molluscs, and many arthropods). In myosin-regulated muscle interaction between actin and myosin is inhibited by the myosin regulatory light chains, and this inhibition is relieved only when  $\text{Ca}^{2+}$  ions bind directly to the myosin molecules (molluscan smooth muscle). In vertebrate smooth muscle regulation involves an enzyme-driven cascade involving calmodulin, and contraction is initiated by the phosphorylation of one of the myosin light chains.

### 1.3 Muscle diversity

It is clear from this introductory chapter that there is a wide variety of muscle types and that diversification exists between these fibre groups. At a very general level muscle fibres are classified into three major groups (skeletal, cardiac, and smooth muscle) on the basis of their functional, structural and biochemical properties. Vertebrate muscle can be subdivided into fast and slow twitch fibres and tonic fibres on the basis of histochemical and biochemical criteria (Pette & Staron, 1990). The APs of the vertebrate slow twitch fibres are smaller in depolarisation amplitude than those of fast twitch fibres. In tonic muscle fibres, which have postural roles within the body, contraction is not initiated by an all-or-nothing action potential, but instead a small potential change recorded as an excitatory postsynaptic potential (EPSP) transmits decrementally across the electrically-inexcitable muscle membrane. Activation of the whole fibre is achieved in this case by multiterminal innervation. Repetitive nerve impulses produce EPSPs which summate to give a maintained change in membrane potential, leading to a graded contraction of the muscle fibre.

The functional unit of vertebrate skeletal muscle is the 'motor unit', which represents the number of muscle fibres innervated by a single motor axon. The size of a motor unit can vary from around 2000 muscle fibres per axon (e.g. frog gastrocnemius muscle) to 20

fibres per axon (e.g. the tensor tympani muscle of mammalian ear) (for review, see Buchthal & Schmalbruch, 1980). In general all the muscle fibres in a given motor unit have the same morphological and physiological properties (as confirmed by the glycogen depletion method) (Ridge, 1989). However, while some muscles are composed of fibres with uniform properties (homogeneous muscles) others are mixtures of muscle fibres (and hence motor units), with different properties (heterogeneous muscles). Such heterogeneity allows a muscle to produce a wide range of contractile responses (in terms of velocity, force and endurance). However, heterogeneous muscles are almost intractable systems in which to study the contractile properties of different fibres types.

Muscle fibres of various invertebrates (nematodes, annelids, crustaceans and insects) can also be classified into phasic and tonic types (Jahromi & Atwood, 1966; Parnas & Atwood, 1966). As with vertebrate skeletal muscle, this division can either be complete, with the existence of separate homogenous fast and slow muscles (e.g. the deep and superficial muscles respectively of the decapod crustacean abdomen (Parnas & Atwood, 1966)) or can be incomplete, forming heterogeneous muscles with mixed fibre types. Example of heterogeneous muscle in crustaceans include claw muscles from the lobster, *Homarus americanus*, the fiddler crab, *Uca pugnax*, and the land crab, *Gecarcinus lateralis* (Mykles, 1985). In fact some muscles which were previously identified to be homogeneous, have since been demonstrated to be heterogeneous from using various histochemical and biochemical techniques (Mykles, 1988).

The concept of the motor unit does not apply to these invertebrate muscles, as each fibre, be it phasic or tonic, receives multiterminal synaptic input from a number of excitatory and inhibitory axons (for review, see Govind, 1995). Although such polyneuronal innervation adds complexity, the number of motor axons is very small (e.g. as few as 2 in crab claw muscles), so it may be easier to identify the muscle fibre types present, following any physiological measurements. In the literature there are examples of studies which have either not attempted to identify fibres, have classed these fibres as anomalous or have simply ignored them, making it impossible to interpret the physiological results in terms of muscle fibre properties. This problem of relating structure to function can be overcome by working on a muscle system in which the fibre types have been identified by reliable methods. Such a system is represented by the superficial abdominal flexor

muscle of the Norway lobster, *Nephrops norvegicus*, and this has been used in the present study.

The abdominal superficial flexor (SF) muscle of the Norway lobster *Nephrops norvegicus* comprises the medial and lateral muscle bundles with two distinct fibres types (Fowler & Neil, 1992). As a result of the work performed in this laboratory the S<sub>1</sub> and S<sub>2</sub> fibre phenotypes have been characterised by their structural properties using histochemical and biochemical techniques (Fowler & Neil, 1992; Neil *et al.*, 1993), by their innervation patterns (Denheem, 1992) and, in collaborative study with Dr. Stefan Galler, by their contractile properties using skinned fibre preparations (Galler & Neil, 1994). Differences in the EC coupling properties of defined fibres phenotypes may be expected, but have not yet been determined.

This project therefore takes advantage of the unique opportunity offered by the SF muscle as an experimental system for investigating the EC coupling properties of different identified fibre types. The following aspects have been addressed:

1. The EC coupling properties of the SF muscle fibre types have been established using membrane-intact fibres preparations (Chapter 2).
2. The EC coupling properties have been investigated in response to the divalent cation Mn<sup>2+</sup> (Chapter 3).
3. The myofibrillar properties of the S<sub>1</sub> and S<sub>2</sub> fast extensor fibre types have been characterised in more detail and related to their roles within the abdomen as well as to their expression of different regulatory protein isoforms (Chapter 4).
4. The effects of Mn<sup>2+</sup> ions on the activation properties of the SF muscle S<sub>1</sub> fibre type have been investigated and related to its Ca<sup>2+</sup> activation properties (Chapter 5).

In Chapter 6 the EC coupling properties (sarcolemmal ion channels, Ca<sup>2+</sup>-release channels, myofibrillar proteins) of the different fibre types are discussed in relation to previous work characterising the different fibres. Future experimental work using the

techniques developed during the course of this study, is also suggested. The role of the heavy metal ion  $Mn^{2+}$  as a tool to investigate the involvement of  $Ca^{2+}$  ions in the different steps of EC coupling is reviewed and the use of the SF muscle system as a biological assay for the accumulation of  $Mn^{2+}$  ions within *Nephrops* is discussed.

**Chapter 2**  
**EC coupling in the *Nephrops* abdominal**  
**superficial flexor muscle**

## 2.1

## INTRODUCTION

In long-bodied macrurous decapod crustaceans, such as the crayfish and lobsters, the abdomen is organised into six segments (Fig. 2.1) whose movements are controlled by the action of four sets of muscles in response to motor patterns generated within each of the six ganglia in the ventral nerve cord (VNC). These muscles demonstrate a division of labour into distinct fast (or phasic) and slow (or tonic) groups

## 2.1.1 Fast muscle

The fast extensor (FE) and fast flexor (FF) muscles occupy most of the central core of the abdomen. They comprise fibres with short sarcomeres, always being less than 5  $\mu\text{m}$  in length when muscles are fixed at resting length, and myofibrils which are closely packed and regularly arranged. These phasic muscle fibres have been found to have electrotonic connections between adjacent fibres (Parnas & Atwood, 1966; Abbott and Parnas, 1965), so that they act as co-ordinated functional units. These fast muscles are involved in generating the rapid flexion and extension of the abdomen seen during escape swimming by tail flipping (Kennedy & Takeda, 1965a; Wine & Krasne, 1982).

## 2.1.2 Slow muscle

The muscles involved in the control of posture are the superficial extensor (SE) and superficial flexor (SF) muscles, which are the thin sheets of slow muscles on the dorsal and ventral sides of the abdomen, spanning the first five abdominal segments (Pilgrim & Wiersma, 1963; Kennedy & Takeda, 1965a). The superficial flexor (SF) muscle of *Nephrops norvegicus* is divided into two muscle bundles of different slow fibre phenotypes. The medial muscle bundle comprises approximately 20  $S_2$  type fibres arranged in a single layer. The lateral muscle bundle is larger, having approximately 60 fibres arranged in a layer  $3/4$  fibres deep. Approximately 90% of these fibres are of the  $S_1$  fibre type, but 10% are of the  $S_2$  type and are distributed across the muscle in a non-

uniform manner (Fowler & Neil, 1992). This chapter will concentrate on the properties of the SF muscle of *Nephrops norvegicus*.

### **2.1.3 Morphological, biochemical and histochemical properties of the SF muscle fibres**

The majority of the fibres in the lateral muscle bundle of the SF muscle have sarcomere lengths 6-8µm, contain a pH-labile isoform of myosin ATPase and low levels of oxidative enzymes, and express the myofibrillar protein pattern characteristic of the S<sub>1</sub> phenotype. Fibres of the medial muscle bundle have sarcomere lengths 9-11 µm, contain a pH-stable isoform of myosin ATPase and higher levels of oxidative enzymes, and express the myofibrillar protein pattern of the S<sub>2</sub> fibre phenotype (Neil *et al.*, 1993) There is also a clear difference in the extent of the tubular systems between the slow fibre phenotypes (Fowler & Neil, 1992).

### **2.1.4 Mechanical properties of the SF muscle fibres**

Using skinned muscle fibres, isometric force measurements on thin (<80 µm) myofibrillar bundles from freeze-dried fibres of the SF muscle have been correlated with subsequent identification of their phenotypes (Galler & Neil, 1994). The observed differences in the mechanical properties of these muscle fibre types provides information about their contractile performance and their probable functional role, and also give insights into their possible underlying contractile mechanisms. On the basis of the above findings it was proposed that S<sub>2</sub> fibres contract at a slower rate, are specialised for long-lasting force maintenance and are more fatigue resistant, while the S<sub>1</sub> fibres are adapted for slow movements.

### **2.1.5 Innervation of the SF muscle fibres**

The SF muscles in each segment of *Nephrops* receive a polyn neuronal innervation from six motor neurones (f1-f6), five of which are excitatory, while the remaining one is an

inhibitor (f5) (Fig. 2.2) (Kennedy & Takeda, 1965b; Winc *et al.*, 1974; Thompson & Page, 1982). The S<sub>1</sub> and S<sub>2</sub> fibre phenotypes of the SF muscle have been classified by their innervation properties (Denhean, 1992). The S<sub>2</sub> fibres in the medial bundle show a characteristic pattern of high post-synaptic activity as a result of synaptic inputs from the majority of the five excitatory axons, which induce relatively large excitatory post-synaptic potentials (EPSPs) (also called excitatory junction potentials, EJPs) that show little facilitation. In contrast, the majority of lateral fibres (of the S<sub>1</sub> type) are activated by the axons f4 and f6, are synaptically 'silent' in response to individual presynaptic spikes, and produce highly facilitating EPSPs in response to spike trains. In the few lateral fibres that are of the S<sub>2</sub> type the pattern of synaptic activity is similar to that normally associated with the medial (S<sub>2</sub>) fibres.

#### 2.1.6 Presynaptic and postsynaptic events in the SF muscle fibres

Experiments investigating presynaptic and postsynaptic events in crab muscle have shown that high levels of facilitation are related to low levels of transmitter being released ('low output synapses'), while low levels of facilitation are associated with higher levels of transmitter release ('high output synapses') (Sherman & Atwood, 1972; Parnas *et al.*, 1982; Rathmayer and Hammelsbeck, 1985). In general, high output synapses are found in muscles which are capable of generating fast 'twitch-like' contractions, while low output synapses are found in muscles which generate slow, sustained contractions (Atwood, 1963; Rathmayer & Ersleben, 1983; Rathmayer & Maier, 1987). However, the differences between the slow fibres in *Nephrops norvegicus* do not follow this trend. The S<sub>1</sub> fibres, which are often synaptically 'silent' on account of their 'low output' synapses and high facilitation properties, contract at a faster rate than the S<sub>2</sub> fibres, which exhibit properties of high output synapses and low facilitation properties, produce large amplitude EPSPs in response to normal levels of activity and facilitate to a small extent (Denhean, 1992).

### 2.1.7 Excitation contraction (EC) coupling in the SF muscle fibres

The clear segregation of abdominal superficial muscles in *Nephrops* into distinct slow fibre types provides the opportunity to study EC coupling in relation to fibre heterogeneity. Despite extensive studies of the SF muscle fibre types, little is known about the steps in EC coupling that give rise to these differences in the kinetics of  $\text{Ca}^{2+}$  activation, and in the  $\text{Ca}^{2+}$  sensitivity of force generation. Using an isolated nerve-muscle preparation of the SF muscle of *Nephrops*, experiments investigating the events both at the fibre surface and within the myoplasm have been conducted in order to establish the relationships between voltage, inward  $\text{Ca}^{2+}$  current, internal free  $\text{Ca}^{2+}$  levels and tension, and to relate these to the structural and functional properties of the different fibre types. These experiments also provide the basic framework upon which later experiments investigating the effects of the heavy metal ion, manganese on the different processes of EC coupling in the SF muscle of *Nephrops* have been based.

## 2.2

## MATERIALS & METHODS

### 2.2.1 The whole SF muscle bundle preparation

#### 2.2.1.1 Dissection of the abdomen

Norway lobsters (*Nephrops norvegicus*, L.) of carapace length 50-90 mm were obtained from the Universities Marine Biology Station, Millport, Isle of Cumbrae, Scotland. Animals were maintained in tanks of aerated circulating sea water at 10-12°C and fed on whitebait. For experiments, animals were anaesthetised by cooling on ice, the brain was destroyed and the abdomen was separated at its junction with the thorax.

The abdominal nerve cord was exposed by removal of the dorsal part of the abdomen and the deep flexor muscles. The first and second roots of all ganglia were cut short, and the superficial third root (Sr3) supplying one of the SF muscles of the first abdominal segment was dissected free. Cuts were made through the ventral membrane and exoskeletal rib in order to isolate the SF muscle without damaging the insertions of its fibres onto the surrounding calcified membrane (Fig. 2.1). In order to make separate

force recordings from the medial and lateral bundles of the SF muscle, an incision was made along the boundary between them, taking care to avoid damage to the nerve supply. The whole preparation (muscle bundles and associated Sr3 nerve) was then lifted free and pinned along its posterior edge, dorsal side up, in a Sylgard-lined perfusion chamber (volume 10 ml).

### **2.2.1.2 Solutions**

The standard *Nephrops norvegicus* saline (Miyau, 1984), had the following composition (mM/l): NaCl, 478; KCl, 12.74; CaCl<sub>2</sub>·2H<sub>2</sub>O, 13.69; MgSO<sub>4</sub>·6H<sub>2</sub>O, 20.47; Na<sub>2</sub>SO<sub>4</sub>, 3.9; HEPES, 5; 1074 mosmol<sup>-1</sup>. Other test solutions were derived from the standard saline. A Ca<sup>2+</sup>-free solution was obtained by substituting the CaCl<sub>2</sub>·2H<sub>2</sub>O with MgSO<sub>4</sub>·6H<sub>2</sub>O; a high concentration K<sup>+</sup> solution was obtained by increasing the KCl content (1-100 mM); the osmolarity was maintained by reducing the NaCl content either in standard saline or Ca<sup>2+</sup>-free saline. Caffeine (0.01-20 mM), 2,3-butanedione monoxime (BDM) (10-20 mM) and tetracaine (31-500 μM) were added at the required concentration to either standard saline or Ca<sup>2+</sup>-free saline. The pH of all the solutions was adjusted to 7.45 using NaOH (1M), or HCL (1M). All the chemicals were obtained from Sigma Ltd. and were stored in the refrigerator (5°C).

### **2.2.1.3 Drug application, cooling and perfusion**

All experiments were performed at 15°C ± 1°C, maintained by means of Peltier heat pump attached to the preparation chamber. The preparations were perfused with standard *Nephrops* saline or with saline containing different pharmacological agents, using a peristaltic pump (Autoclode, Model VL) set to deliver 2 ml per minute.

### **2.2.1.4 Stimulation of the preparation**

Two methods were used to stimulate the preparation: standard nerve stimulation, using a train of DC pulses at 25-30 Hz for 0.25-0.5s at 3V, and electrical field stimulation from

an AC source connected to two platinum electrodes placed alongside the muscle in the perfusion chamber (Fig. 2.3). In experiments using electrical field stimulation the voltage was adjusted to produce a contraction amplitude that matched the maximal contraction evoked by nerve stimulation, in order to produce contractions within the physiological range.

#### **2.2.1.5 Tension measurements and intracellular recording**

The mechanical responses of both the medial and lateral bundles of the SF muscle to nerve or muscle stimulation were recorded by attaching force transducers (Grass FT 03) to the membrane around their anterior insertions. The electrical responses of fibres to nerve stimulation were recorded using intracellular glass microelectrodes filled with 3M KCl (resistance 10-30 M $\Omega$ ). Membrane potential changes were recorded differentially between the microelectrode and bath, grounded through a silver/silver chloride electrode. After amplification, the tension and intracellular recordings were displayed on a digital oscilloscope (Gould 400) and were also fed to an A/D converter (Maclab, AD Instruments) for further analysis (Fig. 2.3).

#### **2.2.1.6 Calibration of the force transducers**

Each force transducer was calibrated by placing it in a horizontal position, and suspending a series of known weights from the point used to attach the muscle bundle. From these data a calibration curve of voltage versus weight in grams (and hence force in Newtons) was constructed, and fitted by regression equations.

#### **2.2.1.7 Data analysis**

The raw data plots of force and EPSPs were recorded by the software program CHART, saved on computer disc and transferred to the drawing package MACDRAW PRO for presentation. The peak force and the height of the first and tenth EPSP and the total depolarisation at the tenth EPSP was measured using the CHART program. The values

were recorded on an internal spreadsheet, recorded on computer disc and transferred to Microsoft EXCEL for further analysis. All results are presented as mean  $\pm$  S.D., the latter being indicated on graphs by vertical error bars. Statistical significance was assessed by the Student t test, with probabilities of less than 5% being considered significant.

## **2.2.2 Single fibre experiments**

### **2.2.2.1 Preparation of membrane-intact single fibres**

Because the medial bundle of the SF muscle contains only  $S_2$  fibres in a single layer whereas the lateral bundle is 3-4 fibres thick and is a mixture of  $S_1$  and  $S_2$  fibre types it is easier to separate medial  $S_2$  fibres intact and to be certain of their identity. For this reason only  $S_2$  fibres were used for membrane-intact single fibre force experiments.

Single fibres were dissected in  $Ca^{2+}$ -free saline to prevent contraction. The dissection was as described for the whole muscle bundle experiments (see Section 2.2.1.1). When the first abdominal segment was cut free from the abdomen, fine forceps were used to tease apart individual  $S_2$  fibres from the medial muscle bundle, being careful to not to damage the insertion points at each end, which were left intact. Single fibres were then cut free using scissors, were pinned in a Sylgard-lined dish containing  $Ca^{2+}$ -free saline and were kept refrigerated (5 °C) until required.

### **2.2.2.2 Experimental set-up**

A purpose-built mechanical apparatus, constructed for detecting signals of force and sarcomere length of single skinned fibres, was adapted to measure force from membrane-intact single fibres (see Fig. 4.1). A cuvette-transporting system enabled rapid solution changes to be made. During this procedure the position of the fibre remained fixed whilst a multiple cuvette holder was lowered, moved horizontally and raised again in a arc. During the transfer the fibre was out of the solution for only 0.2-0.3 seconds. The attachment points for the muscle fibre ends onto the mechanical apparatus were two epoxy carbon needles with tip diameters of 100  $\mu$ m. During the experiments these thin needles were immersed into the bath solutions to a depth of 1 mm. They were attached

by their narrow edges in order to minimise compliance of the needles in the direction of the force (for more detail see Section 4.2).

### **2.2.2.3 Mounting the fibre between the carbon needles**

Immediately before the experiment, fresh fibres were removed from the storage dish and transferred to a coverslip. Using fine forceps, one end of the fibre was attached to the tip of the epoxy carbon needle connected to the force transducer, and the other was attached to the tip of the second needle. Each end of the fibre was secured with a small drop of adhesive (Histacryl Blue Vetseal, Braun, Melsungen, Germany) applied by means of a micro pipette, which rapidly polymerised on immersion in the standard saline. Following this procedure the attached fibre was transferred rapidly into the next cuvette containing fresh standard saline.

Before all experiments the fibre was slackened to record the control zero point, and then adjusted until the fibre length was set to the point where force was just recorded (i.e. adjusted exactly to the slack position). Whilst in standard saline the sarcomere length of the fibre was measured using laser diffractometry, using a He-Ne laser (see Section 4.2). The sarcomere length of each fibre was determined before and after experiments. Fibre length and diameter were measured using an eyepiece micrometer attached to the microscope. All experiments were carried out between 16-18 °C. Temperature was maintained by an external cooling unit (Churchill thermocirculator) which circulated cooled water around the preparation holding block of the mechanical apparatus.

### **2.2.2.4 Activation of the muscle fibre**

All the solutions were as described for the whole muscle bundle experiments (see Section 2.2.1.2) except that in the  $\text{Ca}^{2+}$ -free solution 5 mM ethyleneglycol bis ( $\beta$ -aminoethyl ether) -N-N'-tetraacetic acid (EGTA) was substituted for NaCl. From the cuvette containing standard *Nephrops* saline the fibre was transferred to a cuvette containing the test solution. The fibre produced force under isometric conditions. At the end of each experiment the fibre was transferred to a cuvette containing standard saline.

### 2.2.2.5 Recording system

The fine end of a glass micropipette was bent at right angles by heating and was attached to a micromanipulator. Using the calibrated wheel on the micromanipulator to measure movement, the glass pipette was gradually moved forward against a fine balance, and for a given distance moved the resulting weight on the balance was recorded. This procedure was then repeated with the glass micropipette clamped against the carbon needle attached to the force transducer. Using the micromanipulator attached to the epoxy carbon needle and the force transducer to measure distance, the needle was moved forward against the glass pipette. The force transducer was then calibrated by converting the distance moved by the glass pipette, which corresponded to a known weight, to mV, which could then be converted to force (mN).

Force was recorded by a transducer connected to an A/D converter (Mac Lab, AD Instruments). The forces were measured using automated macros in the software program (CHART), were recorded on an internal spreadsheet (Datapad), recorded on computer disc and transferred to Microsoft EXCEL for further analysis.

## 2.2.3 Two electrode voltage clamp technique

### 2.2.3.1 Preparation of single fibres for voltage clamp

Norway lobsters (*Nephrops norvegicus*, L.) of carapace length 40-50 mm were used for these experiments. All dissections were carried out under  $\text{Ca}^{2+}$ -free saline. The dissection of the SF muscle bundle was as described for the whole muscle bundle experiments (see Section 2.2.1.1). After the SF muscle was lifted free from the abdomen, the Sr3 nerve was removed and the medial and lateral muscle bundles were separated. For some experiments the muscle bundles were cut into smaller groups of fibres and for others the bundles were left intact. The muscle bundles were pinned in a Sylgard-lined dish containing standard saline.

### 2.2.3.2 Voltage clamp solutions

Tetraethylammonium chloride (TEA) blocks the fast outward  $K^+$  currents in crustacean muscle fibres (Mounier & Vassort, 1975). For this reason, and to prolong the inward  $Ca^{2+}$  current ( $I_{Ca}$ ), TEA (100 mM) was added to all solutions, apart from those used to investigate the outward potassium currents. TEA solutions were obtained by substituting NaCl for TEA to maintain the osmolarity. TEA is agrosopic, and was stored as a 1 M stock solution in distilled water. Other test solutions were derived from the standard voltage clamp saline (see Section 2.2.1.2); 5 mM EGTA was substituted for NaCl in the  $Ca^{2+}$ -free solutions. The pH of all the solutions was adjusted to 7.45 using NaOH (1M) or HCL (1M). All the chemicals were obtained from Sigma Ltd. and were stored in the refrigerator (5°C). For Barium ( $Ba^{2+}$ ) solutions, to prevent the formation of a white precipitate only chloride salts were used. Standard  $Ba^{2+}$  saline had the following composition (mM): NaCl, 462.0; KCl, 16.0;  $BaCl_2 \cdot 2H_2O$ , 26.0;  $MgCl_2 \cdot 6H_2O$ , 8.0; HEPES, 5.0; glucose: 11.0. 1036 mosmol<sup>-1</sup>. Other test solutions were derived from the standard saline (see Section 2.2.1.2).

### 2.2.3.3 Electrodes and voltage recording

The muscle fibre segments were pinned in a Sylgard-lined bathing chamber. Solutions were applied to the preparation by tubes connected to a peristaltic pump which allowed the solutions to be changed rapidly. Measurements were not made while the solution was flowing. The muscle fibre was penetrated by two microelectrodes, one to record voltage and the other to pass current. A preamplifier recorded the membrane potential, and the clamping amplifier passed current to control this potential (Geneclamp 500, Axon Instruments). Thin-walled glass microelectrodes (Clarke Electromedical) were filled with 3 mM KCl for both voltage measurement and current injection and had resistances of 5-10 M $\Omega$ . These electrodes were of low resistance and small tip size and allowed large amounts of current to be passed to successfully clamp large fibres. The current electrode and the voltage electrode and head stages were shielded by an aluminium sheet to prevent capacity coupling between the two electrodes. For voltage clamping the current electrode was inserted at the middle of a muscle fibre and a voltage electrode was inserted at a distance of 30-50  $\mu$ m from the current electrode. The membrane potential of the fibre

was clamped to a constant value (-60 mV) by means of a voltage clamp circuit. The clamp potential was changed by a command voltage controlled by the computer software package (Whole Cell Program (WCP), developed by Dr. John Dempster, University of Strathclyde, Glasgow) and was triggered by an external trigger (Digitimer, Neurolog). The effects of electrode/ground capacity were compensated.

The signals from the voltage electrode and current electrode were passed to an A/D converter (CED 1401) and displayed on an oscilloscope (Gould 1400) and a computer monitor. A standard voltage pulse step protocol (a series of six 10 mV depolarising steps, from a holding potential of -60 mV, with four 2.5 mV hyperpolarising steps applied each depolarising step, for leak subtraction) was applied to single muscle fibres, and the results were recorded, leak-subtracted and analysed by the WCP software package.

The traces which are shown in this chapter and Chapter 3 represent preliminary experiments.

## 2.3

## RESULTS

### 2.3.1 Voltage and frequency of neuronal stimulation

The Sr3 nerve which innervates the SF muscle of *Nephrops norvegicus* comprises 6 axons, 5 of which are excitatory and one of which is inhibitory (see Section 2.1.5). To ensure that all these axons were being recruited during neuronal stimulation, a series of experiments was conducted which measured the effects of voltage (0-2.0 V) and frequency (10-100 Hz) on the neuronally-evoked force of the medial and lateral muscle bundles. Figure 2.4 shows the results from a single experiment for the SF medial muscle bundle. Below 0.5 V no force was evoked, at 0.6 V small forces were recorded in both the lateral and medial muscle bundles and at 1.0 V the maximal force was reached. Higher voltages of stimulation produced no further increase in force. This pattern of activation was observed at frequencies of 10 Hz and above (Figs. 2.4, 2.5 & 2.6). These results show that the voltage activation threshold for all 6 axons is between 0.6 and 1.0 V for both muscle bundles.

The level of force evoked also correlated with the frequency of stimulation. Supramaximal stimulation of the preparation (i.e. above 1.0 V) induced very low forces at frequencies up to 10 Hz. An example of the original data is shown in Figure 2.6. Higher frequencies induced higher forces in both muscle bundles (Fig. 2.5). At all frequencies the larger lateral bundle produced greater force than the smaller medial muscle bundle (Figs. 2.5 & 2.6). The level of force produced by individual SF muscle preparations also differed and for this reason in subsequent figures the force results are expressed as a percentage of the maximally-activated control force for each muscle bundle. Data from different experimental series expressed in this way confirm that above the threshold voltage muscle force is dependent on the frequency of stimulation (Fig. 2.7) Below 10 Hz no force or very low levels of force was recorded, and at frequencies above 10 Hz force increased with frequency. A similar relationship was observed for both muscle bundles (Fig. 2.7).

### 2.3.2 Membrane potential

The electrical properties of the  $S_1$  fibres, which comprise the majority of the SF lateral muscle bundle, and the  $S_2$  fibres, which comprise the medial muscle bundle were measured using two microelectrodes inserted into individual fibres of each type. Previous studies of the SF muscle have shown that resting potential of both muscle fibre types is typically around -60 mV (Denhehen, 1992), and this has also been shown in the slow muscle fibres of other crustaceans (Gainer, 1968). For this reason, muscle fibres were only accepted for further electrical measurements if they showed a resting potential between -45 and -70 mV. Measurements of membrane potential from a selection of fibres in a typical preparation are shown in Table 2.1.

### 2.3.3 Excitatory post-synaptic potentials

Excitatory post-synaptic potentials (EPSPs) were measured in the  $S_1$  and  $S_2$  fibre types of the SF muscle. EPSPs from the  $S_2$  fibre type were larger at all frequencies of stimulation, when compared to the  $S_1$  fibre type (Table 2.2). The observed differences were consistent between preparations and usually became apparent when the stimulus frequency was

increased above 10 Hz (Fig. 2.8). In agreement with previous findings (Fowler & Neil, 1992; Denheer, 1992), muscle fibres of the S<sub>1</sub> and S<sub>2</sub> fibre types were found to exhibit different facilitation and summation properties in response to supramaximal stimulation (i.e. recruitment of all 6 SF muscle axons) (Fig. 2.8). The S<sub>1</sub> EPSPs consistently showed strong facilitation with very little summation, whereas the S<sub>2</sub> EPSPs showed a strong summation but very little facilitation. This was demonstrated by comparing the ratio between the first (non facilitated) and 10th (facilitated) EPSP for the two fibre types (Table 2.3; Fig. 2.9). The S<sub>1</sub> fibre type always showed a greater facilitation ratio than the S<sub>2</sub> fibre type and this effect became more pronounced as the frequency of stimulation was increased. Thus at 50 Hz stimulation frequency the S<sub>1</sub> fibre type has a ratio of 3.19:1 while the S<sub>2</sub> fibre type has a ratio of only 1.45:1. The clear differences in the shape and size of the facilitated EPSPs of the S<sub>1</sub> and S<sub>2</sub> fibre types provides a simple and quick method to identify individual muscle fibres for electrical experimentation.

It should also be noted that small differences in facilitation and summation were observed between individual fibres of the same phenotypes, but due to the clear differences in total depolarisation between the EPSPs from the two fibre types this did not affect fibre type identification. This size difference is seen in both the non-facilitated EPSPs and facilitated ones (Fig. 2.9).

From the results of these preliminary experiments a standard protocol for neuronal stimulation was established - a train of pulses at frequencies between 25-30 Hz for 0.25-0.75s at 3V. This protocol meets the following criteria:

1. a voltage above 1V to ensure the recruitment of all 6 axons of the Sr3 nerve.
2. a frequency of stimulation of at least 10 Hz to ensure sufficient summation and facilitation, and thus generate measurable force.
3. a frequency of stimulation that never exceeds 50 Hz, so that the contraction of the muscle fibre does not dislodge the microelectrodes, or distort the EPSP recordings (as seen in Figure 2.8, middle panel).

### 2.3.4 $\text{Ca}^{2+}$

The requirement for  $\text{Ca}^{2+}$  in the activation of SF muscle fibres was examined by recording the neuronally-evoked force produced by the lateral and medial muscle bundles in the presence of saline containing different concentrations of  $\text{Ca}^{2+}$  ions (Fig. 2.10). Increasing the  $\text{Ca}^{2+}$  concentration from 13.7 mM to 20.0 mM (1.5 x  $\text{Ca}^{2+}$  concentration of standard saline) caused an increase in the size of the force responses (Fig. 2.10B), whereas removing  $\text{Ca}^{2+}$  from the saline abolished force production altogether (Fig. 2.10A). Neuronally-induced muscle force was inhibited within 20 minutes under  $\text{Ca}^{2+}$ -free saline (Figs. 2.10A & 2.11B). When this experiment was repeated using  $\text{Ca}^{2+}$ -free saline containing the high affinity  $\text{Ca}^{2+}$  buffer ethyleneglycol bis ( $\beta$ -aminoethyl ether) - N-N'-tetra-acetic acid (EGTA) similar results were obtained (data not shown). Neuronally-evoked force was not observed in saline containing 3.4 mM  $\text{Ca}^{2+}$  or below, and at concentrations above 3.4 mM force increased in a dose-dependent manner (Fig. 2.11A). A similar effect can be seen when the decrease in force is plotted against time during a  $\text{Ca}^{2+}$ -free saline exposure (Fig. 2.11B). The  $\text{Ca}^{2+}$  concentration decreases in the bathing chamber as the  $\text{Ca}^{2+}$  free saline perfuses in, which is reflected in the gradual inhibition of force.

### 2.3.5 Electrical field stimulation

Electrical field stimulation of the SF muscle enables the muscle bundles to be directly stimulated, since it by-passes the synaptic activation steps involved in neuronally-induced contractions. However, it cannot be excluded that field stimulation also activates the motor nerves directly. In experiments in which  $\text{Ca}^{2+}$  ions were removed from the external bathing solution, force responses to both forms of stimulation were inhibited before the response to field stimulation (Fig. 2.12). This suggests that under these specific pharmacological conditions field stimulation can be used to investigate the effects of chemical agents on post-synaptic processes.

The dependence of synaptic transmission at the neuromuscular junctions of SF motor axons on the presence  $\text{Ca}^{2+}$  ions was examined by recording EPSPs intracellularly in response to neuronal stimulation in the presence and absence of  $\text{Ca}^{2+}$  (Fig. 2.13). Under

$\text{Ca}^{2+}$ -free saline the EPSPs were abolished. Significantly, simultaneous recordings of both the EPSPs and the forces produced by the muscle bundles under these conditions demonstrated that the forces disappeared before the EPSPs (Figs. 2.13 & 2.14). This provides further evidence that  $\text{Ca}^{2+}$  is acting at more than one step in the activation sequence, and also suggests that one or more of the postsynaptic processes is more sensitive to a lowering the  $\text{Ca}^{2+}$  concentration than is the presynaptic step leading to transmitter release.

### 2.3.6 $\text{K}^+$ contractures

The role of  $\text{Ca}^{2+}$  in carrying the inward current across the sarcolemma was further defined by using high concentrations of  $\text{K}^+$  in the standard saline to depolarise the muscle fibres, and thus produce contraction (Fig. 2.15). In most experiments 15 mM  $\text{K}^+$  saline was used because higher  $\text{K}^+$  concentrations (30-100 mM) damaged the muscle preparation. Removal of  $\text{Ca}^{2+}$  from the saline abolished both the membrane depolarisation and the contracture induced by high external  $\text{K}^+$ . Significant differences in force were found between the lateral ( $n = 5$ ) and medial ( $n = 6$ ) muscle bundles when contraction was induced by 15 mM  $\text{K}^+$  ( $p = 0.17$ ,  $T = -1.54$ ) (Fig. 2.16).

### 2.3.7 Voltage Clamping muscle fibres

A number of preliminary voltage clamp experiments were performed in order to determine whether differences exist in the sarcolemmal channels of the different SF fibre types.

Under standard *Nephrops* saline containing TEA (to prolong the inward current by inhibiting the fast outward  $\text{K}^+$  currents), an inward  $\text{Ca}^{2+}$  current ( $I_{\text{Ca}}$ ) peak was observed across the membrane of an  $\text{S}_1$  fibre type in response to a series of 10 mV depolarising steps from a holding potential of -60 mV, at approximately 25 ms (Fig. 2.17). When  $\text{Ca}^{2+}$  ions were removed from the external bathing saline, and in the presence of EGTA, the  $I_{\text{Ca}}$  was completely abolished. This confirms that  $\text{Ca}^{2+}$  ions are required to carry the inward current in the  $\text{S}_1$  muscle fibres.  $\text{S}_2$  fibres were more difficult to voltage clamp, but

from the few experiments that were conducted the  $I_{Ca}$  current appeared to be much smaller (data not shown).

One main problem with the voltage clamp technique is that depolarisation of the muscle fibre induces small contractures localised around the insertion points of the current and voltage microelectrodes. These contractures often pulled the electrode out, and damaged the muscle fibre. Localised contractures were never observed under  $Ca^{2+}$ -free saline, and for this reason experiments were conducted using the divalent cation barium ( $Ba^{2+}$ ). It is known that this ion can pass through  $Ca^{2+}$  channels and carry the inward current across cell membranes (Suarez-Kurtz & Sorenson, 1979) but that it does not initiate muscle contraction. Voltage clamp experiments on SF  $S_1$  fibres in the presence of  $Ba^{2+}$  ions confirmed that they were able to carry the inward current without producing contractures (data not shown). The potential therefore exists to apply this procedure in a more extensive series of experiments.

Evidence was also obtained from voltage clamp experiments performed in the absence of TEA that the  $S_1$  and  $S_2$  fibres display different outward  $K^+$  currents (Fig. 2.18). The  $S_2$  fibres showed a much slower and smaller outward  $K^+$  current than the  $S_1$  fibre type

### 2.3.8 Pharmacological agents

These experiments alone do not discriminate between an effect of  $Ca^{2+}$  ions primarily on the membrane depolarisation (which would have consequent effects on later steps) and simultaneous effects on a number of later steps in EC coupling. In order to determine this in more detail, a number of pharmacological agents were employed which are known to act at particular points in the EC coupling pathway.

#### 2.3.8.1 Caffeine

Caffeine induces muscle contraction by triggering release of  $Ca^{2+}$  from sarcoplasmic reticulum (SR) stores (Sandow, 1965; Endo *et al.*, 1970). It may be expected, therefore, that its action will persist even in the absence of extracellular  $Ca^{2+}$ , and that it will

produce its effect without affecting the membrane potential. In the presence of caffeine there was a dose-dependent increase in neuronally-evoked contractions under normal saline, and at higher concentrations (3 mM and above) also an increase in resting or tonic muscle tension, which can be seen as a baseline shift (Fig. 2.19). Distinct differences were observed in the temporal patterns of responses between the lateral and medial muscle bundles. The medial bundle showed a large increase in the size of the neuronally-evoked contractions (up to 6 times the control level) which subsequently decreased again to some extent, with also a decrease in the underlying contracture. The lateral bundle showed a waxing and waning pattern of evoked contractions which were approximately 3 times larger than in standard saline, and a progressively increasing tonic contracture.

The effect of different concentrations of caffeine on the neuronally-evoked forces can be seen more clearly in Figure 2.20, which shows force measurements at 5 minute intervals throughout a series of caffeine experiments. At 5 minutes, low concentrations of caffeine (0.01-0.1 mM) had little effect, but higher concentrations (1.0-3.0 mM) produced a dose-dependent force increase. After 15 minutes of caffeine, lower caffeine concentrations showed a greater effect which was also dose-dependent. This shows that the effects of caffeine are time-dependent, and which can be interpreted as due to a diffusion delay. These results are consistent with an intracellular site of action for caffeine.

The maximal neuronally-evoked force for each caffeine treatment is shown in Figure 2.21. Similar results were obtained when the muscle preparation was stimulated by direct field stimulation under various caffeine concentrations (Fig. 2.22). In Figures 2.21 and 2.22 the maximal forces of both muscle bundles are normalised to control values. In general the maximal neuronally-induced percentage force increase was greater in the medial muscle bundle. Figure 2.21B shows the caffeine-induced force in  $\text{Ca}^{2+}$ -free saline at different caffeine concentrations. Low caffeine concentrations (1-3 mM) induced only a small force response while higher concentrations (20 mM) produced much larger forces. Caffeine (1-3 mM) induced a greater absolute force increase in the lateral muscle bundle (Fig. 2.21B).

In whole muscle bundles exposed to  $\text{Ca}^{2+}$ -free saline, after the evoked contractions became inhibited an application of caffeine nevertheless produced large contraction forces (Fig. 2.23).

Experiments on single membrane-intact fibres define the role of the intracellular SR  $\text{Ca}^{2+}$  stores more clearly. In the presence of external  $\text{Ca}^{2+}$  ions, a first application of 3 mM caffeine induced a force of approximately 530  $\mu\text{N}$  from the  $\text{S}_2$  fibre type, and after a 2 minute wash in standard saline (to reload the SR) a second application of 3 mM caffeine induced a much smaller force. If the preparation was left for a longer time (15 minutes) in standard saline between caffeine applications the force still did not increase to the level induced by the first caffeine application (Fig. 2.24A). These results indicate that the SR is being depleted of  $\text{Ca}^{2+}$  ions by the caffeine. When this experiment was repeated under  $\text{Ca}^{2+}$ -free saline, an application of 3 mM caffeine in the absence of external  $\text{Ca}^{2+}$  ions (2.24B) induced a force similar to that produced by the first caffeine application in the presence of  $\text{Ca}^{2+}$  (2.24A). The preparation was reloaded with  $\text{Ca}^{2+}$  in standard saline for 10 minutes and then immersed in  $\text{Ca}^{2+}$ -solution containing EGTA to absorb the free  $\text{Ca}^{2+}$  ions. A second caffeine application in  $\text{Ca}^{2+}$ -free saline induced a very small force. These results indicate that both external and internal  $\text{Ca}^{2+}$  are important for muscle contraction and that even when external  $\text{Ca}^{2+}$  is present, the force is inhibited if the internal  $\text{Ca}^{2+}$  SR stores are depleted. These results also indicate that during physiological contraction only a small percentage of the  $\text{Ca}^{2+}$  ions in the SR store are used because when caffeine is applied to release the SR stores, the fibre does not appear to be able to reload the SR stores during the time course of the experiment. This effect is exaggerated when  $\text{Ca}^{2+}$  ions are removed from the bathing saline.

### 2.3.8.2 Tetracaine

Tetracaine inhibits SR  $\text{Ca}^{2+}$  release in a number of different muscles (Csernoch *et al.*, 1988; Almers & Best, 1976). When applied to the SF muscle preparation at 62  $\mu\text{M}$  it abolished neurally-evoked force, but had little or no effect on either the membrane potential or EPSP size (Fig. 2.25). At higher concentrations of tetracaine (500  $\mu\text{M}$ ) both the forces and the EPSPs were inhibited (Figs. 2.25 & 2.26). These results are therefore in accordance with its expected effect on SR  $\text{Ca}^{2+}$  release, as was the finding that tetracaine could reverse a caffeine-induced enhancement of neurally-evoked contractions, again without the EPSP being affected (Fig. 2.27). However, the fact that higher concentrations of tetracaine (500  $\mu\text{M}$ ) abolished the EPSPs as well as the force suggests that its actions can be complex.

### 2.3.8.3 Butanedione monoxime (BDM)

BDM is thought to act in a similar way to caffeine by opening  $\text{Ca}^{2+}$  channels in the SR membrane (Györke *et al.*, 1993). It was possible to demonstrate this for the SF muscle fibre bundles by sequential application of the two drugs (Fig. 2.28). When BDM was applied at concentrations between 5 mM and 20 mM to the SF preparation under  $\text{Ca}^{2+}$ -free saline, a large increase in resting force was produced (Fig. 2.29) and when it was applied under normal saline, it induced oscillations in the resting muscle force of both SF muscle bundles (Fig. 2.30). Furthermore, in the  $S_2$  fibres of the medial bundle, but not in the  $S_1$  fibres of the lateral bundle, there was an accompanying, but independent oscillation in the recorded membrane potential (Fig. 2.30).

## 2.4

## DISCUSSION

The results presented in this chapter indicate that, like other decapod crustaceans, the EC coupling mechanism of the SF muscle in *Nephrops norvegicus* involves  $\text{Ca}^{2+}$ -induced- $\text{Ca}^{2+}$ -release (CICR). Furthermore, differences have been demonstrated between the  $S_1$  and the  $S_2$  fibre types.

### 2.4.1 Activation thresholds

In the first experiments, the effects of stimulus voltage and frequency on the force produced by the medial and lateral muscle bundles was investigated. The results provide essential information about the activation thresholds, and allowed a standard neuronal stimulation protocol to be defined. The results show that the voltage thresholds for force generation in the medial and lateral muscle bundles are similar (between 0.6 and 1.0 V when stimulated above a frequency of 10 Hz) (Figs 2.4, 2.5 & 2.6).

### 2.4.2 Excitation contraction coupling in the SF muscle of *Nephrops*

It is known that  $\text{Ca}^{2+}$  ions are involved at least 4 different steps in the neuromuscular pathway that leads ultimately to muscle contraction. The steps of EC coupling have been discussed in detail in Chapter 1 and are summarised below. Step 4 will be addressed in Chapter 4.

1.  $\text{Ca}^{2+}$  influx at the presynaptic terminal follows arrival of the action potential and leads to the discharge of synaptic vesicles containing the excitatory transmitter (which in crustaceans is glutamate), and in turn produces an excitatory postsynaptic potential (EPSP).
2.  $\text{Ca}^{2+}$  ions carry the inward current across the sarcolemma and the T-tubules, leading to the spread of depolarisation.
3. Inward flow of  $\text{Ca}^{2+}$  ions across the base of the T-tubule leads to release of further  $\text{Ca}^{2+}$  from intracellular stores, notably the sarcoplasmic reticulum (SR) - a process known as calcium-induced calcium release (CICR).
4.  $\text{Ca}^{2+}$  released from the SR binds to regulatory proteins, the troponins, along the myofilaments, leading to exposure of sites on actin for myosin cross-bridge interaction.

### 2.4.3 The involvement of $\text{Ca}^{2+}$ in EC coupling

The requirement for  $\text{Ca}^{2+}$  is typical of invertebrate muscle (Zacharova & Zachar, 1967; Reuben *et al.*, 1967; Edwards & Lorkovic, 1967). For example in crayfish fibres it has been shown that myoplasmic  $\text{Ca}^{2+}$  transients which activate the myofibrils are completely dependent on the presence of extracellular  $\text{Ca}^{2+}$  in the bathing saline (Györke & Palade, 1992) and that contraction is only observed in the presence of  $\text{Ca}^{2+}$  (Zacharova & Zachar, 1967). Extracellular  $\text{Ca}^{2+}$  is essential for muscle contraction in the SF muscle bundles of *Nephrops norvegicus* evoked both by neuronal stimulation and by electrical field stimulation which by-passes the synaptic steps, suggesting that postsynaptic  $\text{Ca}^{2+}$ -dependent processes are being affected.

The effects of changes in external  $\text{Ca}^{2+}$  concentration on the mechanical and electrical responses of crustacean muscle of the crayfish *Procambarus clarkii* was investigated by Matsumara (1978). In crayfish, tension was not detected at  $\text{Ca}^{2+}$  ion concentrations below 3.5 mM and tension increased between 7 and 56 mM  $\text{Ca}^{2+}$ . This was also seen in the SF muscle: below 3.42 mM no force was recorded, and above this concentration force increased in a dose-dependent manner (Figs 2.11A) (standard saline: 13.69 mM  $\text{CaCl}_2$ ; 150%  $\text{Ca}^{2+}$  saline: 20.548 mM; 75 %  $\text{Ca}^{2+}$  saline: 10.27 mM; 50 %  $\text{Ca}^{2+}$  saline: 6.84 mM; 25 %  $\text{Ca}^{2+}$  saline: 3.42 mM).

The voltage clamp studies show that in the absence of  $\text{Ca}^{2+}$  ions no inward current or localised contracture is observed, which strongly suggests that  $\text{Ca}^{2+}$  ions are required to carry the inward current across the sarcolemma; the lack of contracture indicates that the CICR mechanism is disrupted. In addition to this, studies using the divalent cation  $\text{Ba}^{2+}$  indicate that the EC coupling in SF muscle appears to be highly selective for  $\text{Ca}^{2+}$  ions: when  $\text{Ca}^{2+}$  was replaced with the divalent cation  $\text{Ba}^{2+}$  no contractions were induced. Preliminary studies using the two electrode voltage clamp technique have shown that  $\text{Ba}^{2+}$  ions can carry the inward current across the muscle membrane but cannot initiate muscle contraction. Gainer (1968) showed the same to be also true for  $\text{Mg}^{2+}$ ,  $\text{Co}^{2+}$ ,  $\text{Sr}^{2+}$ ,  $\text{Ba}^{2+}$  and  $\text{Cd}^{2+}$  which were all capable of depolarising the muscle membrane in the presence of high  $\text{K}^+$  (100 mM) saline, but did not initiate contraction, although  $\text{Cd}^{2+}$  induced slight force.

The necessity for  $\text{Ca}^{2+}$  for synaptic transmission between axons in the Sr3 nerve and the SF muscle fibres was examined by simultaneous recordings of the EPSPs and the force under  $\text{Ca}^{2+}$ -free saline, which demonstrated that the force disappeared before the EPSPs (Figs. 2.13 & 2.14). This is further evidence that  $\text{Ca}^{2+}$  is acting at more than one step in the activation sequence, and also suggests that one or more of the postsynaptic processes is more sensitive to a lowering the  $\text{Ca}^{2+}$  concentration than is the presynaptic step leading to transmitter release. Matsumara (1978) found similar results in crayfish by lowering the  $\text{Ca}^{2+}$  concentration from 14 mM to 0; tension was immediately reduced while the action potential (AP) remained present, although it eventually also disappeared.

#### 2.4.4 Depolarisation using high concentration potassium saline

The activation mechanism of crustacean muscle is coupled to absolute membrane potential (Hodgkin & Horowicz, 1960; Orkand, 1962; Zachar & Zacharova, 1966) and to membrane current (Reuben *et al.*, 1967). The use of a high concentration  $K^+$  saline to depolarise the muscle membrane stimulating muscle contraction is a well-established method of activation (Orkand, 1962; Gainer, 1968). The role of  $Ca^{2+}$  in carrying the inward current across the sarcolemma was further clarified by using high concentrations of  $K^+$  ions in the external medium to depolarise the muscle fibres, and thus produce contraction (Fig. 2.15).

In many studies (e.g. Chiarandini *et al.*, 1970a) high concentrations of  $K^+$  (60-100 mM and above) have been used, but when similar  $K^+$  salines were applied to the SF muscle preparation the force generated was so large that it damaged the muscle preparation. It was impossible to induce a constant force level at  $K^+$  concentrations above 25 mM. Only a small increase in  $K^+$  ions was required to induce a very large contraction. The  $K^+$  concentration of standard *Nephrops* saline is 13.7 mM, and in all experiments raising the  $K^+$  concentration by only a few millimoles induced a large contraction, which was approximately 2-3 times the level of supramaximal neuronally-evoked contractures. At 15 mM  $K^+$  a plateau force was generated (Fig. 2.15), while concentrations below 15 mM produced smaller muscle forces. In contrast to this result, in experiments on single, membrane-intact fibres it was possible to use higher concentrations of  $K^+$  in the saline. Repeated contracture could be induced at 30 mM  $K^+$  saline, although at 60 mM  $K^+$  saline the force peaked rapidly before dropping to a much lower level. For this reason 15 mM  $K^+$  saline was used as standard to depolarise the SF muscle during experiments. Similar  $K^+$  concentrations were used by Orkand (1962) to depolarise crayfish fibres.

This finding may relate to the findings of Galler and Neil (1994) on skinned  $S_1$  and  $S_2$  fibres. They suggested that the fibres of the SF muscle generate force whilst "at rest", due to the presence of low levels of  $Ca^{2+}$  ions. This would also provide one explanation as to why the fibres of the SF muscle contract extensively when cut whilst being bathed in standard *Nephrops* saline, despite the fact that it contains a  $Ca^{2+}$  concentration below that required for activation. Only when the fibres are bathed in  $Ca^{2+}$ -free saline can this

shortening of cut fibres be prevented. Fast muscles do not show this behaviour when cut under the same conditions.

A consistent finding was that depolarisation by 15 mM  $K^+$  induced a significantly larger contraction in the  $S_2$  fibre phenotype when compared to the force generated in the  $S_1$  fibre phenotype, even though the lateral muscle bundle is more than twice the size of the medial one (Fig. 2.16). This difference may reflect differences in the populations of outward  $K^+$  channels in these fibres, a possibility also indicated by preliminary studies using the two electrode voltage clamp technique (Fig. 2.18). Further study of these would prove instructive.

High  $K^+$  solutions do not induce contraction in  $Ca^{2+}$ -free saline, which suggests that movement of  $Ca^{2+}$  ions across the muscle membrane is essential for initiating muscle contraction in the SF muscle, and also shows that  $Ca^{2+}$  ions are important for post-synaptic processes. This is consistent with the voltage clamp studies showing the disappearance of an inward current in the absence of external  $Ca^{2+}$  ions, and is also consistent with mechanism of EC coupling found in other crustacean muscle (Gainer, 1968). In addition to this Gainer (1968) showed that the substitution of other divalent ions for  $Ca^{2+}$  had no effect on  $K^+$ -induced tension.

#### 2.4.5 Caffeine

Caffeine was used to investigate the processes of EC coupling, as it is known to act at a particular point in the activation pathway. Caffeine rapidly penetrates the cell membranes of intact muscle fibres, and produces the  $Ca^{2+}$  fluxes within cells (Bianchi, 1961) which trigger contractile activity in invertebrate (Chiriandini *et al.*, 1970a) and vertebrate (Sandow, 1952, 1965; Endo *et al.*, 1970) skeletal muscle fibres. Caffeine acts by triggering the release of large quantities of  $Ca^{2+}$  from sarcoplasmic reticulum (SR) stores (Sandow, 1965; Endo *et al.*, 1970), as well as reducing or blocking the sequestration of  $Ca^{2+}$  by the SR membranes which leads to a rise in myoplasmic  $Ca^{2+}$  concentration (Weber, 1968; Weber & Herz, 1968). Frog skeletal muscle is very sensitive to caffeine, sustained contractions at maximal tension being induced at 5-10 mM (Lüttgau & Oetliker, 1968). However a concentration 10 mM caffeine induces only 85 % of the

maximal contraction in crayfish muscle fibres, and caffeine contractures are always transient (Chiarandini *et al.*, 1970a). This suggests that the action of caffeine on frog muscle is in some way different from its effect on crustacean muscle.

In crustacean muscle, caffeine is effective even in the absence of extracellular  $\text{Ca}^{2+}$ , and produces no effect on membrane potential. This was demonstrated by Chiarandini *et al.* (1970a) for crayfish muscle fibres: during caffeine-induced contractures the membrane conductance increased, but no membrane depolarisation occurred, even in the presence of high caffeine concentrations (40 mM). The results obtained here for *Nephrops* SF fibres were essentially similar. Under normal saline caffeine increased the force produced by the SF muscle in a dose-dependent manner, and at higher concentrations (3 mM and above) also increased the level of resting tension (Figs. 2.24A & 2.19). Repeated application of high concentrations of caffeine produced tonic contractures which decreased in size. A recovery period was required between each caffeine application in order to allow extracellular  $\text{Ca}^{2+}$  ions to diffuse into the interior of the muscle fibres and replenish the SR. However, even after a long recovery period the initial caffeine-induced force level was not achieved again. Force produced by lower concentrations of caffeine did not require a recovery period.

Higher concentrations of caffeine also induced a tonic contraction in  $\text{Ca}^{2+}$ -free saline with similar levels of force induced. These contractions however, were more transient and often decreased before the preparation was washed in standard saline (Fig. 2.24B). This must reflect the release of  $\text{Ca}^{2+}$  from intracellular SR stores, and subsequent binding to regulatory proteins. It may therefore be concluded that these later processes of CICR are indeed not affected in the SF muscle by the removal of external  $\text{Ca}^{2+}$ , and that the inhibitory action of  $\text{Ca}^{2+}$  removal thus occurs at an earlier step, most probably membrane depolarisation. This was also indicated by the voltage clamp experiments, which showed the disappearance of an inward current in the absence of  $\text{Ca}^{2+}$  ions. When caffeine was repeatedly applied to a preparation in the absence of  $\text{Ca}^{2+}$ , the force induced was not repeatable even when the preparation was allowed a recovery period before the next caffeine application (Fig. 2.24B). This shows that external  $\text{Ca}^{2+}$  influx is essential for replenishing the intracellular  $\text{Ca}^{2+}$  stores of the SR. Therefore both extracellular and intracellular  $\text{Ca}^{2+}$  are required for activation. Similar findings have been made in other crustacean muscle preparations. For example in single crayfish fibres, repeated

application of caffeine produces reproducible responses which are transient and independent of concentration. However, after higher concentrations the fibres require a recovery period (minimum time of 15-20 minutes) to enable the SR to reload its  $\text{Ca}^{2+}$  stores (Chiarandini *et al.*, 1970).

Single fibre experiments are required to obtain more detailed information about the  $\text{Ca}^{2+}$  stores of the SR of the two SF muscle phenotypes. Experiments conducted on mechanically skinned fibres with intact SR would provide one method to investigate this property further. The amount of  $\text{Ca}^{2+}$  released in response to caffeine can then be estimated for each fibre type from the force-time integral (Endo, 1977; Lea, 1996).

#### 2.4.6 Tetracaine

The local anaesthetics tetracaine and procaine have been used to inhibit SR  $\text{Ca}^{2+}$  release in various skeletal muscle preparations (Suarez-Kurtz, 1976; Almers & Best, 1976; Csernoch *et al.*, 1988). In crayfish fibres 300  $\mu\text{M}$  tetracaine completely blocks the SR  $\text{Ca}^{2+}$  transients without affecting the  $I_{\text{Ca}}$  (Györke & Palade, 1992). This enabled the contributions of the SR  $\text{Ca}^{2+}$ -release and of  $I_{\text{Ca}}$  to the  $\text{Ca}^{2+}$  transients to be separated and enabled the steps of CICR to be effectively uncoupled. Only at millimolar concentrations did tetracaine start to inhibit the  $I_{\text{Ca}}$  (Györke & Palade, 1992). Tetracaine also inhibits  $\text{Ca}^{2+}$ -release induced by applying caffeine (Almers & Best, 1976; Weber & Hertz, 1968), which has also been shown in crayfish fibres using procaine (Chiarandini *et al.*, 1970a; Lea, 1996).

The finding that lower concentrations (62 $\mu\text{M}$ ) of tetracaine inhibited the force produced by the *Nephrops* SF muscle and reversed a caffeine-induced increase in evoked-contractions with little or no effect on either the membrane potential or EPSP size (Fig. 2.27), while at higher concentrations (500  $\mu\text{M}$ ) both the force and EPSPs were inhibited (Figs. 2.25 & 2.26), is in accordance with its expected effect on SR  $\text{Ca}^{2+}$  release (Almers & Best, 1976; Weber & Hertz, 1968). This provides further evidence that EC coupling in the SF muscle fibres of *Nephrops norvegicus* involve CICR, although no distinction was evident in the properties of the  $S_1$  and  $S_2$  fibre types.

However, the effects of higher concentrations of tetracaine (500  $\mu\text{M}$ ), which abolished the EPSPs as well as force (Figs. 2.25 & 2.26), suggest that its actions at these concentrations are similar to its effects on crayfish fibres. Similar findings were obtained by Györke & Palade (1992), although the threshold for blocking the  $S_1$  and  $S_2$  fibres is lower. This suggests that higher concentrations of tetracaine are blocking the  $\text{Ca}^{2+}$  channels which are involved in propagation of the EPSP.

#### 2.4.7 Butanedione monoxime (BDM)

BDM has multiple effects on vertebrate smooth, cardiac and skeletal muscle fibres. In cardiac muscle BDM inhibits tension in isolated preparations from rabbit (Alpert *et al.*, 1989) and ferret (Blanchard *et al.*, 1990) by acting directly at the level of the myofilaments to inhibit  $\text{Ca}^{2+}$ -activated force production. BDM reduces adenosinetriphosphatase (ATPase) activity and  $\text{Ca}^{2+}$ -activated force in chemically skinned ventricular muscle (Li *et al.*, 1985) as well as reducing the amount of  $\text{Ca}^{2+}$  released from the SR which inhibits  $\text{Ca}^{2+}$ -activated force (Blanchard *et al.*, 1990; Gwathmay *et al.*, 1991; Steele & Smith, 1993). In smooth muscle BDM decreases maximum tension in guinea-pig taenia coli, which was found to be related to an inhibition of the crossbridge cycle (Warren *et al.*, 1985), and inhibits  $\text{K}^+$ -induced force in skinned fibres by affecting  $\text{Ca}^{2+}$  translocation (Österman *et al.*, 1993). Similar effects occur in vertebrate skeletal muscle: BDM inhibits contraction in both intact and skinned muscle fibre preparations from frog and rabbit (Mulieri & Alpert, 1984; Fryer *et al.*, 1988; Horiuti *et al.*, 1988; Bagni *et al.*, 1992), it reduces isometric tension, shortening speed and instantaneous stiffness, and inhibits ATPase activity (Horiuti *et al.*, 1988, Higuchi & Takemori, 1989; Bagni *et al.*, 1992). BDM inhibits contraction in intact and skinned frog fibres and also enhances the activity of the CICR mechanism. However, in intact fibres the net effect is to reduce tension by acting mainly on the contractile system (Horiuti *et al.*, 1988).

The effects of BDM on crustacean muscle are not well known, with only a few studies having been conducted. In crayfish muscle BDM was found to potentiate, rather than initiate contraction (1-3 mM) and to induce oscillations at higher concentrations (Györke *et al.*, 1993). It increased the size and length of the intracellular  $\text{Ca}^{2+}$  transients induced

by depolarisation, but did not affect the rate of  $\text{Ca}^{2+}$  removal from the myoplasm or the  $I_{\text{Ca}}$ . It was thought that BDM potentiated  $\text{Ca}^{2+}$ -release in crayfish muscle by dephosphorylation of the  $\text{Ca}^{2+}$ -release channel.

In intact lobster slow muscle fibres, BDM (3-50 mM) increases both resting force and peak twitch force (Györke *et al.*, 1993). In skinned fibres BDM has a small effect on the  $\text{Ca}^{2+}$ -activated force, and in saponin treated skinned fibres with intact SR 50 mM BDM produces a contracture of approximately 75% of that produced by a 50 mM caffeine contracture. Both of these effects are blocked by tetracaine and procaine. This suggests that BDM, like caffeine, releases  $\text{Ca}^{2+}$  from the lobster SR, which is consistent with the finding that when caffeine is used to deplete the SR, BDM has no effect (Godt *et al.*, 1993).

BDM (5-20 mM) induced a large increase in the resting force of the *Nephrops* SF muscle bundles under  $\text{Ca}^{2+}$  free saline conditions (Fig. 2.29) and when applied under standard saline, it induced oscillations in the resting muscle force of both SF muscle bundles (Figs. 2.28 & 2.30) which were accompanied by an oscillation in the membrane potential of the  $S_2$  fibre type that was independent of changes of force (Fig. 2.30). This suggests that as well as triggering  $\text{Ca}^{2+}$  release from intracellular stores, BDM also has an action on sarcolemmal  $\text{Ca}^{2+}$  channels of the *Nephrops*  $S_2$  fibre type. In order to characterise such differences more fully, experiments on single intact fibres, including voltage clamp measurements are required.

This series of experiments has established the basic EC coupling mechanism in the SF muscle of *Nephrops norvegicus* and has identified a few characteristics which differ between the  $S_1$  and the  $S_2$  fibre phenotypes. The work which comprises this chapter provides essential information upon which experiments reported in later chapters are based. In particular, the mechanical properties of skinned muscle fibre preparations have been investigated in more detail (Chapter 4).

Table 2.1 Resting potentials recorded from the S<sub>1</sub> and S<sub>2</sub> fibre types of a single SF muscle.

| Fibres<br>(No) | S <sub>1</sub> | S <sub>2</sub> |
|----------------|----------------|----------------|
| 1              | 55             | 58             |
| 2              | 64             | 65             |
| 3              | 60             | 52             |
| 4              | 62             | 61             |
| 5              | 65             | 68             |
| Mean           | 61.2           | 60.8           |
| S.D.           | 3.9            | 6.2            |
| n              | 5              | 5              |

Table 2.2 Total depolarisation at the 10th EPSP at different frequencies of stimulation in the S<sub>1</sub> and S<sub>2</sub> fibre types. Data from three preparations.

| Stimulation<br>frequency<br>(Hz) | S <sub>1</sub><br>depolarisation<br>(mV) | S.D.<br>(n) | S <sub>2</sub><br>depolarisation<br>(mV) | S.D.<br>(n) |
|----------------------------------|--|-------------|--|-------------|
| 20                               | 2.18                                     | 0.74<br>(3) | 16.02                                    | 7.10<br>(7) |
| 30                               | 2.12                                     | 0.83<br>(4) | 19.12                                    | 4.72<br>(7) |
| 40                               | 3.25                                     | *<br>(1)    | 22.57                                    | 6.96<br>(4) |
| 50                               | 2.11                                     | 0.36<br>(6) | 20.87                                    | 7.11<br>(7) |

Table 2.3 Ratio between the 1st and 10th EPSP at different frequencies of stimulation in the S<sub>1</sub> and S<sub>2</sub> fibre types. Data from three preparations.

| Stimulation<br>frequency<br>(Hz) | S <sub>1</sub><br>ratio 1:10<br>EPSP | S.D.<br>(n) | S <sub>2</sub><br>ratio 1:10<br>EPSP | S.D.<br>(n) |
|----------------------------------|--------------------------------------|-------------|--------------------------------------|-------------|
| 20                               | 2.09                                 | 0.37<br>(3) | 1.78                                 | 0.06<br>(3) |
| 30                               | 2.10                                 | 0.30<br>(3) | 1.98                                 | 0.22<br>(3) |
| 40                               | 2.75                                 | *<br>(1)    | 1.73                                 | 0.44<br>(3) |
| 50                               | 3.19                                 | 0.70<br>(3) | 1.45                                 | 0.33<br>(3) |

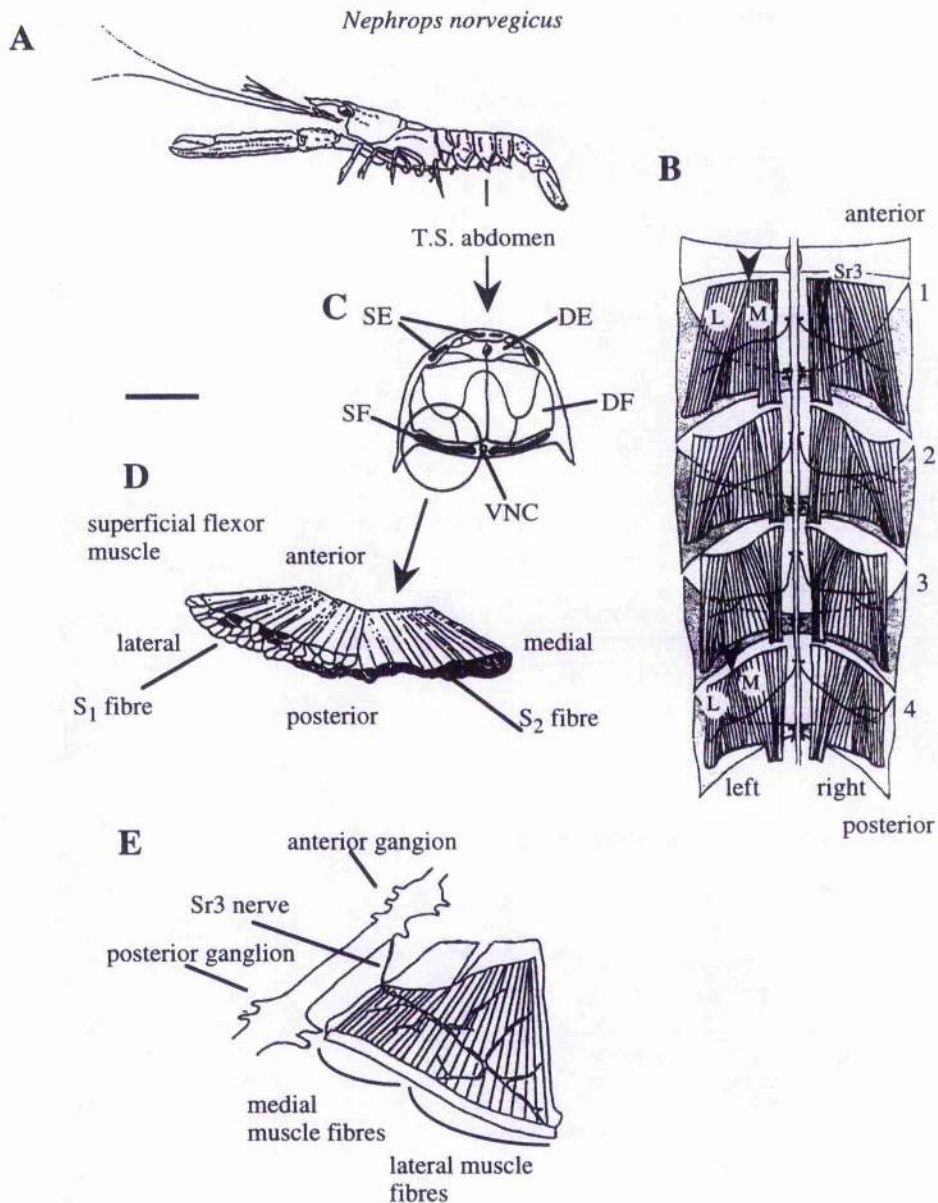


Fig. 2.1  
Morphology of the superficial flexor (SF) muscle in *Nephrops norvegicus*.

(A) The animal (above) has been sectioned transversely in the third segment of the abdomen to show the arrangement of the deep and superficial extensor and flexor muscles (C) SE: superficial extensor muscles; DE: deep extensor muscles; SF: superficial flexor muscles; DF: deep flexor muscles; VNC: ventral nerve cord. The fibre arrangement in the 2 bundles of the SF is shown (D). The SF muscle shows regional segregation of fibre subtypes. The medial bundle is comprised of fibres of the  $S_2$  phenotype (blackened) whilst the lateral bundle is largely comprised of the  $S_1$  phenotype. Scale bar: (A), 30 mm; (C), 10 mm; (D), 1.3 mm.

(B) Dorsal view of the dissected abdomen, showing the arrangement of the SF muscle in segments 1-4. L, lateral bundle; M, medial bundle; Sr3, third superficial root. Arrowheads indicate the medial edge of the lateral bundle. Scale bar: 6.2 mm. (from Fowler & Neil, 1992)

(E) SF system, involved in controlling graded changes in abdominal posture. Dorsal view is shown of nerve cord and SF muscle from 1st segment.. (from Denhean, 1992)

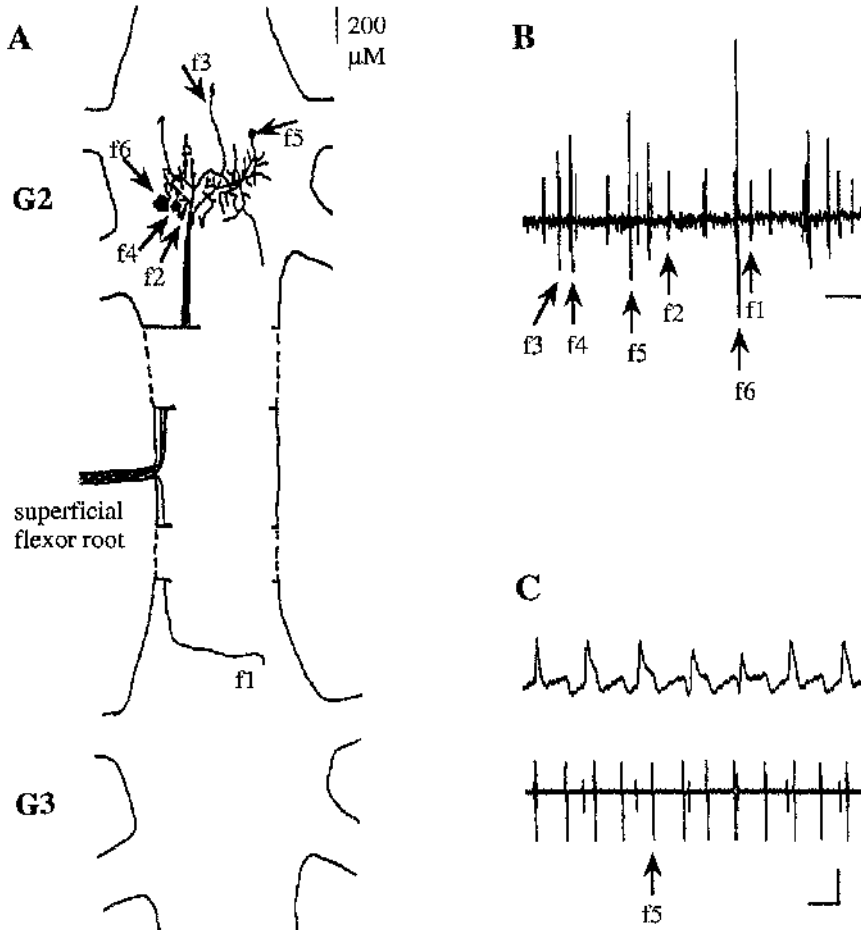


Fig. 2.2  
Six motor neurones innervate the SF muscle of *Nephrops*.

(A) Camera lucida drawing of one of the superficial flexor nerve root retrogradely filled with cobalt. The six motor neurones which are visualised using this technique are labelled according to size of soma. Five motor neurones are located in the ganglion anterior to the Sr3 (in this case abdominal ganglion 2 (G2); three lie ipsilaterally within the ganglion (f2, f4 and f6) while the other two are contralateral (f3 and f5). The remaining motor neurone, f1, has its cell body located contralaterally within the posterior ganglion. Scale bar = 200 μM (from Denhean, 1992).

(B) Identification of six classes of motor neurone according to the amplitude of extracellularly recorded spikes. All motor neurones are firing in this trace. Scale = 50 μM.

(C) The SF muscle inhibitor, f5 can be identified by matching its extracellular spike with an inhibitory post-synaptic potential (IPSP) in the intracellular muscle record. Scale bar = 20 mV, 100 ms (Neil, unpublished data).

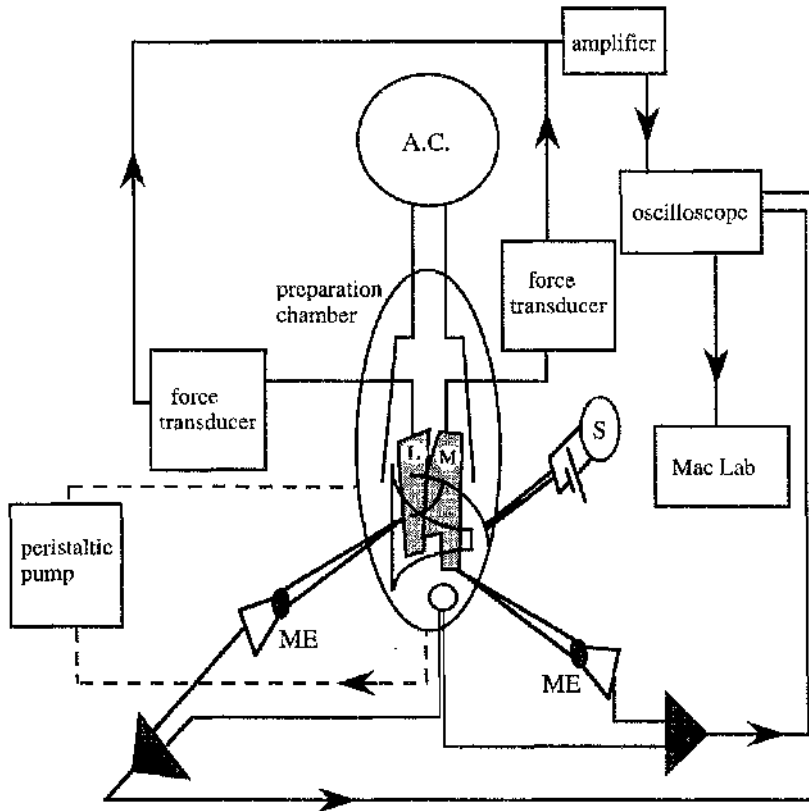


Fig. 2.3  
Experimental setup for the SF muscle bundle experiments.

The SF muscle preparation was pinned in a Sylgard lined bathing chamber and solutions were applied via a peristaltic pump. The preparation was stimulated either by a suction electrode (S) which was connected to the nerve or by field stimulation (A.C.). Force was recorded from the lateral (L) and medial (M) muscle bundles of the SF muscle by two force transducers and the EPSPs were recorded by two intracellular microelectrodes (ME) which were inserted into a  $S_1$  fibre types from the lateral bundle and a  $S_2$  fibre type from the medial bundle. Both force and EPSPs were recorded on the oscilloscope and on the Mac Lab.

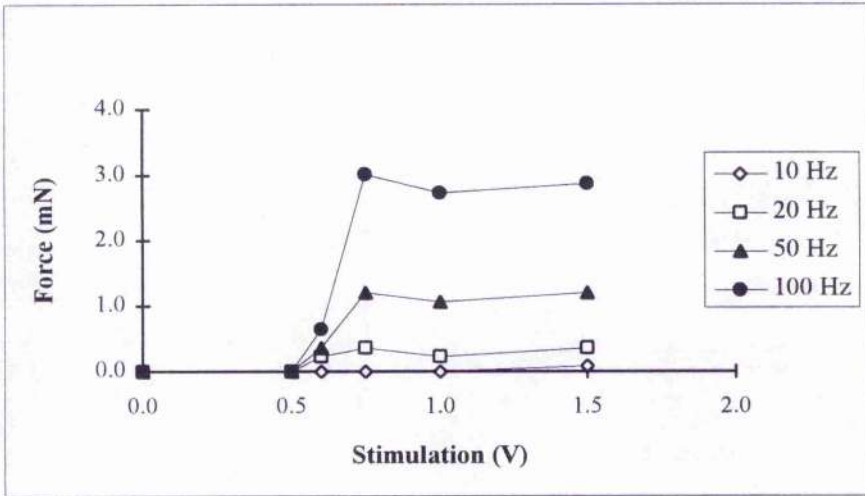


Fig. 2.4

Effect of stimulus frequency and voltage on the neuronally-evoked force from the medial bundle of the SF muscle.

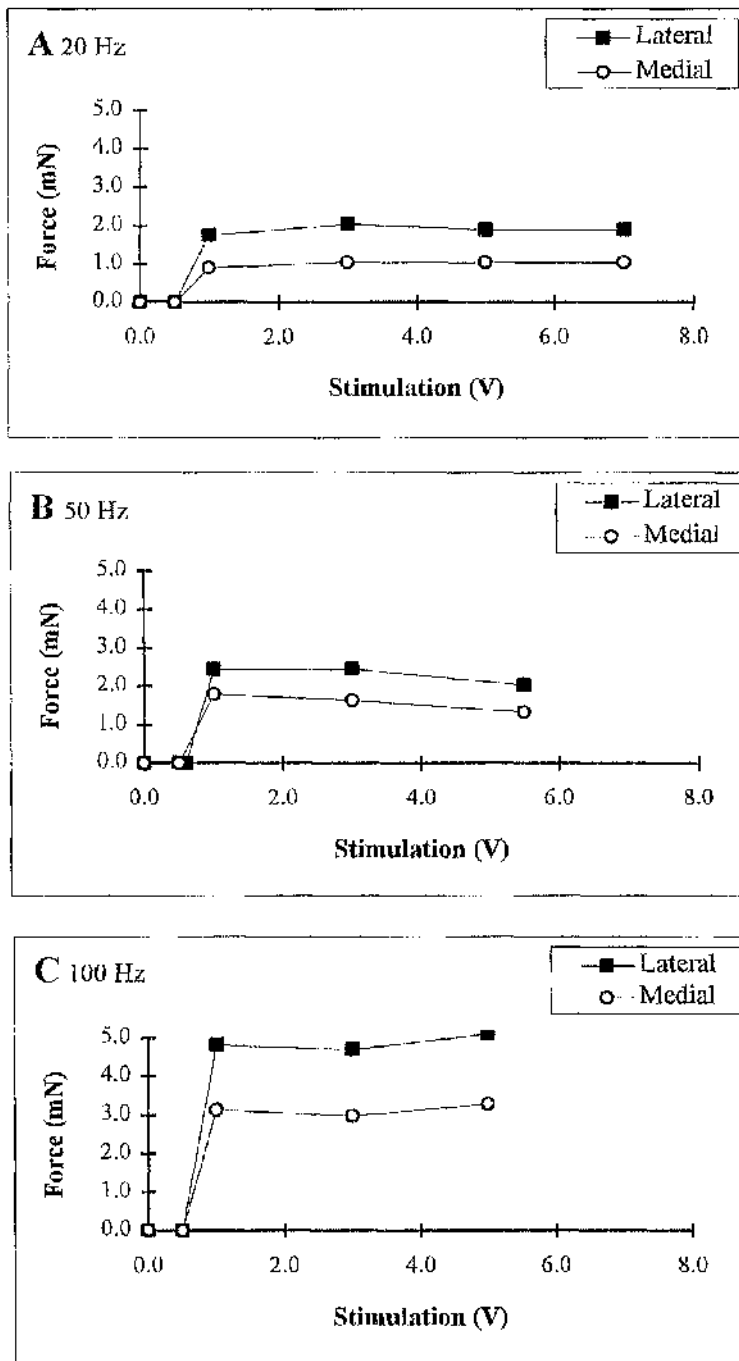


Fig 2.5  
Absolute neuronally-evoked force from the medial and lateral bundles of a single SF muscle stimulated at different frequencies.

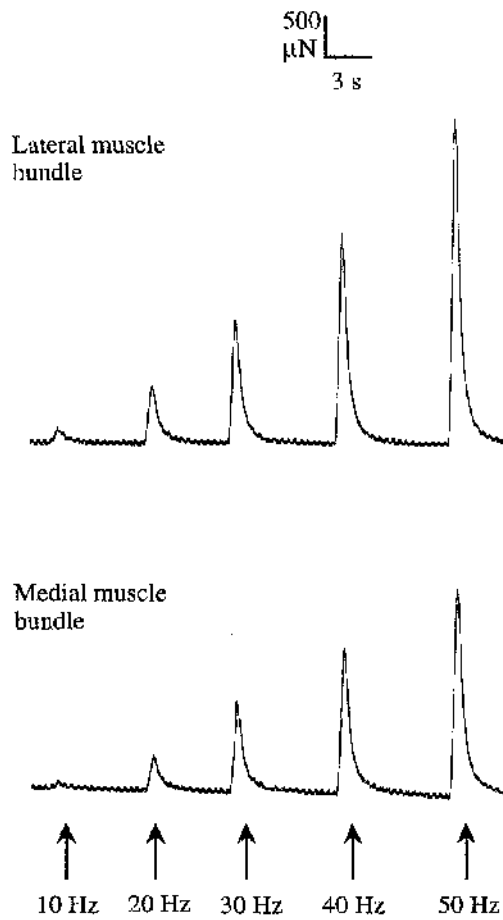


Fig. 2.6  
Effect of stimulus frequency on the force of the SF  
muscle bundles.

Stimulation: a train of pulses at different frequencies  
for 0.5 s at 3V.

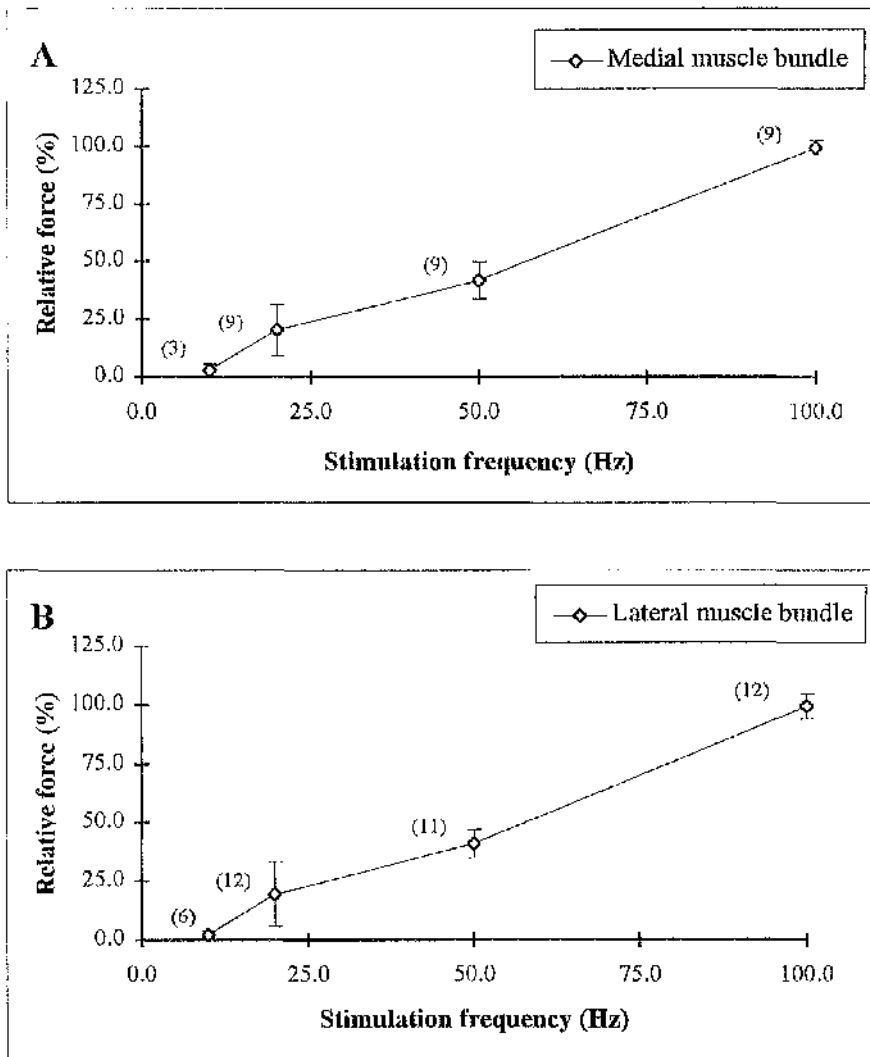


Fig 2.7

Effect of stimulus frequency on the relative force of the SF muscle bundles.

Mean  $\pm$  S.D. values for force from the medial (A) and lateral (B) bundles evoked by standard supramaximal neuronal stimulation; n values are indicated in parenthesis.

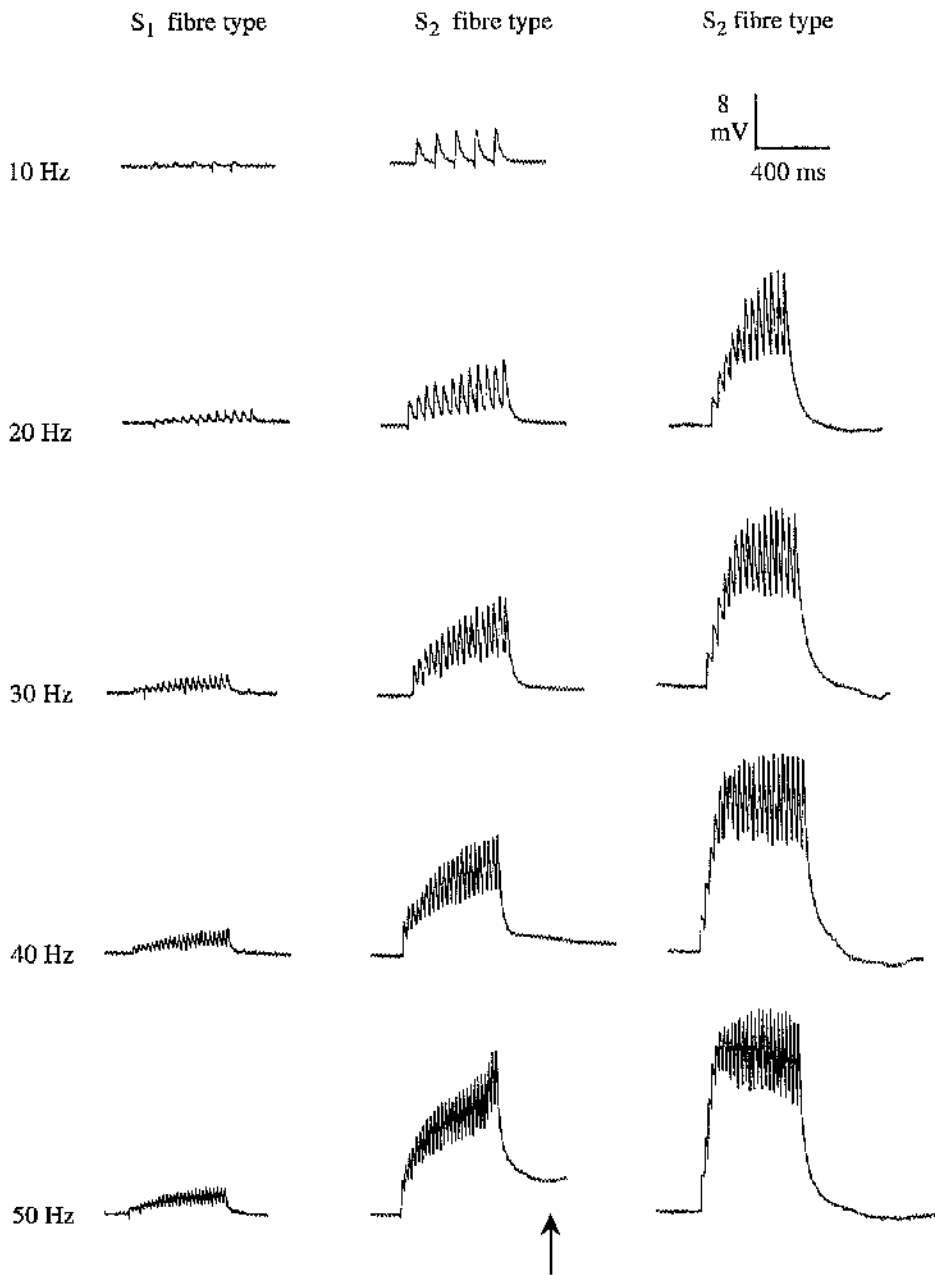


Fig. 2.8  
Effect of stimulus frequency on EPSPs from the S<sub>1</sub> and S<sub>2</sub> fibre types of the SF muscle.

A train of pulses at different frequencies (10-50 Hz) for 0.5s at 3V was used to neuronally stimulate the preparation supramaximally. The arrow indicates an example of the microelectrode being pulled out of the fibre at higher frequencies.

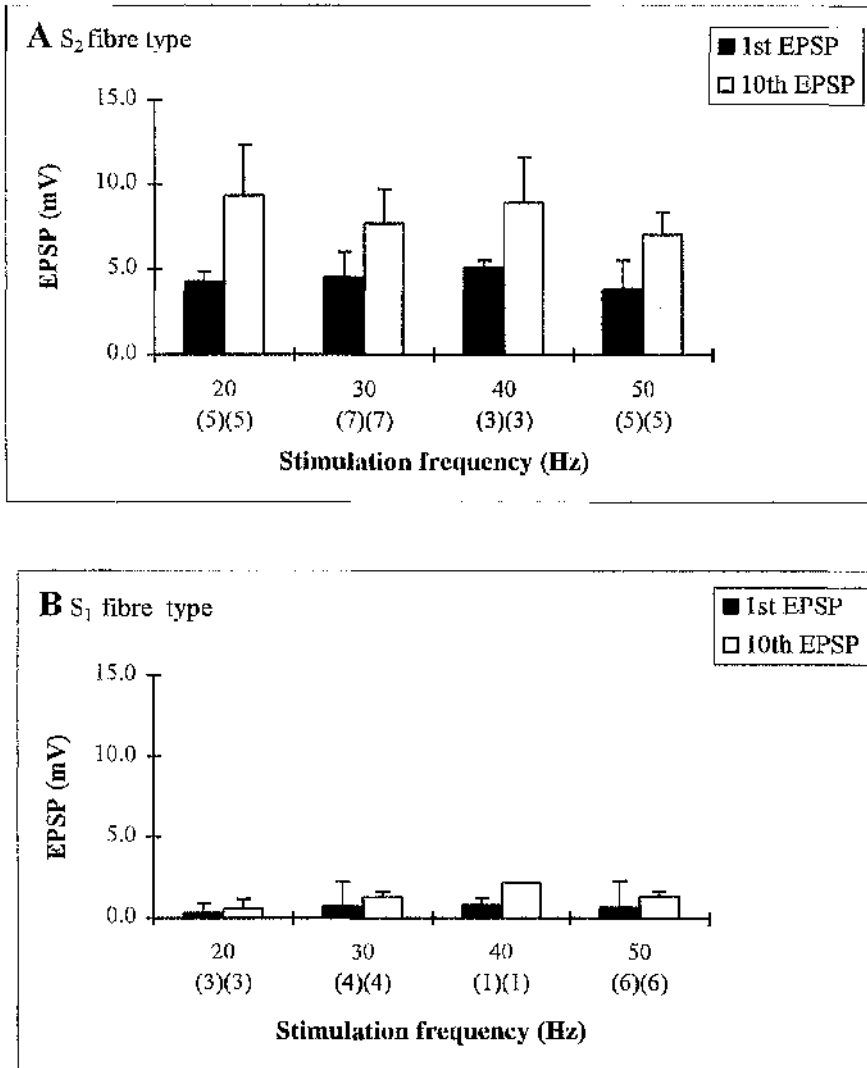


Fig. 2.9  
Facilitation of EPSPs.

- (A) S<sub>2</sub> fibre type
- (B) S<sub>1</sub> fibre type

Mean  $\pm$  S.D. values for the first, non-facilitated and 10th, facilitated, EPSP at different frequencies; n values are indicated in parenthesis.

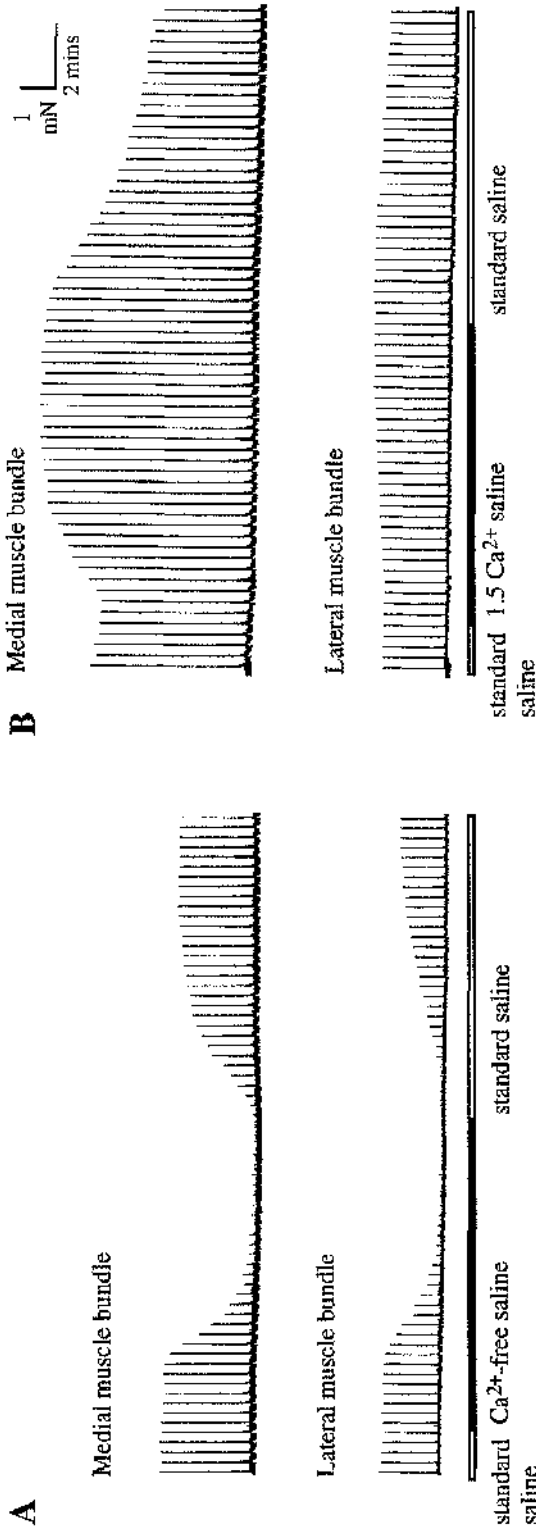


Fig. 2.10

Effects of changes in the  $\text{Ca}^{2+}$  concentration on muscle contraction.

(A)  $\text{Ca}^{2+}$ -free saline inhibited neuronally-evoked force in the two bundles of the SF muscle.

(B) When the concentration of  $\text{Ca}^{2+}$  was increased (standard saline = 13.7 mM; 1.5  $\text{Ca}^{2+}$  saline = 20.0 mM) the neuronally-evoked contractions increased in size.

Standard neuronal stimulation was applied every 20 seconds throughout the experiments.

Bars indicate the application of test solutions in this and all subsequent figures.

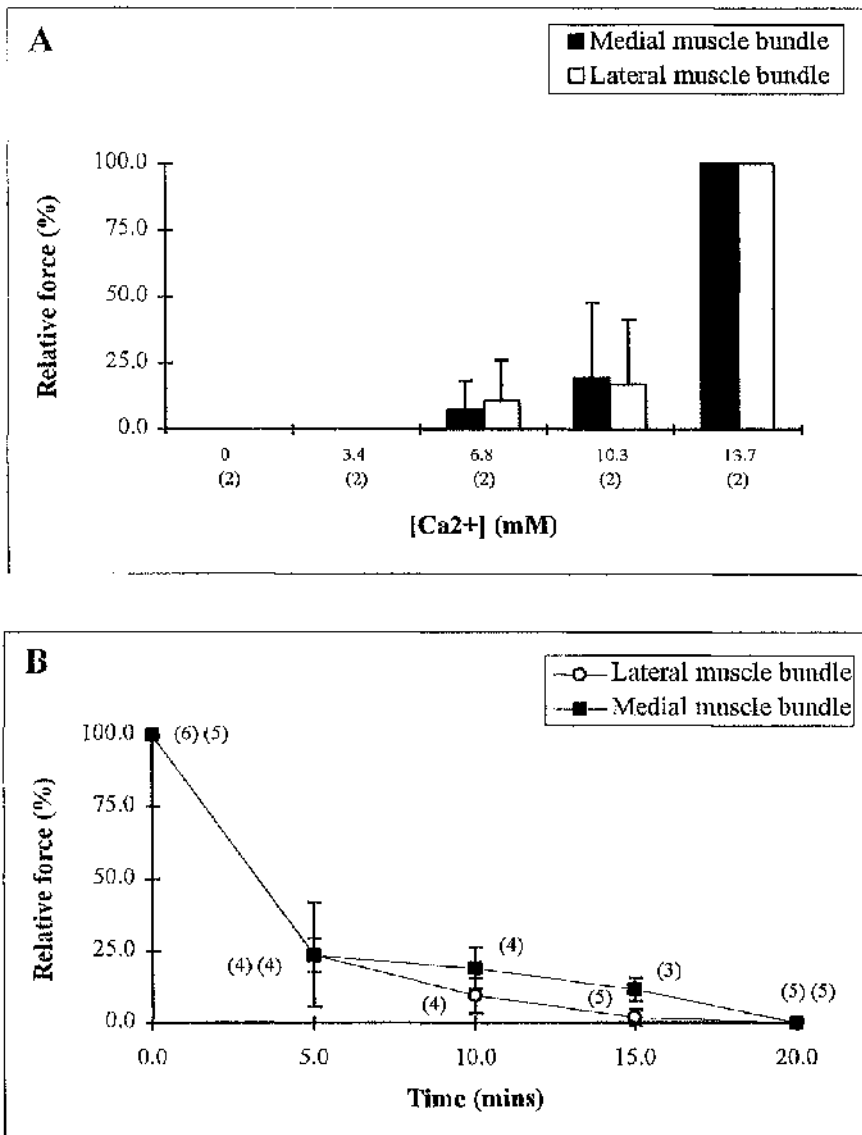


Fig 2.11

Effect of  $\text{Ca}^{2+}$  concentration on the force produced by the SF muscle bundles.

(A) Force at 15 minutes, at different  $\text{Ca}^{2+}$  concentrations; n values are indicated in parenthesis; standard saline contains 13.7 mM  $\text{Ca}^{2+}$ .

(B) Force every 5 minutes during a  $\text{Ca}^{2+}$ -free saline application; n values for the 2 bundles are indicated in parenthesis ((Lateral) (Medial)).

Mean  $\pm$  S.D. values for force evoked by the standard neuronal stimulation.

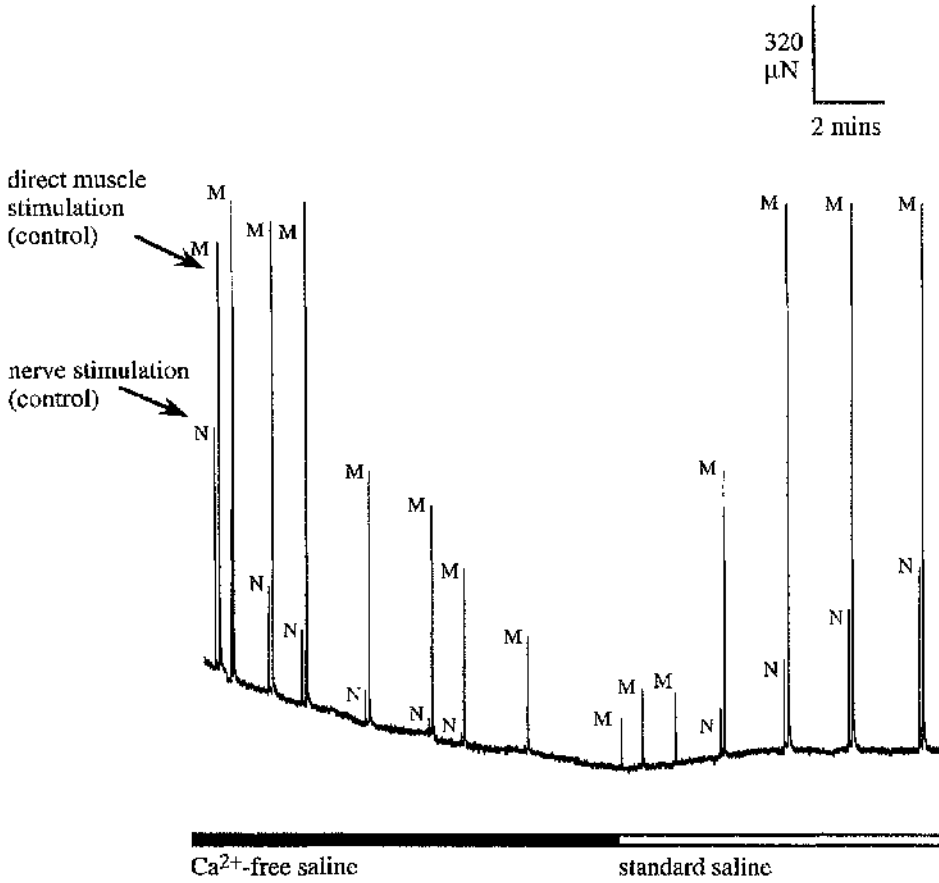


Fig. 2.12  
Effect of  $\text{Ca}^{2+}$ -free saline on the neuronally-evoked force and the force evoked by electrical field stimulation of the medial bundle of the SF muscle.

Arrows indicate the type of stimulation. Note that the force evoked by standard neuronal stimulation (N) disappears completely, while the force evoked by field stimulation (M) is still present.

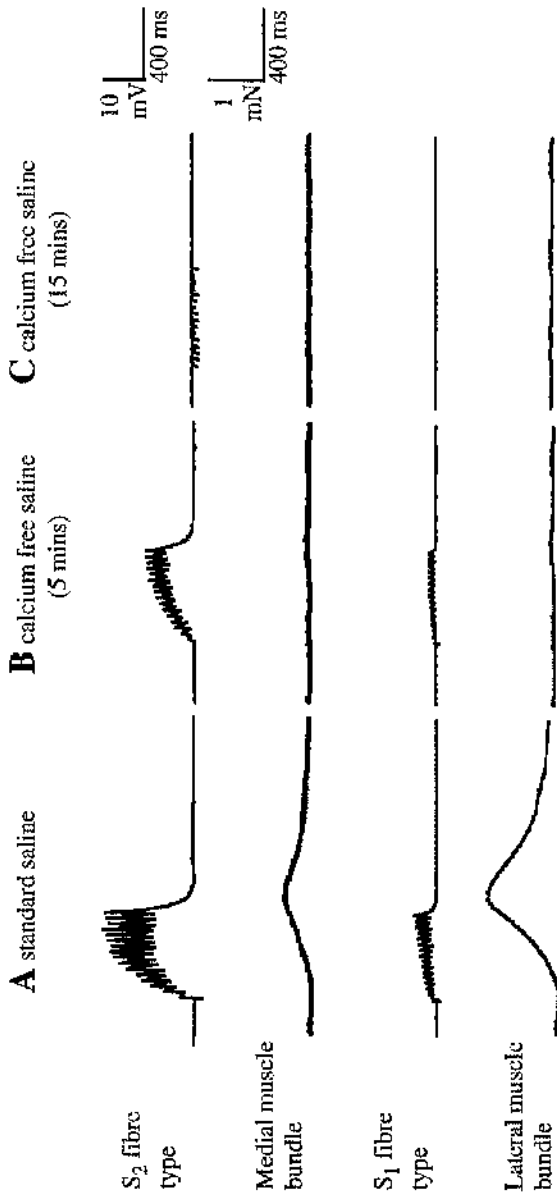


Fig. 2.13 Effect of  $\text{Ca}^{2+}$ -free saline on the force evoked by standard neuronal stimulation and EPSPs recorded from the  $\text{S}_1$  and  $\text{S}_2$  fibre types from the SF muscle.

- (A) Control.
- (B) 5 minutes of  $\text{Ca}^{2+}$ -free saline.
- (C) 15 minutes of  $\text{Ca}^{2+}$ -free saline.

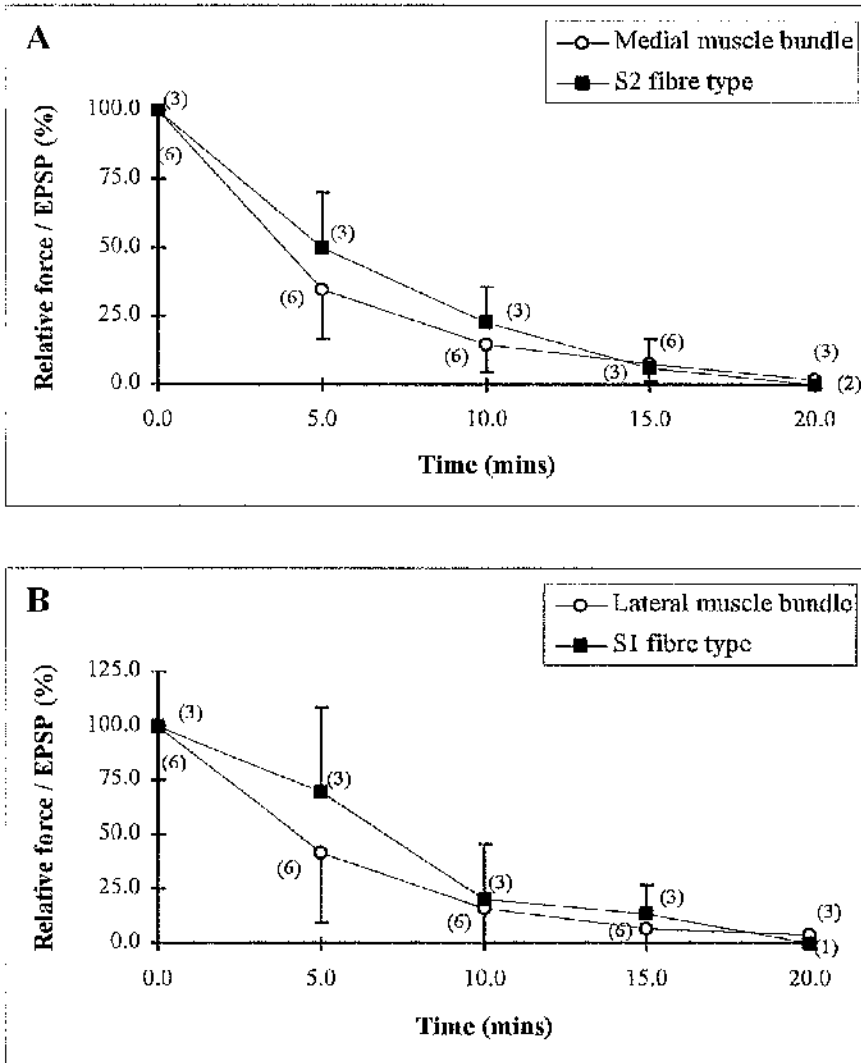


Fig. 2.14

Effect of calcium-free saline on the force and the EPSPs recorded from the SF muscle bundles.

Mean  $\pm$  S.D. values for force from the medial (A) and lateral (B) bundles and for EPSPs from the S<sub>2</sub> (A) and S<sub>1</sub> (B) fibre types, in response to the standard neuronal stimulation; Ca<sup>2+</sup>-free saline was applied at time 0; measurements were taken every 5 minutes; the 10th EPSP in each series of EPSPs was measured; n values are indicated in parenthesis.

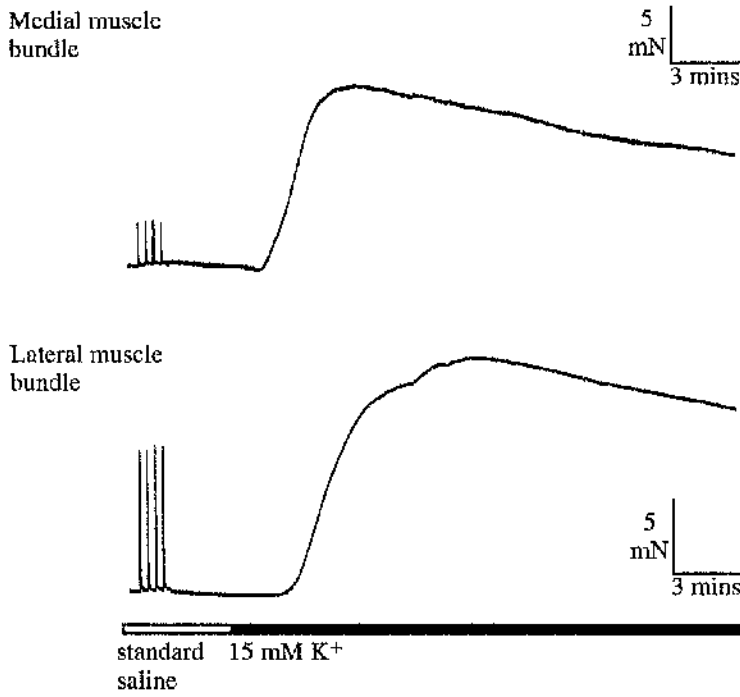


Fig. 2.15  
Potassium-induced contractures in the  $ST^+$  muscle bundles.

Four neuronally-evoked contractions in standard saline are followed by application of a high  $K^+$  saline (15 mM  $K^+$ ).

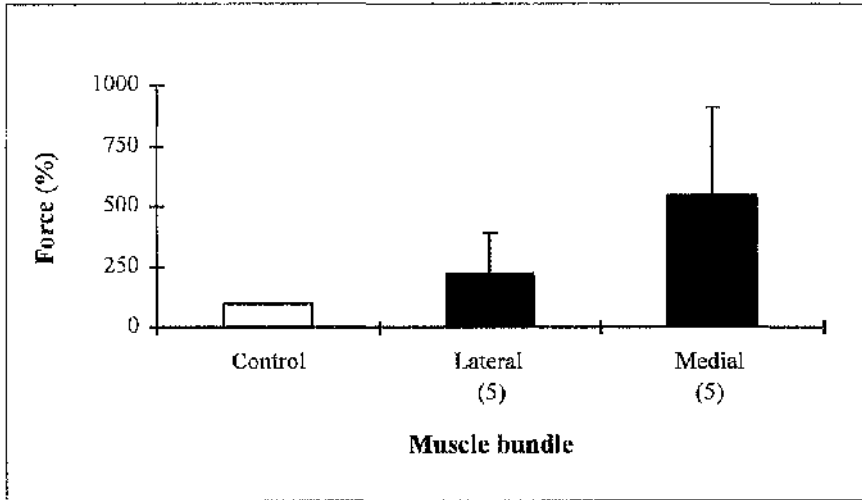


Fig. 2.16  
Potassium-induced contractures in the SF muscle bundles.

Mean  $\pm$  S.D. values for force induced by 15 mM  $K^+$  saline; control (100 %): maximal neuronally-evoked force in standard saline; n values are indicated in parenthesis.

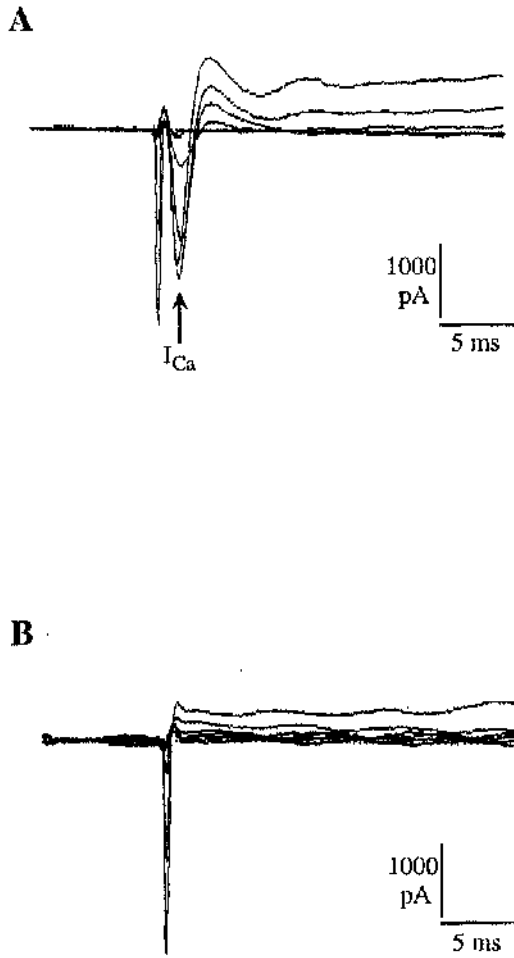


Fig. 2.17  
Voltage clamp recording of fast inward  $\text{Ca}^{2+}$  currents ( $I_{\text{Ca}}$ ) in an  $S_1$  fibre.

(A) Standard saline: note the fast inward  $\text{Ca}^{2+}$  currents.  
(B)  $\text{Ca}^{2+}$ -free saline + EGTA and TEA: the fast inward  $\text{Ca}^{2+}$  currents are abolished.

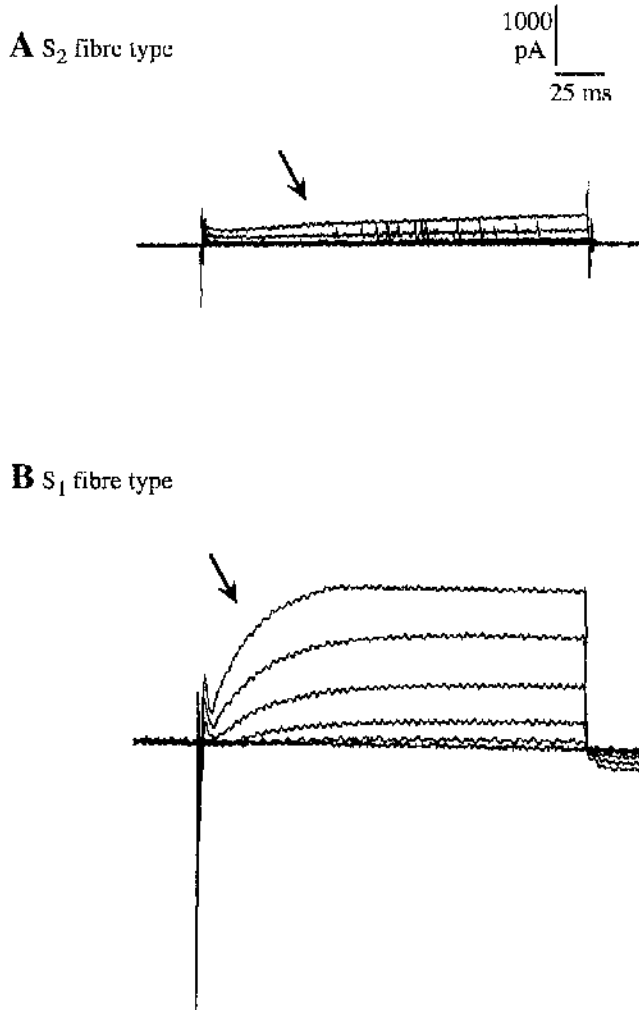
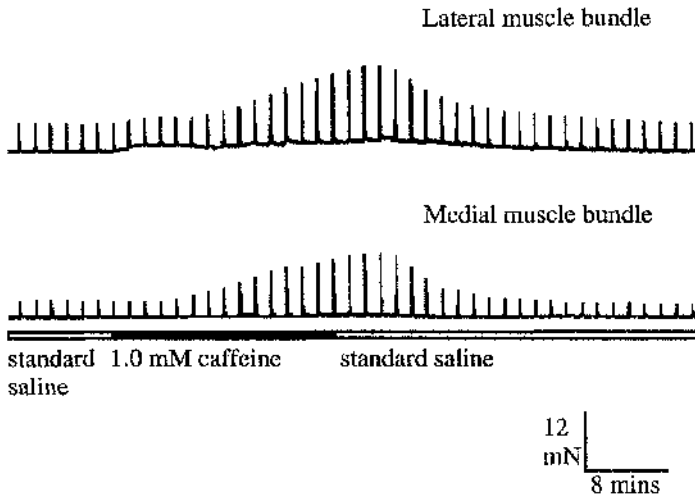


Fig. 2.18  
Voltage clamp recordings showing outward  $K^+$  currents in the  $S_2$  (A)  
and  $S_1$  (B) fibre types.

Arrows indicate the outward  $K^+$  currents; For these measurements no TEA was added to the saline.

**A** 1 mM Caffeine



**B** 3 mM Caffeine

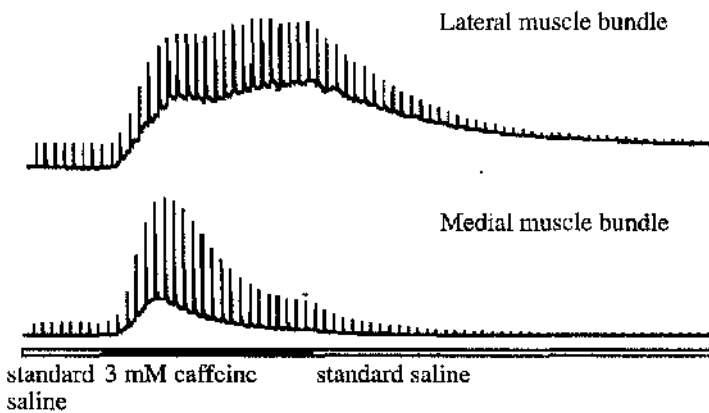


Fig. 2.19  
Caffeine contractures in the SF muscle bundles.

- (A) 1 mM caffeine in standard saline.
- (B) 3 mM caffeine in standard saline. Note the increase in the resting force.

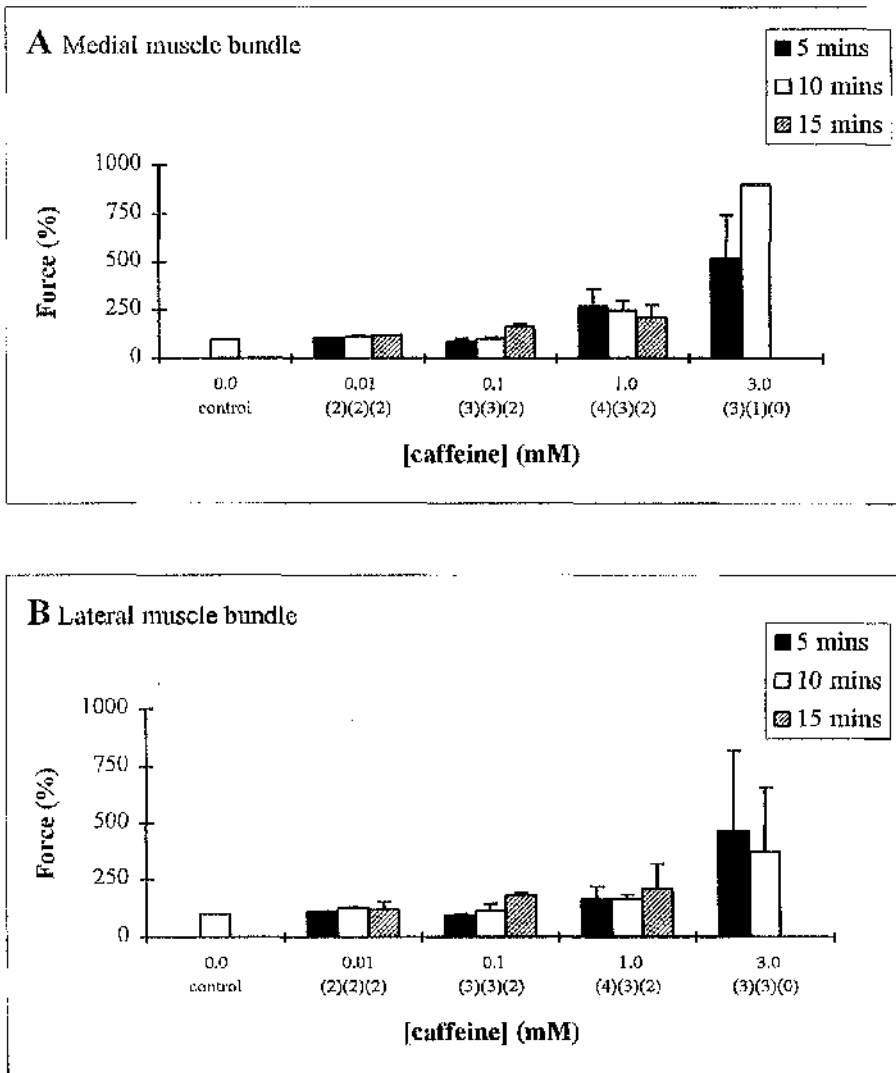


Fig. 2.20

Effect of caffeine on the neurally-evoked forces from the SF muscle bundles.

Force measurements in standard saline containing caffeine taken at 5, 10 and 15 minutes from the medial (A) and lateral (B) muscle bundles; mean  $\pm$  S.D. values for force; n values are indicated in parenthesis.

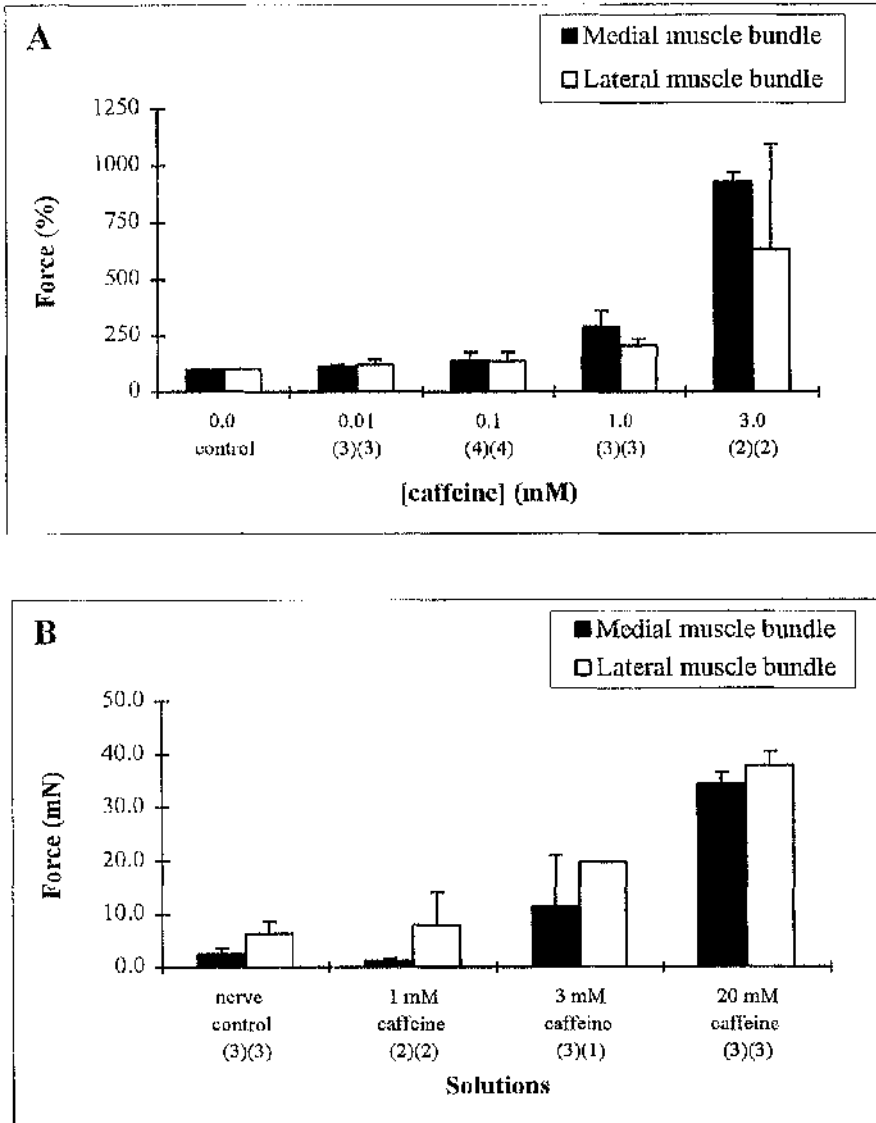


Fig. 2.21  
Effect of caffeine on the SF muscle bundles.

(A) Maximum force (relative to control (100 %): standard neuronal stimulation) in response to different concentrations of caffeine (0.01-3.0 mM) in standard saline.

(B) Maximum absolute force produced by standard neuronal stimulation (control) and different concentrations of caffeine (1.0-20.0 mM) in  $\text{Ca}^{2+}$ -free saline.

Mean  $\pm$  force values, n values are indicated in parenthesis.

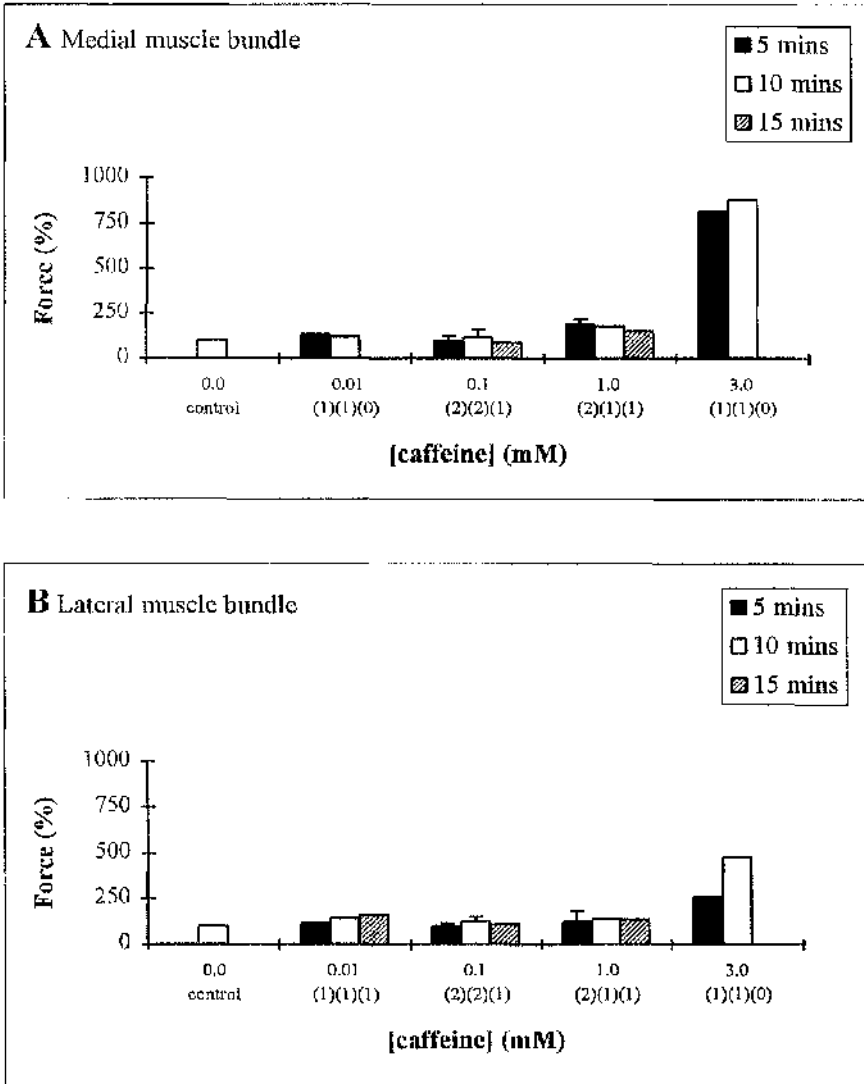


Fig. 2.22

Effect of caffeine on the force evoked by electrical field stimulation of the SP muscle bundles.

Measurements in standard saline containing caffeine taken at 5, 10 and 15 minutes from the medial (A) and lateral (B) muscle bundles; mean  $\pm$  S.D. values for force; n values are indicated in parenthesis.

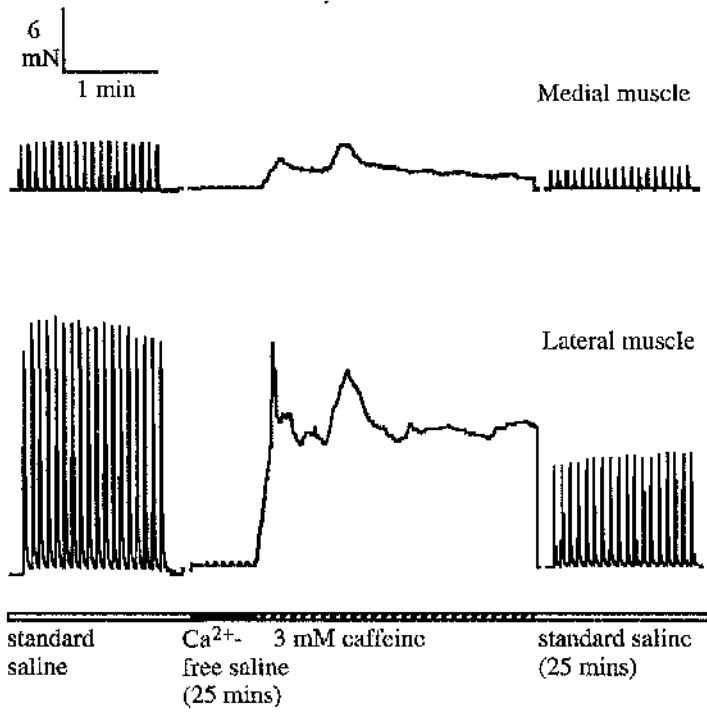


Fig. 2.23

Caffeine-induced contractures in the absence of extracellular  $\text{Ca}^{2+}$ .

Application of caffeine in the presence of  $\text{Ca}^{2+}$ -free saline. Standard neuronal stimulation was applied every 20s throughout the experiment..

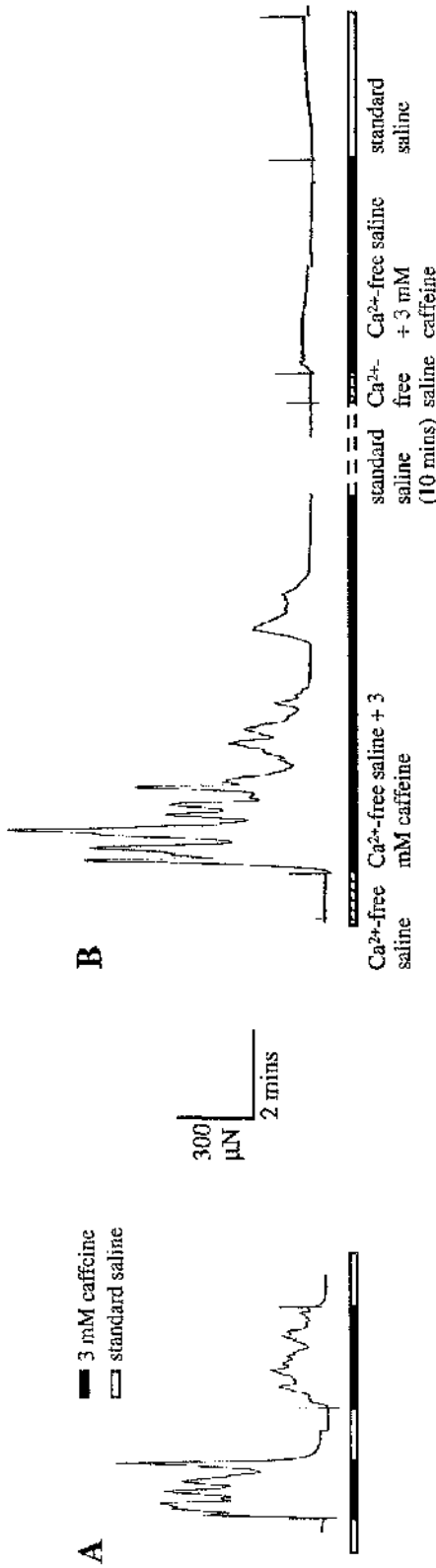


Fig. 2.24

Effect of caffeine on the force produced by a single fibre in the presence and absence of Ca<sup>2+</sup>

(A) Double exposure to 3 mM caffeine in standard saline.

(B) 3 mM caffeine applied in Ca<sup>2+</sup>-free saline; the fibre was then transferred to standard saline to allow the SR to reload with Ca<sup>2+</sup> followed by Ca<sup>2+</sup>-free saline before a second 3 mM caffeine application was made.

All Ca<sup>2+</sup>-free solutions contained 5 mM EGTA; different fibres were used for A and B.

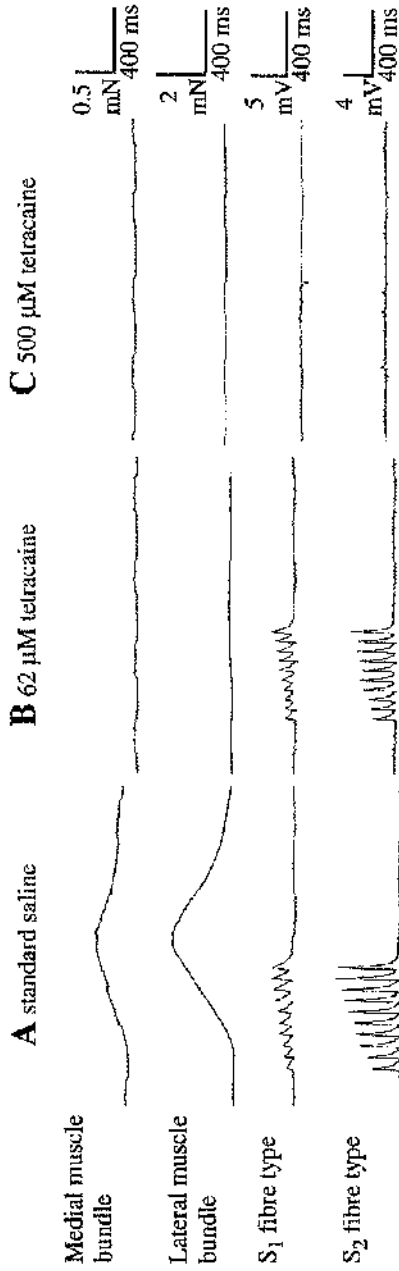


**Fig. 2.25**  
**Effects of tetracaine on the force and EPSPs from the SF muscle bundles.**  
 (A) Control.  
 (B) 62 μM tetracaine. The force of both muscle bundles is inhibited while the EPSPs remain, although slightly reduced in size.  
 (C) 125 μM tetracaine. Both force and EPSPs are blocked.

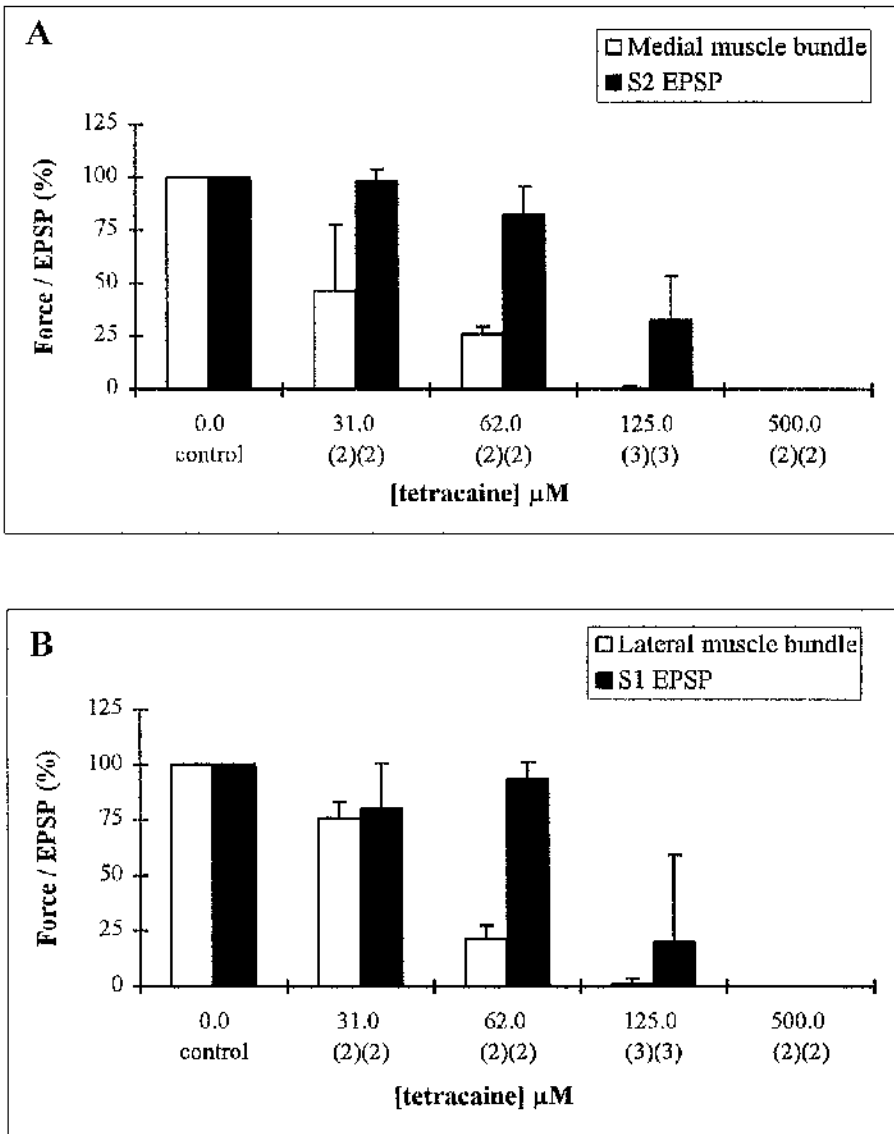
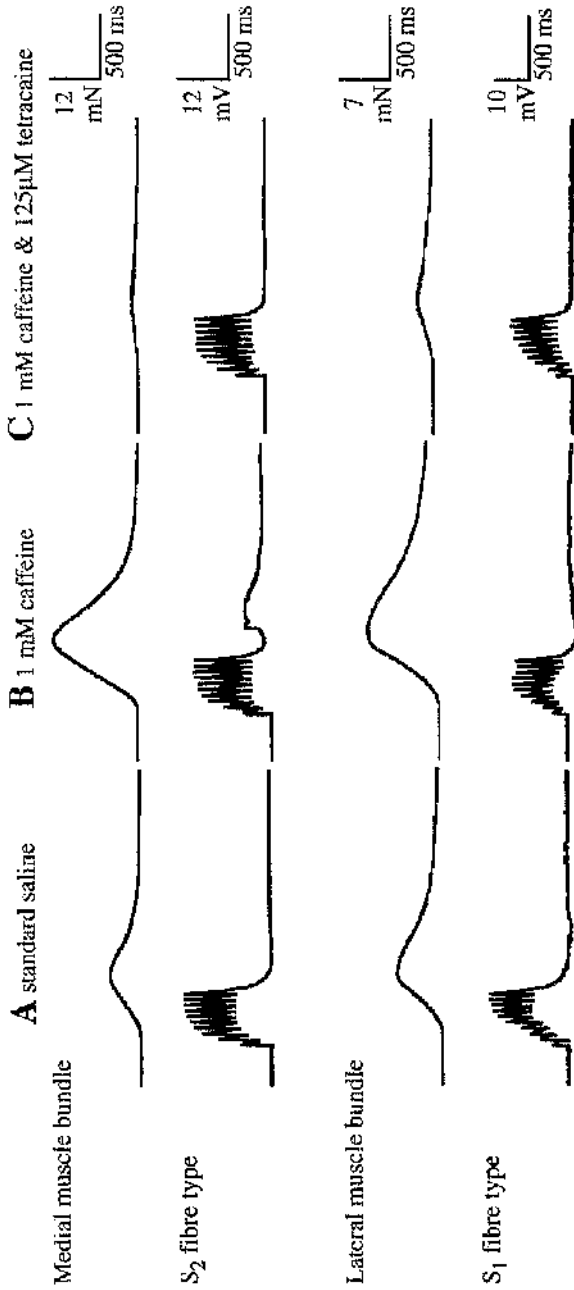


Fig. 2.26

Effect of tetracaine on the force and EPSPs recorded from the SF muscle bundles.

Mean  $\pm$  S.D. values for force from the medial (A) and lateral (B) bundles and on EPSPs from the S<sub>2</sub> (A) and S<sub>1</sub> (B) muscle fibre types in response to standard neuronal stimulation; all measurements were taken after a 15 minute exposure to tetracaine; the 10th EPSP in each series of EPSPs was measured; n values are indicated in parenthesis.



**Fig. 2.27**  
Tetracaine blocks force in the SF muscle bundles and reverses the effects of caffeine.  
(A) Standard saline.  
(B) 1 mM caffeine. The forces of the two muscle bundles are increased but there is no effect on the EPSPs.  
(C) 125 μM tetracaine. The forces are inhibited but there is no effect on the EPSPs.  
All measurements were made after 15 minutes of test solution.

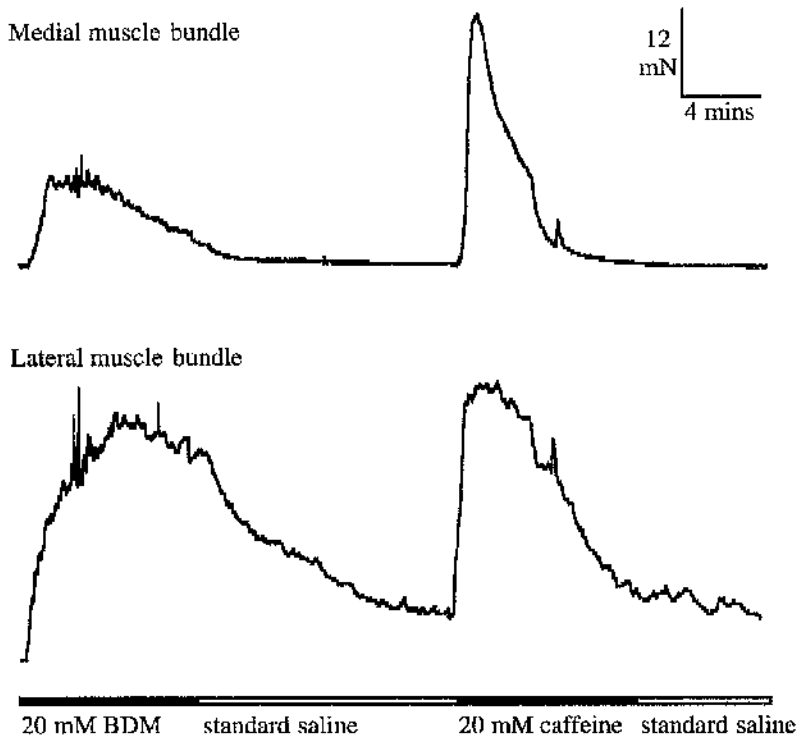


Fig. 2.28  
Caffeine and BDM have similar effects on the resting force of the SF muscle bundles.

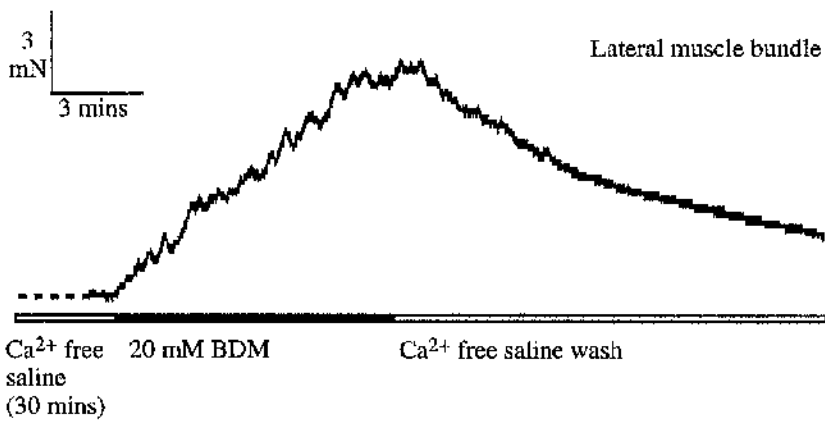


Fig. 2.29  
BDM increases the resting force in the lateral muscle bundle of the SF muscle in Ca<sup>2+</sup> free saline.

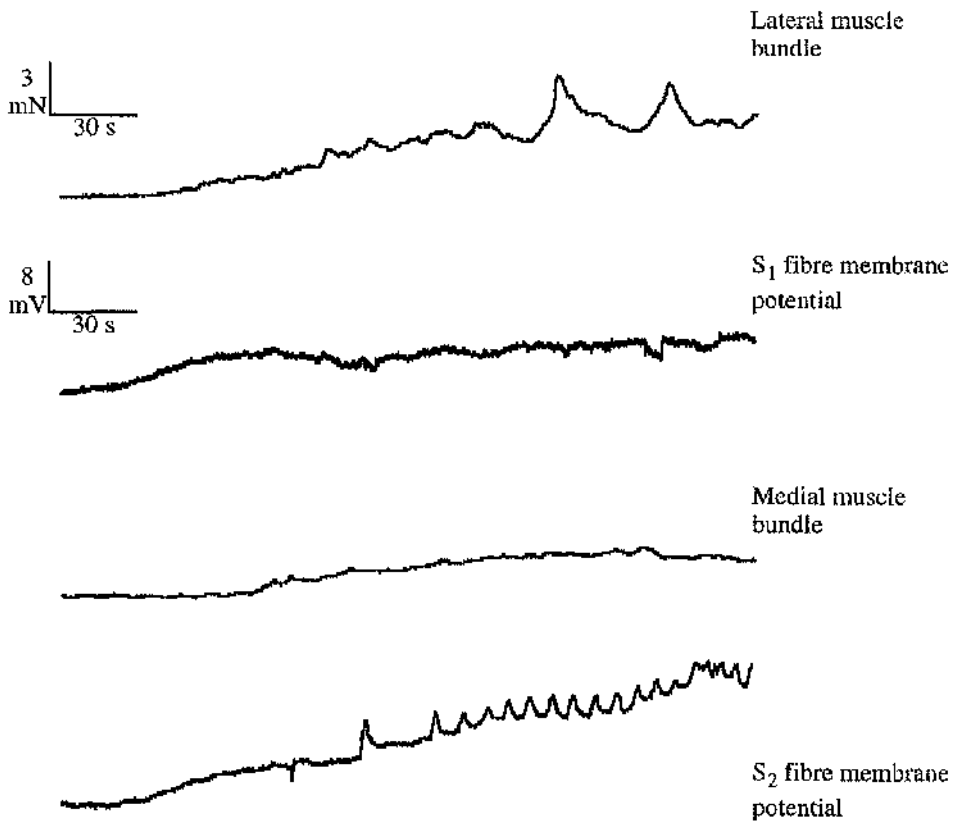


Fig. 2.30  
10 mM BDM increases the resting force of SF muscle bundles and induces an oscillation in the membrane potential of the S<sub>2</sub> fibre type.

**Chapter 3**  
**Effects of Mn<sup>2+</sup> on membrane-intact**  
**muscle fibres**

3.1

INTRODUCTION

3.1.1 Manganese as a  $\text{Ca}^{2+}$  channel blocker

In a variety of excitable cells it is known that the action potentials (APs) are calcium-dependent (Hagiwara, 1973; Reuter, 1973; Hagiwara & Byerly, 1981). Manganese ( $\text{Mn}^{2+}$ ), in common with many other divalent cations such as cobalt ( $\text{Co}^{2+}$ ), nickel ( $\text{Ni}^{2+}$ ) and cadmium ( $\text{Cd}^{2+}$ ), has been shown to block  $\text{Ca}^{2+}$  channels, inhibiting the inward  $\text{Ca}^{2+}$  current across cell membranes (Fatt & Ginsborg, 1958; Hagiwara & Takahashi, 1967). This has led to its use as an experimental tool for establishing the existence and functional importance of membrane  $\text{Ca}^{2+}$  currents in different cellular systems. An example of this is the dependence of transmission at the squid giant synapse on extracellular  $\text{Ca}^{2+}$  (Katz and Miledi, 1969). When injected with tetraethylammonium (TEA), and in the presence of tetrodotoxin (TTX) prolonged APs remain detectable in response to depolarisation. It was demonstrated that this response is due to  $\text{Ca}^{2+}$  currents by showing that the amplitude and duration of the AP increased when the  $\text{Ca}^{2+}$  concentration was increased, that  $\text{Sr}^{2+}$  or  $\text{Ba}^{2+}$  could substitute for  $\text{Ca}^{2+}$ , and that  $\text{Mn}^{2+}$  blocked the response. Consistent with these results, Ross and Stuart (1978) found that  $\text{Mn}^{2+}$  blocked voltage-dependent  $\text{Ca}^{2+}$  channels in the presynaptic membrane of the barnacle photoreceptor.

3.1.2 Excitation-contraction (EC) coupling

Our understanding of the EC-coupling mechanism of invertebrate muscle has been aided by the use of pharmacological agents such as  $\text{Mn}^{2+}$ . For example, in barnacle muscle fibres  $\text{Mn}^{2+}$  has been shown to selectively block the  $\text{Ca}^{2+}$  current, although this effect of  $\text{Mn}^{2+}$  on the  $\text{Ca}^{2+}$  spike becomes less marked when the external  $\text{Ca}^{2+}$  concentration is increased (Hagiwara & Nakajima, 1966a). Hyperpolarisation of the membrane at low  $\text{Ca}^{2+}$  concentrations does not reverse the suppressing effect of  $\text{Mn}^{2+}$  ions, which suggests that the effect of  $\text{Mn}^{2+}$  on the  $\text{Ca}^{2+}$  spike cannot be explained by a shift in the inactivation curve, but is due instead to a direct effect of  $\text{Mn}^{2+}$  on the spike initiation process. These

findings indicate that the  $Mn^{2+}$  ions compete with the  $Ca^{2+}$  ions, and that they can occupy the binding sites on the muscle membrane that are involved in spike initiation.

$Mn^{2+}$  has similar effects on other crustacean muscle fibres. In crayfish muscle fibres  $Mn^{2+}$  reduces the rate of depolarisation and eliminates  $Ca^{2+}$  and  $Ba^{2+}$  APs (Fatt & Ginsborg, 1958; Takeda, 1967). In crab fibres  $Mn^{2+}$  also decreases the size of the AP just before the block (Takeda, 1967; Mounier & Vassort, 1975).

The precise role played by  $Ca^{2+}$  in initiating muscle contraction was established by studies of the inward  $Ca^{2+}$  current and the intracellular  $Ca^{2+}$  stores and by relating these processes to the final event of muscle force. Chiarandini *et al.* (1970a, 1970b) demonstrated that  $Mn^{2+}$  blocks the inward  $Ca^{2+}$  current, which is essential for contraction in crayfish muscle fibres. Caffeine induces a contracture, which is followed by a recovery period. During the recovery period, pharmacologically- and electrically-induced depolarisations of the muscle fibre accelerated the recovery time by inducing an inward  $Ca^{2+}$  current, whereas decreasing the external  $Ca^{2+}$  ion concentration, which reduces the inward movement of  $Ca^{2+}$  ions, or the addition of  $Mn^{2+}$ , which blocks the influx of  $Ca^{2+}$ , had the opposite effect. These results indicate that the influx of  $Ca^{2+}$  ions across the sarcolemma, although small, is critical for muscle contraction.

A second example was demonstrated by Goblet and Mounier (1982) whilst investigating the electrical and mechanical activities of crab muscle fibres. They found that muscle force was associated with the  $Ca^{2+}$  current, and that the quantity of  $Ca^{2+}$  ions entering the cell was important. When  $Mn^{2+}$ -containing or  $Ca^{2+}$ -free solutions were applied, not only was the inward current blocked, but muscle tension was also inhibited. It was concluded that  $Ca^{2+}$  influx was a prerequisite for the development of tension.

### 3.1.3 The passage of $Mn^{2+}$ ions through $Ca^{2+}$ channels

Up till now,  $Mn^{2+}$  has been described as a  $Ca^{2+}$  channel blocker, which contrasts with the property of the divalent cations  $Sr^{2+}$  and  $Ba^{2+}$ , which can replace  $Ca^{2+}$  as carriers of inward current through  $Ca^{2+}$  channels (Fatt & Ginsborg, 1958; Kerkut & Gardner, 1967; Fukuda & Kawa, 1977). However,  $Mn^{2+}$  ions have also been shown to pass through  $Ca^{2+}$

channels in certain preparations. Examples of this include the squid giant axon (Yamagishi 1973) and mammalian cardiac muscle (Ochi 1970, 1975; Delahayes, 1975). In the squid axon it is not clear whether the  $Mn^{2+}$  ions pass through the  $Na^+$  or  $Ca^{2+}$  channels, but in the heart muscle they appear to pass through  $Ca^{2+}$  channels, since  $Mn^{2+}$  APs are blocked by  $La^{2+}$  but not by TTX (Ochi, 1975, 1976).

Myoepithelial cells from the marine polychaete *Syllis spongiphila* have a  $Ca^{2+}$  spike. In  $Ca^{2+}$ -free solutions, low-Na solutions and in the presence of TTX,  $Mn^{2+}$  ions can pass through  $Ca^{2+}$  channels producing  $Mn^{2+}$  APs, which are blocked by  $Co^{2+}$  and  $La^{2+}$  (Anderson, 1979). Consistent with these findings, in voltage-clamp studies of mouse oocytes (Okamoto et al., 1977) and starfish eggs (Hagiwara & Miyazaki 1977) small inward currents were measured when  $Ca^{2+}$  was replaced with  $Mn^{2+}$ .

$Mn^{2+}$  ions have also been shown to carry the inward current in certain skeletal muscle fibres. In larval beetle muscle fibres,  $Mn^{2+}$  ions produce large APs, the size and rate of rise of which increase with increased  $Mn^{2+}$  concentration (Fukunda & Kawa, 1977). This has also been demonstrated in frog skeletal muscle fibres; Palade and Almers (1978) showed that  $Mn^{2+}$  and  $Cd^{2+}$  could substitute for  $Ca^{2+}$ .

### 3.1.4 Theories of how $Mn^{2+}$ ions block and pass through $Ca^{2+}$ channels

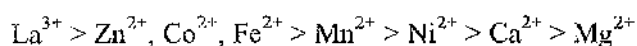
There are many examples, from numerous cell types, of  $Mn^{2+}$  ions being able to pass through  $Ca^{2+}$  channels. However, the mechanism by which  $Mn^{2+}$  and other divalent cations can either pass through or block  $Ca^{2+}$  channels is still not clearly understood, or defined. Two main theories have been suggested:

1. When a second ion competes with  $Ca^{2+}$  for the  $Ca^{2+}$  channel binding site, the inward current ( $I_{Ca}$ ) is given by the equation:

$$I = \frac{I_{max} \cdot C}{C + (1 + M/K_m) \cdot K_{Ca}}$$

where  $[M]$  is the concentration of the second ion and  $K_m$  is the corresponding dissociation constant for the binding site (Hagiwara & Takahashi, 1967; Hagiwara & Byerly, 1981). If this second ion has a low or zero mobility for passing through the  $Ca^{2+}$  channel, the total inward current is reduced and the ion is considered as a blocking ion. Ions such as  $Mn^{2+}$  however, that have a high binding affinity, but a low mobility, can act as both  $Ca^{2+}$  channel blockers and current carriers.

Working on barnacle muscle Hagiwara and Takahashi (1967) concluded that the order of the binding affinity for polyvalent metal ions was:



Other more recent studies have shown slightly different sequences (Van Breemen *et al.*, 1973; Anderson, 1983).

2. The second theory is based upon the energies of hydration of polyvalent and divalent ions, and the fact that, of the divalent transition metal series,  $Mn^{2+}$  ions exhibit the lowest energy of hydration (Noyes, 1962). This theory predicts that  $Mn^{2+}$  ions can pass through  $Ca^{2+}$  channels because they can easily substitute their waters of hydration with ligands of the channel and thus permit the  $Mn^{2+}$  ions to pass through the  $Ca^{2+}$  channel. On this basis, similar transition metal divalent cations with higher energies of hydration should block the  $Ca^{2+}$  channel with an effectiveness that would increase as their energies of hydration increase. This was supported by the fact that the Group IIA metals (earth alkaline metals) that pass through the  $Ca^{2+}$  channel ( $Ca^{2+}$ ,  $Sr^{2+}$  and  $Ba^{2+}$ ) exhibit energies of hydration that are still lower than that of  $Mn^{2+}$  (Ochiai, 1977). This hypothesis was confirmed using the transition metals  $Fe^{2+}$ ,  $Co^{2+}$  and  $Ni^{2+}$  which have successively increasing energies of hydration from that of  $Mn^{2+}$  to block the myoeptithelial cell preparation of the polychaete *Syllis spongiphila* (Anderson 1979) .

Other factors however, should also be taken into consideration. One important one is the ionic radius of  $Mn^{2+}$ , which is smaller than that of  $Sr^{2+}$ ,  $Ba^{2+}$  and

$\text{Ca}^{2+}$  (Basolo & Pearson, 1967), but greater than that of the other transition metals.

### 3.1.5 Muscle contraction

The ability of  $\text{Mn}^{2+}$  in  $\text{Ca}^{2+}$ -free solutions to carry the inward current across membranes has prompted the question of whether it is also capable of activating the muscle proteins involved in contraction. To date the literature on invertebrate muscle says not. Anderson (1979), whilst investigating the ability of  $\text{Mn}^{2+}$  ions to pass through  $\text{Ca}^{2+}$  channels in polychaete myoepithelial cells, reported that although  $\text{Mn}^{2+}$  ions can replace  $\text{Ca}^{2+}$  ions in generating spikes, they do not replace  $\text{Ca}^{2+}$  ions in initiating contraction. Cells exhibiting  $\text{Mn}^{2+}$  spikes are quiescent. Nor were contractions induced by  $\text{Mn}^{2+}$  in larval beetle muscle fibres (Fukuda & Kawa, 1977). Consistent with these results with  $\text{Mn}^{2+}$ , is the observation reported by Suarez-Kurtz and Sorenson (1979) that  $\text{Ba}^{2+}$  is also not capable of initiating muscle contraction in crab muscle fibres.

An equivalent study of the direct action of  $\text{Mn}^{2+}$  on the myofibrillar regulatory and contractile proteins of the  $\text{S}_1$  fibre type from the lateral bundle of the SF muscle from *Nephrops norvegicus* has been carried out using skinned muscle fibres (Chapter 5).

### 3.1.6 Effects of $\text{Mn}^{2+}$ on smooth muscle

$\text{Mn}^{2+}$  ions have been shown to activate smooth muscle when the muscle is depolarised by high  $\text{K}^+$  solutions. Work by Nasu *et al.* (1995a) showed that when guinea-pig ileal longitudinal muscle fibres were activated by high- $\text{K}^+$ , the addition of  $\text{Mn}^{2+}$  (5 mM) rapidly abolished muscle force. However, when the preparation was left under these conditions for about 4 hours, the tonic tension re-developed to a level equivalent to the initial  $\text{K}^+$ -induced contracture.  $\text{Mn}^{2+}$  also induced force in control experiments conducted under  $\text{Ca}^{2+}$ -free conditions (Nasu *et al.*, 1995a). Similar reports show that  $\text{Mn}^{2+}$  can substitute for  $\text{Ca}^{2+}$  in binding to calmodulin (Wolff *et al.*, 1977), and in experiments conducted on skinned smooth muscle preparations,  $\text{Mn}^{2+}$  has been shown to activate the contractile proteins from guinea-pig stomach (Ito *et al.*, 1982).

### 3.1.7 The effects of $Mn^{2+}$ on the SF muscle preparation

Since  $Mn^{2+}$  ions have been shown to either block or pass through  $Ca^{2+}$  channels in  $Ca^{2+}$ -regulated cells, the effects of  $Mn^{2+}$  on the  $Ca^{2+}$ -induced- $Ca^{2+}$ -release (CICR) mechanism of the *Nephrops* SF muscle preparation was investigated. Measurements of force induced both neuronally and pharmacologically, and intracellular recordings (EPSPs) were made in the presence of different  $Mn^{2+}$  concentrations. Pharmacological agents were also used as tools to help to identify the specific action of  $Mn^{2+}$  ions on the different steps of the CICR process.

## 3.2

## MATERIALS & METHODS

The experimental methods for this chapter are as described in Chapter 2 (Section 2.2), and the additional solutions that were used are described below.

### 3.2.1 Solutions

The standard *Nephrops norvegicus* saline (Miyan, 1984), had the following composition (mM/l): NaCl, 478; KCl, 12.74;  $CaCl_2 \cdot 2H_2O$ , 13.69;  $MgSO_4 \cdot 6H_2O$ , 20.47;  $Na_2SO_4$ , 3.9; HEPES, 5; 1074 mosmol<sup>-1</sup>. Other test solutions were derived from the standard saline. A  $Ca^{2+}$ -free saline was obtained by substituting the  $CaCl_2 \cdot 2H_2O$  with  $MgSO_4 \cdot 6H_2O$ . A 15 mM  $K^+$  saline was obtained by increasing the KCl content to 15 mM, and the osmolarity was maintained by reducing the NaCl content accordingly. Caffeine solutions were made by adding caffeine to either the standard saline or a  $Mn^{2+}$ -containing (10 mM) saline at the concentration of 20 mM. Manganese solutions were obtained by the addition of  $MnCl_2 \cdot 4H_2O$  at the required concentration to either the standard saline,  $Ca^{2+}$ -free saline or 15 mM  $K^+$  saline; the osmolarity was maintained by reducing the NaCl content. All the  $Mn^{2+}$  solutions were adjusted to pH 7.45 before the addition of manganese, to prevent the formation of a precipitate. The pH of all the solutions was adjusted to 7.45 using NaOH (1M), HCL (1M). All the chemicals were obtained from Sigma Ltd. and were stored in the refrigerator (5°C).

## 3.3

## RESULTS

Low concentrations of  $Mn^{2+}$  (9-18  $\mu M$ ) added to the standard saline increased the size of the neuronally-evoked force in the SF muscle, with a force increase to  $124 \pm 46.69\%$  in the medial bundle and  $138.18 \pm 88.75\%$  in the lateral bundle of the control level at 9  $\mu M$  (Figs. 3.1 & 3.2). When contraction of the SF muscle was evoked by electrical field stimulation, force enhancement also occurred (Fig. 3.1): low concentrations of  $Mn^{2+}$  (18-364  $\mu M$ ) enhanced muscle force, with a force increase to  $140.65 \pm 73.52$  in the medial bundle and  $144.79 \pm 63.76\%$  in the lateral bundle of the control level at 18  $\mu M$   $Mn^{2+}$  (Fig. 3.3). Figure 3.1 shows an example of the original force traces recorded from the medial and lateral muscle bundles of the SF muscle in response to alternate nerve and electrical field stimuli under 9  $\mu M$   $Mn^{2+}$ .

Concentrations of  $Mn^{2+}$  above 90  $\mu M$  for neuronally-evoked excitation and above 364  $\mu M$  for electrical field stimulation reduced the force in a dose-dependent manner, until it was abolished at 2909  $\mu M$   $Mn^{2+}$  (Figs. 3.2; 3.3). Responses of the medial and lateral muscle bundles were closely similar over these ranges.

Simultaneous measures of EPSPs and neuronally-evoked muscle force indicated that the latter had a lower threshold for blocking by  $Mn^{2+}$  (Fig. 3.4). A 10 minute exposure to 3 mM  $Mn^{2+}$  blocked the neuronally-evoked muscle force in the medial muscle bundle, whereas the EPSPs recorded from a fibre of this bundle were still present, though reduced in size to approximately 25% of the control level. Eventually the EPSPs became blocked by  $Mn^{2+}$  as well.

It has been shown that application of solutions containing high concentrations of  $K^+$  ions causes both depolarisation of the muscle membrane and muscle force generation (see Section 2.3.6 and Fig. 2.15). This method of activation avoids the need for neuronal stimulation, since it by-passes the synaptic input. The SF muscle was activated by saline containing 15 mM  $K^+$  for 15 minutes, or until the plateau force was reached. The muscle contracture that followed this  $K^+$ -induced membrane depolarisation was progressively blocked by  $Mn^{2+}$  concentrations from 1 mM to 10 mM (Fig. 3.5). Inhibition was complete at 10 mM  $Mn^{2+}$  and above (Figure 3.6). In three preparations the  $K^+$ -induced

force was measured before and after the addition of 20 mM  $Mn^{2+}$  and related to the force induced by standard neuronal stimulation (Fig. 3.7).

While the muscle was inactivated by the presence of  $Mn^{2+}$ , application of caffeine (20 mM), which releases intracellularly-stored  $Ca^{2+}$  from the SR (see Section 2.4.5), still produced its normal level of contracture. (Fig. 3.8). No significant difference was found between the caffeine-induced force from the medial muscle bundle in  $Ca^{2+}$ -free saline and in  $Mn^{2+}$ -containing saline ( $p = 0.76$ ,  $T = -0.34$ ) (Fig. 3.9).

A further experiment that was conducted was based upon the procedure used by Nasu *et al.* (1995a) on guinea-pig ileal longitudinal smooth muscle. The SF muscle was depolarised for 30 minutes by 15 mM  $K^+$  saline and the addition of  $Mn^{2+}$  (20 mM) then blocked the  $K^+$ -induced force to a level below the original baseline (Figs 3.6 & 3.7). However, when the preparation was left under these conditions for a minimum period of 3 hours (Fig. 3.10), the force re-developed to a level equivalent to  $53 \% \pm 43.42$  in the lateral muscle bundle and  $29.26 \% \pm 21.52$  in the medial muscle bundle of the maximal standard neuronally-evoked force ( $n = 4$ ) (Fig. 3.11).

Preliminary voltage clamp experiments showed that 10 mM  $Mn^{2+}$  blocks the inward  $Ca^{2+}$  current in the  $S_1$  fibre type (Fig. 3.12).  $Mn^{2+}$  concentrations below 10 mM were not tested, and therefore this result does not exclude the possibility that  $Mn^{2+}$  has a different effect at lower concentrations.

### 3.4

### DISCUSSION

It has been well documented that  $Mn^{2+}$  can have a number of effects on muscle contraction (Fatt & Ginsborg, 1958; Hagiwara & Nakajima, 1966a; Suarez-Kurtz *et al.*, 1972). The results shown in Figures 3.1, 3.2 and 3.3 suggest that the same is true for the muscle fibres of SF muscle preparation of *Nephraps norvegicus*. Two effects were observed when increasing concentrations of  $Mn^{2+}$  were applied to the SF muscle preparation: an inhibition at concentrations above 18  $\mu M$  for the neuronally-induced

force and 364  $\mu\text{M}$  for the force evoked by electrical field stimulation, and an activation below these concentrations.

#### 3.4.1 $\text{Mn}^{2+}$ -inhibits muscle force

The inhibitory effect seen under high concentrations of  $\text{Mn}^{2+}$  (above 90  $\mu\text{M}$ ) is consistent with the inhibitory action of  $\text{Mn}^{2+}$  on voltage-gated  $\text{Ca}^{2+}$  channels found in other crustacean and invertebrate muscle preparations, where  $\text{Mn}^{2+}$  ions have been shown to block the inward current across the sarcolemma, inhibiting muscle force (Fatt & Ginsborg, 1958; Takeda, 1967; Mounier & Vassort, 1975). However, although muscle force was inhibited, the site of action of the  $\text{Mn}^{2+}$  ions is not clear. There are numerous points in the excitation-contraction (EC) coupling pathway where  $\text{Mn}^{2+}$  ions could block muscle force:

1. at the synapse, preventing  $\text{Ca}^{2+}$  ion entry which is required to trigger the discharge of synaptic vesicle.
2. blocking the voltage-gated  $\text{Ca}^{2+}$  channels in the muscle membrane, thereby inhibiting the inward  $\text{Ca}^{2+}$  current.
3. preventing  $\text{Ca}^{2+}$ -activation of the DHP-Ryanodine receptor complex.
4. preventing release of intracellularly stored  $\text{Ca}^{2+}$  from the SR.
5. blocking the  $\text{Ca}^{2+}$  binding site (troponin) of the contractile proteins, inhibiting cross-bridge attachment.

It is well documented that  $\text{Mn}^{2+}$  is a potent inhibitor of synaptic transmission (Katz & Miledi, 1969). If  $\text{Mn}^{2+}$  ions were to block muscle force by inhibiting the nerve synapse, then direct electrical stimulation of the muscle which by-passes the neuromuscular synapse, would be expected to remain effective in inducing muscle force. This was not the case, since  $\text{Mn}^{2+}$  blocks electrical field-induced contraction at approximately the same concentration as it blocks neuronally-evoked contraction (Figs. 3.1, 3.2 and 3.3). This result therefore suggests that  $\text{Mn}^{2+}$  acts beyond the synapse (although, this does not exclude the possibility that  $\text{Mn}^{2+}$  also blocks the synapse). The finding that  $\text{Mn}^{2+}$  blocks contractures induced by high  $\text{K}^+$  saline confirms that the  $\text{Mn}^{2+}$  is acting beyond the nerve synapse and that the sarcolemmal  $\text{Ca}^{2+}$  channels are involved (Figs. 3.5 & 3.6).

Experiments which recorded both the neuronally-evoked muscle force and the excitatory post-synaptic potential (EPSP) of the  $S_1$  and the  $S_2$  fibres types (Fig. 3.4) show that muscle force is blocked at a lower threshold. Thus later steps of the CICR process are inhibited before the earlier steps, and thus it is possible to conclude that  $Mn^{2+}$  blocks at more than one point in the muscle activation process.

Caffeine releases  $Ca^{2+}$  from the SR (see Section 2.4.5.). When force was inhibited by 20 mM  $Mn^{2+}$ , an application of caffeine (20 mM) stimulated a force which was comparable in size to that observed when caffeine was applied in control conditions (Figs. 3.9). This suggests that applied  $Mn^{2+}$  does not affect the intracellular processes of  $Ca^{2+}$  release from the SR, or the  $Ca^{2+}$ -activation of the contractile elements themselves, through the binding to regulatory proteins.

### 3.4.2 $Mn^{2+}$ -evoked muscle force

The second effect, which was observed when  $Mn^{2+}$  was applied at low concentrations (9-45  $\mu M$ ) to the SF muscle, was an increase of muscle force above that of the control level, evoked by neuronal and direct field stimulation (Figs. 3.1, 3.2 and 3.3). As  $Mn^{2+}$  ions have been shown to carry the inward current through membrane  $Ca^{2+}$  channels in a variety of preparations (Yamagishi, 1973; Delahayes, 1975; Fukunda & Kawa, 1977; Palade & Almers, 1978; Anderson, 1979), this result suggests that the  $Mn^{2+}$  ions can also pass through ion channels in the sarcolemma of lobster SF fibres. However, at the moment there is no direct evidence for this. Against this idea, if  $Mn^{2+}$  ions were capable of penetrating the muscle fibres by membrane  $Ca^{2+}$  channels, it would be expected that in the absence of  $Ca^{2+}$  ions,  $Mn^{2+}$  ions could induce muscle force. However, no force was recorded in experiments where  $Mn^{2+}$  was applied under  $Ca^{2+}$ -free conditions (data not shown).

One possible explanation for this response is that  $Mn^{2+}$  might selectively block the inhibitory nerve which innervates the SF muscle. Work by Nichols and Nakajima (1975) has shown that 5 mM  $Mn^{2+}$  completely blocked the inhibitory post-synaptic potentials (IPSPs) recorded from lobster and crayfish stretch receptor neurones. The Sr3 nerve which innervates the SF muscle comprises 5 excitatory axons and one inhibitory axon

(see Fig. 2.2 and Section 2.1.5). At  $Mn^{2+}$  concentrations which are too low to block the inward  $Ca^{2+}$  current across the sarcolemma, it is possible that the inhibitory nerve is selectively blocked, thus leading to the observed increase in force. EPSPs are not inhibited by low  $Mn^{2+}$  concentrations. At higher concentrations, the voltage clamp experiments show that the inward current is blocked by  $Mn^{2+}$ . As the  $Mn^{2+}$  concentration was increased throughout an experiment the force increase observed at low concentrations will be masked as  $Mn^{2+}$  ions block inward current. In crustaceans,  $\gamma$ -aminobutyric acid (GABA) is the inhibitory neurotransmitter (Dudel *et al.*, 1980). Picrotoxin is known to selectively block the GABA-activated chloride conductances in invertebrate neuromuscular systems (Nistri & Constanti, 1979; Tallman & Gallagher, 1985). A series of experiments using picrotoxin to block the inhibitory nerve innervating the SF muscle preparation was conducted to see if a similar force increase under picrotoxin was observed to that recorded under low  $Mn^{2+}$  solutions. Unfortunately the results from these experiments were inconclusive and consequently could not be directly compared to the  $Mn^{2+}$  results.

One argument against this theory is that a similar force increase was observed at low  $Mn^{2+}$  concentration in response to electrical field stimulation of the muscle, which is thought to by-pass the neuronal activation step. It is possible however, that this method also activates the Sr3 nerve. This needs to be further elucidated before any firm conclusions can be made.

Force induced by  $Mn^{2+}$  ions was also observed in the long term  $Mn^{2+}$  exposures, which were based upon the work of Nasu and colleagues on smooth muscle (Nasu *et al.*, 1995a). They showed that when guinea-pig ileal longitudinal muscle fibres were activated by high- $K^+$ , the addition of  $Mn^{2+}$  abolished muscle force, but that after a period of 4 hours force re-developed to a level equivalent to the initial  $K^+$ -induced contracture. The addition of the L-type channel blockers, nifedipine and D-600 dose-dependently inhibited the redevelopment of tension, whereas the addition of the T-type channel blocker nickel ( $Ni^{2+}$ ) had no effect on tension. Further experiments using labelled  $^{45}Ca$  showed that during the  $Mn^{2+}$ -induced re-development of tension, the  $^{45}Ca$  uptake remained unchanged from the control level (Nasu *et al.*, 1995a). This result is consistent with the experiments conducted under  $Ca^{2+}$  free conditions which showed that muscle force was not correlated to the influx of  $Ca^{2+}$ . Other workers have also shown that  $Mn^{2+}$

can activate smooth muscle under  $\text{Ca}^{2+}$ -free, high  $\text{K}^+$  conditions (Lategan & Brading, 1988; Sakai and Uchida, 1981). These effects of  $\text{Mn}^{2+}$  do not seem to involve the SR. Pre-treatment of the ileal longitudinal muscle fibres with the  $\text{Ca}^{2+}$ -release blocker ryanodine, and the specific  $\text{Ca}^{2+}$ -ATPase blocker cyclopiazonic acid, have no effects on the contractions evoked by  $\text{Mn}^{2+}$ , or on  $\text{Mn}^{2+}$  uptake in a  $\text{Ca}^{2+}$ -free, high- $\text{K}^+$  medium (Nasu et al., 1995b). From these results it was suggested that  $\text{Mn}^{2+}$  was able to penetrate the muscle fibres via L-type  $\text{Ca}^{2+}$  channels. In addition to this the use of labelled  $\text{Ca}^{2+}$  ions showed that the  $\text{Mn}^{2+}$ -induced force did not correlate to the influx of  $\text{Ca}^{2+}$  and these effects of  $\text{Mn}^{2+}$  do not seem to involve the SR (Nasu *et al.*, 1995b). It was concluded from these results that  $\text{Mn}^{2+}$  initially reduced the  $\text{K}^+$ -induced tonic tension by inhibiting the  $\text{Ca}^{2+}$  influx through L-type  $\text{Ca}^{2+}$  channels, but that after a long period of depolarisation the  $\text{Mn}^{2+}$  is able to penetrate via the same L-type  $\text{Ca}^{2+}$  channels, where it by-passes the SR and directly activates the contractile elements.

When the results obtained by Nasu *et al.* (1995a, 1995b) and Nasu (1995) are compared to the results for the SF muscle preparation of *Nephrops* the following similarities are observed, which suggest that  $\text{Mn}^{2+}$  is capable of penetrating intact fibres:

1. the increase in muscle force above the control level, seen when low  $\text{Mn}^{2+}$  concentrations (9-45  $\mu\text{M}$ ) were applied (Fig. 3.1, 3.2 and 3.3).
2. the rapid inhibition of  $\text{K}^+$ -induced tonic tension by  $\text{Mn}^{2+}$  (Fig. 3.6).
3. the release of intracellular  $\text{Ca}^{2+}$  by caffeine, in the presence of  $\text{Mn}^{2+}$ , indicating that the  $\text{Mn}^{2+}$  does not affect the release of  $\text{Ca}^{2+}$  from the SR (Fig. 3.8), although this does not exclude the possibility that  $\text{Mn}^{2+}$  is not affecting an amplification step involving the DHP/ryanodine receptor complex.
4.  $\text{K}^+$ -induced tension was inhibited by 20 mM  $\text{Mn}^{2+}$ , but when the preparation was left for a period of 3 hours under the same conditions, the tension re-developed to a level approximately 50% that of the control.

### 3.4.3 How does $\text{Mn}^{2+}$ increase muscle force?

There are two main mechanisms by which  $\text{Mn}^{2+}$  ions could potentiate the muscle force:

1. the  $Mn^{2+}$  could be directly activating the contractile proteins. The neuronally-evoked depolarisations of the sarcolemma cause voltage-gated  $Ca^{2+}$  channels to open and it is possible that  $Mn^{2+}$  could have moved through these open channels into the fibres, diffused to the contractile apparatus, bound to the troponin regulatory proteins and induced contraction. This explanation seems very unlikely, since the response is seen only at low  $Mn^{2+}$  concentrations (Figs. 3.1-3.3) and the time scale is very short for the  $Mn^{2+}$  ions to reach the contractile proteins. It would also be expected that there would be an increase in the resting force with time during these experiments as more  $Mn^{2+}$  ions reached the contractile proteins, but this was not observed.

the only situation in which such an effect may have operated was when the fibres were exposed to high concentrations of  $Mn^{2+}$  ions for long periods while contracting in response to  $K^+$  depolarisation (Figs. 3.10 & 3.11). The actual amount of  $Mn^{2+}$  entering the membrane-intact fibres is not known, but is likely to be small. This is considered further in Chapter 5, which describes experiments performed on skinned fibres.

2. it is possible that although  $Mn^{2+}$  does not directly affect  $Ca^{2+}$  release from the SR, as demonstrated by the caffeine experiments (Figs. 3.8 & 3.9), it may affect the amplification step which involves the SR  $Ca^{2+}$ -release ( $Mn^{2+}$ -induced- $Ca^{2+}$ -release (MICR)). Small depolarisations induced by neuronal stimulation or by electrical field stimulation of the muscle may facilitate the entry of small numbers of  $Mn^{2+}$  ions as well as  $Ca^{2+}$  ions through voltage-gated  $Ca^{2+}$  channels, which may subsequently bind to the ryanodine receptors. Higher concentrations of  $Mn^{2+}$  (5 mM and above) blocked the inward  $Ca^{2+}$  current across the sarcolemma (Figure 3.12) and caused an inhibition of force. This is in accord with the fact that MICR is observed only at low  $Mn^{2+}$  concentrations.

The fact that this Chapter only deals with the effects of  $Mn^{2+}$  on intact fibres means that the results can only be interpreted at the level of the muscle membrane and intracellular stores. As yet the mechanism by which  $Mn^{2+}$  enters SF muscle fibres has not yet been determined, and further investigations involving the voltage clamp technique, which can be used to measure the inward current carried by  $Ca^{2+}$  ions through the voltage-gated

$\text{Ca}^{2+}$  channels of muscle membrane, are needed to clarify this. However, the work conducted on smooth muscle (Lategan & Brading, 1988; Sakai & Uchida, 1981; Nasu *et al.*, 1995a, 1995b, & Nasu, 1995), would suggest that under certain conditions the  $\text{Mn}^{2+}$  ions are passing through L-type  $\text{Ca}^{2+}$  channels and are able to activate muscle force above that of the control level. Further experiments involving the voltage clamp technique are required to elucidate this theory further, but from the preliminary voltage clamp data it seems that higher concentrations of  $\text{Mn}^{2+}$  ions block the inward  $\text{Ca}^{2+}$  current.

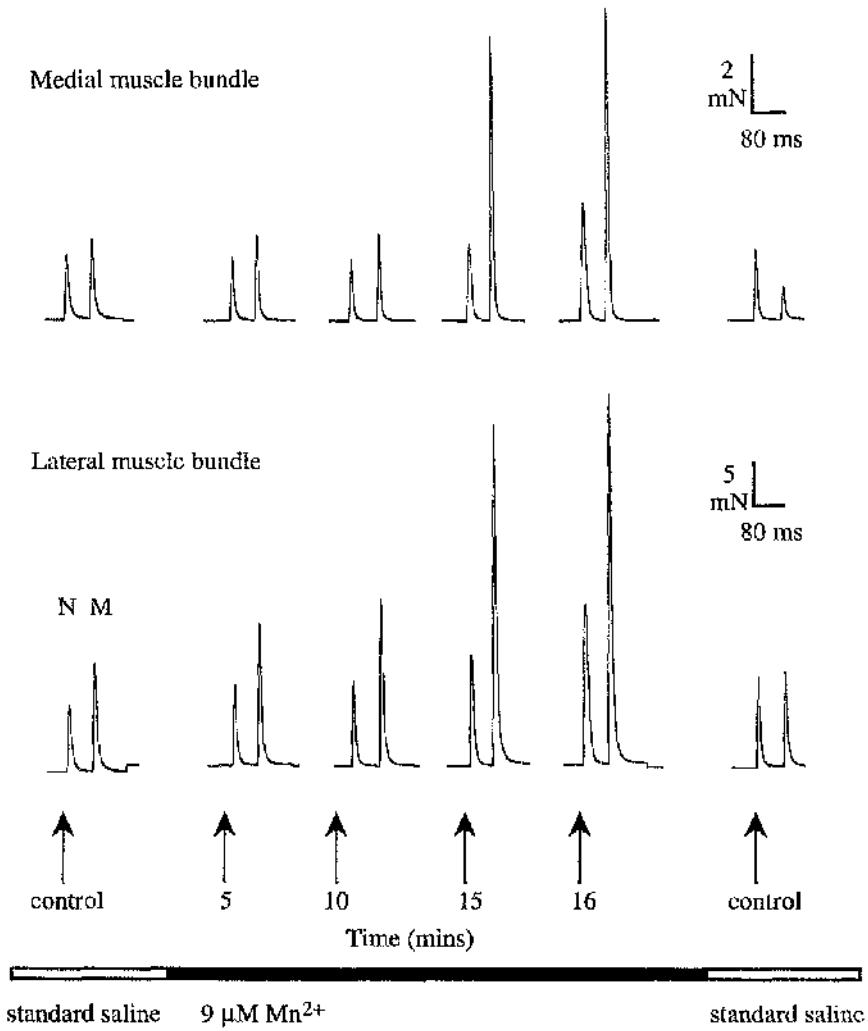


Fig.3.1  
Enhancement of force by low concentrations of manganese.

The effect of manganese on the neuronally-evoked force (N) and the force evoked by electrical field stimulation (M) of the SF muscle bundles.

Note that the force produced by electrical field stimulation at 16 minutes is greater than that produced by neuronal stimulation; arrows indicate the time of stimulation.

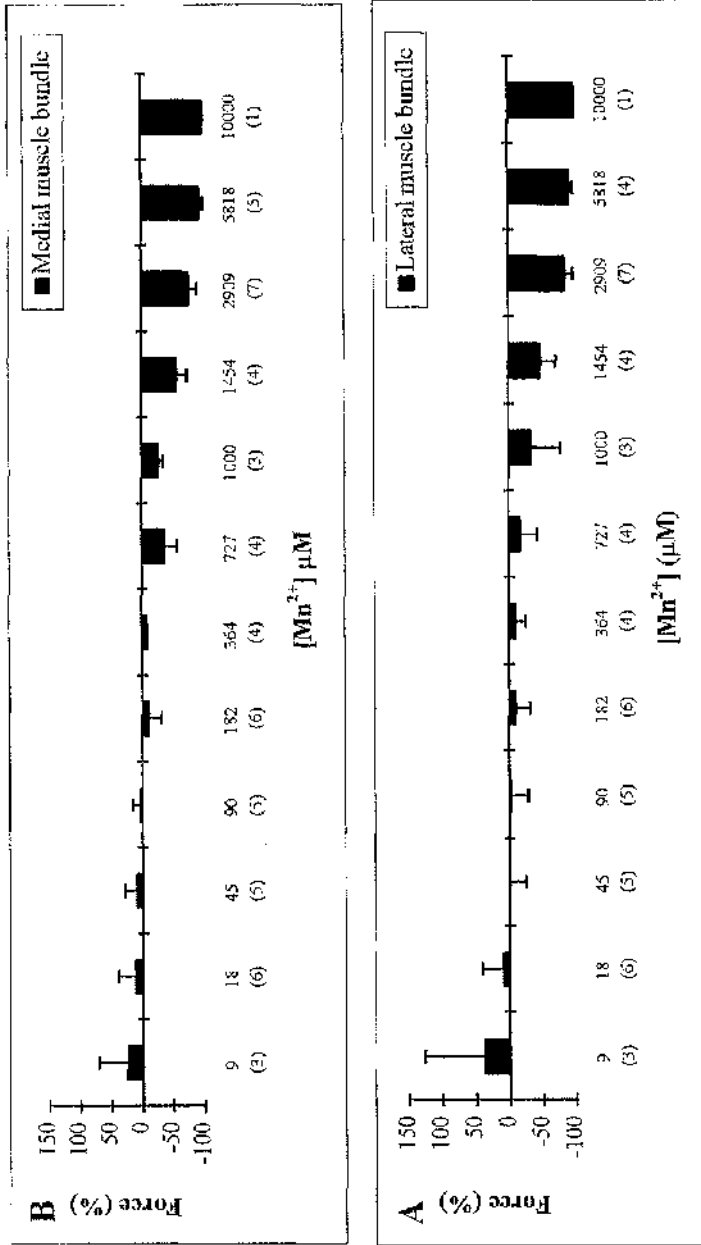


Fig. 3.2  
Effects of Mn<sup>2+</sup> on the neurally-evoked force of the SF muscle bundles.  
Mean ± S.D. values for force from the lateral (A) and medial (B) muscle bundles in response to standard neuronal stimulation; control force = 0 %; negative values represent a reduction in muscle force and positive values represent an increase in muscle force above the control level, n values are indicated in parenthesis.

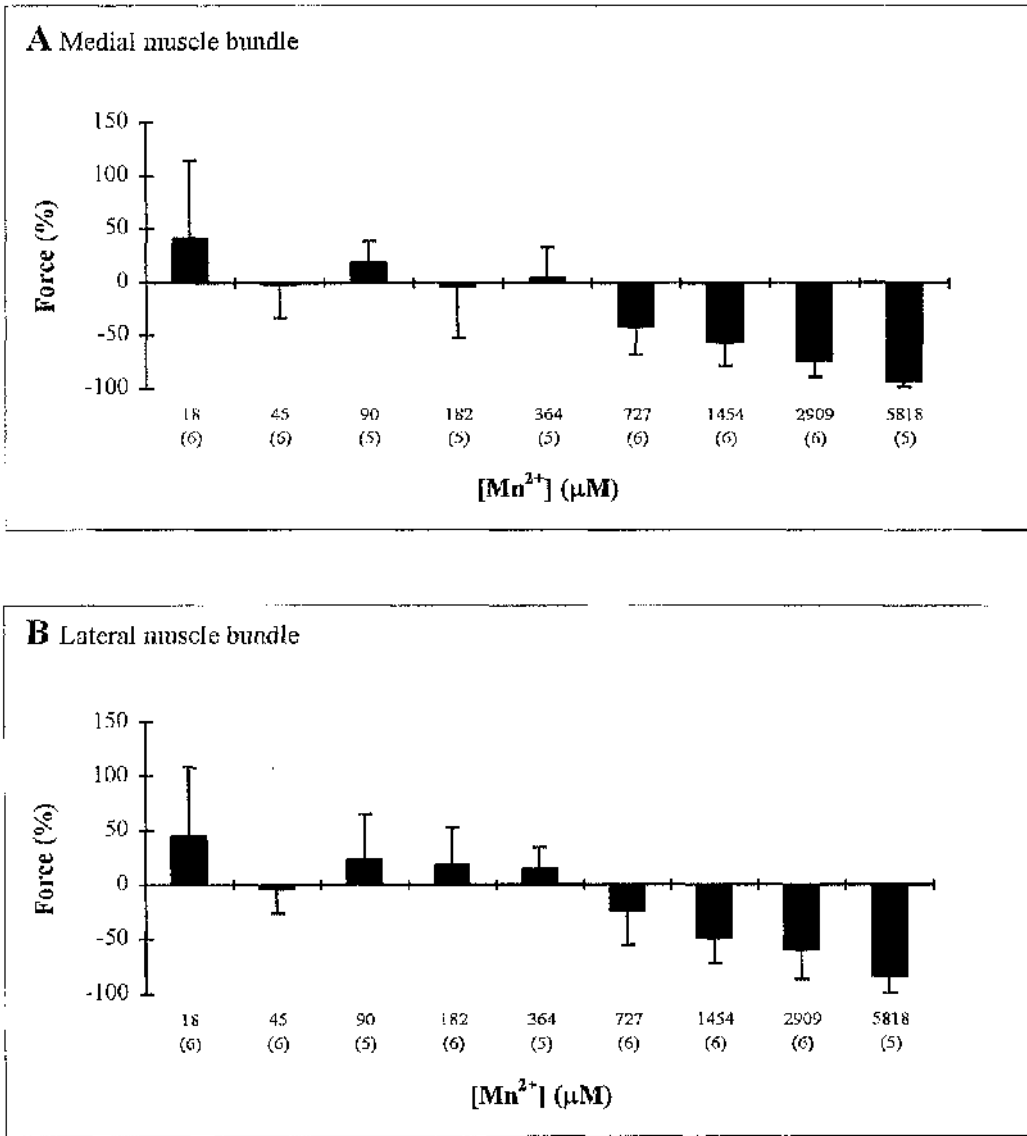


Fig. 3.3

Effects of Mn<sup>2+</sup> on the force evoked by electrical field stimulation of the SF muscle bundles.

Mean ± S.D. values for force from the medial (A) and lateral (B) bundles; control = 0 %; negative values represent a reduction in muscle force and positive values represent an increase in muscle force above the control level; n values are indicated in parenthesis.

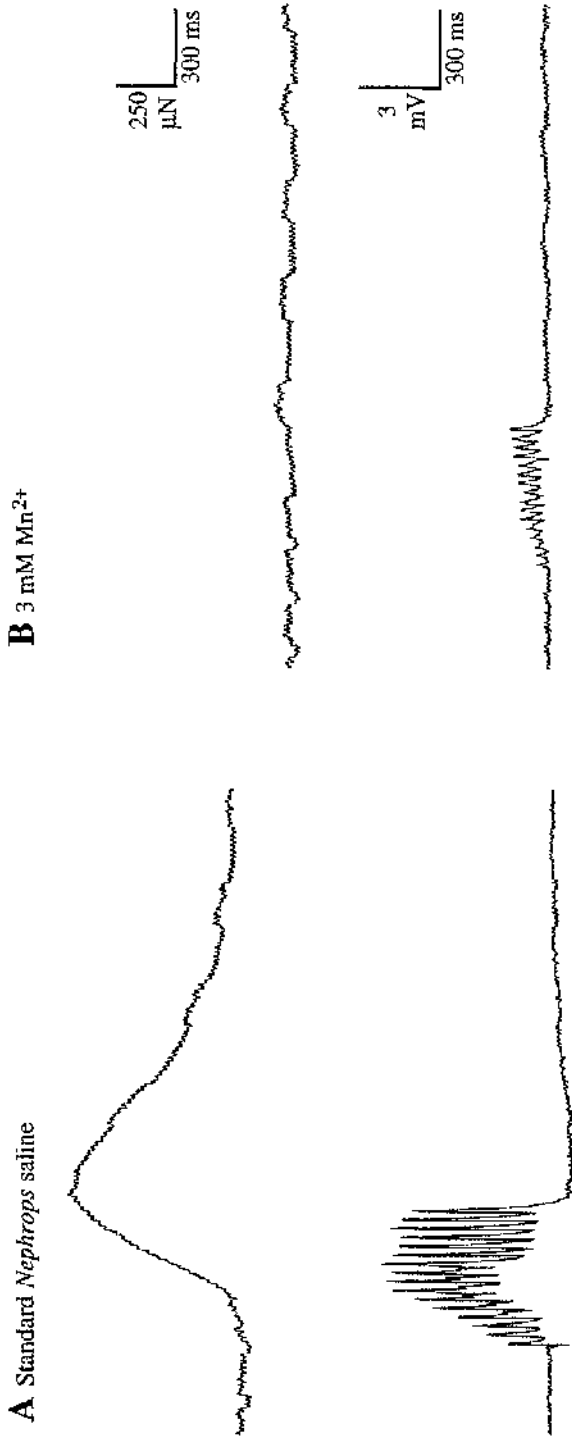


Fig. 3.4  
Effect of  $Mn^{2+}$  on force and EPSPs.

(A) Standard *Nephrops* saline: Force produced by the medial bundle in response to standard neuronal stimulation of the SF muscle and EPSPs from the S<sub>2</sub> fibre type.

(B) 3 mM  $Mn^{2+}$ : a 10 minute  $Mn^{2+}$  exposure blocks the force while the EPSPs still remains present, although reduced in size.

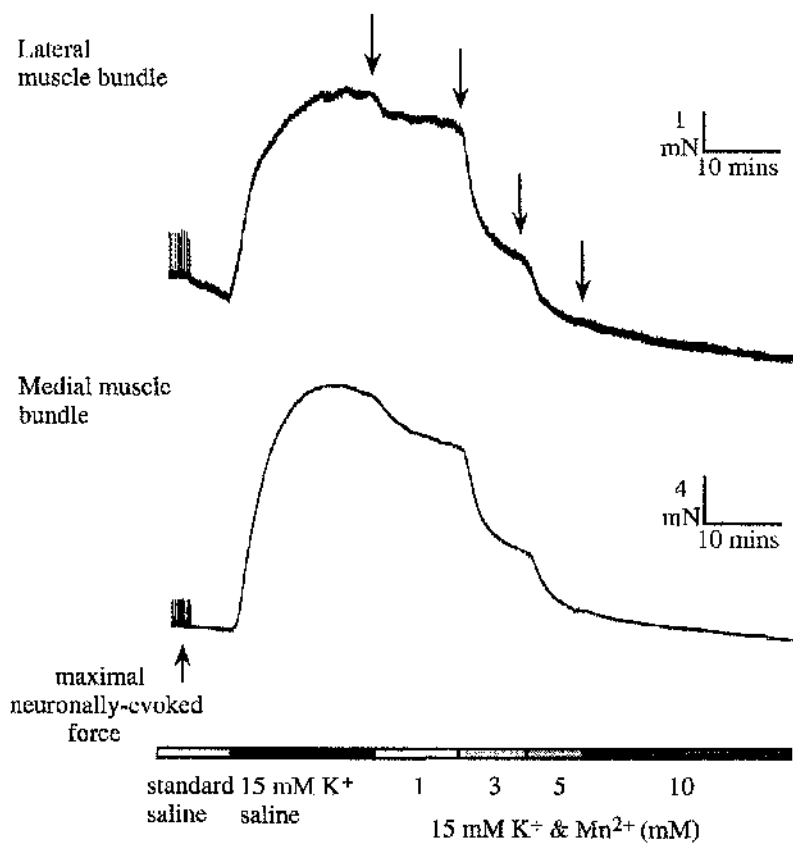


Fig. 3.5  
Mn<sup>2+</sup> inhibits K<sup>+</sup>-induced force.

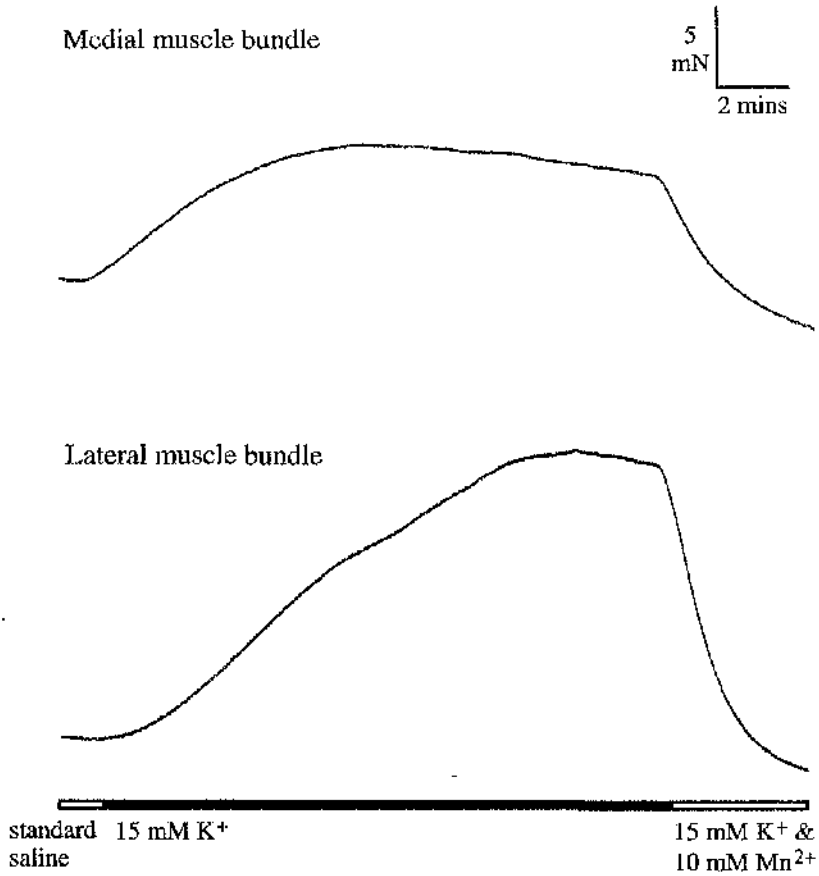


Fig. 3.6  
K<sup>+</sup>-induced force is blocked by 10 mM manganese in the SF muscle bundles.

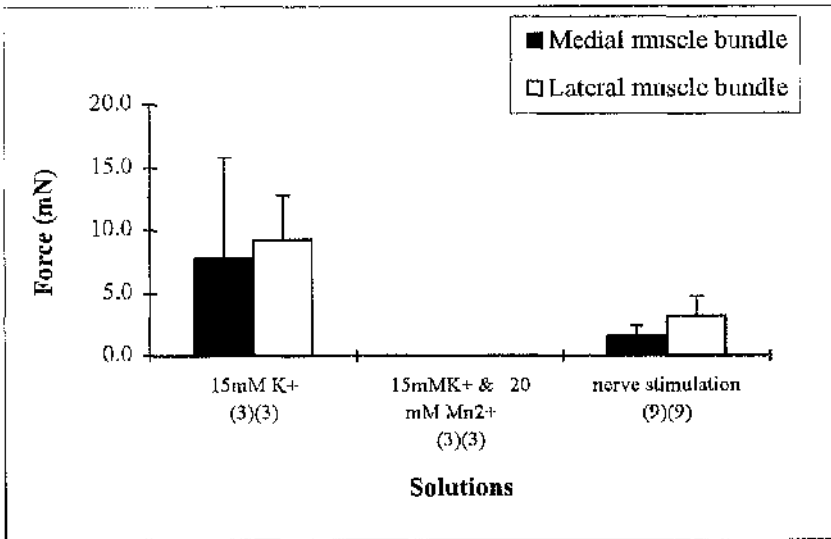


Fig. 3.7

Mn<sup>2+</sup> blocks K<sup>+</sup>-induced force.

Mean  $\pm$  S.D. values for force recorded from the medial and lateral bundles of the SF muscle when depolarised by 15 mM K<sup>+</sup> saline for 15 minutes and after the addition of 20 mM Mn<sup>2+</sup>. Values for the maximal neuronally-evoked force are shown for comparison (3 measures from each preparation); n values are indicated in parenthesis.

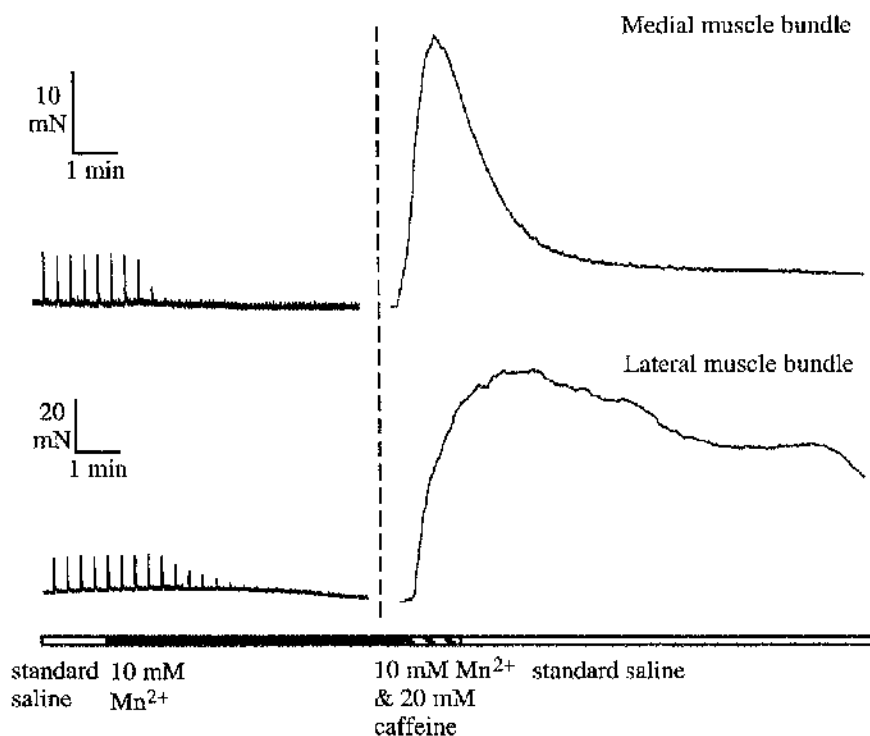


Fig. 3.8  
Application of caffeine induces force after application of high concentration manganese.

Standard neuronal stimulation of the SF muscle bundles was blocked by manganese and subsequently 20 mM caffeine induces large contractures in both muscle bundles. The application of high manganese saline lasted for 15 minutes; the vertical dashed line indicates that there is a break in the force traces

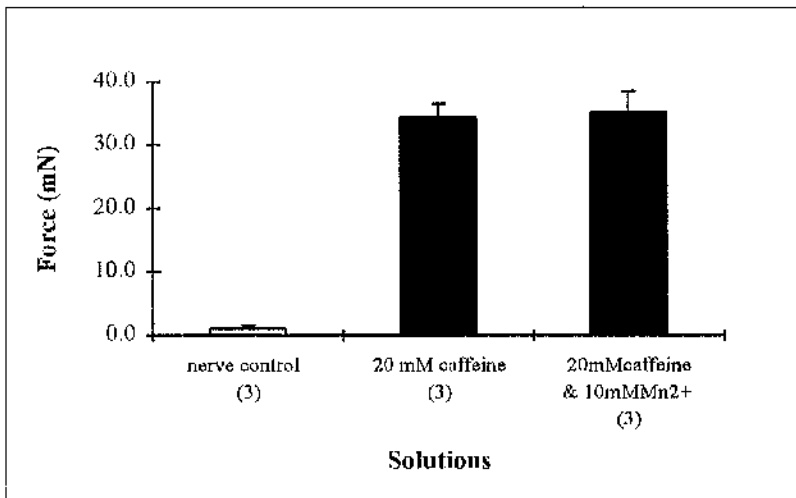


Fig. 3.9

Caffeine-induced contractures in the presence of  $Mn^{2+}$ .

Mean  $\pm$  S.D. values for caffeine-induced force from the medial bundle of the SF muscle; control: maximal neuronally-induced force; n values are indicated in parenthesis.

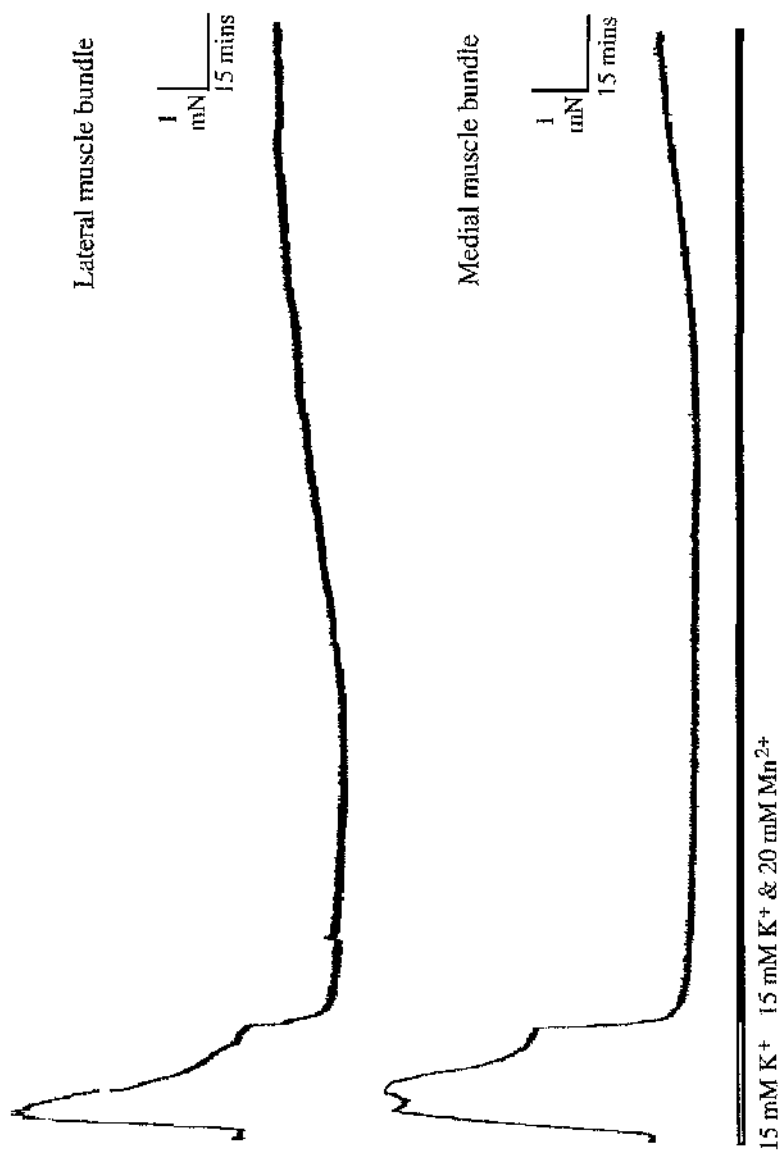


Fig. 3.10  
Long term Mn<sup>2+</sup> experiment.

The initial force induced by K<sup>+</sup> is inhibited by Mn<sup>2+</sup>, but re-develops after 3 hours.

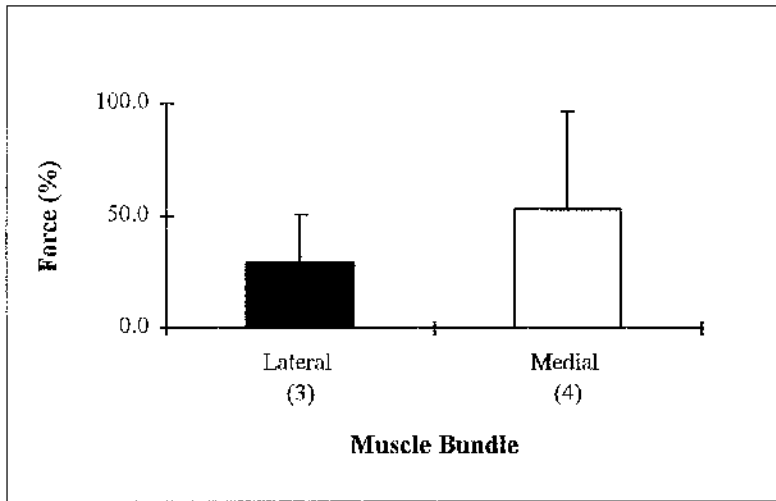
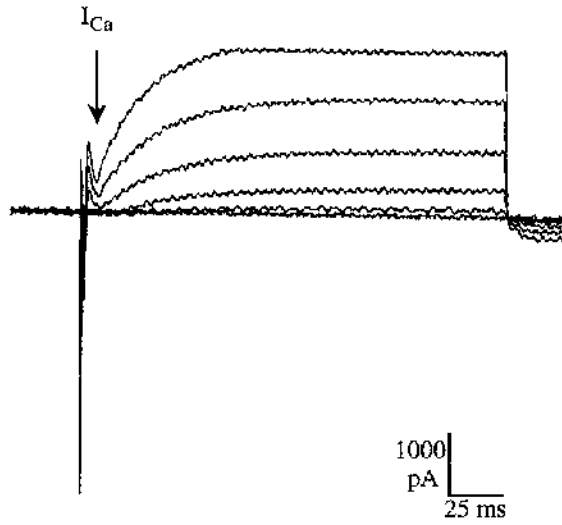


Fig. 3.11

Delayed force increase induced by  $Mn^{2+}$  in the presences of high  $K^+$  saline.

Mean  $\pm$  S.D. values for resting force in the muscle bundles of the SF muscle when exposed to 20 mM  $Mn^{2+}$  (3 hours) under  $K^+$ -induced (15 mM) depolarisation. 100 % = the maximal force evoked by standard neuronal stimulation; n values are indicated in parenthesis.

**A** Standard *Nephrops* saline



**B** 10 mM  $\text{Mn}^{2+}$

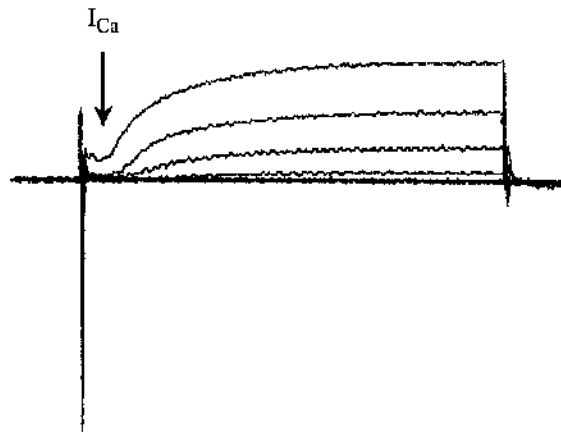


Fig. 3.12  
The inward  $\text{Ca}^{2+}$  currents are blocked by  $\text{Mn}^{2+}$ .

(A) Voltage clamp recording of inward  $\text{Ca}^{2+}$  currents in standard saline containing TEA.

(B) 10 mM  $\text{Mn}^{2+}$  blocks the inward  $\text{Ca}^{2+}$  currents. Inward currents indicated by the arrow.

## **Chapter 4**

### **Myofibrillar force kinetics of different fibre types measured in chemically skinned fibres**

## 4.1

## INTRODUCTION

## 4.1.1 The role of troponin (Tn) in muscle contraction

The studies of Ebashi and workers have established in actin-regulated muscles such as vertebrate skeletal, vertebrate cardiac and certain invertebrate skeletal muscles including those of decapod crustaceans (see Section 1.2.8) that the protein troponin which is associated with the thin filaments, activates contraction (Ebashi & Endo, 1968). The thin filaments are composed of 2 inter-twining helical chains of actin monomers, with 2 linear chains of tropomyosin molecules lying in the grooves between the actin chains. Two troponin molecules are attached at regular intervals (40 nm) along the helix, and for every troponin molecule there is a tropomyosin molecule and 7 actin subunits (Squire, 1981).

Troponin acts as the intracellular  $\text{Ca}^{2+}$  receptor which transmits the  $\text{Ca}^{2+}$  signal in the myoplasm to the actin filaments. By influencing filament structure troponin regulates potential crossbridge binding sites and hence the activity of the contractile ATPase (Leavis & Gergely, 1984; Ohtsuki *et al.*, 1986; Zot & Potter, 1987). The rise in intracellular  $\text{Ca}^{2+}$  to 1-10  $\mu\text{M}$  during muscle activation is detected by the troponin subunit C (Tn-C). In general Tn-C binds four  $\text{Ca}^{2+}$  ions per molecule, but the number of  $\text{Ca}^{2+}$  binding sites is dependent on muscle type. For example, the Tn-C of vertebrate skeletal muscle contains four  $\text{Ca}^{2+}$ -binding domains, whereas crustacean Tn-C has only one (Wnuk *et al.*, 1984). In vertebrate fast muscle there are 2 types of  $\text{Ca}^{2+}$  binding site:  $\text{Ca}^{2+}$ -specific or low-affinity sites which bind only  $\text{Ca}^{2+}$ , and high affinity or Ca-Mg binding sites which are less specific and can bind both  $\text{Mg}^{2+}$  and  $\text{Ca}^{2+}$  (Potter & Gergely, 1975). Crustacean Tn-C displays simple  $\text{Ca}^{2+}$ -binding properties (Wnuk & Stein, 1980; Wnuk *et al.*, 1984) in crayfish there are no Ca-Mg sites with high affinity for  $\text{Ca}^{2+}$  and only a single  $\text{Ca}^{2+}$ -specific site with an affinity in the range of physiological free  $\text{Ca}^{2+}$  concentration (binding constant ( $K_{\text{Ca}}$ ) =  $2 \times 10^5 \text{ M}^{-1}$ ) (Wnuk, 1989).

Troponin is anchored to tropomyosin by the subunit Troponin T (Tn-T). Tropomyosin amplifies the action of troponin (Ebashi *et al.*, 1969; Perry *et al.*, 1973). In the absence of  $\text{Ca}^{2+}$ , tropomyosin is held in its peripheral position, with the inhibitory subunit (Tn-I) bound to actin, and thus inhibits the actomyosin-ATPase activity. Tn-I is regulated by

Tn-C (Hartshorne, 1969) and only when Tn-C and Tn-I are activated together do they form the  $\text{Ca}^{2+}$  switch that regulates actomyosin-ATPase in a  $\text{Ca}^{2+}$ -dependent manner.  $\text{Ca}^{2+}$  binding to Tn-C relieves the inhibitory action of Tn-I and initiates a change in the interaction of the thin filament proteins and in the position of tropomyosin. The bonds between Tn-C and Tn-I are strengthened, which in turn weakens the interaction between Tn-I and actin. As Tn-I no longer binds the actin filament, the tropomyosin-troponin complex moves into the central groove between the actin strands, thereby exposing the binding sites for myosin crossbridges. In this position tropomyosin no longer blocks the attachment of myosin crossbridges to the actin, and activates the myosin-ATPase, thus initiating the contractile process. Myosin subfragment S-1 of the crossbridges contains both the actin binding site and the myosin ATPase (Lowey, 1971). These 2 sites influence each other, so that as soon as myosin binds ATP the actin binding site dissociates from actin and ATP is hydrolysed. Interaction with actin accelerates the rate-limiting step of the ATP splitting mechanism, which results in the release of  $\text{ADP-P}_i$  from the nucleotide binding site.

#### **4.1.2 Regulation of muscle contraction**

##### **4.1.2.1 Steric hindrance hypothesis**

X-ray diffraction studies have led to the proposal that actin-regulation occurs through steric hindrance (Haseigrove, 1973; Huxley, 1973; Parry & Squire, 1973), whereby in the resting state, tropomyosin sterically hinders the interaction of myosin and actin.  $\text{Ca}^{2+}$  binding to Tn produces movement of tropomyosin such that myosin can now interact with actin. However, more recent studies indicate that the process is more complex than this simple model suggests (Weber & Murray, 1973; Eisenberg & Hill, 1985; El-Saleh *et al.*, 1986). The original version of the steric block hypothesis was abandoned when it became clear that crossbridges were attached to actin, albeit weakly, even in the relaxed state. It has since been suggested that both  $\text{Ca}^{2+}$  binding and crossbridge attachment play a role in regulating actin-myosin interaction, ATPase activity, and force generation (Greene & Eisenberg, 1980; Brenner, 1988).

#### 4.1.2.2 $\text{Ca}^{2+}$ binding and crossbridge attachment regulation

There is strong evidence from studies on isolated muscle proteins, skinned fibres and intact muscle fibres that both  $\text{Ca}^{2+}$  binding and crossbridge attachment play roles in the regulation of contraction (Greene & Eisenberg, 1980; Brenner, 1988). For example, it has been proposed that the lag between force development and stiffness is due to the transition of cross-bridges between a low- and a high-force producing state and that this is dependent on the number of attached crossbridges (Bagni, *et al.*, 1988). The biochemical results of Greene and Eisenberg (1980) and the skinned fibre data of Brenner (1988) support the theory that  $\text{Ca}^{2+}$  regulates a rate constant leading to strong crossbridge attachment and force production. In addition to this, the occurrence of weak crossbridge attachments in resting muscle fibres in the absence of  $\text{Ca}^{2+}$  supports the view that  $\text{Ca}^{2+}$  mediates strong binding between actin and myosin.

#### 4.1.3 Skinned fibre experiments

Skinned muscle fibres have had their muscle membranes destroyed, either mechanically, chemically or by a freeze-drying process, which exposes the contractile proteins. The functionally isolated contractile machinery of skinned muscle fibres provides an ideal preparation with which to investigate the mechanical properties of different fibre types. Kinetic experiments on skinned muscle fibres and myofibrillar bundles provide information about the contractile performance and functional role of muscle fibres. In addition to this, by comparing the mechanical properties of fibres with different myofibrillar protein isoforms, information can be obtained about the underlying contractile mechanisms.

#### 4.1.4 Co-operativity

The binding of  $\text{Ca}^{2+}$  to isolated Tn may be described in terms of Michaelis-Menton kinetics.  $\text{Ca}^{2+}$  binding to specific sites depends on the  $\text{Ca}^{2+}$  concentration in a hyperbolic manner over a concentration range of two orders of magnitude (Zot *et al.*, 1983). In crustacean and vertebrate muscle fibres co-operativity is thought to be based on the

interaction of separate molecules, rather than on the interaction of several binding sites within the same molecule (Galler & Rathmayer, 1992). The Hill coefficient is a measure of co-operativity of the  $\text{Ca}^{2+}$ -force relationship. If Hill coefficient values of greater than 2 are obtained, the relationship between force development or ATPase activity and  $\text{Ca}^{2+}$  is highly co-operative. Mammalian (Stephenson & Forest, 1980) and arthropod fast fibres (Galler & Rathmayer, 1992) fulfil this criterion having Hill coefficients  $>2$  while slow fibres do not.

#### 4.1.5 Isoforms of troponin

The differences in the force/pCa relationship may also reflect differences in the properties of the regulatory proteins. Crustacean muscle fibres have been shown to express multiple isoforms of Tn-C (crayfish: Kobayashi *et al.*, 1989; barnacle: Collins *et al.*, 1991; lobster: Miegel *et al.*, 1992), and the  $\text{Ca}^{2+}$ -binding properties of the two main isoforms have been determined (Wnuk, 1989; Ashley, *et al.*, 1991). In lobsters three main isoforms occur (Garone *et al.*, 1991) and unique combinations of these are expressed in *Homarus americanus* (Mykles, 1985)

#### 4.1.6 Stretch activation

When small rectangular length changes (stretches) of up to 0.5% of the resting fibre length and lasting less than 0.5 ms are applied to maximally  $\text{Ca}^{2+}$ -activated (pCa 4.7) muscle fibres, stretch-induced delayed force increase (stretch activation) is observed. This is seen after completion of the length change, whereby a decrease in force is followed by a delayed transient increase. Stretch activation can be recorded from most fibre types but is not as pronounced in some. For example, insect flight muscle shows very pronounced stretch activation, whereas in vertebrate skeletal and heart muscle this property is less apparent (Steiger, 1977). Recent studies on rat, fish, crayfish and locust muscle fibres have shown that the differences in the kinetics of stretch activation show a strong correlation to fibre type (Galler, 1994).

In addition to providing a means for fibre identification, stretch activation also provides information about the crossbridge cycling steps in different fibre types. The force transients during stretch activation are thought to represent certain steps of crossbridge turnover and the myosin ATPase cycle under isometric conditions (Steiger & Abbott, 1981). The large variation in the velocity of stretch activation between different fibre types indicates that there are considerable differences in the isometric crossbridge steps, and it is thought that velocity is determined by the myosin heavy chain (MHC) isoforms that are present (Galler *et al.*, 1994).

#### 4.1.7 $\text{Ca}^{2+}$ -sensitivity

The processes involved in the force increase observed during  $\text{Ca}^{2+}$ -activation of the myofibrils include both the regulatory processes ( $\text{Ca}^{2+}$  binding and conformational changes in the regulatory proteins) and the subsequent steps of crossbridge cycling. The contribution of myofibrillar kinetics to fibre activation and relaxation under physiological conditions has been investigated by measuring the dynamics of  $\text{Ca}^{2+}$ -activation (Stephenson & Williams, 1981). As well as this, the relationship between the free  $\text{Ca}^{2+}$  and the steady state isometric force provides information about the ability of individual fibres to regulate their force output under various intracellular  $\text{Ca}^{2+}$  conditions (Stephenson & Forest, 1980).

#### 4.1.8 Stiffness

In the relaxed state of muscle, detached crossbridges are in dynamic equilibrium with weakly attached ones, and  $\text{Ca}^{2+}$ -activation transforms the weakly attached crossbridges to a strongly bound, force-generating state, giving rise to increased stiffness (Brenner, 1988). During maintained contraction, crossbridges are continuously cycling between strongly bound states and various forms of weakly bound state, and the apparent rate constants are affected by the crossbridges entering and leaving the force-generating crossbridge states.

Mechanical and X-ray diffraction experiments indicate that there are two types of attached crossbridge state: those with low stiffness and those with high stiffness (Huxley, 1980). The low stiffness crossbridges are involved at the beginning and end of the crossbridge cycle, whereas the high stiffness crossbridges are important for the generation of force (Huxley & Kress, 1985).

Fibre stiffness can be estimated by determining the instantaneous tension change produced by a small length change imposed on one end of the fibre whilst maximally activated. Under these conditions most of the compliance originates from the crossbridges themselves (Ford *et al.*, 1981), and it is assumed that crossbridge elasticity is the same during lengthening as in isometric conditions, and that in this state any changes in stiffness indicate corresponding changes in the number of attached crossbridges.

#### 4.1.9 Speed of muscle contraction and shortening velocity

Many different parameters control the speed of muscle contraction. Some of these are structural, such as the delivery of  $\text{Ca}^{2+}$  ions to the interior of the muscle fibre, which is affected by the extent of the transverse tubule system and the number of triadic junctions. Faster contraction is generally correlated with a larger junctional area between the T-system and the SR, which increases the delivery rate of  $\text{Ca}^{2+}$  ions to the contractile units. Others parameters are chemical, such as the myosin ATPase activity, which has been related to the speed of contraction. In studies on the crab *Eriphia spinifrons* it has been shown that slow muscle fibres contain myosin of low ATPase activity, whereas the fast types contain myosin with high ATPase activity (Maier *et al.*, 1984) suggesting that the rate of contraction may be determined by the rate of ATP splitting by actin-myosin crossbridges.

Maximal isometric force is equivalent to the load that can be supported by a fibre without causing a change in muscle length. Removal of the load (slackening) enables shortening to occur at its maximal speed (unloaded shortening velocity) and can be determined by measuring the time taken for the fibre to begin to re-develop force. Shortening velocity is thought to be related to crossbridge kinetics. Faster shortening requires a

greater rate of filament sliding, of attachment and detachment of crossbridges and of ATP splitting. The slack test method has been used to determine the unloaded shortening velocity of skinned muscle fibres (Galler & Rathmayer, 1992). The constant load method is another test which measures shortening velocity as well as providing other information such as the maximal power of a muscle fibre (the load at which the fibre is most energy efficient) (Woledge, 1985).

In skeletal muscle comprising different fibre types, shortening velocity has been found to be correlated with both the type of myosin heavy chain expression (Reiser *et al.*, 1988) and with the expression of different alkali light chain isoforms (Greaser *et al.*, 1988). The P-light chain may also be important in determining contraction speed (Hoffman *et al.*, 1990).

#### 4.1.10 Sarcomere length

Crustacean muscles of different types differ in sarcomere length (Jahromi & Atwood, 1971). Sarcomere length affects the speed of shortening and the energy expenditure required for the maintenance of a given force (tension cost). If the rate of filament sliding is dependent on the rate of crossbridge cycling, and hence on ATPase activity, and the force development is a function of the number of attached crossbridges, then, for a given rate of crossbridge cycling, two short sarcomere fibres will shorten at twice the rate of an equally long contractile unit made up of one long sarcomere. As force development is dependent on the number of crossbridges per sarcomere length, one long sarcomere fibre can have twice as many crossbridges attached as one short sarcomere fibre, which means that force development is twice as large. However, the maintenance of this large force requires only half as many ATP-splitting crossbridges, which means that it is less costly.

#### 4.1.11 Fibre identification

The gel electrophoresis technique has been used to divide crustacean muscle fibres into a number of phenotypic categories according to their myofibrillar protein assemblages, (Lehman & Szent-Györgyi, 1975; Silverman *et al.*, 1987). Individual fibres can express

multiple isoforms of certain contractile and regulatory proteins (Mykles, 1985; Mykles, 1988; Neil *et al.*, 1993) and since these differences remain distinguishable in skinned fibres, the different Tn isoforms can be used to reliably identify individual fibres using the gel electrophoresis technique (Neil *et al.*, 1993).

In a number of studies, the identification and classification of muscle fibre phenotypes has been based on either the myosin heavy chain (MHC) isoforms, which correspond to the histochemically determined myofibrillar adenosine triphosphatase (mATPase) activity and its pH stability (Staron & Pette, 1986), or on differences in the maximal unloaded shortening velocity ( $V_{max}$ ) (Eddinger & Moss, 1987). Studies on subtypes of rat fast muscle fibre show that only a weak correlation exists between MHC isoforms,  $V_{max}$  and fibre type (Bottinelli *et al.*, 1991). This raises the question of what is a reliable method for fibre type identification, and for this reason stretch activation was recorded in all experiments of this study, in order to provide a quick physiological method to identify individual fibres.

#### 4.1.12 The $S_1$ and $S_2$ fibre types of *Nephrops norvegicus*

The  $S_1$  and the  $S_2$  fibre phenotypes of the SF muscle of *Nephrops norvegicus* have been identified on the basis of their morphological, histochemical and biochemical properties (Fowler & Neil, 1992; Neil *et al.*, 1993; Galler & Neil, 1994) (see Section 2.1). This section discusses differences between the fibre types in their mechanical properties.

Using skinned muscle fibres, isometric force measurements on thin (<80  $\mu\text{m}$ ) myofibrillar bundles from freeze-dried fibres of the SF muscle have been correlated with subsequent identification of their phenotypes (Galler & Neil, 1994). Differences were observed in their kinetics following  $\text{Ca}^{2+}$  activation, as expressed in the half times of force development ( $S_1$ :  $416 \pm 174$  ms,  $S_2$ :  $762 \pm 199$  ms plus a delay of 280 ms) and relaxation ( $S_1$ :  $162 \pm 75$  ms,  $S_2$ :  $257 \pm 53$  ms), the  $\text{Ca}^{2+}$  sensitivity of force generation ( $\text{pCa}_{50}$ ) ( $S_1$ :  $5.40 \pm 0.12$ ,  $S_2$ :  $5.55 \pm 0.08$ ), their relatively flat pCa/force relationship, Hill coefficient values ( $S_1$ :  $2.78 \pm 0.35$ ;  $S_2$ :  $2.66 \pm 0.37$ ) and the kinetics of stretch activation, as determined by the delay of peak of stretch-induced force increase ( $S_1$ :  $91$  ms  $\pm$  30,  $S_2$ :  $493 \pm 436$  ms).

From these results it has been concluded that:

1. force production by the  $S_2$  myofibrillar bundle is more sensitive to the  $Ca^{2+}$  level than is force production by the  $S_1$  bundle. This is thought to reflect the different properties of the Tn isoforms expressed in the two fibre types (Tn-T<sub>1</sub>, Tn-I<sub>2</sub>, Tn-C<sub>1</sub> and Tn-C<sub>3</sub> are expressed in the  $S_2$  fibres, while  $S_1$  fibres express Tn-T<sub>2</sub>, Tn-I<sub>4</sub> and Tn-C<sub>2</sub> as the major isoforms).
2. changes in force output with changing intracellular free  $Ca^{2+}$  concentration are controlled over a relatively wide range and that complete activation and relaxation of the fibres requires large changes in  $Ca^{2+}$  concentration, which have the effect of slowing down the force response.
3. the low  $Ca^{2+}$  threshold of the  $S_2$  fibres may allow  $Ca^{2+}$ -dependent force production to occur at below the threshold  $Ca^{2+}$  concentrations that are required for other  $Ca^{2+}$ -dependent intracellular processes. The  $S_2$  fibres are used for long-lasting holding work and this would allow the medial fibres to be activated to some extent under normal resting conditions (Galler & Neil, 1994).
4. both fibre types are slowly contracting and exhibit low myofibrillar ATPase activity.
5. intrinsic myofibrillar kinetics are not the main time-limiting factor for either activation or relaxation of intact fibres under physiological conditions.
6. processes which precede crossbridge cycling seem to be the main time-limiting factors for the  $Ca^{2+}$  activation of the myofibrils.

The observed differences in the mechanical properties of these muscle fibre types provide information about their contractile performance and their probable functional role, and also give insights into their possible underlying contractile mechanisms. On the basis of the above findings it was proposed that  $S_2$  fibres have slow kinetics of activation and relaxation, slower crossbridge cycling and a higher  $Ca^{2+}$ -sensitivity of force generation. These characteristics suggest that the  $S_2$  fibres are specialised for long lasting force maintenance, appropriate for maintaining abdominal posture with a high economy of energy consumption and are more fatigue resistant, while the  $S_1$  fibres have faster kinetic characteristics and lower  $Ca^{2+}$ -sensitivity, suggesting that they control slow movements of the abdomen.

This chapter extends these mechanical studies on skinned  $S_1$  and the  $S_2$  fibres and in addition investigates the fast (F) fibre phenotype from the deep extensor muscle of *Nephrops norvegicus*. The work conducted in this chapter also provides relevant background information for a study of the effects of manganese on the contraction of skinned fibres (Chapter 5).

## 4.2

## MATERIALS & METHODS

### 4.2.1 Animal preparation

Adult *Nephrops norvegicus* of 50-90 mm carapace length were obtained from the Universities Marine Biological Station, Millport, Isle of Cumbrae, Scotland, UK. They were maintained in communal tanks of aerated, filtered, circulating sea water, at a temperature of 10-12°C, and fed on whitebait. For experiments, animals were anaesthetised by cooling on ice, the brain was destroyed and the abdomen was separated at its junction with the thorax.

### 4.2.2 The SF muscle bundle preparation

The dorsal part of the abdomen and the deep flexor muscles were removed to expose the slow flexor (SF) muscles. Cuts were made through the ventral membrane and exoskeletal rib in order to isolate the SF muscle without damaging the insertions of its fibres onto the surrounding calcified membrane. The whole SF muscle was then lifted free and pinned in a slightly stretched position on a Sylgard-lined dish containing relaxation solution at room temperature. This could then be stored for up to 14 days at -25°C.

### 4.2.3 Fast extensor muscle preparation

Removal of the whorls of deep fast muscle from the ventral half of the abdomen exposed the fast extensor muscles. The lateral-most bundle of each muscle, which is composed of

long straight muscle fibres, was dissected away from the rest of the fast extensor muscle. Cuts were made through the dorsal membrane and exoskeleton beyond the insertion point of the lateral bundle, to separate the anterior end of the bundle from the dorsal side of the abdomen without damaging the muscle fibres. The whole fast extensor muscle was then lifted free and pinned in a slightly stretched position on a Sylgard-lined dish containing relaxation solution at room temperature.

#### 4.2.4 Preparation of single fibres

Whilst in relaxation solution, individual (1-4 mm in length)  $S_1$ -type fibres from the lateral bundle and  $S_2$ -type fibres from the medial bundle of the SF muscle and individual fast extensor muscle fibres were dissected out using fine forceps. These were split into myofibrillar bundles with mean diameters of between 40 and 150  $\mu\text{m}$ .

All the fibres were chemically skinned whilst attached to the experimental apparatus by exposure to a relaxation solution containing 1% Triton X-100 (10 min, room temperature).

#### 4.2.5 Solutions

Solutions were prepared according to Moisesescu and Thieleczek (1978a) and are as described by Galler and Neil (1994). All solutions contained 60 mM N-2-(Hydroxyethyl)piperazine-N'-2-ethansulfonic acid (HEPES) (free acid), 8 mM  $\text{Na}_2\text{H}_2\text{ATP}$  (total), 10 mM sodium phosphocreatine and 1 mM free  $\text{Mg}^{2+}$ . In addition, all solutions contained 646 mM sucrose in order to adjust the osmolarity to 1 osmol  $\text{l}^{-1}$  which corresponds to that of the haemolymph and dextran (40g/l) to prevent swelling of the muscle fibres (Godt & Maughan, 1977). The relaxation solution (solution B) contained 50 mM ethyleneglycol bis ( $\beta$ -aminoethyl ether) -N-N'-tetraacetic acid (EGTA), the activation solution (solution A) contained 50 mM CaEGTA, and the preactivation solution (solution H, low  $\text{Ca}^{2+}$  buffer capacity) contained 50 mM hexamethylenediamine-N,N,N',N'-tetraacetic acid (HDTA). The pH of all the solutions was adjusted to 7.10 at 22-24 °C. Twenty units  $\text{ml}^{-1}$  creatine phosphokinase (Sigma) were

added immediately before experiments to solutions A, B and H. The glycerol relaxation solution for fibre storage consisted of B solution and 50% (v/v) glycerol. A low ionic strength rigor solution (10 mM imidazole, 2.5 mM EGTA, 7.5 ethylene diaminetetraacetic acid (EDTA) 134 mM  $K^+$  propionate, pH 6.8) was used for the fixation procedure of the fibre ends (see Section 4.2.12). All the solutions were stored at  $-25^{\circ}C$  and were brought to room temperature immediately prior to use. All the experiments were conducted at  $22^{\circ}C$ .

#### 4.2.6 Experimental set-up

All experiments followed the basic method described by Galler and Rathmayer (1992) and Galler and Hilber (1994). Briefly, a purpose-built mechanical apparatus was constructed for detecting signals of force, fibre length and sarcomere length of single fibres (Fig. 4.1). Rapid length changes were carried out by a feedback-controlled stepping motor. A cuvette-transporting system enabled rapid solution changes to be made. During this procedure the position of the fibre remained fixed whilst a multiple cuvette holder was lowered, moved horizontally and raised again in an arc. During the transfer the fibre was out of the solution for only 0.2-0.3 seconds. The attachment points for the muscle fibre ends onto the mechanical apparatus were two epoxy carbon needles with tip diameters of 100  $\mu m$ . During the experiments these thin needles were immersed into the bath solutions to a depth of 1 mm. Force artefacts due to the varying surface tension between the fibre and the bath solution were minimal because of this flattened profile and small diameter. One of the needles was glued onto the lever arm of the stepping motor (which varied the fibre length in non-isometric measurements) and the feedback unit (Fig. 4.2). The needles were attached by their narrow edge to the force transducer and the stepping motor in order to minimise the compliance of the needles in the direction of the force (total compliance of the attachment system was  $1.8 \mu m mN^{-1}$ , corresponding to a maximal fibre shortening of 0.1% in the worst case).

## 4.2.7 Measurements of shortening velocity

### 4.2.7.1 Manual constant load experiments

For these experiments a constant load unit (Scientific Instruments, Heidelberg Germany) was used to 'clamp' the force at a desired value by controlling the position of the stepping motor (Fig. 4.2). After maximal activation (pCa 4.7), the force was clamped at an adjustable value between 2 and 98% of the actual force for approximately 1500 ms (and in each series of experiments had at least 3 loads set to less than 10%  $P_0$  ( $P_0$  = isometric force)). Each series of force clamps was preceded and followed by a slackening of the fibre to detect the actual force zero point. From the length changes the shortening velocity of the muscle could be determined at different force levels. From the force-velocity relationship values for unloaded shortening velocity ( $V_{max}$ ) and maximal power were extrapolated.

### 4.2.7.2. Force clamp ramp experiments

Different voltage sources were used to control the stepping motor. A BASIC computer program was used to instruct the digital-analogue (A/D) converter (RT1815) to make a staircase-like voltage ramp (Fig. 4.3A). For setting the absolute amplitude of the voltage-ramp, the actual force just before the ramp was measured by the A/D converter and fed into the output of this device. The voltage ramp was fed into the external input of the constant load unit. In addition, a Digitimer (Master 8) was used for timing the events. To enable evaluation of the force-velocity data, the zero point of the force was precisely determined in each force clamp experiment. At the end of each load ramp the voltage source from the stepping motor was switched from the constant load output to the DC voltage unit to create complete slackening of the fibre. Measurements were made in the same way as for the manual constant load experiments.

## 4.2.8 Force measurements

Force measurements were made by force sensor elements (Type AE801, Sensor, Norway), which were used in combination with a force bridge amplifier (Fig. 4.2). The

resonance frequency of the force measuring system was  $10 \pm 0.5$  kHz. The sensitivity of the force measuring system (about  $0.1 \text{ mN V}^{-1}$ ; output limit 5V) was calibrated by simulating the pulling force of a muscle fibre with a thin glass needle of known resistance. The linearity of the system was determined and a linear relationship between the force and length signal was obtained up to a voltage output of 5V from the bridge amplifier. As the force output of the sensor was affected by light, the sensitive part was shaded with black paint.

#### **4.2.9 Changes in fibre length**

The feedback-controlled stepping motor (based on a Ling Dynamics vibrator, model V101) was able to perform quick rectangular length changes on the muscle fibre (up to 100  $\mu\text{m}$  in 0.5 ms and up to 500  $\mu\text{m}$  in less than 1 ms). Measurements of length changes were calculated using the equations described by Galler and Hilber (1994).

#### **4.2.10 Measurements of sarcomere length**

The sarcomere lengths of muscle fibres was measured by laser diffractometry, using a He-Ne laser (632.8 nm, 4 mW, Spectra Physics) (Zite-Ferenczi & Rüdell, 1978). The sarcomere length of each fibre was determined before and during activation. All calculations of sarcomere length were determined using the goniometric function (Zite-Ferenczi & Rüdell, 1978).

#### **4.2.11 Recording system**

Electrical signals of fibre length and force were recorded on a digital tape recorder (DTR 1802, Fa. Biologic) and an A/D converter (Mac Lab, AD Instruments). The force and length values were measured using automated macros in the software program (CHART), were entered onto an internal spreadsheet (Datapad), were recorded on computer disc and transferred to Microsoft EXCEL) for further analysis. All experiments were also recorded on a chart recorder.

#### 4.2.12 Experimental procedure

Immediately before the experiment, fresh fibres were removed from storage (-25 °C in glycerol -B solution) and transferred to a coverslip at room temperature. One end of the fibre was attached to the tip of the epoxy carbon needle connected to the force transducer, and the other was attached to the needle connected to the stepping motor. Each end of the fibre was secured with a small drop of adhesive (Histacryl Blue Vetscal, Braum, Melsungen, Germany) applied by means of a micro pipette, which rapidly polymerised on immersion in the low ionic strength 'pre-rigor' solution. Whilst submerged in this solution, an 8% gluteraldehyde + 10% toluidine blue solution was applied to the fibre ends just adjacent to the needles. The rest of the fibre was not contaminated since the gluteraldehyde solution, having a lower specific weight than the low ionic strength rigor solution, quickly flowed to the bottom of the cuvette. This provided a sharp border between the active segment of the skinned fibre and the inactive fixated and glued ends, thereby eliminating irregularities which might arise due to interference with the sarcomeres near the site of attachment (Chase & Kushmerick, 1988). Following this procedure the attached fibre was transferred rapidly into the next cuvette containing glycerol-free relaxation solution ('B').

Before all experiments the fibre was slackened to record the control zero point, and was then adjusted until the fibre length was set to the point where force was just recorded (i.e. adjusted exactly to the slack position). Whilst in 'B' solution the sarcomere length of the fibre was measured using laser diffraction. Fibre length and diameter were measured using an eyepiece micrometer attached to the microscope. The passive force level was not normally more than 5%. All experiments were carried out at 22 °C.

#### 4.2.13 Activation of the muscle fibre

From B solution the fibre was transferred to preactivation 'H' solution, followed by maximally-activating  $\text{Ca}^{2+}$  'A' (pCa 4.7) solution. The fibre produced force under isometric conditions. At the end of each experiment the fibre was transferred to a cuvette containing relaxation 'B' solution (Fig. 4.5A).

#### 4.2.14 Kinetic measurements

A series of kinetic experiments was conducted on maximally  $\text{Ca}^{2+}$ -activated (pCa 4.7) fibres, whilst under isometric conditions (Fig. 4.5A).

1. *Stiffness measurements.* The force responses to small rectangular stretches and releases of the fibre were measured.
2. *Stretch activation and quick releases.* Small fast stretches (Fig. 4.6) and releases were applied to each fibre (Fig. 4.5B). Each stretch resulted in a force increase which was followed by a force decrease when the muscle fibre had reached a new length. Stretch activation was observed during the force decay period when the decay was interrupted by a transient force increase. The amplitude of this transient force increase differs depending on fibre type. Similar phases are observed in the force transient in response to quick release experiments.
3. *Constant load experiments.* Manual constant loads (Fig. 4.3C) and constant load ramps (Fig. 4.3A) were used to measure the shortening velocity of the fibres. A comparison was made between the two methods.

#### 4.2.15 Determination of the fibre types using gel electrophoresis

After all the tests were complete, the fibres were deposited in small tubes and stored in the freezer (-25 °C). Under these conditions the fibres could be stored for up to 3 months. SDS-polyacrylamide gel electrophoresis was performed to confirm the identity of the fibres as the  $S_1$  phenotype as distinct from the  $S_2$  phenotype, following the method used by Laemmli (1970) and Neil *et al.* (1993). Gels containing a 2.5 % acrylamide and 0.8 % (w/v)  $N,N'$ -methylene bisacrylamide stock solution. Single fibres were transferred to 100  $\mu\text{M}$  of SDS sample buffer (62.5 mM Tris-HCl, pH 6.8; 12.5 % glycerol; 1.25 %  $\beta$ -mercaptoethanol). Samples were immediately boiled for 3 minutes, then stored at -25 °C until required. Samples and standards of known molecular mass ( $M_r$ ) (Sigma Dalton Mark VII-L) were applied to the wells in the stacking gel. The gels were then mounted in a chamber containing a reservoir buffer of 0.2 M glycine, 25 mM Tris HCl and 0.1 % SDS, and run with applied currents of up to 40 mA per gel. Gels were fixed and stained

in 2 % (w/v) Coomassie Blue in 45 % (v/v) methanol and 10 % (v/v) acetic acid for up to 8 hours and subsequently destained in a methanol/acetic acid mixture.

#### 4.2.16 Analysis of data

1. *Shortening velocity.* Fibre length changes were determined within individual time intervals which are given separately in the results. The force was measured automatically using the software package Chart on the Mac Lab, taking an average of 5-10 data points from the middle of the individual time intervals. For velocity data the change in fibre length was divided by the corresponding time period.
2. *Stiffness.* Fibre length changes and force measurements were made automatically using the software package Chart, taking an average of 5-10 data points from the middle of the individual time intervals.
3. *Graphical representation of results.* All results were expressed as mean  $\pm$  S.D. and analysed using a Students t-test.

### 4.3

## RESULTS

#### 4.3.1 Sarcomere length

After transferring the fibre into B solution, fibre length was adjusted to the just slack position and the sarcomere length was measured. If the sarcomere length was not observed in B solution it was measured during the first maximal activation, which in some instances made the laser diffraction pattern more distinct. Sarcomere length values for the S<sub>1</sub> fibres were  $6.83 \pm 0.88 \mu\text{m}$ , for the S<sub>2</sub> fibres were  $6.62 \pm 0.93 \mu\text{m}$  and the fast fibres were  $2.07 \pm 0.36 \mu\text{m}$  (Fig. 4.6A). Significant differences were observed between the fast and the S<sub>1</sub> ( $p = 0.0000$ ,  $T = 11.03$ ) and S<sub>2</sub> ( $p = 0.0000$ ,  $T = 11.03$ ) fibre types, although the difference between the S<sub>1</sub> and S<sub>2</sub> types was not significant ( $p = 0.7$ ,  $T = 0.39$ ), which made identification of the S<sub>1</sub> and S<sub>2</sub> fibre types by measuring the sarcomere

length not possible. For this reason all the fibres were identified using the SDS gel electrophoresis technique (see Section 4.2.15) (Figure 4.4).

### 4.3.2 Maximal tension

Fresh, chemically skinned fibres were transferred to the maximally-activating (A) solution (pCa 4.7) after immersion in relaxation (B) and pre-activation (H) solutions. Force increased to a plateau level (Fig. 5.4A) and in most cases the sarcomere length of the myofibrillar bundle remained detectable. Plateau forces were related to the cross-section area of individual fibres. This was calculated by assuming an elliptical or circular shape and determining the largest and smallest diameters using a stereo microscope with an eyepiece micrometer. Mean values for maximal tension were  $10.51 \pm 3.87 \text{ Ncm}^{-2}$  ( $n = 9$ ) for the  $S_1$  fibres,  $3.06 \pm 0.84 \text{ Ncm}^{-2}$  ( $n = 8$ ) for the  $S_2$  fibres and  $5.06 \pm 0.91 \text{ Ncm}^{-2}$  ( $n = 5$ ) for the fast (F) fibres (Fig 4.7D). Significant differences occurred between all three fibre types  $S_1$ - $S_2$ :  $T = 5.3$ ,  $p = 0.0007$ ;  $S_1$ -fast:  $T = 3.78$ ,  $p = 0.0044$ ;  $S_2$ -fast:  $T = -3.61$ ,  $p = 0.0087$ .

### 4.3.3 Quick stretches and releases

Figure 4.5B shows original recordings of fibre length (upper traces) and force (lower traces) during a stretch activation and during a series of 3 release experiments on a maximally  $\text{Ca}^{2+}$ -activated fibre (from Galler *et al.*, 1996). Huxley and Simmons (1971a) and Ford *et al.*, (1977, 1981) recognised four phases in the tension response to quick stretch and release. The initial response is the change during the actual length step which is due to elastic elements of the fibre (phase 1). After the length step is complete, the partial recovery in force is classed as phase 2. This is followed by a reversal of force recovery (phase 3), and finally a much slower return to the original tension (phase 4). In addition to the phases individual terms are used to describe particular force measurements. Following a quick stretch,  $t_0$  is the time when the length change is initiated,  $t_1$  is the time of the extreme minimum value, and  $t_2$  is the time of the secondary delayed and transient rise in force (stretch activation). Following a quick release,  $t_0$  is the time when the length change is initiated,  $t_1$  is the time of the extreme minimum value,

and  $t_2$  is the time of the partial recovery of force. In addition,  $t_3$  is the time from the beginning of the release and the end of phase 3.

#### 4.3.3.1 Stretch activation

Stretches of up to 0.5 % of resting fibre length were applied for 0.5 ms to myofibrillar bundles which had been maximally  $\text{Ca}^{2+}$ -activated, and the force response were recorded. After completion of the length change there was a decrease in force ( $t_1$ ), followed by a delayed transient increase ( $t_2$ ). The force decreased more rapidly in the myofibrillar bundle of the  $S_1$  type (point of minimum force at  $21.33 \pm 8.67$  ms; range, 11-33 ms;  $n = 9$ ) than in the  $S_2$  type ( $85.25 \pm 52.35$  ms; range, 45-187 ms;  $n = 8$ ) (Figs. 4.8 & 4.9). These values are significantly different ( $p = 0.011$ ,  $T = 3.41$ ). The time of  $t_2$  occurred at  $122 \pm 17.97$  ms (range 90-150 ms;  $n = 9$ ) in the  $S_1$  fibre type, but was later in the  $S_2$  fibre type ( $412.5 \pm 201.85$  ms; range 240-840 ms;  $n = 8$ ) (Figs. 4.8 & 4.9). The  $t_2$  values of the  $S_1$  and  $S_2$  fibre types are significantly different ( $p = 0.007$ ,  $T = -3.78$ ). These results ( $t_1$  and  $t_2$  values) are consistent with the findings of Galler and Neil (1994). Only one myofibrillar bundle of the fast fibre type showed stretch activation (Fig. 4.10), and this showed very brief phases ( $t_1 = 10$  ms;  $t_2 = 35$  ms). The mean  $\pm$  S.D. values for the  $t_2$  time of stretch activation in the three fibre types is shown in Figure 4.7B.

The relationship between the force at the end of the length step ( $t_1$ ) and the force after the subsequent partial recovery of force ( $t_2$ ) differs for each fibre type and can be used to identify differences in crossbridge cycling. Figure 4.11. shows an example of a  $t_1$ - $t_2$  plot for each fibre type.

#### 4.3.3.2 Quick releases

Quick releases were applied to isometrically  $\text{Ca}^{2+}$ -activated  $S_1$ ,  $S_2$  and fast muscle fibres. The phases of release were only observed in the  $S_1$  and  $S_2$  fibre types (Figs. 4.12 & 4.13) and only when small releases (0.1-0.2 % of the fibre length) were applied. The force transients from the  $S_1$  and  $S_2$  fibre types thus show a time course symmetry with distinct

differences in time behaviour of force. The fast fibre type never showed distinct phases of release (Fig. 4.14).

#### 4.3.4 Stiffness

For stiffness measurements, stretches of up to 0.5 % and larger releases of up to 5 % of fibre length were applied. Larger releases were applied because the measurements made ( $t_1$  and  $t_2$ ) are after phase 1 of the release and are necessary in order to slacken the fibre, and to detect the zero point of force ( $Y_0$  value). Force and fibre length were measured immediately after the length change was completed, or at the peak of the overshoot which was present in some experiments. The relationship between the force change and length change is linear for stretches, and also for releases (Fig. 4.15) although for larger releases the relationship becomes less apparent. The fibre stiffness was determined in the linear part of the curve by dividing the change in force (as a percentage of isometric force) by the calculated change in sarcomere length (unit: percentage of  $T_0$   $\text{nm}^{-1}$  per half sarcomere). Examples of  $t_1$  plots demonstrating differences in stiffness for each fibre type are shown in Figure 4.15. Direct stiffness is expressed in  $\text{N}/\text{cm}^2$  per  $\text{nm}$  half sarcomere, and mean  $\pm$  S.D. values for stiffness of the three fibre types are shown in Figure 4.7H ( $S_1$ :  $0.36 \pm 0.19$ ,  $n = 6$ ;  $S_2$ :  $0.09 \pm 0.03$ ,  $n = 8$ ; fast:  $0.64$ ,  $n = 5$ ). Significant differences exist between the  $S_1$  and the  $S_2$  fibre types and the  $S_2$  and fast fibre types ( $S_1$ - $S_2$ :  $p = 0.027$ ,  $T = 3.08$ ;  $S_2$ -fast,  $p = 0.018$ ,  $T = -3.87$ ), although no significant difference exists between the  $S_1$  and the fast fibre type ( $p = 0.14$ ,  $T = -1.7$ ).

The  $Y_0$  value is not a direct measure of stiffness, but it is related to stiffness by the equation  $Y_0 = P_0/K$  where  $P_0$  is the isometric force and  $K$  is stiffness.  $Y_0$  is the amount of length change required to bring the actual force generated by the fibre to zero. ( $Y_0$  is the point where the  $t_1$  curve crosses the X axis). Crustacean muscles have very large  $Y_0$  values and these were found to differ between the three fibre types.  $Y_0$  values are expressed as  $\mu\text{m}/\text{half sarcomere length}$ ,  $S_1$ :  $31.66 \pm 0.19$ ,  $n = 6$ ;  $S_2$ :  $26.77 \pm 2.91$ ,  $n = 8$ ; fast:  $7.57 \pm 2.55$ ,  $n = 5$ ). Significant differences were found between the fast and the  $S_1$  and  $S_2$  fibre types ( $S_1$ -fast:  $p = > 0.0001$ ,  $9.44$ ;  $S_2$  -fast  $p = > 0.0001$ ,  $T = 11.41$ ), but no significant difference was found between the  $S_1$  and  $S_2$  fibre type ( $p = 0.088$ ,  $T = 11.83$ ). These  $Y_0$  values show a similar wide range to  $Y_0$  measurements from freeze dried  $S_1$  and

$S_2$  fibres (data not shown) but are reversed compared with the results obtained by Galler and Neil (1994). Possible explanations for this is that the condition of the muscle fibre preparations was different in the two sets of experiments. Certainly Galler and Neil, (1994) found distinct differences between sarcomere length between fibres types while no difference was found in this study.

#### 4.3.5 Shortening velocity

Figure 4.3 shows the original traces of the shortening velocity at different loads measured by the manual constant load method and by the load ramp method for a SF muscle  $S_1$  fibre. The shortening velocity measured by the manual constant load method for a crayfish fibre is shown for comparison (from Galler, 1994). The upper traces of Figure 4.3 A and B represent the fibre length change and the lower traces represent the force response. In the manual constant load method the force was decreased stepwise in a series of individual experiments from the isometric force plateau controlled by the constant load unit, whereas in the ramp method the load was decreased in a stepwise manner during a single experiment. Examples of original force-velocity plots by the manual constant load method at three different time intervals (indicated in the figure legend), the constant load ramp method for the time interval 5-200 ms and for intrapolated shortening which is the extrapolated shortening values from the manual constant load method for an  $S_1$ ,  $S_2$  and fast fibre type are shown in Figures 4.16, 4.17 and 4.18 respectively.

When the  $S_1$ ,  $S_2$  and fast fibres are maximally  $Ca^{2+}$ -activated and are released to shorten at constant load by the manual and constant load ramp methods, the fibre length decreases in a steady curved manner (Figs. 4.3A 4.3B). The velocity of fibre shortening decreases continuously from the beginning to the end of the isotonic releases.

Clearer differences can be observed between the fibres types when the force-velocity plots are compared (Figs. 4.16, 4.17 and 4.18). The shape of the force-velocity plots gives information about the velocity of shortening at a given load.  $S_1$  and fast fibres exhibit a very curved force-velocity relationship (Fig. 4.16 & 4.18), which shows that these fibres shorten very slowly at high load but that the velocity increases very quickly

as the load is lowered. Maximal shortening velocity occurs at zero load. The  $S_2$  fibres exhibit very different force-velocity profiles, which approximate to a linear relationship (Fig. 4.17). This indicates that the velocity of shortening in the  $S_2$  fibre type does not increase as the load is reduced.

To compare all three fibre types, their force-velocity relationships (measured by the constant load ramp method) have been plotted together on the same axes (Fig. 4.19). Differences between the shapes of the curves can be seen more distinctly when plotted in this way.

Mean  $\pm$  S.D. values for unloaded shortening ( $V_{max}$ ) measured by the ramp method (5-200 ms time interval) and by the manual constant load method for 3 different time intervals are shown in Table 4.1. The  $S_1$  fibre type has the fastest maximal unload shortening velocity for all different time intervals and the  $S_1$  fibre type is significantly different from the  $S_2$  fibre type ( $S_1$ - $S_2$ :  $p = 0.0001$ ,  $T = 5.74$ ). The  $S_2$  and fast fibre types show similar  $V_{max}$  values, which are not significantly different ( $p = 0.45$ ,  $T = -0.80$ ). Mean  $\pm$  S.D. values for the extrapolated unloaded shortening velocity expressed as a percentage of fibre length per second have also been calculated for each fibre type (values are taken from the 500 ms time interval at  $0.2 P_0$ ,  $S_1$ :  $-0.077 \pm 0.014$ ,  $n = 9$ ;  $S_2$ :  $-0.047 \pm 0.012$ ,  $n = 8$ ; fast:  $-0.028 \pm 0.012$ ). These results are consistent with the measurements of shortening velocity by the constant load experiments, showing that the  $S_1$  fibres shorten at a faster rate than either the  $S_2$  and fast muscle fibre types.

From the force-velocity plots the mean  $\pm$  S.D. values for maximal power have been extrapolated for the three fibre types (Fig. 4.7C) ( $S_1$ :  $0.137 \pm 0.03$ ,  $n = 9$ ;  $S_2$ :  $0.199 \pm 0.05$ ,  $n = 8$ ;  $0.07 \pm 0.01$ ,  $n = 5$ ) (for calculation method, see Woledge, 1985). The linear relationship observed in the  $S_2$  fibre type means that  $S_2$  fibres are most energy-efficient at high loads, while the curved relationship of the  $S_1$  and fast fibres shift the maximal power values to lower loads.

A linear relationship exists between the values for maximal unloaded shortening velocity ( $V_{max}$ ) measured by the manual constant load method for three different time intervals and by the constant load ramp method for the three fibre types (Fig. 4.20) indicating that there is a good correlation between the two constant load methods. No significant

difference was found between values of the first time interval measured by the manual constant load method (0.005-0.1 s) and the time interval measured by the ramp method (0-0.2 s) in any of the fibre types ( $S_1$ :  $p = 0.8$ ,  $T = -0.26$ ;  $S_2$ :  $p = 0.79$ ,  $T = -0.27$ ; fast:  $p = 0.75$ ,  $T = 0.33$ ). This shows that the more rapidly performed constant load ramp method provides a reliable way to measure shortening velocity, and for this reason it has been used as the preferred method in other experiments (Chapter 5).

#### 4.3.6 Filament sliding

Assuming a uniform shortening of all sarcomeres within a muscle fibre, the speed of filament sliding was calculated from the shortening velocity of the whole fibre by multiplication with half sarcomere length. The mean  $\pm$  S.D. values for filament sliding are expressed as  $\mu\text{m/s}$  per half sarcomere length ( $S_1$ :  $1.73 \pm 0.45$ ,  $n = 6$ ;  $S_2$ :  $0.89 \pm 0.22$ ,  $n = 8$ ; fast:  $0.54 \pm 0.41$ ) (Fig. 4.7E). The  $S_1$  fibres have significantly faster filament sliding than the  $S_2$  fibres ( $p = 0.0082$ ,  $T = 3.88$ ) and the fast fibres ( $p = 0.018$ ,  $T = 3.84$ ), but no significant difference occurs between the  $S_2$  and fast fibre types ( $p = 0.29$ ,  $T = 1.43$ ).

## 4.4

## DISCUSSION

Previously the  $S_1$  and  $S_2$  fibres which comprise the SF muscle of *Nephrops norvegicus* have been characterised by their mechanical properties (Galler & Neil, 1994) and these results have been related to their histochemistry and biochemistry (Fowler & Neil, 1992). This study confirms the work of Galler and Neil and develops their study further, as well as characterising the properties of the fast extensor muscle fibre type.

#### 4.4.1 Shortening velocity

Measurements of shortening velocity at different loads by the manual constant load method and the constant load ramp method and the velocity of filament sliding which

takes into account the sarcomere length of the fibres, have been determined. The data from the fast fibres was very inconsistent and for this reason only the  $S_1$  and  $S_2$  fibre type will be considered in detail.

Similar measurements of unloaded shortening velocity by the constant load method and slack test method have been made on rabbit, rat and human skeletal muscle fibres (Galler and Hilber, 1994). When these fibres are maximally  $Ca^{2+}$ -activated and are released to shorten at constant load, the fibre length decreases in a steady curved manner. The velocity of fibre shortening decreases continuously from the beginning to the end of the isotonic releases. This contrasts with the more linear length change found in frog fibres (Julian *et al.*, 1986). It is proposed by Galler *et al.* (1996) that the curvature of the length trace during isotonic releases is due to internal forces which accelerate or slow down the fibre shortening. Compressive force, which is based upon the properties of stretched myofibrils, could accelerate the fibre shortening at the early stage (phase 1) of release (Tameyasu, 1992). The internal loads which result from the increasing mechanical stress of the interfilamentary network during fibre shortening could slow down fibre shortening at later stages (phase 3) of isotonic release (Brenner, 1980).

A similar relationship between fibre length and fibre shortening was found in the  $S_1$  and  $S_2$  fibre types. When these fibres are released to shorten at constant load, the fibre length decreases in a steady curved manner (Fig. 4.3C). The slower  $S_2$  fibres showed an even stronger curved profile than the  $S_1$  fibres, and no rapid early phase can be distinguished from phase 2. This suggests that all the fibres have lower levels of compressive force because of the slow velocity of phase 1. The curvature of the length profiles is also very similar to the length change during shortening in crayfish fibres (Fig. 4.3B).

More distinct differences between the three fibre types were observed in the force-velocity relationships. The  $S_1$  have very curved force velocity profile (Fig. 4.16) which shows that these fibres shorten very slowly at high load but that the velocity increases very quickly as the load is lowered. The  $S_2$  fibres exhibit a more linear relationship (Fig. 4.17) which indicates that the velocity of shortening in the  $S_2$  fibre type does not increase, but increases at a relatively constant rate as the load is lowered.

From the force-velocity plots the parameter of maximal power can be deduced. This is the value at which the fibre can produce the maximum mechanical power output and is most energy-efficient. Greater curvature of the force-velocity relationship shifts the maximal power output to a lower load. The strong curvature of the force-velocity plots from the  $S_1$  fibres shifts the maximal power output to a lower load than for the  $S_2$  fibres ( $S_1$ :  $0.137 \pm 0.03$ ;  $S_2$ :  $0.199 \pm 0.05$ ). As well as the curvature of the force velocity relationship, other parameters can be extrapolated to give more information about the fibre types. Examples of these include: values of maximal unloaded shortening velocity ( $V_{max}$ ) and filament sliding which takes into account differences in sarcomere length between the fibre types.  $S_1$  fibres have faster velocities of unloaded shortening ( $V_{max}$ ) than the  $S_2$  fibres (for the 0-200 ms time interval,  $S_1$ : 0.53 FL/s;  $S_2$ : 0.27 FL/s), and when this parameter is combined with the similar sarcomere lengths of the  $S_1$  and  $S_2$  fibre types, the result is much faster filament sliding in the  $S_1$  fibre type. Assuming uniform shortening along the length of the whole fibre, the  $S_1$  fibres shorten almost twice the distance per unit time as the  $S_2$  fibre type.

These differences agree with the findings by Galler and Neil (1994) which defines the different roles of the  $S_1$  and  $S_2$  fibre types within the abdomen. The slower, long lasting, fatigue resistant contractures of the  $S_2$  fibre type control abdominal posture, which requires the  $S_2$  fibres to be activated at a low level even when the animal is at rest. This was indicated by the  $S_2$  fibres being slightly activated at below-threshold levels of  $Ca^{2+}$  ions. The higher maximal power of the  $S_2$  fibres enables them to maintain reasonably high loads very efficiently for long periods of time. However, because the  $S_2$  fibres do not have to contract rapidly (are not involved in fast movements such as the escape response), but are constantly maintaining a low level of contraction, they have a much lower unloaded shortening velocity and rate of filament sliding. Lower maximal tension was also measured in maximally  $Ca^{2+}$ -activated  $S_2$  fibres ( $3.06 \pm 0.84 \text{ N cm}^{-2}$ ). Due to the support of the body by the medium, the  $S_2$  fibres will be required to maintain only low levels of tension in order to hold the abdominal posture.

In contrast, the  $S_1$  fibres are adapted for shorter more rapid contractions which are involved in slow movements of the abdomen. The  $S_1$  fibres have a much higher velocity of fibre shortening and filament sliding, higher levels of maximal tension ( $10.51 \pm 3.87 \text{ N cm}^{-2}$ , which is about three times that of the  $S_2$  fibres) but are less energy-efficient and

have lower maximal power. Due to the nature of synaptic input (see Section 2.1.5) these fibres are not activated at rest, but are recruited to contract to contribute to postural change.

#### 4.4.2 What determines the shortening velocity?

Although differences in shortening velocity, filament sliding, maximal power and tension can be related to the different roles of the  $S_1$  and  $S_2$  fibre types this still does not explain how these differences are brought about, or what are the underlying control mechanisms. Many different factors could be involved in altering these parameters, such as the presence of different muscle protein isoforms or the kinetics of crossbridge cycling.

$V_{\max}$  represents the velocity of muscle fibre shortening at zero load and is the maximal speed at which the fibre can shorten.  $V_{\max}$  therefore represents crossbridge cycling at its highest rate. In the literature it has been suggested that only the detachment rate of crossbridges determines the velocity of fibre shortening (Eisenberg *et al.*, 1980). If the velocity of unloaded filament sliding is an indication of the rate of crossbridge detachment (Woledge, 1985; Eisenberg *et al.*, 1980), then the different unloaded shortening velocities of the  $S_1$  and  $S_2$  fibre types imply that they do differ.

Differences in shortening velocity have also been related to the presence of different myosin heavy chain (HC) isoforms, different myosin light chain (LC) isoforms and different ratios of HC and LC isoforms that are expressed. In general fast fibres express different myosin isoforms to slow fibres and differences also exist between subgroups of slow and fast fibre types. For example many different workers have found that Type I and Type II mammalian fibres have different  $V_{\max}$  values which correlate with the presence of different myosin heavy chain (HC) isoforms (Reisner *et al.*, 1985a; Eddinger & Moss, 1987; Greaser *et al.*, 1988; Bottinelli *et al.*, 1991; Galler *et al.*, 1994). Greaser *et al.* (1988) identified three groups of muscle fibres from rabbit. One has exclusively the slow type myosin heavy chain and myosin light chains and has low velocities, another group has mixtures of fast type and slow type myosin HCs and LCs and has intermediate shortening velocities, and the third group of fibres has fast type myosin HCs and LCs and high shortening velocities. Myosin heavy chain isoform composition is strongly

correlated with maximal unloaded shortening velocity ( $V_{max}$ ) in rabbit soleus muscle fibres (slow twitch muscle) (Reiser *et al.*, 1985a) and from neonatal rabbit psoas (fast twitch) muscle (Reiser *et al.*, 1985b). Differences in the ratio of myosin alkali light chains, myosin heavy chain types or the ratio of the two have been correlated with shortening velocity in rabbit muscle fibres (Sweeney *et al.*, 1988). Julian *et al.*, (1981) found that fast rabbit psoas fibres containing myosin light chains of the fast type consistently had higher  $V_{max}$  values than rabbit soleus muscle segments which contained myosin light chains of the slow type. Since the different  $S_1$ ,  $S_2$  and fast fibre types of *Nephrops* have been shown to express different myosin heavy chain components, but not myosin light chains components (Neil *et al.*, 1993), it is possible that the myosin heavy chains are responsible for the differences seen in their shortening velocity.

In addition to its relationship to myosin isoforms expression,  $V_{max}$  has been strongly correlated with myofibrillar ATPase (mATPase) activity (Galler & Rathmayer, 1992; Bottinelli *et al.*, 1994b). However, it should be noted that when the ATPase activity was measured by histochemical means, levels were not similar to those found under normal physiological conditions. In crustacean muscle ATPase activity is almost 4 times higher in fast muscle than slow muscle (Li & Mykles, 1990). Differences also exist between the  $S_1$  and  $S_2$  fibres:  $S_1$  fibres have higher mATPase activity and faster shortening velocity while the  $S_2$  fibres exhibit lower ATPase activity and slower shortening velocities (Fowler & Neil, 1992).

#### 4.4.3 Force transients in response to quick changes in fibre length

##### 4.4.3.1 Stretch activation

Crossbridge kinetics vary between different fibre types, and the kinetics of stretch-induced delayed force increase (stretch activation), which is thought to represent certain steps of crossbridge cycling (Huxley & Simmons, 1970, 1971a & b, 1973; Ford *et al.* (1977, 1981, for review see Woledge, 1985) has been shown to correlate with different fibre types from rat, fish, frog, locust and crayfish (Galler, 1994; Galler *et al.*, 1994). Clear differences exist in the temporal behaviour of force responses of the individual phases following quick changes (stretches) in fibre length between the  $S_1$ ,  $S_2$  and fast fibre types, although it should be noted that only one example of the fast fibre type was

recorded. Similar values to those obtained by Galler and Neil (1994) for  $t_1$  and  $t_2$  were recorded. These measurements are also in a similar range to those recorded from slow muscle fibre phenotypes from crayfish, locust and rat (Galler, 1994), while the  $t_2$  values from the fast fibre type is in a similar range to the rat fast fibres.

#### 4.4.3.2 Quick release

Examples of quick release experiments for each fibre type are shown in Figures 4.12, 4.13 and 4.14. However, because the force transients were not recorded in response to a controlled length step, no absolute measurements could be determined. This is because the time parameters of force transients following releases are dependent on the amplitude of the length change (Huxley & Simmons, 1971; Ford *et al.*, 1977; Woledge *et al.*, 1985; Galler *et al.*, 1996). The force transients from the  $S_1$  and  $S_2$  fibre types both show a time course symmetry, but have distinct differences. These results are similar to those observed by Galler *et al.*, (1996) showing that the different force transients in response to quick releases vary between fibre type. These differences may relate to variations in myosin head isoforms, which exhibit different kinetic properties in rat fibres (Galler *et al.*, 1996).

Based upon the original theoretical considerations of stretch and release experiments (Huxley & Simmons, 1970, 1971a & b, 1973; Ford *et al.* (1977, 1981), recent studies suggest that molecular mechanisms underlie the force transients in response to length steps. It was proposed by Irving *et al.*, (1992, 1995) that the quick force recovery after release in fibre length (phase 2) results from force-generating movements of attached myosin heads. The following interruption or reversal of force recovery (phase 3) seems to be correlated with regeneration of the ability to execute force-generating movements (Lombardie *et al.*, 1992). The duration of this regeneration period may provide information about the time course of cyclic interactions between the myosin heads and the actin filament (attachment/detachment process). Based on these theories, and the fact that the time course behaviour of the force transients induced by stepwise length changes has been shown to be similar for stretches and release (Galler *et al.*, 1996), the apparent differences between the  $S_1$ ,  $S_2$  and fast fibres in the results from the quick release and

stretch experiments suggest that the crossbridge kinetics differ between fibre type, and that the kinetics cyclic interactions of the myosin molecules are different.

Another possible explanation for these data is the presence of different myosin isoforms in the different fibre types. The different parameters of stretch (Galler *et al.*, 1994) and release (Galler *et al.*, 1996) which exists between fibre types have also been shown to correlate with the myosin heavy chain complement as well as with the maximal unloaded shortening velocity. This correlation is observed in the results for the  $S_1$  and  $S_2$  fibres:  $S_1$  fibres show faster unloaded shortening velocity and the more rapid force transients ( $t_1$  and  $t_2$ ) while the  $S_2$  fibres exhibit low  $V_{max}$  values and much slower force transients.

#### 4.4.4 Muscle fibre stiffness

Originally the instantaneous stiffness (change in tension per change in length (phase 1 of the force transient) was thought to be proportional to the number of attached crossbridges, which would mean that stiffness could be used as a measurement of attached crossbridges (Ford *et al.*, 1981). However, more recent studies suggest that not all muscle fibre compliance is in the crossbridges, as initially proposed by Ford *et al.* (1981). X-ray diffraction studies on intact muscle (Huxley *et al.*, 1994; Wakabayashi *et al.*, 1994) and other methods (Kojimi *et al.*, 1994; Higuchi *et al.*, 1995) have shown that about half the measured compliance originates in the thin actin filaments. This results in higher stiffness measurements for attached crossbridges during isometric contraction.

Measurements of muscle fibre stiffness from the  $S_1$  and  $S_2$  fibres are similar, though not identical to the results of Galler and Neil (1994). Greater releases are required to reach zero force in the  $S_1$  fibre type than in the  $S_2$  fibres type. As stiffness has been shown to decrease in crustacean fibres following a short exposure to liquid nitrogen, used by Galler and Neil (1994), the fact that in the present study fibres were chemically skinned may explain this difference. In addition to this the deterioration of structures in series with the force generating elements may also contribute to the stiffness of the activated fibres (Galler & Neil, 1994), and these may differ between preparations and the skinning procedure used.

#### 4.4.5 The fast fibre type

The constant load experiments performed on the fast fibre type produced very inconsistent results, which may reflect fibre damage as a result of the skinning procedure. One possible explanation as to why the fast fibres responded in the opposite manner to the  $S_1$  and  $S_2$  fibres is that the internal structure (for example the T-tubules) of fast fibres is different to that of the slow muscle fibres (Crowe & Baskin, 1981). The chemical skinning procedure used for these experiments may cause an osmotic shock which damages the T-tubules of the fast fibres which could prevent  $Ca^{2+}$  ion diffusing to the contractile proteins in the same way, although it should be noted that similar results were obtained from freeze dried fast fibre preparations. Other workers report similar problems with mechanical experiments on skinned fast fibres from cod (Altringham & Johnston, 1982). The force velocity relationships for the fast fibres showed a curved profile: the speed of shortening was very slow at high loads, but as the load was reduced the velocity of shortening increased rapidly. The values for maximal power ( $0.07 \pm 0.01$ ), and maximal unloaded shortening velocity (for the 0-200 ms time interval,  $0.34 \pm 0.203$  FL/s) for the fast fibre type are very low. Fast muscle fibres are adapted to contract rapidly and powerfully for brief periods of time. It would be expected therefore that the fast muscle fibres would show a less curved force velocity relationship (reflecting an ability to contract powerfully at high loads), high maximal unloaded shortening velocity, and a high maximal tension level. The results from the fast fibres do not fit this description, but are similar to the values obtained from the  $S_2$  fibre type but with a low maximal power level. In other studies which have compared fast and slow skeletal muscle fibres, such as those of rat, the maximal power output is much higher in the fast fibre type (Bottinelli *et al.*, 1991). All these results indicate that the fast fibres are damaged. However, what is interesting from the stiffness measurements is that the fast fibres show higher levels of fibre stiffness in comparison to the  $S_1$  and  $S_2$  fibres (fast:  $0.642 \pm 0.314$  N cm<sup>2</sup>/mm;  $S_1$ :  $0.363 \pm 0.209$  N cm<sup>2</sup>/mm;  $S_2$ :  $0.096 \pm 0.034$  N cm<sup>2</sup>/mm). Mechanically damaged muscle fibres have been shown to have low levels of fibre stiffness (Galler, Pers. com.), which would suggest that the fast fibres results are reliable. One possible explanation for this result is that elements other than the myofibrils are contributing to the stiffness. It was suggested by Galler and Neil (1994) and by West *et al.* (1992) working on mechanically skinned fibres from the Yabby, the Australian crayfish that the differences observed in muscle fibre stiffness are due to structural

differences outside the crossbridges. Electron microscopy would be helpful to examine this possibility for the muscle fibres of *Nephrops norvegicus*.

Table 4.1 Maximal unloaded shortening at different time intervals

| Time           | $S_1$<br>(FL/s) | S.D. | n | $S_2$<br>(FL/s) | S.D. | n | Fast<br>(FL/s) | S.D. | n |
|----------------|-----------------|------|---|-----------------|------|---|----------------|------|---|
| 0.005-0.1 s    | 0.54            | 0.10 | 9 | 0.29            | 0.10 | 8 | 0.29           | 0.23 | 7 |
| 0.1-0.5 s      | 0.28            | 0.09 | 9 | 0.11            | 0.04 | 7 | 0.10           | 0.06 | 7 |
| 0.5-1.0 s      | 0.10            | 0.01 | 9 | 0.06            | 0.02 | 8 | 0.04           | 0.02 | 7 |
| 0-0.2 s (ramp) | 0.53            | 0.10 | 9 | 0.27            | 0.06 | 8 | 0.34           | 0.20 | 7 |

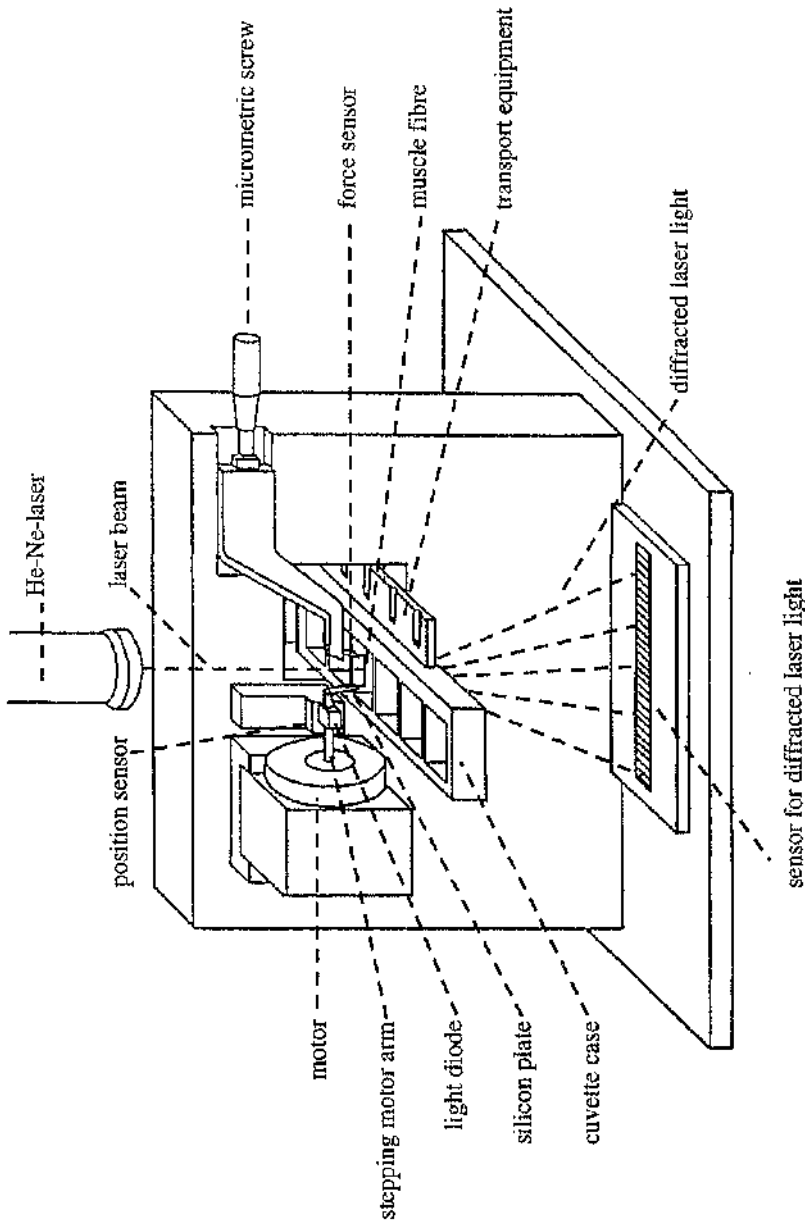


Fig. 4.1  
 Mechanical part of the experimental apparatus.

The muscle fibre is mounted between the force sensor and the stepping motor (from Galler & Hilber, 1994)



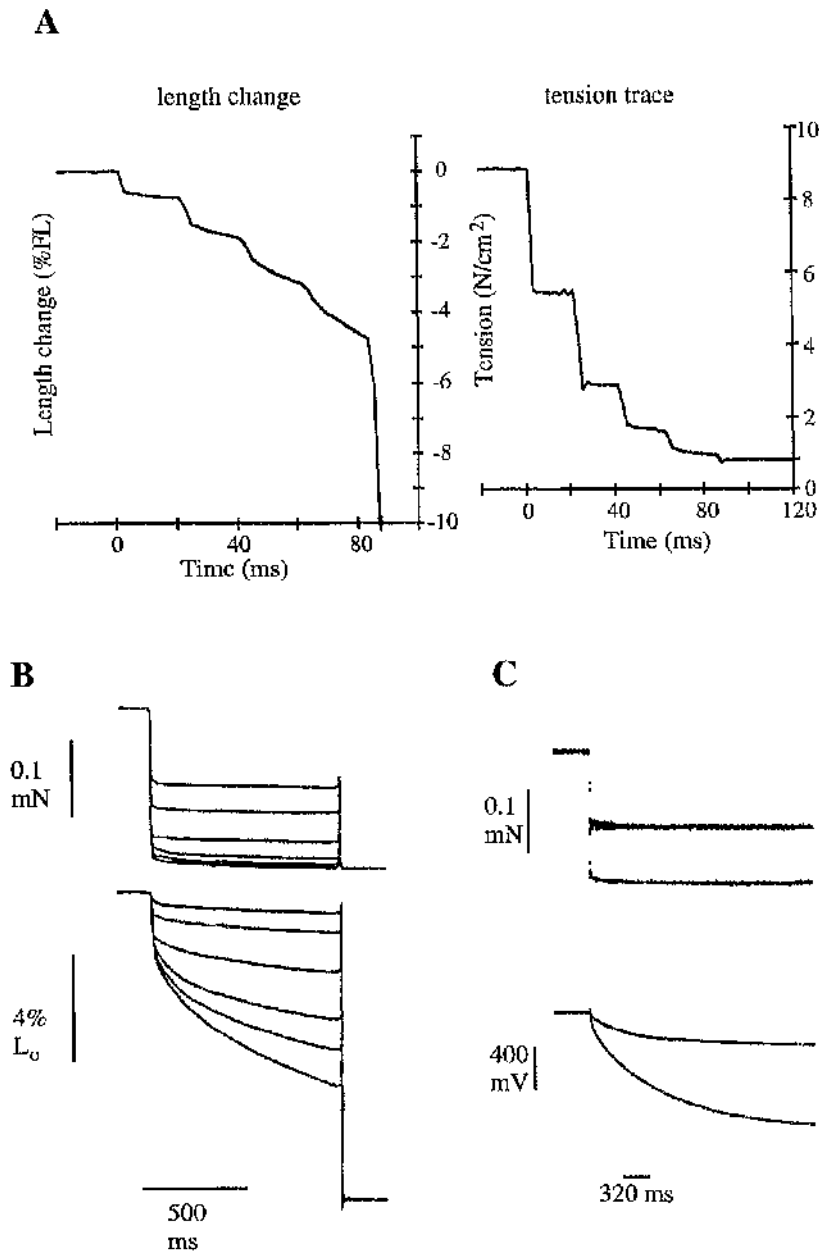


Fig. 4.3  
Force and length changes during constant load experiments.

Constant load ramp: original traces of force (right panel) and fibre length (left panel) during a load ramp; the beginning of each trace corresponds to with the maximally Ca<sup>2+</sup>-activated isometric force (A).

Superimposed force (upper panel) and fibre length (lower panel) traces during subsequent load steps for measuring shortening velocities in crayfish (B) (from Galler, 1994) and *Nephrops norvegicus* (C).

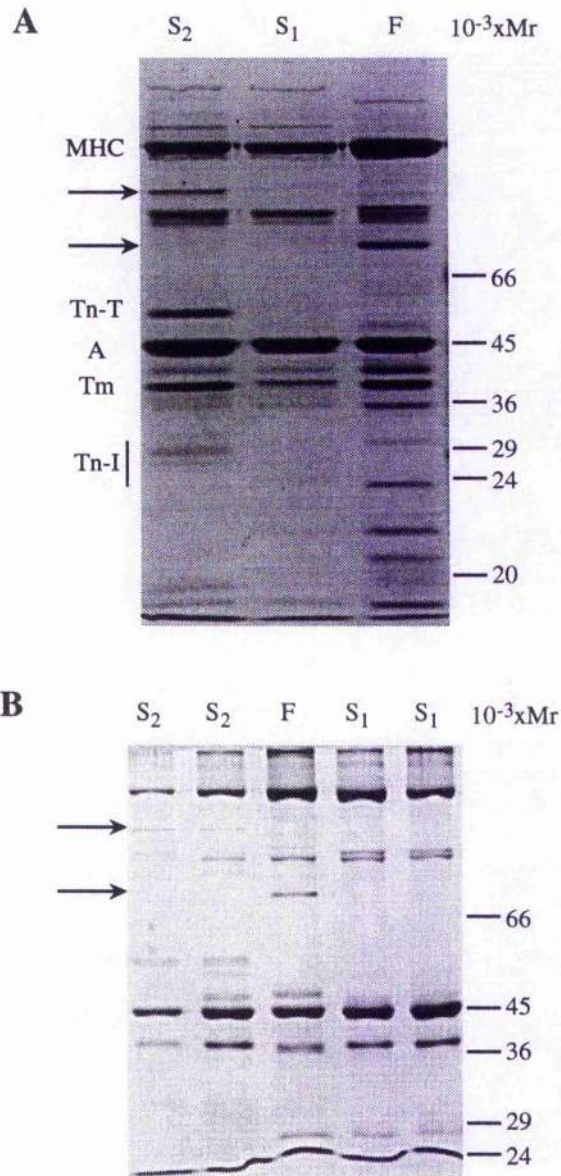


Fig. 4.4  
SDS-PAGE (10 % gel) of membrane-intact (A) and skinned (B) S<sub>1</sub>, S<sub>2</sub> and fast (F) fibres.

Note that the gel performed on skinned fibres following mechanical experiments provides an unambiguous method for fibre identification. Arrows indicate the important bands for fibre identification; MHC, myosin heavy chain; Tn-T, troponin T; A, actin; Tm, tropomyosin; Tn-I, troponin I; 10<sup>-3</sup>xMr indicates the relative molecular mass of the proteins.

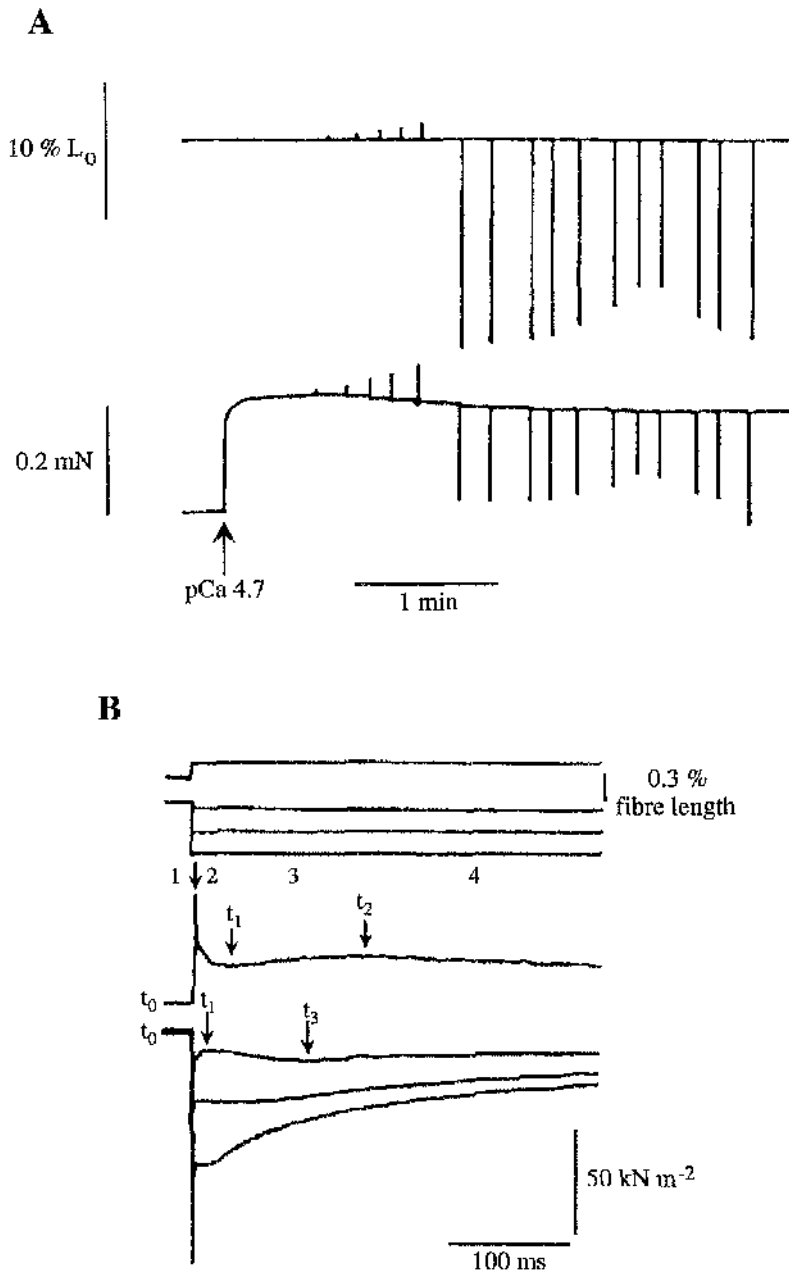


Fig. 4.5  
Original traces of force and fibre length during an experiment.

(A) Force and fibre length during calcium-activation and subsequent application of length (stretch activation) and force (measurements of shortening velocity) steps.

(B) Fibre length (upper traces) and force (lower traces) during a stretch and three release experiments on a maximally calcium-activated fibre; 1-4 represents the 4 phases of the force transients, an arrow indicates the end of each phase; other time parameters are indicated by the labelled arrows (from Gallier *et al.*, 1996)

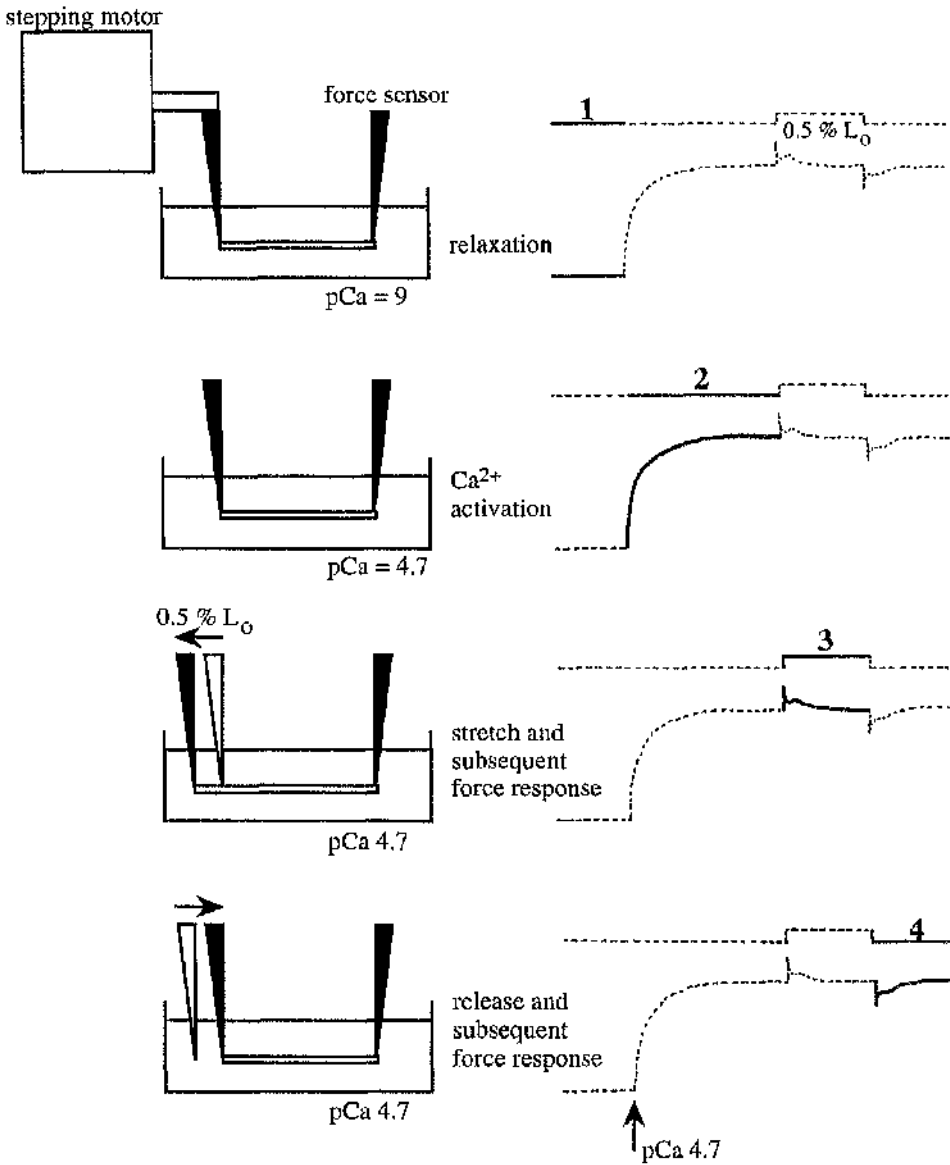


Fig. 4.6 Length changes applied to a muscle fibre and the force response during stretch activation.

1. In relaxation (B) solution: no force is recorded.
2.  $pCa 4.7$  (A) solution maximally activates the fibre under isometric conditions.
3. Whilst maximally activated the fibre is stretched ( $0.5\%$  of the original resting fibre length), this results in a force increase which is followed by a force decrease when the fibre has reached a new length. Stretch activation is observed during the decay period when it is interrupted by a transient force increase.
4. When the fibre is released from stretch, an initial drop in the force occurs, which is followed by a gradual increase until the force returns to the original plateau force level (from Galler, 1994)

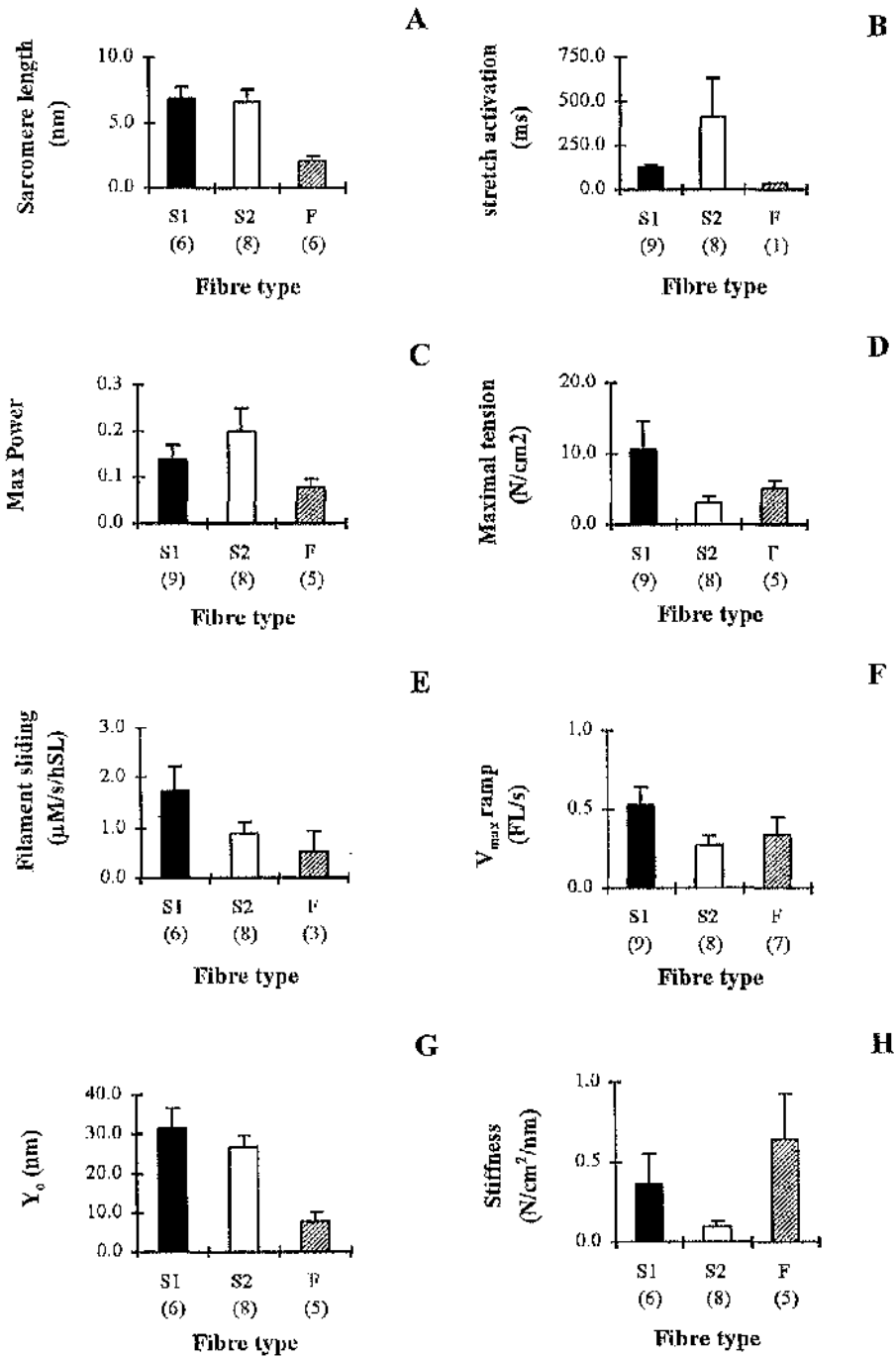
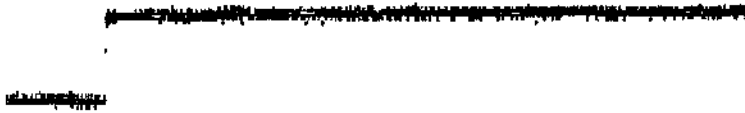


Fig 4.7  
Properties of the S<sub>1</sub>, S<sub>2</sub> and fast fibre types.

Mean  $\pm$  S.D. values for sarcomere length (A), stretch activation (B), maximal power (C), maximal tension (D), maximum velocity of filament sliding (E), shortening velocity (F), stiffness ( $Y_0$  values) (G) and stiffness (H); n values are indicated in parenthesis.

Length change



Force response

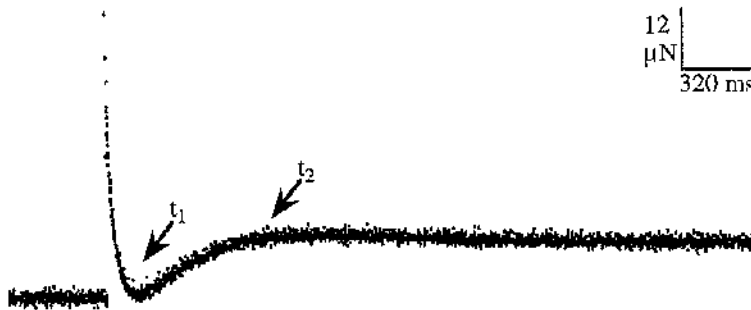
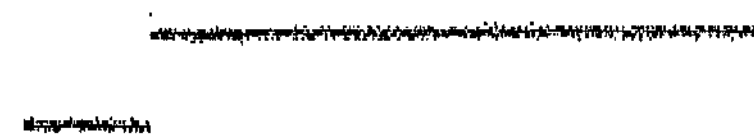


Fig. 4.8  
Stretch activation in the  $S_2$  fibre type.

The force response to a small stretch, 0.5 % of the original fibre length, was measured. The different time parameters of stretch are indicated by the arrows ( $t_1 = 147$  ms,  $t_2 = 840$  ms).

Length change



Force response

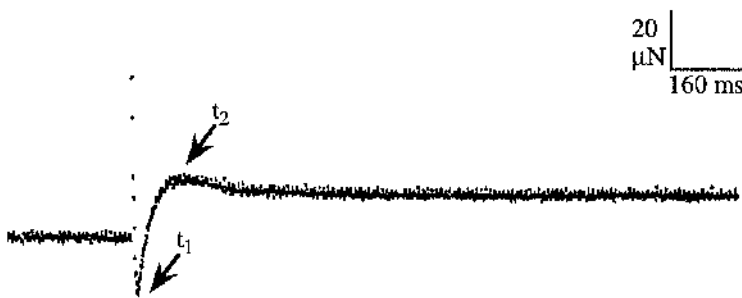
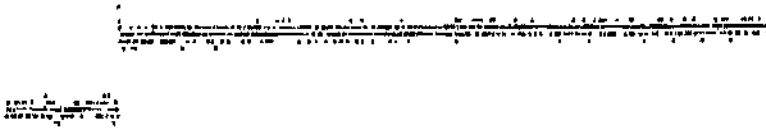


Fig. 4.9  
Stretch activation in the  $S_1$  fibre type.

The force response to a small stretch, 0.4 % of the original fibre length, was measured. The different time parameters of stretch are indicated by the arrows ( $t_1 = 14$  ms,  $t_2 = 115$  ms).

Length change



Force response

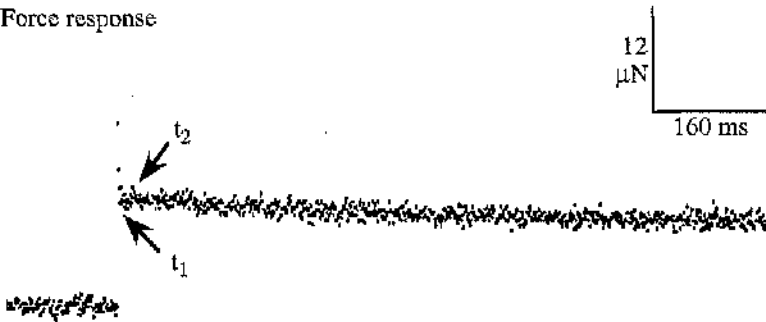


Fig. 4.10  
Stretch activation in the fast fibre type.

The force response to a small stretch, 0.2 % of the original fibre length, was measured. The different time parameters of stretch are indicated by the arrows ( $t_1 = 10$  ms,  $t_2 = 35$  ms).

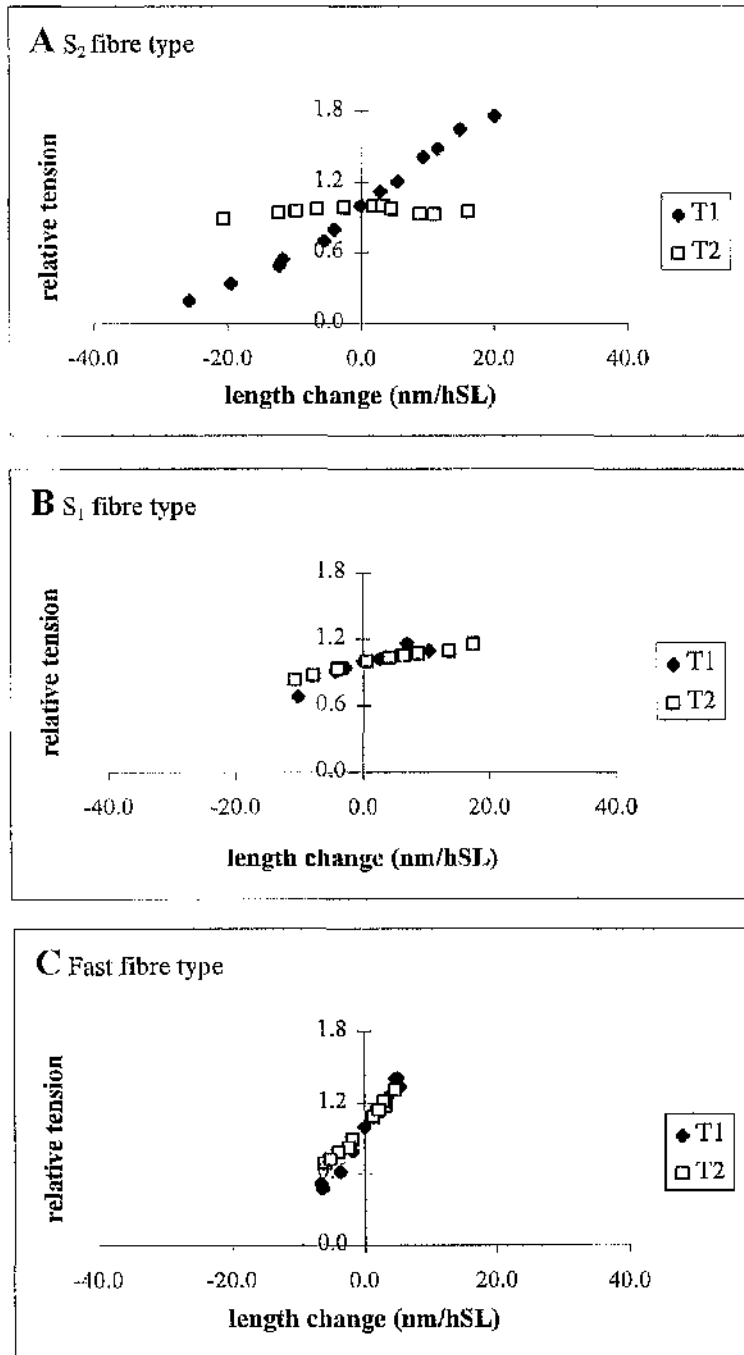
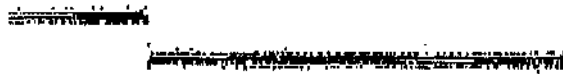


Fig. 4.11  
Force-length relationships of the different fibre types.

The relationship between the applied length change (nm per half sarcomere length) and resulting force ( $t_1$  curve,  $t_1/t_0$ ;  $t_2$  curve,  $t_2/t_0$ ) for the S<sub>2</sub> (A), S<sub>1</sub> (B) and fast (C) fibre types.  $t_1$  is the force at the end of the length step,  $t_2$  is the force after the subsequent quick recovery, and  $t_0$  is the isometric force before the length change.

Length change



Force response

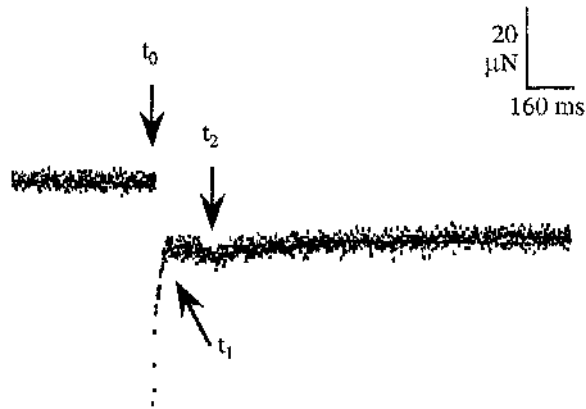


Fig. 4.12  
Quick release experiment in the  $S_1$  fibre type.

The force (lower trace) response to a quick release, 0.1 % of the original fibre length (upper trace) was measured. The different time parameters of release are indicated by the arrows.

Length change

1000 μm

1000 μm

Force response

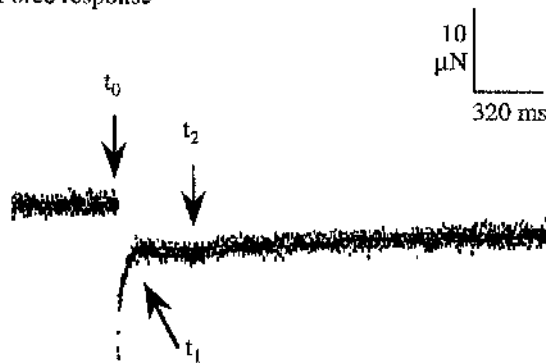
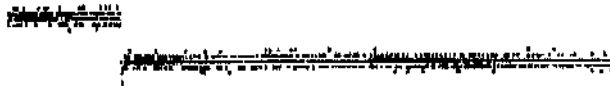


Fig. 4.13  
Quick release experiment in the  $S_2$  fibre type.

The force (lower trace) response to a quick release, 0.2 % of the original fibre length (upper trace) was measured. The different time parameters of release are indicated by the arrows.

Length change



Force response

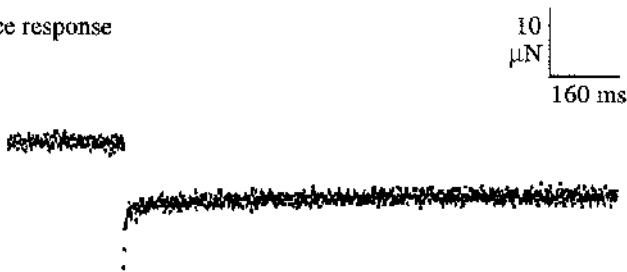


Fig. 4.14  
Quick release experiment in the fast fibre type.

The force (lower trace) response to a quick release, 0.01 % of the original fibre length (upper trace) was measured. The different time parameters of release were never observed in the fast fibre type.

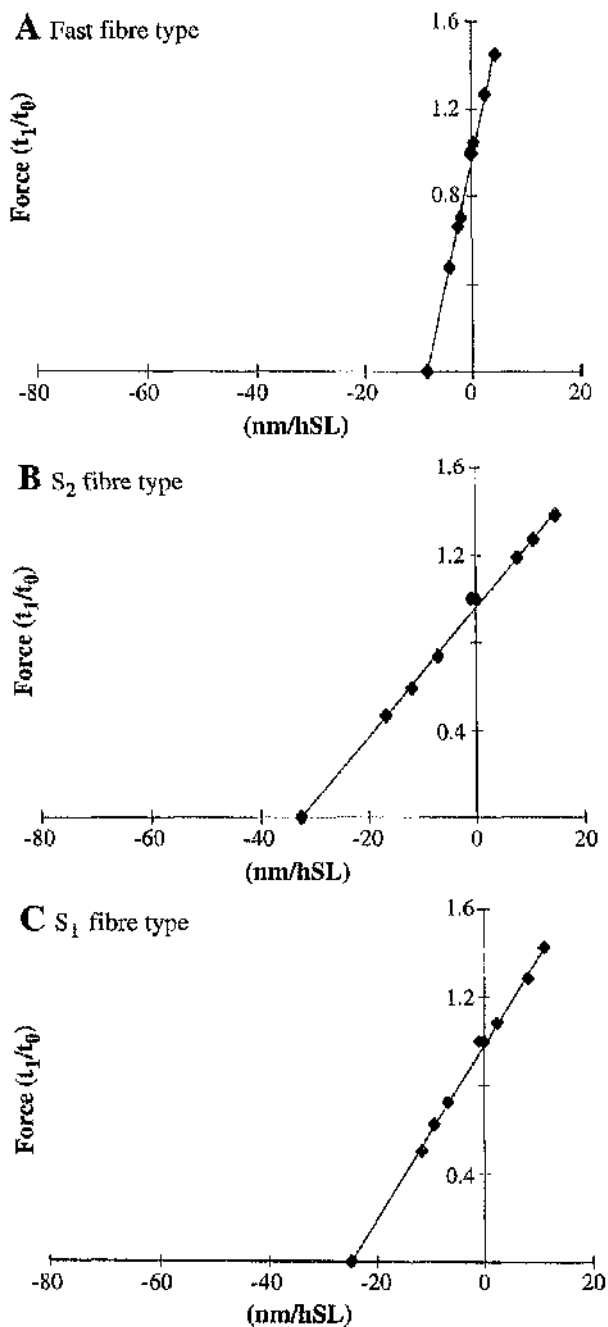


Fig. 4.15  
 $t_1$  plots for the fast (A),  $S_2$  (B) and  $S_1$  (C) fibre types.

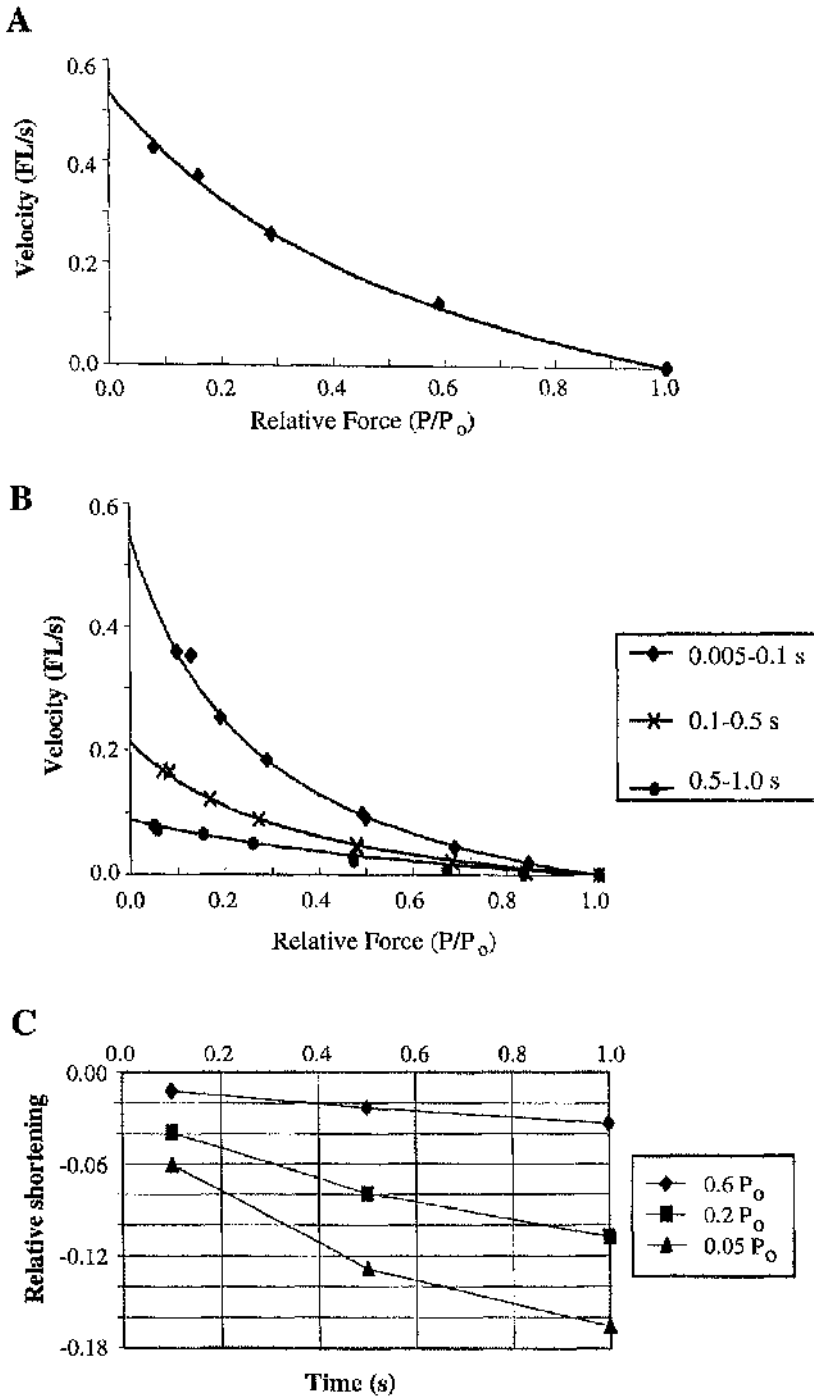


Fig. 4.16 Examples of the original force-velocity and intrapolated shortening plots for the  $S_1$  fibre type.

(A) shortening velocity measured by the constant load ramp method between 0.0 and 0.2 ms; (B) shortening measured by the manual constant load method at three different time intervals; (C) intrapolated shortening at 3 defined loads.

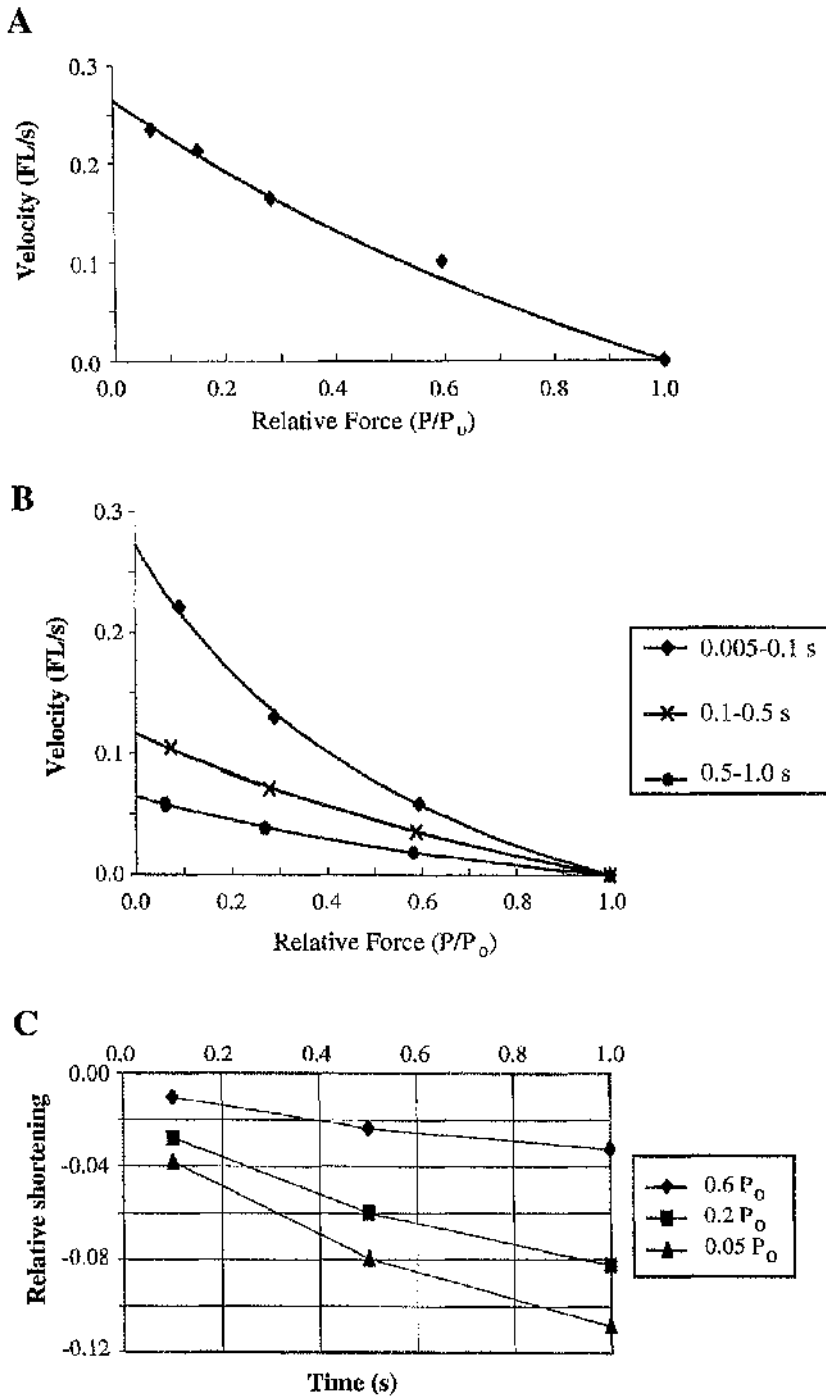


Fig. 4.17 Examples of the original force-velocity and intrapolated shortening plots for the  $S_2$  fibre type.

(A) shortening velocity measured by the constant load ramp method between 0.0 and 0.2 ms; (B) shortening measured by the manual constant load method at three different time intervals; (C) intrapolated shortening at 3 defined loads.

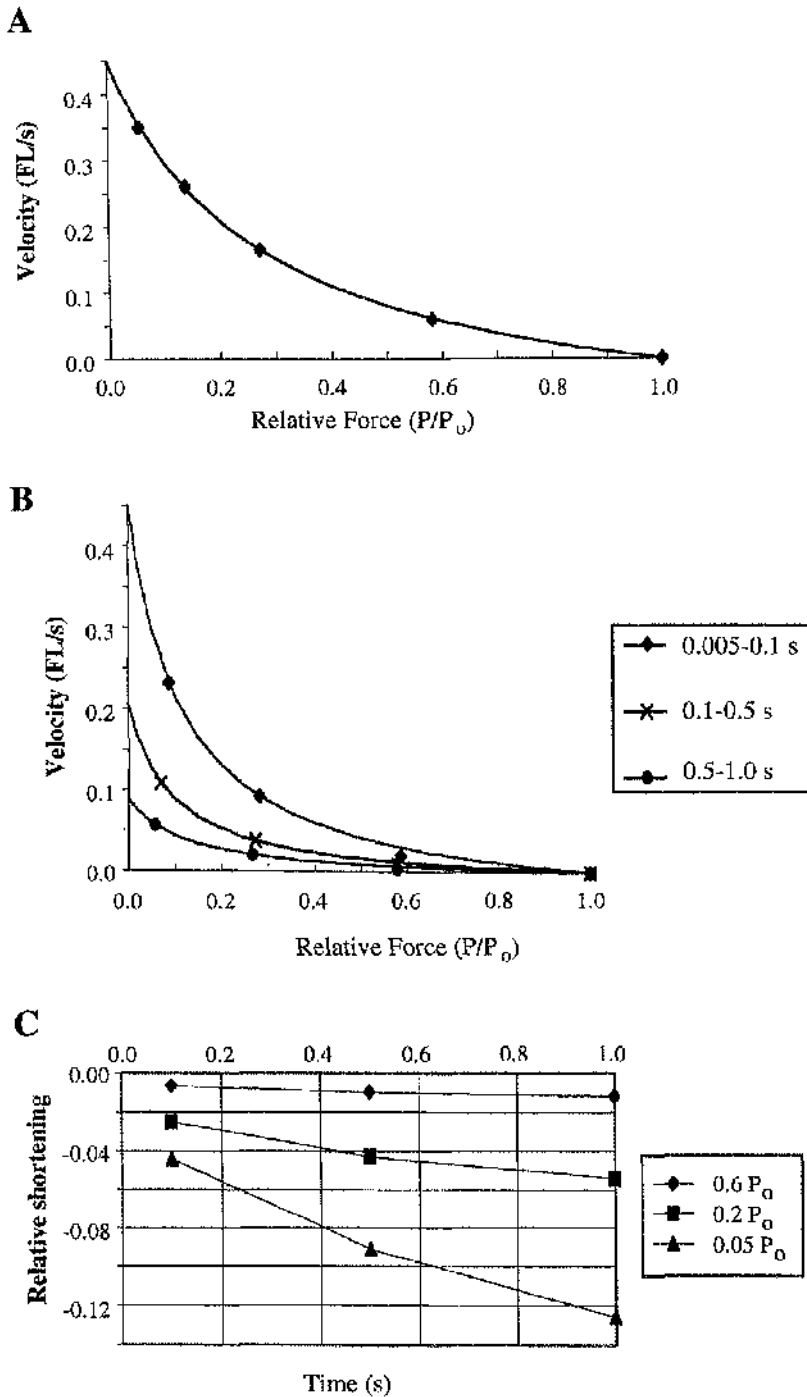


Fig. 4.18  
Examples of the original force-velocity and intrapolated shortening plots for the fast fibre type.

(A) shortening velocity measured by the constant load ramp method between 0.0 and 0.2 ms; (B) shortening velocity measured by the manual constant load method at three different time intervals; (C) intrapolated shortening at 3 defined loads.

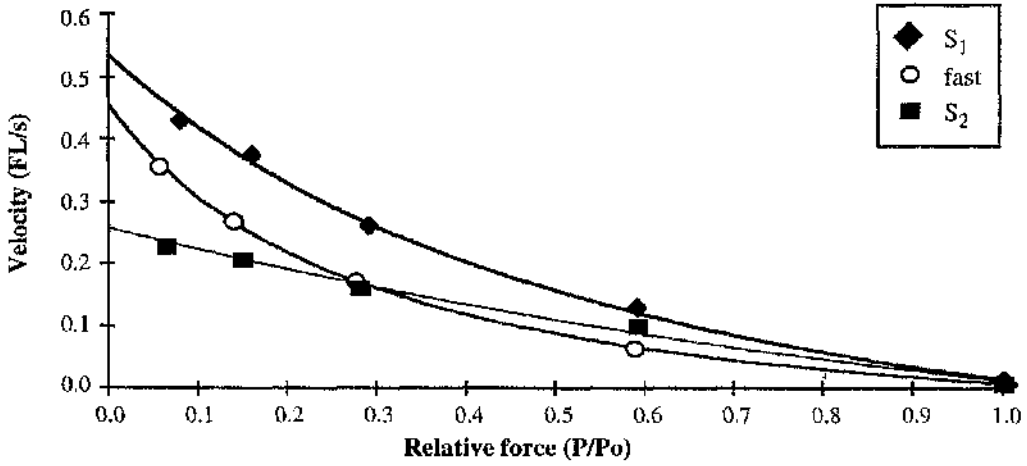


Fig 4.19  
Examples of force-velocity plots for the S<sub>1</sub>, S<sub>2</sub> and fast fibre types.

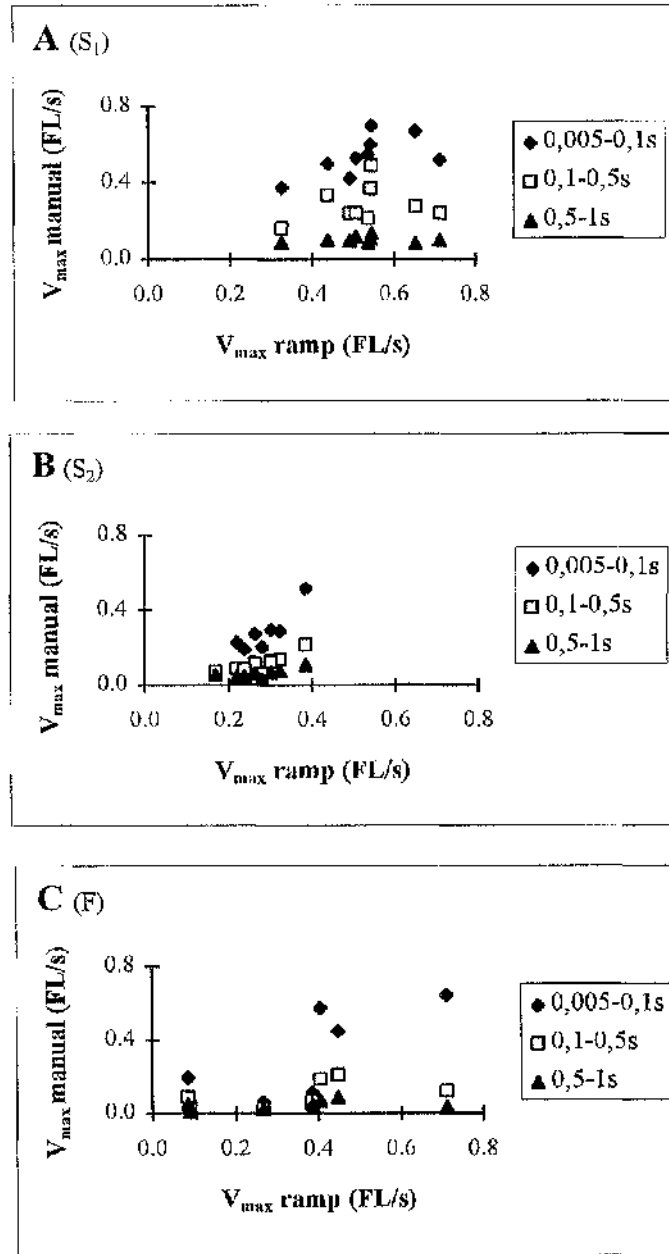


Fig. 4.20

Relationship between shortening velocity measured by the manual and constant load ramp methods.

Maximal shortening velocity ( $V_{\max}$ ) expressed as fibre lengths/second for the  $S_1$  (A),  $S_2$  (B) and fast (C) fibre types. Measurements by the manual constant load method at three different time intervals (indicated in the key) are plotted against the values measured by the constant load ramp method ( $S_1$ :  $n = 9$ ;  $S_2$ :  $n = 8$ ; Fast:  $n = 7$ ).

**Chapter 5**  
**Effects of  $Mn^{2+}$  on the activation of**  
**skinned fibres**

5.1

INTRODUCTION

Little is known about the ability of divalent cations, other than  $\text{Ca}^{2+}$ , to activate the contractile proteins and hence initiate force development in skeletal muscle. Skinned muscle fibres, which have had their sarcolemma destroyed either chemically by exposure to detergents such as Triton X-100, mechanically by splitting the fibres, or by a freeze drying process, have been used to investigate this property of divalent cations.

5.1.1 Activation of skinned muscle fibres with divalent cations

The activation properties of strontium ions ( $\text{Sr}^{2+}$ ) have been most extensively studied.  $\text{Sr}^{2+}$  can substitute for  $\text{Ca}^{2+}$  in activating cardiac and skeletal muscle of vertebrates (Heilbrunn & Wiercinski, 1947; Donaldson & Kerrick, 1975; Donaldson *et al.*, 1978; Moisescu & Thieleczek, 1978a) as well as the skeletal muscle of invertebrates (Caldwell & Walster, 1963). In vertebrate skeletal muscle it has been demonstrated by Moisescu and Thieleczek (1979) that  $\text{Sr}^{2+}$  can induce the same level of force as  $\text{Ca}^{2+}$ .

Although  $\text{Sr}^{2+}$  has been shown to generate force in both vertebrate and invertebrate preparations, the extent to which they are activated differs. An extensive study by Stephenson and Williams (1980) has shown that  $\text{Sr}^{2+}$  cannot activate the contractile apparatus of some invertebrates, and only partially activates others. Distinct differences were also observed by Moisescu and Thieleczek, (1979) in the ability of  $\text{Sr}^{2+}$  to replace  $\text{Ca}^{2+}$  in arthropod skeletal muscles, compared with vertebrate skeletal muscle. Similarly, with these results, experiments by West *et al.* (1992) have shown that both the long and short sarcomere muscle fibres from the claw of the Yabby, *Cherax destructor*, an Australian crayfish can be only partially activated by  $\text{Sr}^{2+}$ .

As well as  $\text{Sr}^{2+}$ , other divalent cations have been shown to generate force in skinned preparations. Frog muscle fibres for example, are maximally activated by  $\text{Ba}^{2+}$ ,  $\text{Cd}^{2+}$  and  $\text{Sr}^{2+}$ , whereas  $\text{Ni}^{2+}$  induces only a transient force response that irreversibly damages the contractile apparatus (Stephenson & Thieleczek, 1986).

### 5.1.2 Skinned fibre experiments with manganese

The activation of invertebrate muscle, vertebrate skeletal and vertebrate cardiac muscle by  $Mn^{2+}$  has not been studied in any detail. The only reported examples of  $Mn^{2+}$ -activation of vertebrate skinned fibres involve rabbit skeletal muscle. For example Yoshida and Tawada (1976), working on rabbit psoas fibres, found that  $Mn^{2+}$ -activation produces 80-89% of the contraction force produced by normal  $Ca^{2+}$ -activation. Consistent with this result,  $Mn^{2+}$  ions activate rabbit soleus muscle fibres (Hoar & Kerrick, 1988).

### 5.1.3 The activation of vertebrate smooth muscle by $Mn^{2+}$

The activation of skinned smooth muscle cells by  $Mn^{2+}$  has been studied more extensively. It is generally agreed that smooth muscle contraction involves the phosphorylation of myosin light chains (Aldelstein & Klee, 1983; Hartshorne & Siemankowski, 1981; Kamm & Stull, 1985). In turn phosphorylation of myosin light chain kinase by  $Ca^{2+}$  and calmodulin (which acts as the main  $Ca^{2+}$  receptor), allows activation of the actomyosin ATPase and contraction. Removal of  $Ca^{2+}$  inactivates the kinase and phosphatases then dephosphorylates myosin light chains, bringing about relaxation. In addition to this proposed mechanism there have been reports that smooth muscle contractile proteins can be activated by other mechanisms, such as direct activation by  $Ca^{2+}$  (Chacko, 1981; Marston & Smith, 1984).

It has been found that  $Mn^{2+}$  can activate smooth muscle contraction. In the presence of the reducing agent dithiothreitol,  $Mn^{2+}$  maximally activates chicken gizzard smooth muscle (Hoar & Kerrick, 1988). It was thought that this activation does not require myosin light chain phosphorylation, and consequently may be useful in studying the mechanisms by which smooth muscle is regulated. A similar study of guinea-pig stomach muscle has shown that in skinned muscle fibres of the antrum,  $Mn^{2+}$  only partially activates the contractile proteins. To produce a given force,  $Mn^{2+}$  is required at a concentration 1000 times greater than  $Ca^{2+}$  (Itoh *et al.*, 1982). Since it has been reported that  $Mn^{2+}$  can bind calmodulin in a similar way to  $Ca^{2+}$  (Chao *et al.*, 1984), this suggests that  $Mn^{2+}$  bound to this  $Ca^{2+}$  receptor incompletely activates them. However, whether

these properties directly reflect the actions of  $Mn^{2+}$  ions smooth skinned muscle cells still remains to be clarified.

#### 5.1.4 The activation of *Nephrops* skinned fibres by $Mn^{2+}$

This chapter investigates the effects of  $Mn^{2+}$  on the isometric force of skinned muscle fibres of the superficial flexor (SF) muscle of *Nephrops norvegicus*. The experiments that have been performed were conducted for two main reasons:

1. experiments on isolated neuromuscular SF muscle preparations have shown that in the presence of low  $Mn^{2+}$  concentrations (9-45  $\mu$ M) there is an increase in the neuronally-evoked force in both the medial ( $S_2$ ) and lateral ( $S_1$ ) bundles (see Section 3.3). One possible explanation for this response is that  $Mn^{2+}$  binds to the myofibrillar regulatory proteins, and leads to the activation of the contractile proteins. In skinned muscle fibres the outer sarcolemmal membrane is disrupted and  $Mn^{2+}$  ions in the external solution have direct access to the regulatory proteins.
2. at present there is no detailed information about the kinetics of  $Mn^{2+}$ -activation in invertebrate skeletal muscle. Therefore measurements of shortening velocity, stretch activation and stiffness have been made with the fibres activated by different concentrations of  $Mn^{2+}$ . The results make it possible to compare the kinetics of  $Mn^{2+}$ -activation with those of normal  $Ca^{2+}$ -activation.

Due to the limitations of time, experiments were performed only on the  $S_1$  fibres from the lateral bundle of the SF muscle. The  $S_1$  fibres was chosen for the  $Mn^{2+}$  experiments because  $S_1$  fibres showed shorter activation times than the  $S_2$  fibres and preliminary experiments have shown that  $Mn^{2+}$ -activation is slower than  $Ca^{2+}$ -activation.

5.2

MATERIALS & METHODS

All experiments followed the basic methodology described by Galler and Rathmayer (1992) and Galler and Hilber (1994). Details of these methods are given in Chapter 4 (Sections 4.2.1-4.2.16). Only additional information is given here.

5.2.1 Preparation of single fibres

Muscle fibres of the  $S_1$  type (1-4 mm in length) were dissected from the lateral bundle of the SF muscle using fine forceps, and were split into myofibrillar bundles with mean diameters of between 40 and 80  $\mu$ M. Myofibrillar bundles of less than 80  $\mu$ m in diameter were used for the  $Ca^{2+}$ - $Mn^{2+}$ -activation experiments because the rate of diffusion of  $Ca^{2+}$  ions appears not to limit force-development below diameters of 80  $\mu$ m (Galler & Neil, 1994).

5.2.2 Solutions

Solutions were prepared according to Moisescu and Thielezek (1978a). All solutions contained 60 mM HEPES (free acid), 10 mM ethyleneglycol bis ( $\beta$ -aminoethyl ether) -N-N'-tetraacetic acid (EGTA) and 8 mM  $Na_2H_2ATP$  (total). In addition, all solutions contained 646 mM sucrose (in order to adjust the osmolarity to 1 osmol) and dextran (40g/l). The pH of all the solutions was adjusted to 7.10 at 22-24 °C. The composition of the solutions is shown in Tables 5.1 and 5.2 and the binding constants for calculating the ATP and EGTA content of the solutions are listed in Tables 5.8 and 5.9. The glycerol relaxation solution for fibre storage consisted of B solution and 50% (v/v) glycerol. A low ionic strength rigor solution (10 mM imidazole, 2.5 mM EGTA, 7.5 (EDTA) 134 mM  $K^+$ propionate, pH 6.8) was used for the fixation procedure of the fibre ends (see Section 4.2). Solutions A and B were mixed according to the proportions shown in Table 5.3, to give a range of pCa values (where pCa = negative logarithm of free  $Ca^{2+}$  concentration). Quantities of A and B solution were measured on a fine balance (accuracy 0.001g) in order to achieve maximum accuracy. All the solutions were stored at -25°C

and were brought to room temperature immediately prior to use. All the experiments were conducted at 22°C.

### 5.2.3 Activation of the muscle fibre

From 'B' solution the fibre was transferred to either  $Mn^{2+}$  solutions,  $Ca^{2+}$  solutions, or low ATP solutions, depending on the experiment conducted. Under a higher  $Ca^{2+}$  concentration ('A' solution pCa 4.7), the fibre produced force under isometric conditions. At the end of each experiment the fibre was transferred to a cuvette containing 'A' solution, followed by relaxation in 'B' solution.

### 5.2.4 Experimental protocols

#### 5.2.4.1 pCa and pMn force relationships

The relationship between the free  $Ca^{2+}$  concentration (expressed as pCa), the free  $Mn^{2+}$  concentration (expressed as pMn) and isometric force was studied. Series of free pCa solutions (pCa 2.82-4.7) and free  $Mn^{2+}$  solutions (pMn 5.66-1.52) were prepared (see Tables 5.1 and 5.3). Single fibres were split into two myofibrillar bundles, and one bundle was exposed to a range of  $Mn^{2+}$  solutions and the other bundle was exposed to a range of  $Ca^{2+}$  solutions, in order of ascending concentration. This enabled a direct comparison to be made between the  $Mn^{2+}$ - and  $Ca^{2+}$ -sensitivity for each fibre. The fibre remained in the activation solution for 2 minutes, or until a plateau force was reached. Between each measurement the fibre was fully relaxed in 'B' solution. The maximal tension was determined, and the quotient of force at maximal  $Ca^{2+}$  or  $Mn^{2+}$  activation was calculated from the cross sectional area.

#### 5.2.4.2 Low ATP experiments

A series of low-concentration ATP solutions was prepared (see Table 5.2). Each ATP solution contained the same amount of free MgATP as one of the high-concentration  $Mn^{2+}$  solutions (See Tables 5.1 & 5.3). When  $Mn^{2+}$  was added to the skinned fibre

solutions and used to activate muscle fibres, due to the high affinity of  $Mn^{2+}$  ions for ATP, MnATP is formed instead of MgATP which is essential for the cycling of cross-bridges and muscle force. Since it is not known whether MnATP can substitute for MgATP, control experiments were conducted to determine the effect of low MgATP concentrations.

### 5.2.5 Kinetic measurements

Whilst under isometric conditions in  $Mn^{2+}$ ,  $Ca^{2+}$  or ATP solutions, a series of kinetic experiments was conducted:

1. *stiffness measurements*; the force responses to small rectangular stretches and releases of the fibre were measured.
2. *stretch activation*; small fast stretches were applied to each fibre (Fig. 4.5). Stretch activation times were compared between  $Mn^{2+}$ - and  $Ca^{2+}$ -activated fibres at different free ion concentrations.
3. *constant load experiments*; the shortening velocity of the fibres was measured, and comparisons were made between the  $Mn^{2+}$ - and the  $Ca^{2+}$ - activated fibres at different free ion concentrations.

### 5.2.6 Analysis of data: pCa and pMn force curves

The effect of  $Ca^{2+}$  ions on force production is represented as the relative force ( $P/P_o$ ), where P is the steady-state force level at a given  $Ca^{2+}$  concentration ( $[Ca^{2+}]$ ), and  $P_o$  is the maximum  $Ca^{2+}$ -activated force as a function of the pCa ( $pM = -\log_{10} [M^{2+}]$  where  $[M^{2+}]$  is the concentration of the divalent cation). The relationship between  $P/P_o$  and pCa is described by the Hill equation (1):

$$P/P_o = K [Ca^{2+}]^{n_{Ca}} / (1 + K [Ca^{2+}]^{n_{Ca}}) \quad (1)$$

where  $n_{Ca}$  is the Hill coefficient (n) for  $Ca^{2+}$ , and K is the constant which is related to the pCa value corresponding to 50%  $P_o$  ( $pCa_{50}$ ) by the expression (2):

$$\log_{10} K = npCa_{50} \quad (2)$$

The  $pCa_{50}$  value describes the sensitivity of the contractile apparatus to  $Ca^{2+}$ . The  $pCa_{10}$  value describes the level of  $[Ca^{2+}]$  required to produce 10 %  $P_o$ , which then gives an indication of the  $Ca^{2+}$  required to initiate contraction. The Hill coefficients are directly proportional to the maximum slope of the sigmoidal curves relating  $P/P_o$  to  $pCa$  and gives an indication of the level of co-operativity within that functional unit. Equivalent functions  $pMn$ ,  $pMn_{50}$  and  $pMn_{10}$  apply in the case of  $Mn^{2+}$  solutions.

### 5.2.7 Graphical representation of results

All results are expressed as mean  $\pm$  S.D. and analysed using a Students t-test. The  $pCa_{50}$ , the  $pMn_{50}$  and the Hill coefficient values were measured for each myofibrillar bundle and are expressed as mean  $\pm$  S.D. However, the fitted curve for the averaged  $pCa$ - and  $pMn$ -force plot uses the average  $P/P_o$  regression values.

## 5.3 RESULTS

### 5.3.1 Force transients induced by $Mn^{2+}$

Manganese activated the contractile apparatus of the SF  $S_1$  fibres at low concentrations ( $pMn$  5.33-4.0) in the absence of  $Ca^{2+}$ . At higher concentrations ( $pMn$  4.0-2.69) there was a force plateau, but at concentrations above  $pMn$  2.3 the force produced was lower (Fig. 5.1). These results refer to the steady state force.

Different types of activation were observed, depending on the  $Mn^{2+}$  concentration. 5 mM  $Mn^{2+}$  ( $pMn$  2.3) induced approximately half- maximal tension, with either a stable plateau force (5.2B) or an activation with a small overshoot in force (Fig. 5.2A). At 10 mM  $Mn^{2+}$  ( $pMn$  2.0) the force responses were transient, with an initial increase to a level of about half maximum force followed by a decrease to either a small force plateau or to zero force (Fig. 5.3). This response was also observed at higher  $Mn^{2+}$  concentrations (15,

30 mM (pMn 1.8, 1.52)); under 30 mM  $Mn^{2+}$  the initial force increase was smaller than that at 10 mM and the subsequent force decrease was to below the passive force level (Fig. 5.3).

### 5.3.2 Relaxation after $Mn^{2+}$ activation

In general, a rapid force decrease was observed when the solution was changed from  $Mn^{2+}$  to B solution. The relaxation was similar to, and in many cases faster than the relaxation after  $Ca^{2+}$ -activations. When higher  $Mn^{2+}$  concentrations (5-30 mM) were applied, the change to B solution induced a transient increase in force (3-20 sec), before it decreased to zero (Fig. 5.3).

### 5.3.3 Comparison with maximal $Ca^{2+}$ activation

Maximal  $Ca^{2+}$  activation always induced a slightly higher force than maximal  $Mn^{2+}$  activation, although the rate of force rise in  $Ca^{2+}$  solutions appeared to be lower than for  $Mn^{2+}$  solutions. When the fibres were activated submaximally, a delay in the force increase was observed with both  $Mn^{2+}$  and  $Ca^{2+}$  solutions. This delay appeared to be longer with  $Mn^{2+}$  solutions. However, since this has not been evaluated, no direct comparison can be made between submaximal  $Mn^{2+}$  and  $Ca^{2+}$  activations on the same myofibrillar bundle.

### 5.3.4 pMn- and pCa-tension relationship

Individual  $S_1$ -type fibres were split into myofibrillar bundles. Using a different bundle for each force experiment, a direct comparison was made between the pMn- and pCa-tension relationship of a fibre (Figs. 5.4, 5.5 and 5.6). The fibres were more sensitive to  $Ca^{2+}$  than to  $Mn^{2+}$  (pCa<sub>50</sub>:  $6.33 \pm 0.26$  (n = 3); pMn<sub>50</sub>:  $4.86 \pm 0.115$  (n = 5)) (see Tables 5.4 and 5.5). These values are significantly different ( $p = 0.011$ ,  $T = 9.27$ ). The mean pCa<sub>50</sub> value differs from the value of  $5.4 \pm 0.12$  obtained by Galler and Neil (1994) from freeze-dried fibres using solutions containing 50 mM EGTA and 10 mM creatine

phosphate. The solutions in the present experiments contained 10 mM EGTA, due to the added  $Mn^{2+}$ . To control for this difference, a single  $S_1$  fibre was split, and individual myofibrillar bundles were tested separately in the 10 mM EGTA solution (myofibrillar bundle Ca-1) and the 50 mM EGTA solution (myofibrillar bundle Ca-1a). The  $pCa_{50}$  value decreased to a value similar to that obtained by Galler and Neil (1994) (10 mM EGTA  $pCa_{50}$ : 6.04; 50 mM EGTA + 10 mM creatine phosphate  $pCa_{50}$ : 5.84).

### 5.3.5 Hill coefficients

Using the Hill equation, the mean Hill coefficients were calculated (see Tables 5.4 and 5.5). The values obtained for  $Ca^{2+}$  and  $Mn^{2+}$  solutions ( $n(Ca^{2+})$ :  $1.7 \pm 0.6$  ( $n = 3$ );  $n(Mn^{2+})$ :  $3.4 \pm 1.2$  ( $n = 5$ ) are significantly different ( $p = 0.044$ ,  $T = 2.68$ ). The results show that the  $pMn$ -tension relationship has a steeper slope than the  $pCa$ -tension relationship (Fig. 5.6). However, the gradient of these curves is very sensitive to the free metal ion concentrations in the solutions and, is especially dependent on the EGTA (total) / metal ion (total) relationship.

### 5.3.6 $Ca^{2+}$ contamination

Although low levels of  $Ca^{2+}$  may have been present in the solutions, the amount of  $Ca^{2+}$  was undetectable with the  $Ca^{2+}$ -sensitive electrode developed by Galler, *et al.* (1994). The free  $Ca^{2+}$  concentration due to  $Ca^{2+}$  contamination was calculated for the worst case conditions, and was found to be too low to activate the fibres.

### 5.3.7 EGTA

$Mn^{2+}$  has a much higher affinity for EGTA than does  $Ca^{2+}$ . Consequently, in the  $Mn^{2+}$  solutions it is impossible to control for  $Ca^{2+}$  contamination. The EGTA concentration was reduced to 10 mM EGTA in all the solutions, including the ones without  $Mn^{2+}$ . A direct comparison between these results and those from living fibres cannot be made,

since the ionic strength in living fibres is higher than in the solutions with 10 mM EGTA used in the skinned fibre experiments.

### 5.3.8 Effects of ionic strength on the $\text{Ca}^{2+}$ activated force

The  $\text{Ca}^{2+}$  sensitivity was lower at high ionic strength (solutions with 50 mM EGTA compared with 10 mM EGTA). Plotting stiffness against tension (steady state levels at different activations), the values obtained at different ionic strengths lie on the same relationship (data not shown).

### 5.3.9 ATP control experiments

#### 5.3.9.1 Muscle fibre force

Under normal physiological conditions ATP binds to  $\text{Mg}^{2+}$  to form MgATP, which is essential for crossbridge cycling and force generation (Woledge *et al.*, 1985). At high free  $\text{Mn}^{2+}$  concentrations,  $\text{Mn}^{2+}$  has a higher affinity for ATP than does  $\text{Mg}^{2+}$  and binds ATP to form MnATP, which decreases the MgATP concentration of the solution (see Table 5.6). It is not known whether MnATP can be used by the muscle fibre instead of MgATP, but it is possible that the decrease of MgATP as a result of the formation of MnATP in the  $\text{Mn}^{2+}$  solutions is the source of the force decrease seen at high free  $\text{Mn}^{2+}$  concentrations. A comparison was therefore made between the high  $\text{Mn}^{2+}$  activation solutions (above pMn 3.0 (1 mM)) and  $\text{Ca}^{2+}$  solutions containing the same concentrations of MgATP (Table 5.6).

The results show that the force in the low MgATP solution (0.16 mM) was higher than that reached in the  $\text{Mn}^{2+}$ -solution (10 mM) with the corresponding MgATP concentration. At lower concentrations of  $\text{Mn}^{2+}$  (1-5 mM), the forces were similar to those in the MgATP solutions (Fig. 5.8). The  $\text{Mn}^{2+}$ -activations at 1-5 mM showed a different force behaviour than the corresponding low-ATP  $\text{Ca}^{2+}$ -activations.  $\text{Mn}^{2+}$  activations showed a stable plateau force whereas the low-ATP  $\text{Ca}^{2+}$ -activations showed decreasing force with continuing activation time (Fig. 5.8).

When the isometric force is plotted against the MnATP it can be seen that tension decreases with increasing MnATP concentrations (Fig. 5.10). This decrease appears not to be due to increased levels of MnATP limiting the levels of available MgATP (Fig. 5.9). The relationship between MgATP and tension has a hyperbolic function similar to that of the Michaelis Menten relationship. The  $K_m$  value of the relationship under  $Mn^{2+}$  activations is around 0.2 mM MgATP. Under these conditions the concentration of the presumed inhibitor is relatively constant (6.53-7.93 mM see Table 5.6). Under  $Ca^{2+}$ , the isometric force is much more sensitive to the MgATP concentration; in the presence of 50  $\mu$ M MgATP the force was still more than 80 % of the maximum level, whereas the comparable  $Mn^{2+}$  solution produced only 50 % maximal force. This trend continued for the lower-ATP concentration- $Mn^{2+}$  solutions, but not for the control low-ATP solutions. MgATP concentrations below 0.05 mM were not used for this study.

### 5.3.9.2 Muscle fibre stiffness

If MgATP were limiting in the higher  $Mn^{2+}$  solutions, an increase in muscle fibre stiffness would occur, since the attached crossbridges would be unable to detach and the fibre would be in a state of rigor. Therefore small stretches were made under each  $Mn^{2+}$  solution and the low MgATP solution, to test for rigor.

Stiffness increased only in the 30 mM (pMn 1.52) solution (Fig. 5.11), and this was accompanied by a decrease in muscle force (Fig. 5.12). However, the stiffness at pMn 1.5 (30 mM solution) is not significantly different from that measured at pCa 4.7 (A solution) ( $p = 0.46$ ,  $T = -0.91$ , solution, A:  $n = 6$ ; pMn 1.52:  $n = 3$ ). When stiffness is plotted against the change in MnATP concentration (Fig. 5.13) the increase in stiffness at 30 mM  $Mn^{2+}$  is shown to be correlated with increased levels of MnATP. However, when stiffness is plotted against the MgATP concentration (Fig 5.14) there is no significant difference in stiffness between the MgATP activations (1.3-0.105 mM) and the  $Mn^{2+}$ -activations (1-15 mM), but at 30 mM  $Mn^{2+}$  the stiffness increases. This result suggests that a rigor-like state is present at 30 mM  $Mn^{2+}$ , whereas in the solution with the corresponding low MgATP (53  $\mu$ M) there is no rigor present. This is in agreement with the theory that MnATP competes with MgATP on the binding site of the myosin

ATPase. MnATP seems to induce a rigor-like state only if a low MgATP concentration (50  $\mu$ M) is present.

### 5.3.9.3 Maximal shortening velocity

Measurements of the maximal unloaded shortening velocity ( $V_{\max}$ ) (Fig. 5.15) and of filament sliding (Fig. 5.16) were made under different  $Mn^{2+}$  and MgATP solutions. Both the  $V_{\max}$  and filament sliding during maximal  $Mn^{2+}$  activation (0.1-2 mM) did not differ significantly from the values recorded during maximal  $Ca^{2+}$ -activation ( $V_{\max}$ , 0.1 mM  $Mn^{2+}$ :  $p = 0.13$ ,  $T = -1.57$ ; 1 mM  $Mn^{2+}$ :  $p = 0.48$ ,  $T = -0.74$ ; 2 mM  $Mn^{2+}$ :  $p = 0.75$ ,  $T = -0.33$ , Filament sliding, 0.1 mM  $Mn^{2+}$ :  $p = 0.15$ ,  $T = -1.51$ ; 1 mM  $Mn^{2+}$ :  $p = 0.52$ ,  $T = -0.68$ ; 2 mM  $Mn^{2+}$ :  $p = 0.81$ ,  $T = -0.25$ , solution A:  $n = 28$ ;  $Mn^{2+}$  solutions (mM) 0.1:  $n = 12$ ; 1:  $n = 6$ ; 2:  $n = 5$ ). Submaximal  $Mn^{2+}$ -activations (below 1 mM), had lower  $V_{\max}$  values (i.e. lower shortening velocity), as had submaximal  $Ca^{2+}$ -activations. Filament sliding (Fig. 5.18) and  $V_{\max}$  (Fig. 5.17) were also measured in low-MgATP solutions: the 2 mM  $Mn^{2+}$  solution and the 0.72 mM MgATP solution contained the same amount of free-MgATP. A significant difference was observed between both measurements of shortening velocity made in these two solutions ( $V_{\max}$ :  $p = 0.03$ ,  $T = 3.0$ ; filament sliding:  $p = 0.023$ ,  $T = 3.23$ ) (Fig. 5.17 and 5.18).

### 5.3.10 Stretch activation experiments

Stretch activations in all the experiments were faster (by 2-3 times) in maximal  $Mn^{2+}$  activations (pMn 4.33-1.52) than those recorded in A solution (pCa 4.7) (Figs. 5.19a, 5.19b and Table 5.4). At  $Mn^{2+}$  concentrations above 2 mM (pMn 2.69) the stretch activation disappeared (Figs. 5.20a and 5.20b). In  $Ca^{2+}$  activations with low MgATP (1.3-0.053 mM) stretch activation was never observed, and only exponentially shaped stretches were recorded (Figs 5.21a and 5.21b). Stretch activation was present at lower  $Mn^{2+}$  concentrations (1-5 mM), but was absent in the corresponding low ATP solutions.

## 5.4

## DISCUSSION

The experiments conducted in this chapter demonstrate that  $\text{Mn}^{2+}$ , like other divalent ions such as  $\text{Sr}^{2+}$ , can activate the contractile proteins of a crustacean skeletal muscle. They also confirm the results of the previous chapter. If  $\text{Mn}^{2+}$  ions can diffuse to the contractile elements of the membrane-intact fibres, this provides a possible explanation for the increase of muscle force seen when low concentrations are applied to intact muscle fibres (Chapter 3).

5.4.1 Activation of  $\text{S}_1$  fibres by  $\text{Mn}^{2+}$ 

The experiments described in this chapter demonstrate that  $\text{Mn}^{2+}$  ions can activate the  $\text{S}_1$  fibres of *Nephrops norvegicus*, although the maximal force induced by  $\text{Mn}^{2+}$  (at pMn 4.0) was lower than that induced by maximal  $\text{Ca}^{2+}$ -activation (Figs. 5.4, 5.5 and 5.6). This finding is in agreement with that of other workers, who have shown that the divalent cations  $\text{Sr}^{2+}$ ,  $\text{Ba}^{2+}$ , and  $\text{Cd}^{2+}$  can activate frog muscle fibres (Stephenson & Thieleczek, 1986). However, this response was gradually reversed with increasing  $\text{Mn}^{2+}$  concentrations (beyond pMn 3.0) and the force was dose-dependently inhibited until it was completely abolished at 30 mM  $\text{Mn}^{2+}$  (pMn 1.52) (Fig 5.1). These changes accompany decreasing levels of MgATP and increasing levels of MnATP, which raises the question of whether either of these changes can themselves cause the force changes.

## 5.4.2 The role of MgATP and MnATP

Under normal physiological conditions ATP binds to  $\text{Mg}^{2+}$  to form MgATP, which is essential for myofilament crossbridge cycling and force generation (Woledge *et al.*, 1985).  $\text{Mn}^{2+}$  has a higher affinity for ATP than  $\text{Mg}^{2+}$ , and binds ATP to form MnATP, which decreases the MgATP concentration of the solution (Table 5.6). It is not known whether MnATP can be used by the muscle fibre in the place of MgATP, but it is possible that the decrease of the MgATP concentration as a result of the formation of MnATP in the  $\text{Mn}^{2+}$  solutions is the cause of the force decrease seen at high free  $\text{Mn}^{2+}$

concentrations. Two main theories have been put forward to explain the inhibition of muscle force by  $Mn^{2+}$ :

1. MgATP concentration is limiting due to the high levels of MnATP which the muscle fibre is unable to use, and consequently enters a rigor like state.
2. the MnATP inhibits the myosin ATPase, and thereby competes with MgATP for binding sites on the myosin ATPase.

#### 5.4.2.1 Does MgATP limit force production?

With reference to the first hypothesis, when a comparison was made between the high- $Mn^{2+}$  activation solutions (above 1 mM) and the corresponding MgATP solutions, the results show that the decreasing levels of MgATP did not cause the depression of muscle force seen at  $Mn^{2+}$  concentrations higher than 5 mM (pMn 2.3). The force in the low MgATP solutions was always higher than in the corresponding  $Mn^{2+}$  solution (Fig. 5.8). This result suggests that MgATP is not force-limiting.

#### 5.4.2.2 Does competitive inhibition between MnATP and MgATP limit force production?

As the MgATP level was decreased, the tension-MgATP relationship changed, even in the presence of a relatively constant concentration of MnATP (6.53-7.93 mM) (Table 5.6). This strongly suggests that competitive inhibition does occur between MnATP and MgATP, and that it is much more pronounced when the MgATP level is low, as in the 30 mM  $Mn^{2+}$  solution (Fig. 5.9). The relationship between MgATP and tension has a hyperbolic function similar to that of the Michaelis-Menten relationship (Fig. 5.9). The  $K_m$  value of the relationship under  $Mn^{2+}$  solutions was  $\cong 0.2$  mM MgATP. Under these conditions, the concentration of the presumed inhibitor MnATP was relatively constant (6.53-7.93 mM). Under  $Ca^{2+}$  the isometric force was much more sensitive to the MgATP concentration; for example in the presence of 50  $\mu$ M MgATP, the force was still more than 80% of maximum, whereas the comparable  $Mn^{2+}$  solution produced a force of only 50% of maximum. This trend continued in the lower ATP concentration- $Mn^{2+}$  solutions,

but not for the control low ATP solutions. In the literature,  $K_m$  values of 1 to 7.5  $\mu\text{M}$  MgATP are known under  $\text{Ca}^{2+}$  activation (Pferrer *et al.*, 1988). According to these values, the formation of MnATP would lead to a large change of the  $K_m$  value.

The work of Stephenson and Thieleczek (1986) also suggests that the binding of divalent metal ions to ATP competitively inhibits MgATP. They reported that the force response declined markedly when the myofibrillar preparations were activated by  $\text{Cd}^{2+}$ . When a fibre was transferred to a solution containing a high concentration of CdATP (6.7 mM) and a low concentration of MgATP (1.1 mM), the force initially reached about 80% of the maximal force due to the rapid increase in  $\text{Cd}^{2+}$  ions, and then decreased to about 50% maximal force, as the CdATP gradually increased in the preparation. It was concluded that the CdATP had an inhibitory effect on the force response due to the CdATP competing for the MgATP binding site on the myosin. A similar response is seen in *Nephrops* S<sub>1</sub> fibres at 5 mM  $\text{Mn}^{2+}$  (Fig. 5.2).

#### 5.4.3 Kinetic measurements made under $\text{Mn}^{2+}$

The questions of whether force is limited by low levels of MgATP and whether MnATP competes with MgATP have been addressed further using kinetic measurements. If MgATP were limiting in the higher  $\text{Mn}^{2+}$ -solutions, an increase in muscle fibre stiffness would be expected. The attached crossbridges would be unable to detach and the fibre would be in a state of rigor. Small stretches were made under each  $\text{Mn}^{2+}$  solution and low ATP solution, to test for rigor. No significant difference was observed between the  $\text{Mn}^{2+}$ -solutions (1-15 mM) and their corresponding low ATP solutions. Muscle fibre stiffness increased only at 30 mM  $\text{Mn}^{2+}$  (Figs. 5.11 & 5.13). This result suggests that a rigor-like state was present at 30 mM  $\text{Mn}^{2+}$ , whereas in the solution with corresponding low MgATP (53  $\mu\text{M}$ ) there was no rigor present (Fig. 5.14). This is in agreement with the model above in which MnATP competes with MgATP for the binding sites of the myosin ATPase. MnATP seems to induce rigor-like states only if a low MgATP concentration (50  $\mu\text{M}$ ) is present.

#### 5.4.4 Stretch Activation

Stretch activation experiments also highlight discrepancies between  $Mn^{2+}$  activation at high concentrations and the corresponding low ATP solutions. It is interesting that  $Mn^{2+}$  is able to prevent the effects of low MgATP with regard to stretch activation. Stretch activation was never observed in any of the low ATP solutions (Fig. 5.21), whereas it was recorded in the  $Mn^{2+}$  solutions up to a concentration of 5 mM (Table 5.7, Fig. 5.20). This difference suggests that there is no simple answer to how  $Mn^{2+}$  acts. These results suggest that  $Mn^{2+}$  may not only reduce the levels of MgATP in solutions, but may also affect the kinetics of certain steps of the crossbridge cycle.

The same response was recorded when the stretch activation time was measured for a fibre immersed in  $Ca^{2+}$  solutions containing different concentrations of  $Mn^{2+}$ . Stretch activation was much faster in the presence of  $Mn^{2+}$  ions (Table 5.7).

#### 5.4.5 Ionic concentration

One other possible explanation is based on the fact that  $Ca^{2+}$  and other divalent ions change the surface charges of the filaments, thus affecting the attachment of the crossbridges (Julian & Moss, 1981). It is thought that the thick filaments carry a positive charge and the thin filaments carry a negative charge and that increasing the concentrations of the divalent ions may decrease the affinity of the crossbridges and lead to a decrease in isometric force. Experiments using high concentrations of  $Mn^{2+}$  (15-30 mM) could be affected in this way, due to the high ionic strength of the solutions.

#### 5.4.6 Can $Mn^{2+}$ bind to troponin?

Troponin (Tn) is composed of three subunits, Tn-C, Tn-I and Tn-T. The troponin molecule reconstituted from these three subunits has all the properties of the native protein: in conjunction with tropomyosin it switches the actomyosin-ATPase on and off, depending on whether the Tn-C subunit is occupied by  $Ca^{2+}$  or is not (see Section 4.1).

The sensitivity of skeletal muscle actomyosin is a reflection of the  $\text{Ca}^{2+}$ -binding ability of Tn-C, and in view of the important regulatory role that this protein plays in the EC coupling of skeletal muscle, a clarification of its functional role in relation to the binding of  $\text{Ca}^{2+}$  is essential for a better understanding of muscle function. For this reason the ability of cations such as  $\text{Mn}^{2+}$  to bind to Tn has received attention, and it has been found that they provide useful tools for studying the ion binding properties of Tn (West *et al.*, 1992).

Evidence from electron spin resonance techniques suggests that  $\text{Mn}^{2+}$  binds to troponin at the high affinity  $\text{Ca}^{2+}$ -binding site, although the binding affinity for  $\text{Mn}^{2+}$  is lower ( $\text{Mn}^{2+}$  to Tn:  $n = 2.5$  moles  $\text{Mn}^{2+}$  per  $10^5$  g Tn and  $k \cong 2 \times 10^5 \text{ M}^{-1}$ ;  $\text{Ca}^{2+}$  to Tn:  $n = 3$  moles per  $10^5$  g Tn and  $k \cong 4 \times 10^6 \text{ M}^{-1}$ , where  $n$  represents the number of  $\text{Mn}^{2+}$  sites and  $k$  the binding constant for these sites) (Hartshome & Boucher, 1974).

Consistent with these findings, absorption and fluorescence spectrophotometry techniques have been used to show that metal ions bind to Tn-C with affinities in the order of  $\text{Ca}^{2+} \cong \text{Cd}^{2+} \cong \text{Yb}^{3+} > \text{Sr}^{2+} \cong \text{La}^{3+} \geq \text{Mn}^{2+} > \text{Zn}^{2+} \cong \text{Co}^{2+} \cong \text{Ba}^{2+} > \text{Mg}^{2+} \cong \text{Ni}^{2+}$  (Winter *et al.*, 1974). The spectroscopic changes observed with lower affinity cations are quantitatively different from those produced by those of high affinity ( $\text{Ca}^{2+}$ ,  $\text{Cd}^{2+}$  and  $\text{Sr}^{2+}$ ), indicating that the nature or extent of the conformational change brought about by the low affinity cations may be different from those produced by  $\text{Ca}^{2+}$ . It is thought that these differences reflect the inability of these cations to fit the metal binding sites (Winter *et al.*, 1974).

However, although  $\text{Mn}^{2+}$  has been shown to bind to the same binding site as  $\text{Ca}^{2+}$  it has also been reported that  $\text{Mn}^{2+}$  cannot substitute for  $\text{Ca}^{2+}$  as an activator of muscle contraction (Hartshome & Boucher, 1974). This would suggest that the occupancy of the receptor sites is not significant for activation, and that only specific activating cations can induce the conformational changes that ultimately lead to the activation of actomyosin ATPase. The results presented in this chapter and in Chapter 3 show, however, that  $\text{Mn}^{2+}$  can activate the contractile proteins and induce muscle force.

The question that arises from these investigations is: what makes a particular cation bind to Tn? Other factors such as the chemical properties are important in the binding of

divalent cations to Tn. However, when these have been investigated for other metal ions there does not appear to be any clear differences between the chemical properties of a given cation and its affinity for Tn (Hartshorne & Boucher, 1974). For example cations with the highest affinity for the Tn receptor site can differ in their co-ordination chemistry.  $\text{Ca}^{2+}$  forms ionic bonds with oxygen ligands and it seems very likely that it binds to Tn via carboxyl groups.  $\text{Cd}^{2+}$  also binds very strongly to oxygen, and it would therefore be expected to prefer nitrogen and sulphur as electron donors and form bonds of a more covalent character.

What is increasingly evident is that the size of the cation is critical in the selectivity of the receptor site. The  $\text{Ca}^{2+}$ -binding site of Tn will only accept divalent cations within a relatively restricted range of ionic radii (Fuchs, 1974), for example  $\text{Cd}^{2+}$  has an ionic radius (0.97Å) which is extremely close to that of  $\text{Ca}^{2+}$  (0.99 Å). Cations with an ionic radius of less than 0.8 Å ( $\text{Mn}^{2+}$ ) or greater than 1.2 Å ( $\text{Pb}^{2+}$ ) appear to be effectively excluded from the  $\text{Ca}^{2+}$ -binding sites (Fuchs, 1974), and as  $\text{Mn}^{2+}$  fits within these limits it is able to bind Tn.

It appears from the  $\text{Mn}^{2+}$  studies that the ability of  $\text{Mn}^{2+}$  to pass through the membrane- $\text{Ca}^{2+}$  channels and activate the contractile elements, is due to the ionic properties of the  $\text{Mn}^{2+}$  ions. The ionic radius appears to be critical for both the above steps of  $\text{Mn}^{2+}$  activation and the energies of hydration (see Sections 3.1 and 3.4) are important in the movement of  $\text{Mn}^{2+}$  ions through the  $\text{Ca}^{2+}$  channels.

Table 5.1 Composition of B, A and Mn<sup>2+</sup> solutions

| Solution | Free Ca <sup>2+</sup><br>(M) | Free Mg <sup>2+</sup><br>(mM) | Free Mn <sup>2+</sup><br>(mM) | MgATP<br>(mM) | MnATP<br>(mM) | Total Ca <sup>2+</sup><br>(M) | Total Mg <sup>2+</sup><br>(mM) | Total Mn <sup>2+</sup><br>(mM) |
|----------|------------------------------|-------------------------------|-------------------------------|---------------|---------------|-------------------------------|--------------------------------|--------------------------------|
| B        | 1.0x10 <sup>-9.0</sup>       | 1                             | 0.00                          | 7.14          | 0.00          | 0                             | 8.51                           | 0.00                           |
| A        | 1.0x10 <sup>-4.7</sup>       | 1                             | 0.00                          | 7.07          | 0.00          | 9.9x10 <sup>-3.0</sup>        | 8.11                           | 0.00                           |
| pMn 1.52 | *                            | 1                             | 30.00                         | 0.05          | 7.93          | 5.0x10 <sup>-6.0</sup>        | 1.05                           | 47.94                          |
| pMn 1.80 | *                            | 1                             | 15.00                         | 0.10          | 7.87          | 5.0x10 <sup>-6.0</sup>        | 1.10                           | 32.88                          |
| pMn 2.00 | *                            | 1                             | 10.00                         | 0.16          | 7.81          | 5.0x10 <sup>-6.0</sup>        | 1.16                           | 27.82                          |
| pMn 2.30 | *                            | 1                             | 5.00                          | 0.30          | 7.65          | 5.0x10 <sup>-6.0</sup>        | 1.49                           | 22.65                          |
| pMn 2.69 | *                            | 1                             | 2.00                          | 0.72          | 7.19          | 5.0x10 <sup>-6.0</sup>        | 1.72                           | 19.19                          |
| pMn 3.00 | 1.0x10 <sup>-8.0</sup>       | 1                             | 1.00                          | 1.30          | 6.53          | 2.0x10 <sup>-6.0</sup>        | 2.31                           | 17.54                          |
| pMn 4.00 | 1.0x10 <sup>-8.0</sup>       | 1                             | 0.10                          | 4.90          | 2.47          | 8.0x10 <sup>-8.0</sup>        | 5.95                           | 12.57                          |
| pMn 4.33 | -                            | 1                             | 0.010                         | 5.90          | 1.39          | -                             | 6.93                           | 11.43                          |
| pMn 4.66 | -                            | 1                             | -                             | 6.50          | 0.71          | -                             | 7.53                           | 10.73                          |
| pMn 4.80 | -                            | 1                             | -                             | 6.66          | 0.53          | -                             | 7.69                           | 10.53                          |
| pMn 5.00 | 1.0x10 <sup>-7.0</sup>       | 1                             | 0.001                         | 6.83          | 0.34          | -                             | 7.86                           | 10.34                          |
| pMn 5.33 | -                            | 1                             | -                             | 6.99          | 0.16          | -                             | 7.87                           | 10.13                          |
| pMn 5.66 | -                            | 1                             | -                             | 7.07          | 0.08          | -                             | 7.88                           | 10.02                          |

\* The Ca<sup>2+</sup> concentration is below detectable levels

Table 5.2 Composition of low ATP solutions

| Solution  | MgATP<br>(mM) | MnATP<br>(mM) | Total Ca <sup>2+</sup><br>(mM) | Total Mg <sup>2+</sup><br>(mM) | Total Mn <sup>2+</sup><br>(mM) | Total ATP<br>(mM) |
|-----------|---------------|---------------|--------------------------------|--------------------------------|--------------------------------|-------------------|
| 1.3 ATP   | 1.300         | -             | 9.90                           | 2.340                          | -                              | 1.500             |
| 0.72 ATP  | 0.720         | -             | 9.90                           | 1.715                          | -                              | 0.800             |
| 0.305 ATP | 0.305         | -             | 9.90                           | 0.311                          | -                              | 0.345             |
| 0.159 ATP | 0.159         | -             | 9.89                           | 1.164                          | -                              | 0.190             |
| 0.105 ATP | 0.105         | -             | 9.87                           | 1.110                          | -                              | 0.119             |
| 0.053 ATP | 0.053         | -             | 9.90                           | 1.058                          | -                              | 0.060             |

Table 5.3 Mixing proportions of solutions A and B used for the pCa-tension experiments, and the final pCa of the mixtures

| Free pCa | Free pMg | Total Ca <sup>2+</sup> (mM) | Total Mg <sup>2+</sup> (mM) | % A solution |
|----------|----------|-----------------------------|-----------------------------|--------------|
| 8.18     | 2.75     | 1.50                        | 10.184                      | 3.00         |
| 7.94     | 2.75     | 2.50                        | 10.140                      | 5.00         |
| 7.76     | 2.76     | 3.75                        | 10.085                      | 7.50         |
| 7.57     | 2.76     | 5.50                        | 10.008                      | 11.0         |
| 7.27     | 2.78     | 10.0                        | 9.810                       | 20.0         |
| 7.03     | 2.78     | 15.0                        | 9.590                       | 30.0         |
| 6.84     | 2.82     | 20.0                        | 9.370                       | 40.0         |
| 6.67     | 2.84     | 25.0                        | 9.130                       | 50.0         |
| 6.49     | 2.87     | 30.0                        | 8.930                       | 60.0         |
| 6.30     | 2.89     | 35.0                        | 8.710                       | 70.0         |
| 6.12     | 2.91     | 39.0                        | 8.534                       | 78.0         |
| 5.95     | 2.93     | 42.0                        | 8.402                       | 84.0         |
| 5.76     | 2.94     | 44.5                        | 8.292                       | 89.0         |
| 5.55     | 2.95     | 46.5                        | 8.204                       | 93.0         |
| 5.30     | 2.96     | 48.0                        | 8.138                       | 96.0         |
| 5.02     | 2.96     | 49.0                        | 8.094                       | 98.0         |
| 4.49     | 2.96     | 49.5                        | 8.072                       | 99.0         |
| 4.47     | 2.94     | 50.0                        | 8.050                       | 100.0        |

Table 5.4 Hill coefficients, constants and pMn<sub>50</sub> values for the Mn<sup>2+</sup>-activation experiments

| Fibre   | pMn <sub>50</sub> | Hill constant | Hill coefficient |
|---------|-------------------|---------------|------------------|
| Mn-12   | 4.84              | 24.7          | 5.26             |
| Mn-13   | 4.87              | 10.7          | 2.3              |
| Mn-14   | 4.96              | 12.5          | 2.6              |
| Mn-15   | 4.96              | 14.2          | 2.94             |
| Mn-17   | 4.68              | 19.3          | 4.17             |
| average | 4.86              | 16.24         | 3.45             |
| S.D.    | 0.115             | 5.62          | 1.23             |
| n       | 5                 | 5             | 5                |

Table 5.5 Hill coefficients, constants and  $pCa_{50}$  values for the  $Ca^{2+}$ -activation experiments

| Fibre   | $pCa_{50}$ | Hill constant | Hill coefficient |
|---------|------------|---------------|------------------|
| Ca-1a   | 6.04       | 6.91          | 1.2              |
| Ca-3    | 6.53       | 9             | 1.43             |
| Ca-4    | 6.44       | 15.2          | 2.4              |
| average | 6.33       | 10.57         | 1.677            |
| S.D.    | 0.26       | 4.31          | 0.637            |
| n       | 3          | 3             | 3                |

Table 5.6 Lists the MnATP and MgATP concentrations that are in the different pMn solutions, As MnATP increased, MgATP decreases

| Free Mn (pMn) | MgATP (mM) | MnATP (mM) |
|---------------|------------|------------|
| 4             | 4.9        | 2.47       |
| 4.33          | 5.903      | 1.384      |
| 4.66          | 7          | 0.743      |
| 4.8           | 6.66       | 0.529      |
| 5             | 6.834      | 0.34       |
| 5.33          | 6.994      | 0.164      |
| 5.66          | 7.07       | 0.077      |
| 3             | 1.3        | 6.53       |
| 2.69          | 0.72       | 7.186      |
| 2.3           | 0.305      | 7.647      |
| 2             | 0.159      | 7.81       |
| 1.82          | 0.105      | 7.871      |
| 1.52          | 0.053      | 7.93       |

Table 5.7 The stretch activation ( $t_2$ ) times (ms) for 5  $S_1$  fibres when exposed to different concentrations of  $Mn^{2+}$  and when maximally  $Ca^{2+}$ -activated. ( $t_2$  represents the time from the beginning of stretch to the peak value of the delayed force increase).

| Fibre (No) | pCa (ms) | pMn (ms) |
|------------|----------|----------|----------|----------|----------|----------|----------|----------|----------|----------|
| 1          | 400      | 140      | 140      | -        | 130      | 115      | 105      | 170      | 170      | 130      |
| 2          | 400      | -        | 160      | -        | 125      | 130      | 160      | -        | 160      | 150      |
| 3          | -        | -        | 180      | 160      | 160      | 160      | 190      | -        | 220      | -        |
| 4          | 570      | -        | 170      | 170      | 160      | 160      | -        | 230      | 200      | 190      |
| 5          | 440      | -        | 150      | 110      | 100      | 100      | 120      | 130      | -        | -        |
| Mean       | 452.5    | 140.0    | 160.0    | 146.6    | 135.0    | 133.0    | 143.7    | 176.6    | 187.5    | 156.6    |
| S.D.       | 80.6     | -        | 15.8     | 32.1     | 25.5     | 26.8     | 35.6     | 50.3     | 27.5     | 30.5     |
| n          | 4        | 1        | 5        | 3        | 5        | 5        | 4        | 3        | 4        | 3        |

Table 5.8 Binding constants for EGTA

| Chemical                                    | Concentration<br>(M)  |
|---|-----------------------|
| HEGTA/(H. EGTA)                             | $1 \times 10^{9.27}$  |
| H <sub>2</sub> EGTA/(H <sub>2</sub> EGTA.H) | $1 \times 10^{8.67}$  |
| H <sub>3</sub> EGTA/(H <sub>3</sub> EGTA.H) | $1 \times 10^{2.66}$  |
| H <sub>4</sub> EGTA/(H <sub>4</sub> EGTA.H) | $1 \times 10^{2.40}$  |
| MgEGTA/(Mg. EGTA)                           | $1 \times 10^{5.21}$  |
| MgHEGTA/(MgEGTA.H)                          | $1 \times 10^{7.62}$  |
| CaEGTA/(Ca. EGTA)                           | $1 \times 10^{10.97}$ |
| CaHEGTA/(CaEGTA.H)                          | $1 \times 10^{3.79}$  |
| MnEGTA/(Mn. EGTA)                           | $1 \times 10^{12.28}$ |
| MnHEGTA/(MnEGTA.H)                          | $1 \times 10^{4.10}$  |

\* H = proton concentration, ionic strength = 0.1 M, binding constants at 20°C

Table 5.9 Binding constants for ATP

| Chemical                                  | Concentration<br>(M) |
|---|----------------------|
| HATP/(H. ATP)                             | $1 \times 10^{6.51}$ |
| H <sub>2</sub> ATP/(H <sub>2</sub> ATP.H) | $1 \times 10^{4.06}$ |
| MgATP/(Mg. ATP)                           | $1 \times 10^{4.06}$ |
| MgHATP/(MgATP.H)                          | $1 \times 10^{4.55}$ |
| CaATP/(Ca. ATP)                           | $1 \times 10^{3.77}$ |
| CaHATP/(CaATP.H)                          | $1 \times 10^{4.69}$ |
| MnATP/(Mn. ATP)                           | $1 \times 10^{4.76}$ |
| MnHATP/(MnATP.H)                          | $1 \times 10^{4.14}$ |

\* H = proton concentration, ionic strength = 0.1 M, binding constants at 20°C

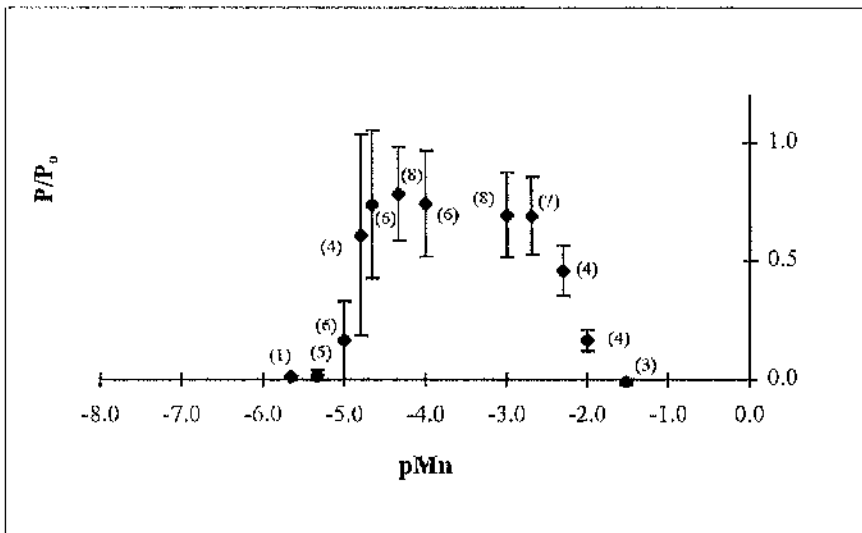


Fig. 5.1

Relationship between the relative isometric steady-state force and the free  $Mn^{2+}$  concentration.

Mean  $\pm$  S.D. values for relative isometric force ( $P/P_0$ ); pMn expressed as the negative logarithm of the free  $[Mn^{2+}]$  of the bath solutions; n values are indicated in parenthesis.

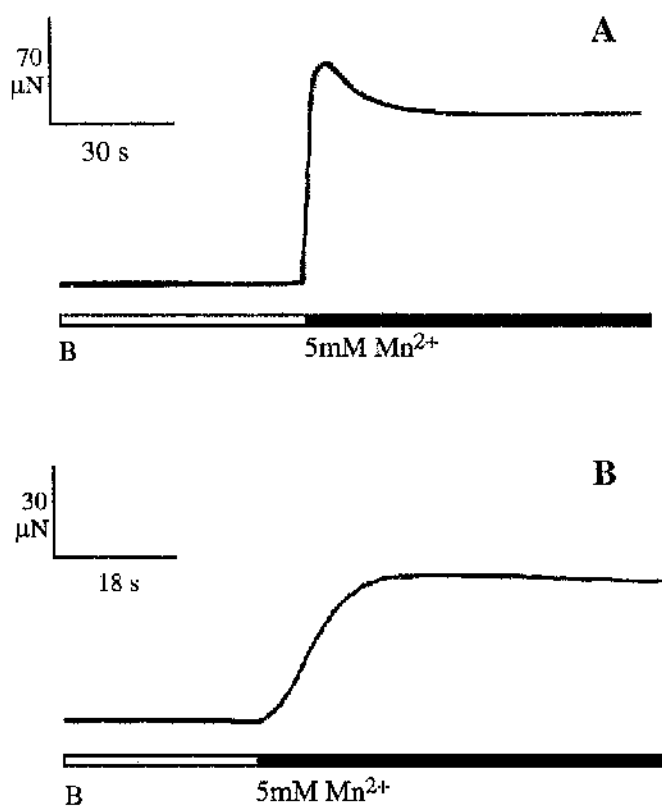


Fig. 5.2  
Activations recorded under 5 mM manganese solution.

A and B data for 2 different fibres.

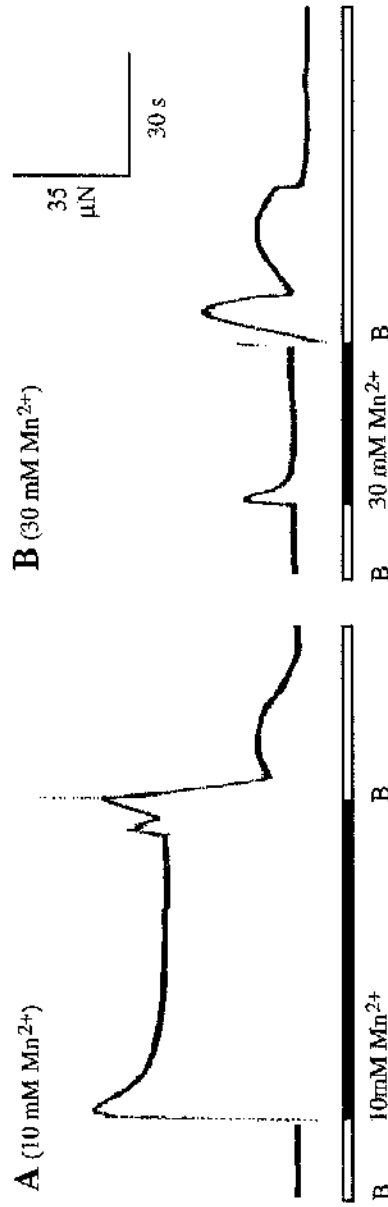


Fig. 5.3 Actuations recorded under 10 mM (A) and 30 mM (B) manganese solutions.

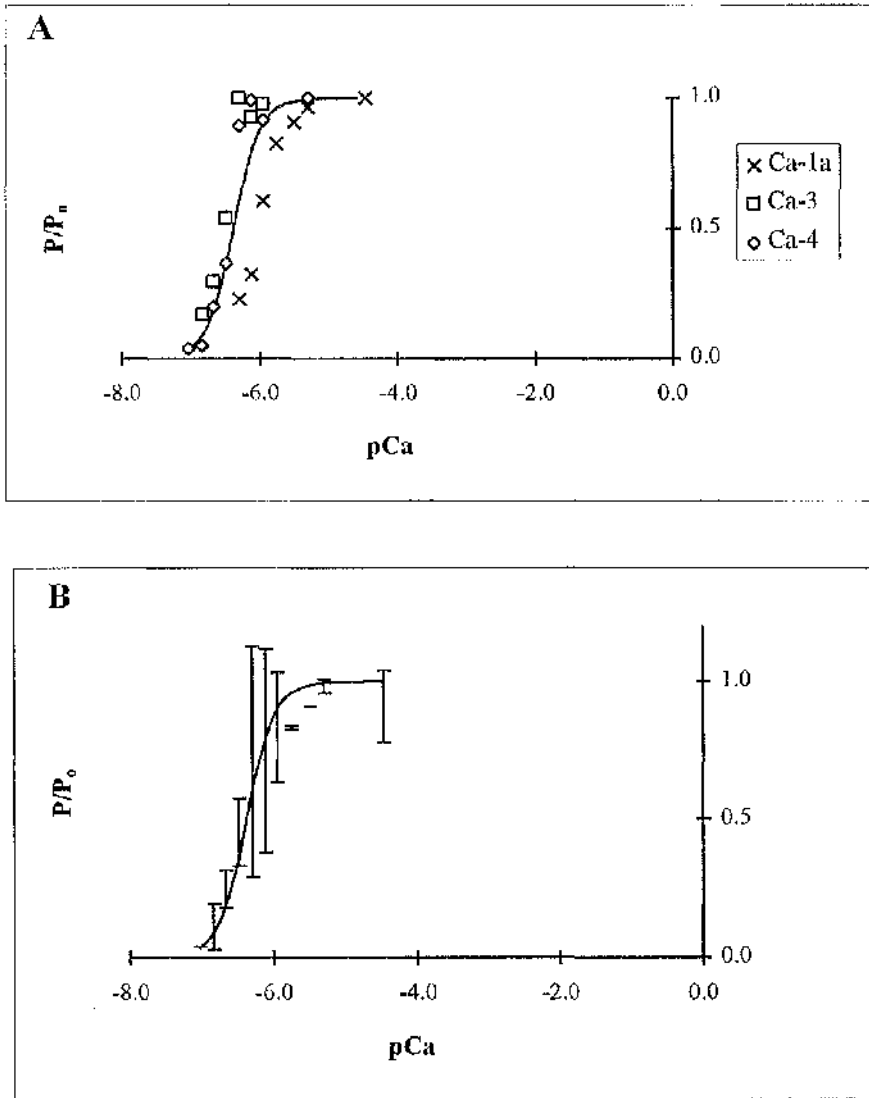


Fig.5.4  
Relationship between the relative isometric steady-state force ( $P/P_0$ ) and  $pCa$ .

(A) Values for 3 different fibres; (B) mean  $\pm$  S.D. for data in A.  
 $pCa$  expressed as the negative logarithm of the free  $[Ca^{2+}]$  of the bath solutions.

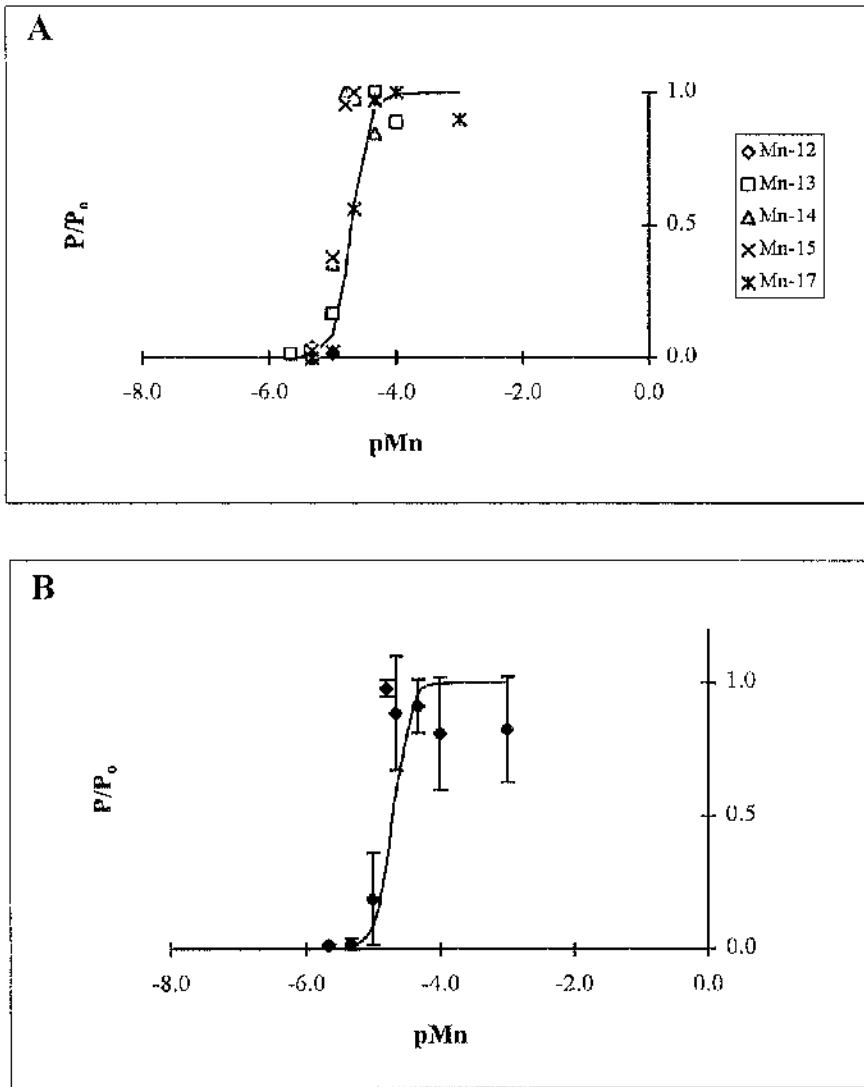


Fig. 5.5

Relationship between the relative isometric steady-state force ( $P/P_0$ ) and the free  $Mn^{2+}$  concentration ( $pMn$ ).

(A) Values for 5 different fibres; (B) mean  $\pm$  S.D. for data in A.  $pMn$  expressed as the negative logarithm of the free  $[Mn^{2+}]$  of the bath solutions

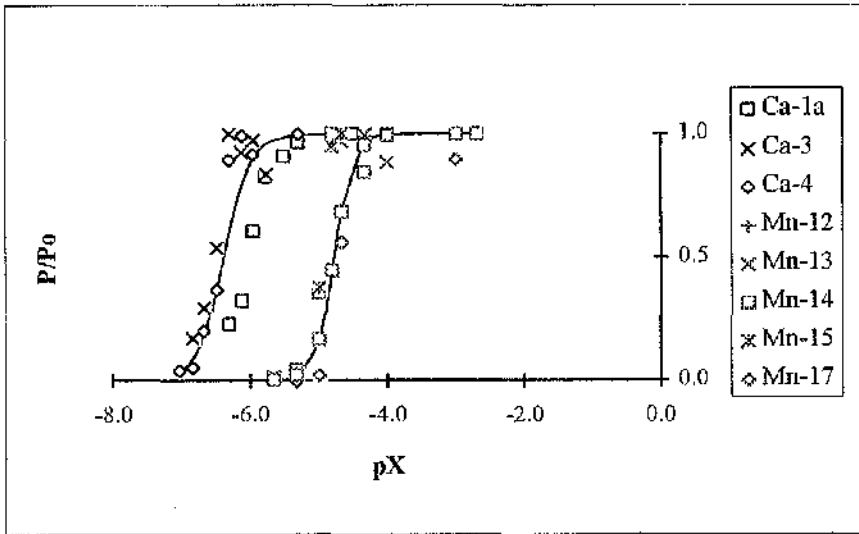


Fig. 5.6  
Relationship between the relative isometric steady-state force ( $P/P_0$ ) and  $pCa$  and  $pMn$ .

Data derived from different myofibrillar bundles of the same fibres.  $pX$  expressed as the negative logarithm of the  $[Ca^{2+}]$  or  $[Mn^{2+}]$  of the bath solutions,  $n = 5$ .

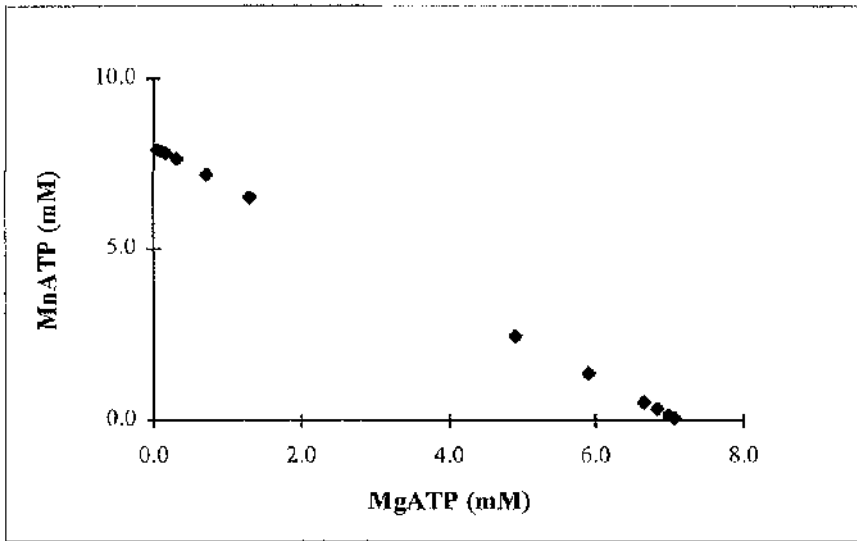


Fig. 5.7  
The relationship between MgATP and MnATP when they are in solution together.

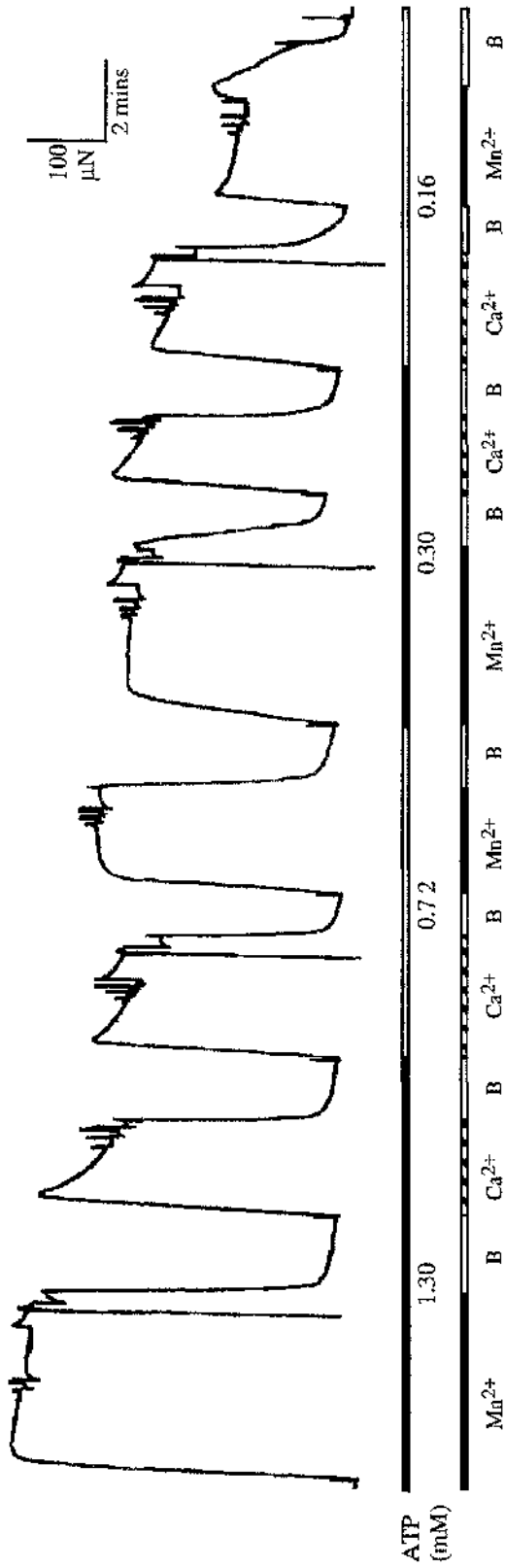


Fig. 5.8 Original force traces of a single S<sub>1</sub> fibre in response to different Mn<sup>2+</sup> solutions (pMn 4.0-1.52) and their equivalent low MgATP solutions (pCa 4.7) (See Table 5.6).

Kinetic experiments were performed under each solution which can be seen as rapid changes of force during each activation. The top bars indicate the Ca<sup>2+</sup> and Mn<sup>2+</sup> solutions which contain the same amount of ATP.

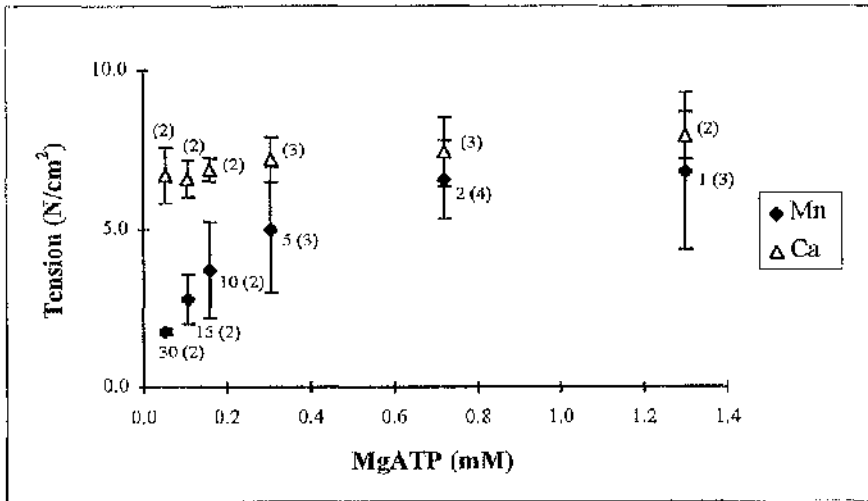


Fig. 5.9  
Effect of MgATP on muscle fibre maximal tension.

Maximal tension was measured under  $Mn^{2+}$  solutions containing low levels of MgATP and under A solutions with the same MgATP concentrations (eg. the 30 mM  $Mn^{2+}$  solution contains the same [MgATP] as the 0.05 mM MgATP solution). Mean  $\pm$  S.D. values for maximal tension;  $[Mn^{2+}]$  (mM) is indicated by each data point; n values are indicated in parenthesis.

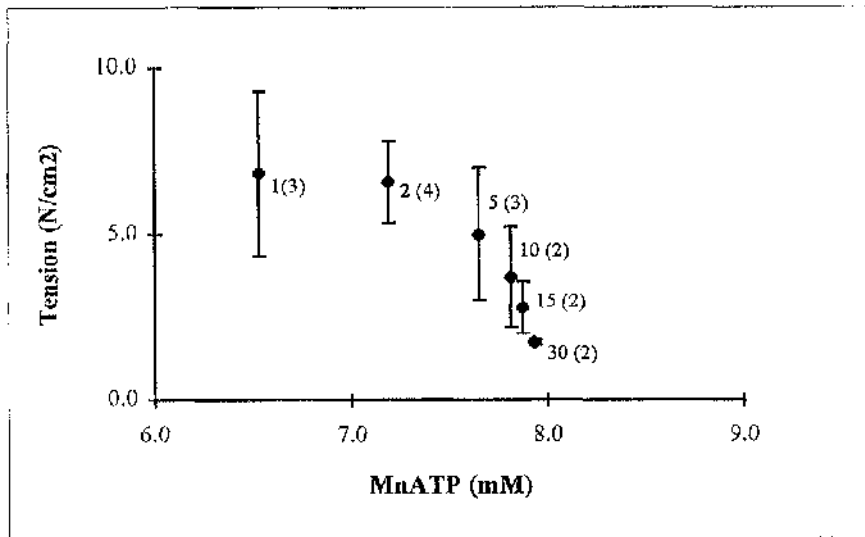


Fig. 5.10  
Effect of MnATP on muscle fibre maximal tension

Mean  $\pm$  S.D. values of maximal tension;  $[Mn^{2+}]$  (mM) is indicated by each data point; n values are indicated in parenthesis.

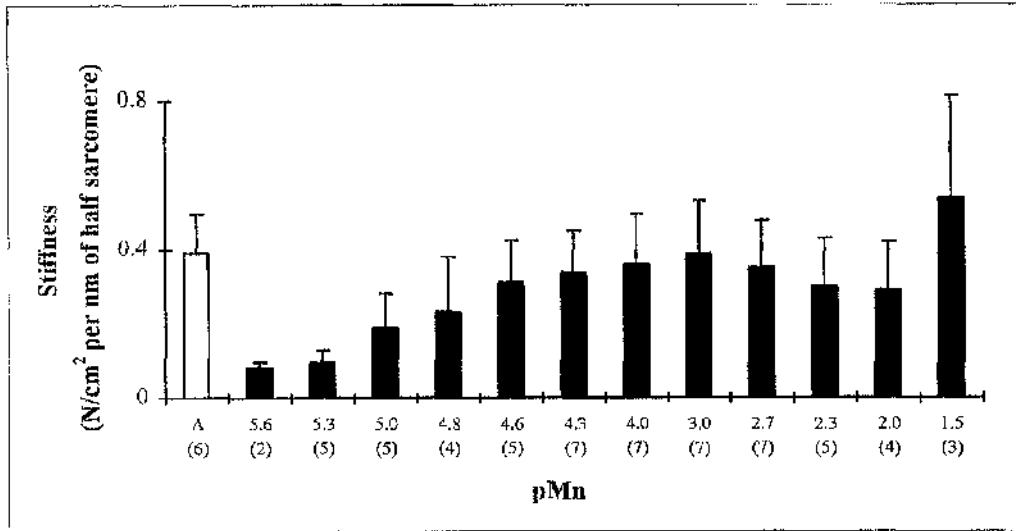


Fig. 5.11

The effect of  $Mn^{2+}$  on muscle fibre stiffness

Mean  $\pm$  S.D. values for stiffness; pMn is expressed as the negative logarithm of the free  $[Mn^{2+}]$ ; 'A' (pCa 4.7) = control; n values are indicated in parenthesis.

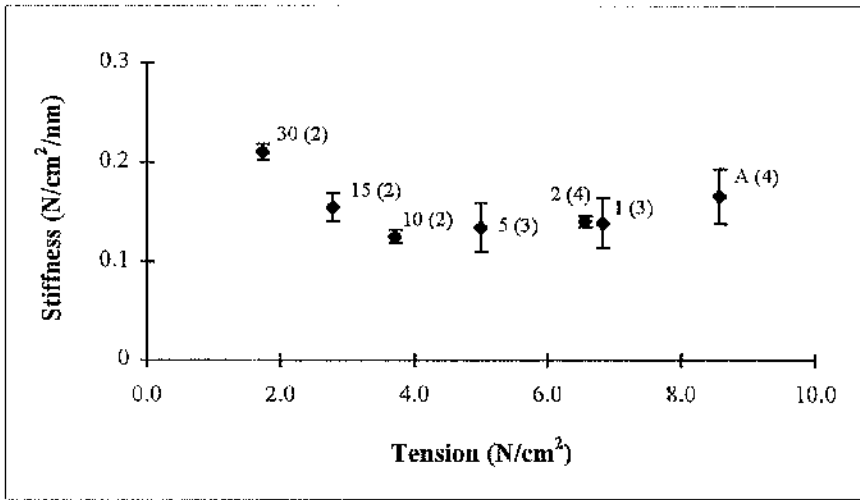


Fig. 5.12  
Relationship between stiffness and maximal tension.

Mean  $\pm$  S.D. values for stiffness at different  $Mn^{2+}$  concentrations. Only 30 mM  $Mn^{2+}$  increased fibre stiffness above the control level (A); 'A' solution (pCa 4.7) = control;  $Mn^{2+}$  concentration is indicated next to each data point (mM), n values are indicated in parenthesis.

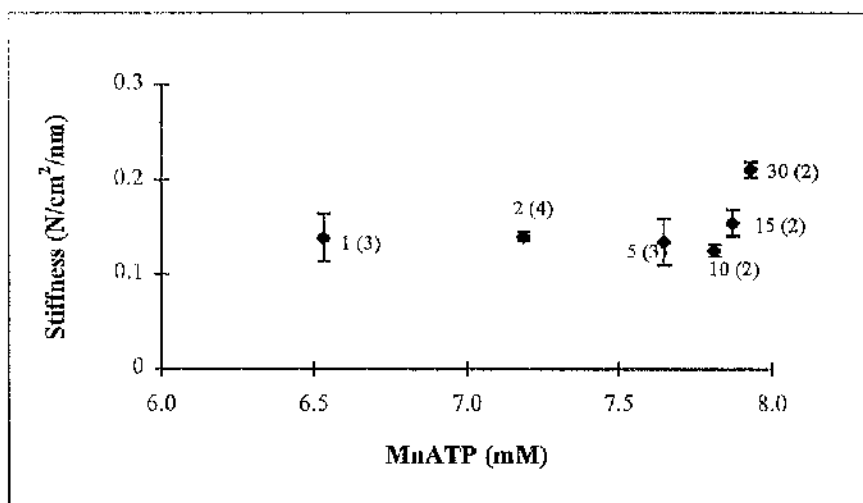


Fig. 5.13

The effect of MnATP on muscle fibre stiffness at different  $Mn^{2+}$  concentrations.

Mean  $\pm$  S.D. values for stiffness;  $[Mn^{2+}]$  (mM) is indicated by each data point; n values are indicated in parenthesis.

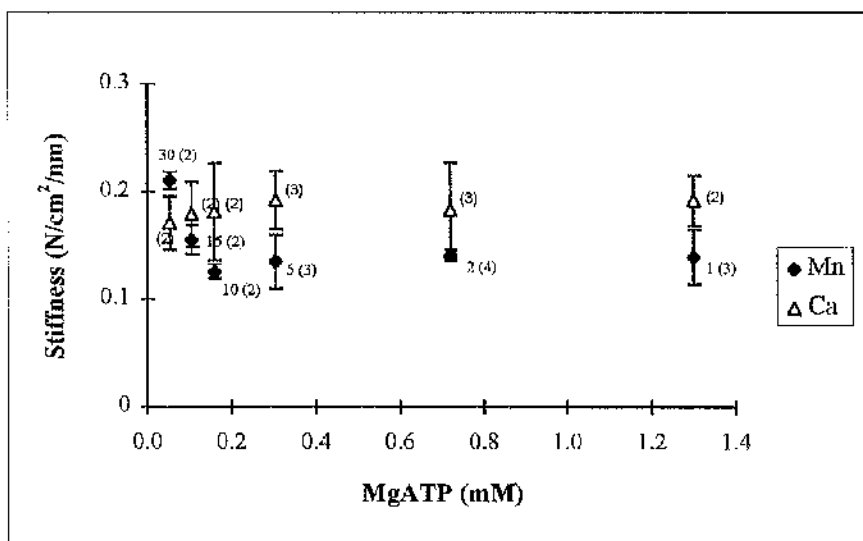


Fig. 5.14

The effect of MgATP on muscle fibre stiffness.

Stiffness was measured under different  $Mn^{2+}$  solutions containing low levels of MgATP and under A solutions with the same MgATP concentrations (eg. the 30mM  $Mn^{2+}$  solution contains the same  $[MgATP]$  as the 0.05mM ATP solution) Mean  $\pm$  S.D. values of stiffness;  $[Mn^{2+}]$  (mM) is indicated by each data point; n values are indicated in parenthesis.

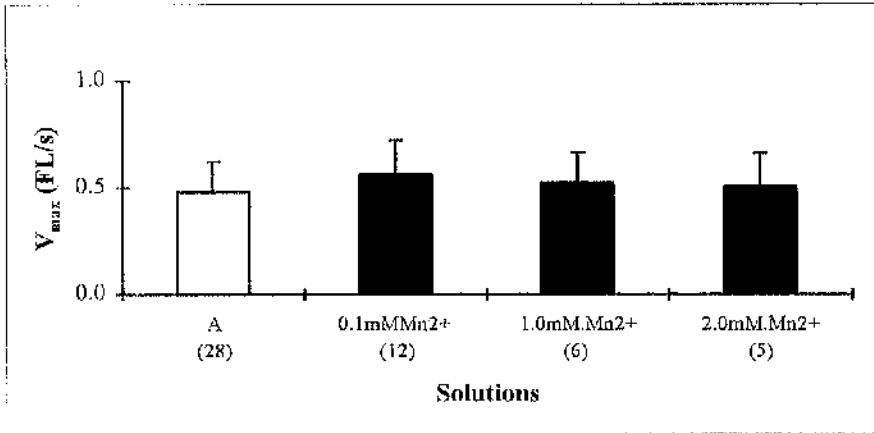


Fig. 5.15

Effect of Mn<sup>2+</sup> on maximal shortening velocity (V<sub>max</sub>).

Mean ± S.D. values for V<sub>max</sub> are expressed as fibre lengths/second; 'A' solution (pCa 4.7) = control; n values are indicated in parenthesis.

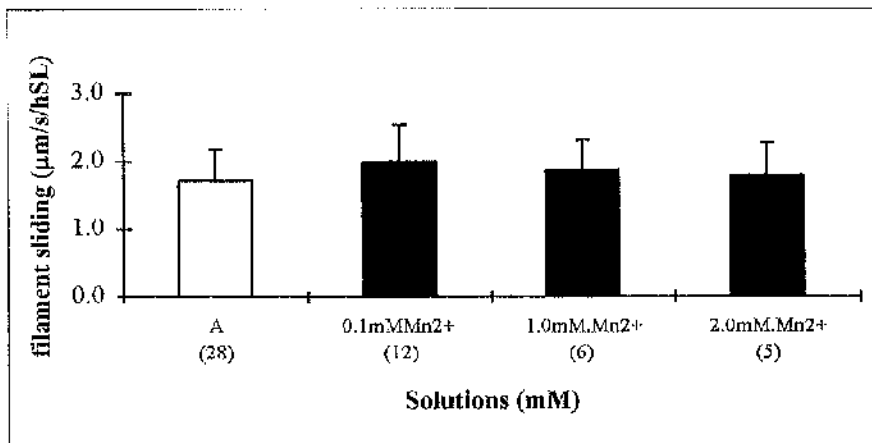


Fig. 5.16

Effect of Mn<sup>2+</sup> on the rate of filament sliding.

Mean ± S.D. values for filament sliding are expressed per half sarcomere length; 'A' solution (pCa 4.7) = control; n values are indicated in parenthesis.

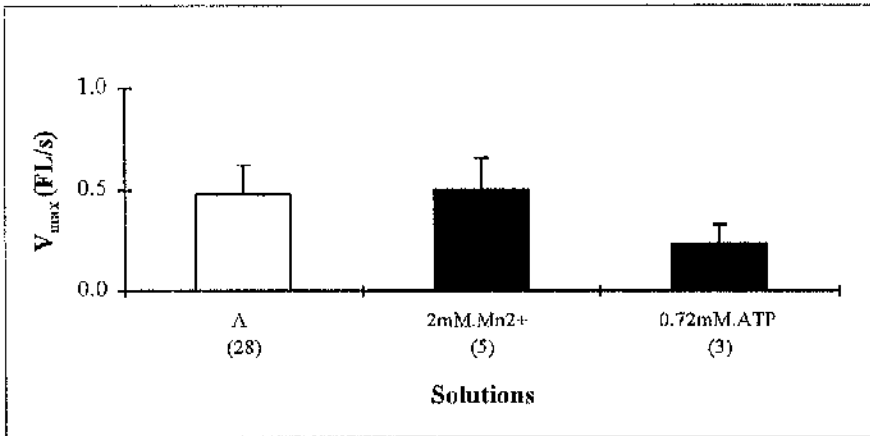


Fig. 5.17

Comparison of the  $V_{max}$  of the 2 mM  $Mn^{2+}$  solution which contains 0.72 mM MgATP with the equivalent low MgATP  $Ca^{2+}$  solution.

Mean  $\pm$  S.D. values for  $V_{max}$  are expressed as fibre lengths/s; 'A' solution (pCa 4.7) = control; n values are indicated in parenthesis.

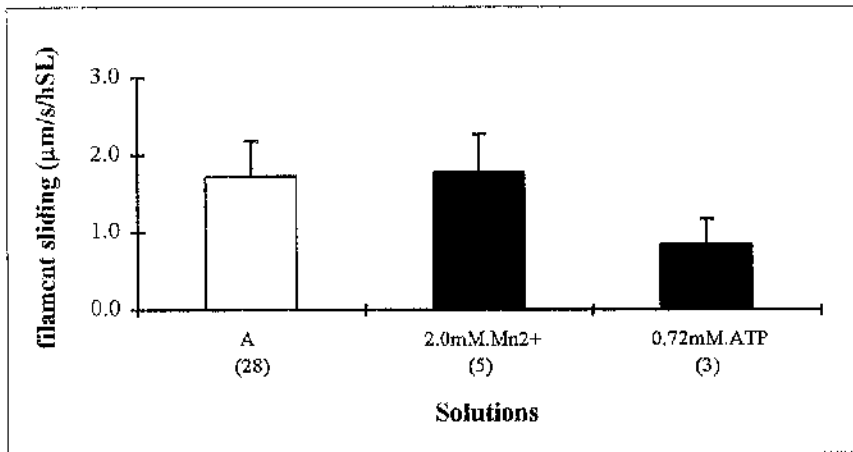


Fig. 5.18

Comparison of the rate of filament sliding in the 2mM  $Mn^{2+}$  solution which contains 0.72 mM MgATP with the equivalent low MgATP  $Ca^{2+}$  solution

Mean  $\pm$  S.D. values for filament sliding are expressed per half sarcomere; 'A' solution (pCa 4.7) = control; n values are indicated in parenthesis.

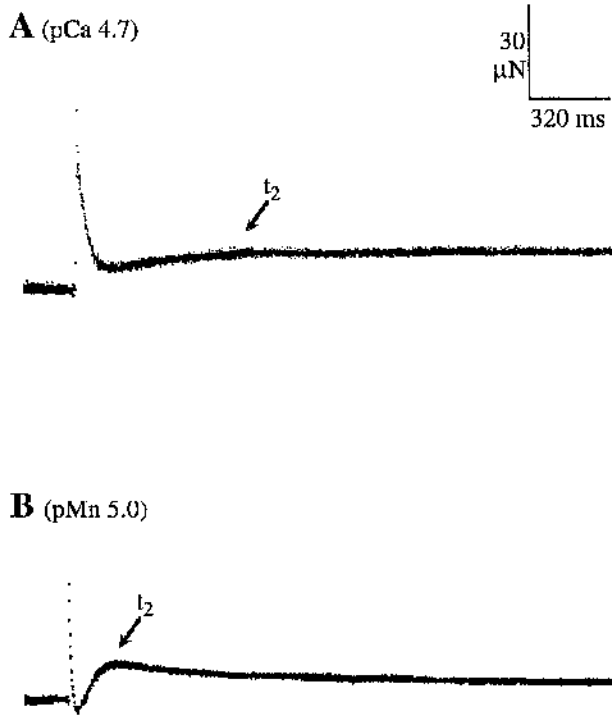
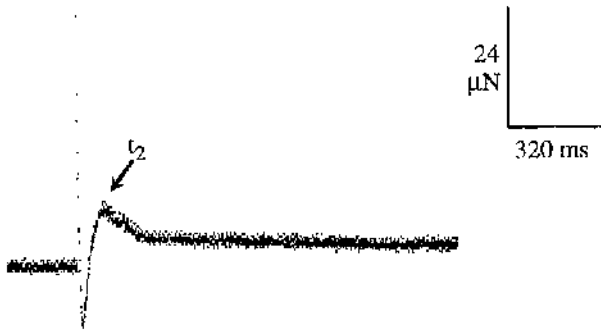


Fig. 5.19  
Effect of  $\text{Mn}^{2+}$  on stretch activation.

The force response to small stretches (0-0.5 % of the original fibre length) was measured in  $\text{Ca}^{2+}$ - (A) and  $\text{Mn}^{2+}$ - (B) activation solutions containing 10 mM EGTA. The  $t_2$  time parameter of stretch is indicated by the arrows (pCa 4.7:  $t_2 = 570$  ms, pMn 5.0:  $t_2 = 160$  ms).

**A** (pMn 4.66)



**B** (pMn 1.52)



Fig. 5.20  
Effect of high and low concentrations of  $Mn^{2+}$  on stretch activation.

The force response to small stretches (0-0.5 % of the original fibre length) was measured in low (A) and high (B) concentration  $Mn^{2+}$  solutions. The  $t_2$  time parameter of stretch is indicated by the arrows (pMn 4.66:  $t_2 = 120$  ms, pMn 1.52: Stretch activation is absent)

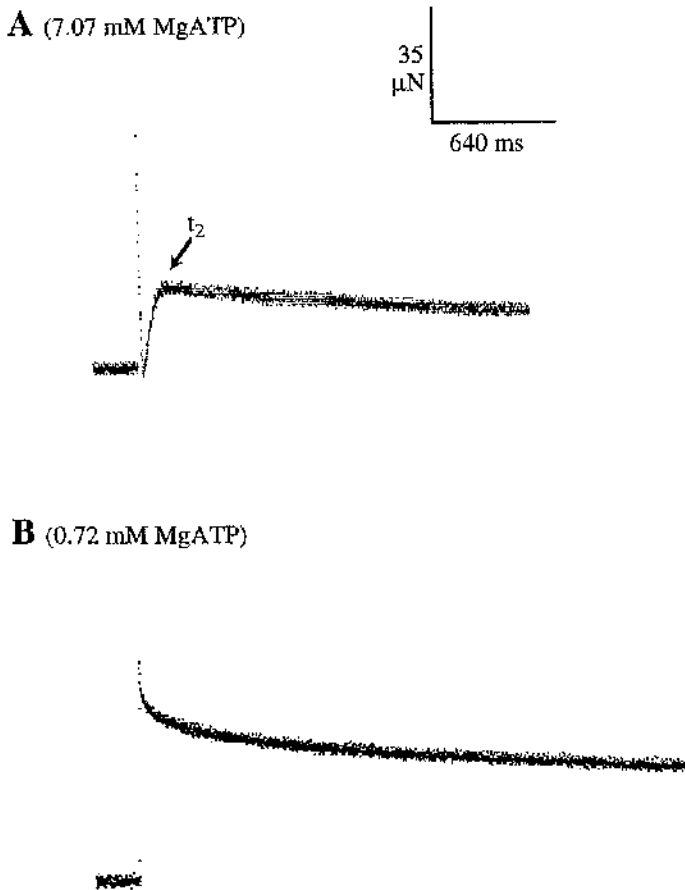


Fig. 5.21  
Effect of low MgATP on stretch activation.

The force response to small stretches (0-0.5 % of the original fibre length) was measured in low (B) and high (A) concentration MgATP solutions. The  $t_2$  time parameter of stretch is indicated by the arrow (pCa 4.7, 7.07 mM MgATP:  $t_2 = 150$  ms, pCa 4.7, 0.72 mM MgATP: Stretch activation is absent).

**Chapter 6**  
**General Discussion**

## GENERAL DISCUSSION

The different experimental approaches described in this thesis have attempted to demonstrate the properties of EC coupling in a typical crustacean slow muscle, and to identify differences between identified slow fibres types. Different steps in the EC coupling process have been investigated using the appropriate experimental techniques:

1. single membrane-intact fibres and fibre bundles to investigate the intracellular stores.
2. voltage clamp recordings to investigate the different ion channels which are present in the sarcolemma.
3. skinned fibre preparations to look at the contractile proteins and crossbridge kinetics.

## 6.1 EC coupling properties of the SF muscle of *Nephrops*

### 6.1.1 EC properties identified using membrane-intact fibres

The experiments conducted on membrane-intact fibres demonstrate the EC coupling mechanism in the medial and lateral bundles of the SF muscle. The main points of evidence for this are:

1. the inhibition of both the neuronally-induced force and the force induced by electrical field stimulation in  $\text{Ca}^{2+}$ -free saline shows that external  $\text{Ca}^{2+}$  ions are essential for contraction (Fig. 2.12).
2. the increase in the size of the neuronally-evoked force (Fig. 2.20) and force evoked by electrical field stimulation (Fig. 2.22) by caffeine indicates that in the presence of external  $\text{Ca}^{2+}$  ions caffeine effects the force amplification step of EC coupling.
3. high concentrations of caffeine (1-20 mM) applied to the SF muscle in  $\text{Ca}^{2+}$ -free saline induce large contractures (Fig. 2.21B). Since  $\text{Ca}^{2+}$  ions are known to

activate the contractile proteins by binding to the regulatory protein troponin (Ebashi & Endo, 1968), this experiment indicates that internally stored  $\text{Ca}^{2+}$  ions are essential for contraction in the SF muscle bundles.

In addition this experiment shows that by removing external  $\text{Ca}^{2+}$  from the saline, which is the trigger for EC coupling, the subsequent steps of activation are inhibited. Caffeine induces contraction by activating a later step in the EC coupling process: the release of  $\text{Ca}^{2+}$  ions from the SR which activate the myofibrillar proteins (muscle contraction).

4. single fibre experiments show that if the SR is depleted of  $\text{Ca}^{2+}$  by an application of caffeine, subsequent caffeine-induced contractures are inhibited, even in the presence of saline containing  $\text{Ca}^{2+}$  ions. This confirms that both external and internal  $\text{Ca}^{2+}$  ions are required for contractions, that the external  $\text{Ca}^{2+}$  ions themselves cannot directly activate the myofibrillar proteins and that an intermediate step is involved (release of  $\text{Ca}^{2+}$  from the SR).
5. tetracaine blocks the release of  $\text{Ca}^{2+}$  ions from the SR (Csernoch *et al.*, 1988; Almers & Best, 1976). Tetracaine inhibited the neuronally-induced force (Fig. 2.26), the force evoked by electrical field stimulation (data not shown) and the caffeine-induced force (Fig. 2.27). This confirms that SR  $\text{Ca}^{2+}$  release occurs in the SF muscle and also that it is essential for muscle contraction.
7. BDM is thought to release  $\text{Ca}^{2+}$  ions from the SR in a similar manner to caffeine in crustacean muscle (Györke *et al.*, 1993). BDM had an almost identical effect to caffeine on the SF muscle bundles of *Nephrops* (Fig. 2.28). It increased the tonic force levels in standard saline as well as releasing intracellular  $\text{Ca}^{2+}$  from the SR to initiate contraction in  $\text{Ca}^{2+}$ -free saline (Fig. 2.29). The BDM results confirm the findings demonstrated by the caffeine experiments.

The results described above have demonstrated the processes of EC coupling in the SF muscle fibres. However, it is not clear from these experiments whether any differences occur between the two fibre phenotypes. In general the intact muscle bundle experiments

indicate that the  $S_1$  and  $S_2$  fibre types exhibit very similar EC coupling properties. For example, the  $Ca^{2+}$ -release properties of the two muscle bundles, which were demonstrated by the caffeine experiments, are very similar.

However, this finding is not really surprising, since studies by Franzini-Armstrong *et al.* (1992) show that the arrangement of junctional feet connecting the T-tubules and SR together forming the  $Ca^{2+}$ -release channels (ryanodine receptors) in invertebrate muscle are very similar in size and shape, and that very little difference occurs between species. It is therefore unlikely that significant structural differences exist between the  $Ca^{2+}$  release channels in two slow fibre types originating from the same muscle.

An appropriate experimental method which could be applied to further investigate the  $Ca^{2+}$ -release properties of the different fibre types uses mechanically skinned fibres with intact SR (Lea, 1996), unlike the chemically skinned fibres used in this study in which the SR is destroyed. Lea showed that in crab and lobster striated muscle caffeine and micromolar concentrations of  $Ca^{2+}$  released  $Ca^{2+}$  from the ryanodine-sensitive SR store. This technique would allow the content of the SR stores and the CICR properties of the RyR to be investigated in the  $S_1$  and  $S_2$  fibre types. This technique also complements the work conducted on the chemically skinned muscle fibres and on the intact muscle bundles. The advantages of this technique are:

1. the  $Ca^{2+}$ -release mechanism can be accessed directly, because the first step of EC coupling, the flux of  $Ca^{2+}$  ions across the sarcolemma is not involved (since the sarcolemma has been removed) but the SR is intact and functional.
2. the preparation of single fibres will be reasonably quick, unlike the preparation of membrane-intact single fibres. For comparison, experiments should also be carried out on single membrane-intact fibres.

One other aspect which is often ignored, but which has been shown to differ between the  $S_1$  and  $S_2$  fibre types is the extent and invagination of the of T-tubules (Fowler & Neil, 1992), which consequently affects the delivery of  $Ca^{2+}$  ions to interior of the fibre. Crowe and Baskin (1981) showed using electron-microscopy that the T-tubules were very different between fast and slow fibres types. The highly invaginated tubular system within fast muscle fibres was implicated as an external  $Ca^{2+}$  store and for this reason the

flux of  $\text{Ca}^{2+}$  ions across the sarcolemma was thought to be responsible for activating the contractile proteins. This contrasts with the situation in the slow fibre types, in which the internal  $\text{Ca}^{2+}$  stored in the SR initiates contraction through CICR. Since differences do occur between the  $\text{S}_1$  and  $\text{S}_2$  fibre types in the extent of their tubular systems (Fowler & Neil, 1992) this factor should be taken into consideration in when studying the activation properties of CICR.

Experiments using high concentrations of  $\text{K}^+$ -ions in the saline to induce contraction indicate that subtle differences do occur between the  $\text{S}_1$  and  $\text{S}_2$  fibres types and that they are related to the first step of EC coupling, membrane depolarisation. The  $\text{S}_2$  fibre type from the medial muscle bundle is very sensitive to depolarisation of the muscle membrane, producing much higher levels of force than the  $\text{S}_1$  fibres of the lateral muscle bundle.

### **6.1.2 Sarcolemmal ion channel properties**

Preliminary voltage clamp experiments indicate that the  $\text{S}_1$  and  $\text{S}_2$  fibres express different populations of ion channels in their muscle membranes. Differences were observed in both the inward  $\text{Ca}^{2+}$  currents the outward  $\text{K}^+$  currents. The  $\text{S}_1$  fibres appear to express faster inward  $\text{Ca}^{2+}$  ( $I_{\text{Ca}}$ ) and outward  $\text{K}^+$  currents which are large in amplitude while the  $\text{S}_2$  fibres appear to express much slower  $I_{\text{Ca}}$  and outward  $\text{K}^+$  currents which are small in amplitude. These characteristics are consistent with those derived from mechanical (Galler & Neil, 1994), biochemical and histochemical tests (Fowler & Neil, 1992) and may explain some of the different fibre properties. Thus the faster, larger  $I_{\text{Ca}}$  current of the  $\text{S}_1$  fibres would provide the rapid influx of  $\text{Ca}^{2+}$  ions needed to initiate the more rapid contractions produced by these fibres while the faster larger outward  $\text{K}^+$  currents would limit their contraction duration. The  $\text{S}_2$  fibres are more sensitive to lower levels of  $\text{Ca}^{2+}$  ions. Conversely the slower, smaller  $I_{\text{Ca}}$  flux into  $\text{S}_2$  fibres would provide enough  $\text{Ca}^{2+}$  ions to activate the low levels of tension observed in these more  $\text{Ca}^{2+}$ -sensitive fibres, while the slower smaller outward  $\text{K}^+$  currents would ensure that contraction is not reversed quickly. These properties of the  $\text{S}_2$  fibres are required to maintain abdominal posture for long period of time.

Further investigations of the ion channels of fibres require the development of alternative techniques to the two-electrode voltage clamp method which is not ideal for crustacean muscle fibres. The large size and surface area of the invaginated membrane which forms the tubule system mean that large amounts of current are required to voltage clamp the muscle fibres. In addition to this the  $I_{Ca}$  flux across the membrane at larger depolarising steps induces small localised contractures which damage the fibre and can dislodge the electrodes. One method to overcome this problem is to use  $Ba^{2+}$  ions to carry the inward current as they do not initiate contraction, but this does not provide the ideal solution. An alternative approach is to use a sarcolemmal membrane preparation, these are called sarcolemmal vesicles or 'blebs' which was first developed for vertebrate skeletal muscle (Burton *et al.*, 1988). Treatment of the muscle fibres with specific enzyme solutions causes the muscle membrane to develop blebs. It is thought that the blebs comprise sarcolemma and that the inside is in communication with the cytoplasm. However, this does not exclude the possibility that the parts of the blebs could originate from the sarcoplasmic reticulum and T-tubules. The blebs form with intact ion channels and have a small surface areas which makes them a very convenient preparation to use in the study of ion channel populations within muscle membrane using the patch clamp method. Using sarcolemmal vesicles from the lobster skeletal muscle and the patch clamp technique, a series of single channel conductances and gating behaviours have been detected in the sarcolemmal vesicle membranes which were attributed to a diverse family of potassium-conducting channels that are thought to be present in intact muscle membranes in lobsters (Worden *et al.*, 1994). These channels have similarities to cation channels identified by other workers using excised patches of membrane from sarcoplasmic reticulum (Tang *et al.*, 1989) and from lobster olfactory receptor neurones (McClintock & Ache, 1990). These results also correlate with the preliminary voltage clamp findings in that the  $S_1$  and  $S_2$  fibres appear to express different population of outward  $K^+$  channels.

Patch clamping sarcolemmal vesicles formed from individual  $S_1$  and  $S_2$  fibres may provide a better alternative to the voltage clamp technique and would provide a method to identify the populations of ion channels expressed in the membranes of the different fibre phenotypes. However, it is also important to remember that the properties of the channels recorded in lobster membrane blebs may differ from those in native membrane due to the enzyme treatment applied, and the loss of underlying cytoplasm.

### 6.1.3 Myofibrillar properties

As discussed in Chapter 4 (Section 4.4) the mechanical information recorded from skinned fibres has been correlated to the myofibrillar protein isoforms which expressed in different muscle fibre types (Reiser *et al.*, 1988; Bottinelli *et al.*, 1994a; Galler *et al.*, 1996), and the expression of different myosin HC isoforms has been related to variations in the kinetics of the crossbridge cycle. The different stages of the crossbridge cycle are thought to be responsible for the force transients measured in response to quick stretches and release of fibre length.

The S<sub>1</sub> and S<sub>2</sub> fibres express very different mechanical properties which probably relate to the different roles of these fibres within the abdomen of *Nephrops norvegicus* (see Section 4.4). The cause of these differences remains to be determined, but one very plausible explanation is that the S<sub>1</sub> and S<sub>2</sub> fibre types express different myosin heavy chain isoforms. This has been demonstrated by the peptide mapping technique (Neil *et al.*, 1993) but this needs to be confirmed by more sensitive methods such as those developed by Cotton and Mykles (1993) using cloned fast and slow MHC from the lobster *Homarus americanus*. Peptide mapping of the myosin heavy chains produced 7 peptides unique to slow muscle myosin and 11 unique to fast muscle myosin. This more detailed information on the MHC isoforms can then be correlated to the mechanical data from the S<sub>1</sub>, S<sub>2</sub> and fast fibres.

No difference was found in the complements of myosin light chains, indicating that the myosin light chains are probably not responsible for differences between the different fibre phenotypes. Using two dimensional PAGE gel electrophoresis Li and Mykles (1990) also showed that both the fast and slow myosin light chains were identical in size and net charge.

One other possible explanation for these results is the presence of different troponin isoforms (Fowler & Neil, 1994) (see Section 4.1). Although, this does not seem likely, since the expression of different troponin isoforms is normally associated with differences in the Ca<sup>2+</sup>-sensitivity of force generation (Moss *et al.*, 1986; Babu *et al.*, 1987). However, in rabbit plantaris muscles it has been correlated with maximal

unloaded shortening velocity (Greaser *et al.*, 1988), so this possibility should not be ruled out.

#### 6.1.4 Acto-myosin regulation in decapod crustaceans

Another consideration of relevance in relation to the expression of different Tn isoforms but not myosin light chain isoforms, is that decapod crustaceans are classed by Lehman and Szent-Györgyi (1975) as having actin-regulated muscle. However, the muscles which comprise the crusher claw of the lobster *Homarus Americanus* are classed as being dual-regulated. This poses the question of whether other slow muscle systems in crustaceans are dual-regulated, and whether the S<sub>1</sub> and S<sub>2</sub> fibre types of the SF muscle fall within this dual-regulated category. The existing histochemical studies by Fowler and Neil (1992) on the SF muscle do not resolve this problem: they showed that the S<sub>1</sub> and S<sub>2</sub> fibre types express various Tn isoforms, and thus may vary in their actin-regulation, but express myosin light chains with no type-specific differences. It is possible that the myosin light chain could play a similar regulatory role in both fibre types.

#### 6.1.5 Fibre heterogeneity within single populations

In the introduction to this thesis the issue of muscle fibre heterogeneity within single fibre populations was discussed in relation to muscle fibre identification. This factor may explain results obtained by other workers which were either inconsistent with the majority, and which are often described in the literature as anomalies or are excluded from publication. One example of this is the work of Tameyasu (1992) on the crayfish *Procambarus clarkii* slow extensor muscle which was described as a single population of homogenous fibres. Using the slack test method to measure shortening velocity, two responses were identified in fibres, one response, which was observed for most fibres had a biphasic time course of shortening consisting of an initial high velocity phase followed by a slow velocity phase. However, a few fibres exhibited a linear shortening with a constant velocity. These results indicate the presence of two fibre types within the slow extensor muscle that are similar to the S<sub>1</sub> and S<sub>2</sub> fibres types of *Nephrops norvegicus*: S<sub>1</sub>

fibres exhibit a very curved force velocity profile, with an initial higher velocity phase followed by a slower phase while the  $S_2$  fibres exhibited a much more linear profile.

Work of the  $Ca^{2+}$ -release properties of lobster abdominal muscle provides a further example (Lca, 1996). Of 17 fibres tested in this study 14 gave caffeine-induced contractions, while 3 gave no response. It was suggested that the different responses could be attributed to the presence of two fibre types within the fibres chosen at random from the abdominal flexor muscle, although this was not directly determined.

## 6.2 Manganese

### 6.2.1 The activation properties of $Mn^{2+}$ ions

1. The whole muscle bundle experiments show that  $Mn^{2+}$  can increase the neurally-evoked muscle force and the force evoked by electrical field stimulation as well as increasing the resting force when the fibres are depolarised by high  $K^+$  solutions.
2. The skinned fibre experiments have established that  $Mn^{2+}$  can activate the contractile proteins directly, thus providing one possible explanation for the responses seen in the intact muscle bundles.

Comparative studies investigating the effect of other heavy metal ions, including cobalt and cadmium, on the intact neuromuscular SF muscle preparation (A. S. Granz, D. M. Neil & S. Baden, unpublished observation) have shown that at low concentrations, in a similar range to  $Mn^{2+}$ , the size of muscle contraction was increased above the control level. At higher concentrations, force was inhibited dose-dependently. These results indicate that the ion channels which are responsible for carrying the inward current across the sarcolemma of  $S_1$  and  $S_2$  fibres are not specific to  $Ca^{2+}$  ions and that when present in the correct concentration other ions can pass through these channels and activate the contractile proteins either directly or by activating the release of  $Ca^{2+}$  from the SR through the CICR mechanism.

From these studies it is clear that  $Mn^{2+}$  induced force in the intact SF muscle preparation but what is not clear is how the  $Mn^{2+}$  ions enter across the sarcolemma. One likely

explanation is that  $Mn^{2+}$  ions can pass through L-type  $Ca^{2+}$  channels. The L-type channel blocker nifedipine and the T-type channel blocker nickel may provide useful pharmacological tools to identify this mechanism. Nasu *et al.* (1995) showed that in  $Ca^{2+}$ -free saline, the long term re-development of force induced by  $Mn^{2+}$  was inhibited by nifedipine but not by nickel. The ability of one of these agent to block the  $Mn^{2+}$ -induced force in the SF muscle preparation would provide firm evidence for the  $Mn^{2+}$  entry mechanism. In addition to this the effects of nifedipine on the different muscle bundles may provide useful information about the populations of L-type  $Ca^{2+}$  channels in the different fibres types. The results of such experiments could be independently corroborated using the voltage clamp technique on whole fibres, or patch clamp studies on sarcolemmal vesicles.

It would also be useful to directly measure the distribution of the  $Mn^{2+}$  ions inside the different fibres using radio-isotope measurements, or by Electron Energy Loss Spectroscopy (EELS) linked to an EM, in order to determine whether these divalent ions can enter the fibres.

Voltage clamp studies show that  $Ba^{2+}$  ions can carry the inward current in *Nephrops norvegicus*  $S_1$  fibres. Thus measuring the inward current across the sarcolemma in the presence of  $Ca^{2+}$ -free saline containing  $Mn^{2+}$  or other divalent cations, would provide firm evidence that  $Mn^{2+}$  and these other divalent ions are able to carry the current across the sarcolemma at low concentrations. Indeed, in preliminary voltage clamp studies it has already been shown that 10 mM  $Mn^{2+}$  blocks the inward current in  $S_2$  fibres.

Experiments on skinned  $S_1$  fibres showed that  $Mn^{2+}$  can activate the contractile proteins (Chapter 5). A series of experiments using the other divalent ions which were shown to affect force from the isolated muscle bundle preparation would provide an interesting comparison to the  $Mn^{2+}$  experiments, as well as investigating if any of these other divalent cations and heavy metal ions are capable of activating the contractile proteins. A similar study was performed by Stephenson and Thieleczek (1986) using  $Sr^{2+}$ ,  $Ni^{2+}$ ,  $Cd^{2+}$  and  $Ba^{2+}$  which showed that  $Sr^{2+}$ ,  $Cd^{2+}$  and  $Ba^{2+}$  activated skinned muscle fibres of frog while  $Ni^{2+}$  caused only a transient increase in force. Only  $Ba^{2+}$  activated to a similar level as maximal  $Ca^{2+}$ -activated force.

Preliminary skinned fibre experiments conducted on the S<sub>2</sub> fibre type showed that these fibres were much more sensitive to Mn<sup>2+</sup> ion than the S<sub>1</sub> fibre type, while the sensitivities of the S<sub>1</sub> and S<sub>2</sub> fibre types to Ca<sup>2+</sup> ions were very similar. This indicates that different Tn isoforms which are expressed in the S<sub>1</sub> and S<sub>2</sub> fibre types have a greater variance in binding Mn<sup>2+</sup> ions than in binding Ca<sup>2+</sup>. For this reason the use of divalent cations such as Mn<sup>2+</sup> to activate skinned fibres may provide a useful tool with which to identify different fibre types within a single population of fibres. A similar study conducted by West *et al.* (1992) on skinned fibres from the freshwater crustacean *Cherax destructor* showed that when the fibres were activated by Sr<sup>2+</sup> ions large differences were observed between the activation of long- and short-sarcomere fibres. In addition to this the short and long sarcomere fibres were also differentially activated in the presence of 2,3-butanedione monoxime (BDM) (West *et al.*, 1992), with the short sarcomere fibre being more sensitive to BDM. It was suggested that these differences are also related to possible differences in the properties of the myosin expressed in the two fibre. Similar effects of BDM have been shown in fast and slow twitch fibres in mammalian muscle (Fryer *et al.*, 1988). The whole muscle bundle experiments performed in this present study show that BDM induces force in the SF muscle bundles, although differential effects between fibre types were only observed at the level of the muscle membrane. It would therefore be interesting to see the effects of BDM on the activation of skinned fibres preparations. BDM may provide another useful tool with which to identify differences between the S<sub>1</sub>, S<sub>2</sub> and fast fibre types, and to identify heterogeneous populations of fibres.

### 6.2.2 Ecological effects of Mn<sup>2+</sup> in the environment

Manganese (Mn) is an important and abundant trace metal in marine sediments, which occurs as insoluble and stable Mn (III, IV) oxides under oxic conditions but is readily reduced to mainly Mn<sup>2+</sup> under hypoxic conditions (Hall *et al.*, 1989; Gerringa 1991). Hypoxic and even anoxic conditions in the bottom water occurs in many marine coastal areas around the world due to eutrophication caused by excess of nutrients running off the land. The dissolved Mn<sup>2+</sup> then becomes bioavailable and accumulates in the benthic fauna (Hall *et al.*, 1989, Gerringa 1991). Following autumnal hypoxia in the Kattegat along the Swedish west coast the Norway lobster *Nephrops norvegicus* has been found to

have 2-4 times higher  $Mn^{2+}$  concentrations in internal tissues as haemolymph and muscle, which have therefore been identified as potential targets for the effects of  $Mn^{2+}$  (Baden *et al.*, 1994).

The concentrations used in the present study are about a factor of 10 higher than the concentrations occurring during hypoxic events in the sea, although higher levels of accumulation cannot be excluded. Therefore it cannot at present be predicted whether the levels accumulated by *N. norvegicus* under eutrophic conditions would be sufficient to depress neuromuscular performance. However, the isolated neuromuscular preparation from *Nephrops norvegicus* offers a potential bioassay for  $Mn^{2+}$  in the environment.

## References

REFERENCES

- Abbott, B.C. and Parnas, I. (1965). Electrical and mechanical responses in deep abdominal extensor muscles of crayfish and lobster. *J. gen. Physiol.* **48**, 919-931.
- Adelstein, R. S. and Klee, C. B. (1983). Purification and characterisation of smooth muscle myosin light chain kinase. *J. biol. Chem.* **256**, 7501-7509.
- Almers, W. and Best, P.M. (1976). Effects of tetracaine on displacement currents and contraction of frog skeletal muscle. *J. Physiol., Lond.* **262**, 583-611.
- Alpert, N. R., Blanchard, E. M. and Mulieri, L. A. (1989). Tension independent heat in rabbit papillary muscle. *J. Physiol., Lond.* **414**, 433-1989.
- Altringham, J. D. and Johnston, I. A. (1982). The pCa-tension and force-velocity characteristics of skinned fibres isolated from fish fast and slow muscle fibres. *J. Physiol., Lond.* **333**, 421-449.
- Anderson, M. (1979).  $Mn^{2+}$  ions pass through  $Ca^{2+}$  channels in myoepithelial cells. *J. exp. Biol.* **82**, 227-238.
- Anderson, M. (1983).  $Mn^{2+}$  ions pass through calcium channels. *J. gen. Physiol.* **81**, 805-827.
- Arispe, N., Olivares, E., Jainovich, E. and Rojas, E. (1992). Screening of ryanodine (RYA) sensitive channels in sarcoplasmic reticulum vesicles from crustacean muscle. *Biophys. J.* **61**, A24.
- Ashley, C. C. Lea, T. J., Hoar, P. E., Kerrick, W. G. L., Strang, P. F. and Potter, J. D. (1991). Functional characterisation of the two isoforms of troponin C from the arthropod *Balanus nubilus*. *J. Muscle Res. Cell Motil.* **12**, 532-542.

- Ashley, C.C., Griffiths, P.J., Lea, T.J., Mulligan, I.P., Palmer, R.E. and Simnott, S.J. (1993). Barnacle muscle,  $Ca^{2+}$ , activation and mechanics. *Rev. Physiol. Biochem. Pharmacol.* **122**, 149-258.
- Atwood, H. L. (1963). Differences in muscle fibre properties as a factor in 'fast' and 'slow' contraction in *Carcinus*. *Comp. Biochem. Physiol.* **10**, 17-32.
- Babu, A., Scordilis, S. P., Somenblich, E. H. and Gulati, J. (1987). The control of myocardial contraction with skeletal fast muscle troponin C. *J. biol. Chem.* **262**, 5815-5822.
- Baden, S. P., Depledge, M. H. and Hargeman, L. (1994). Glycogen depletion and altered copper and manganese handling in *Nephrops norvegicus* following starvation and exposure to hypoxia. *Marine Ecol. Prog.* **103**, 105-112.
- Bagni, M. A., Cecchi, G. and Schoenberg, M. (1988). A model of force production that explains the lag between crossbridge attachment and force after electrical stimulation of striated muscle fibres. *Biophys. J.* **54**, 1105-1114.
- Bagni, M. A., Cecchi, G., Colomo, F. and Garzella, P. (1992). Effects of 2,3-butanedione monoxime on the crossbridge kinetics in frog single muscle fibres. *J. Muscle Res. Cell Motil.* **13**, 516-522.
- Basolo, F. and Pearson, R. G. (1967). *Mechanisms of inorganic reactions*, 2nd edition. John Wiley and Sons Inc., New York.
- Bean, B.P. (1984). Nitrendipine block of cardiac calcium channels, high-affinity binding to the inactive state. *Proc. natn. Acad. Sci. USA* **81**, 6388-6392.
- Berridge, M. J. (1990). Calcium oscillations. *J. biol Chem.* **265**, No 17, 9583-9586.
- Berridge, M. J. (1993). Inositol triphosphate and calcium signalling. *Nature* **361**, 315-325.

- Berridge, M. J. and Irvine, R. F. (1989). Inositol phosphates and cell signalling. *Nature* **341**, No 6239, 197-205.
- Beukelman, D. J. and Wier, W. G. (1988). Mechanism of release of calcium from sarcoplasmic reticulum of guinea-pig cardiac cells. *J. Physiol., Lond.* **405**, 233-255.
- Bianchi, C.P. (1961). The effects of caffeine on radiocalcium movement in frog sartorius. *J. gen. Physiol.* **44**, 845-858.
- Bianchi, P. C. (1969). Pharmacology of excitation-contraction coupling in muscle *Fed. Proc.* **28**, 1624-1627.
- Blanchard, E. M., Smith, G. L., Allen, D. G. and Alpert, N. R. (1990). The effects of 2,3-butanedione monoxime on initial heart tension, and aequorin light output in ferret papillary muscles *Pflügers Arch.* **416**, 219-221.
- Block, B.A., Imagawa, T., Campbell, K.P., Franzini-Armstrong C. (1988). Structural evidence for direct interaction between the molecular components of the transverse tubule /SR junction in skeletal muscle. *J. Cell. Biol.* **107**, 2587-2600.
- Bottinelli, R. S., Schiaffino, S. and Reggiani, C. (1991). Force-velocity relations and myosin heavy chains isoform compositions of skinned fibres from rat skeletal muscle, *J. Physiol., Lond.* **437**, 655-672.
- Bottinelli, R. S., Betto, R., Schiaffino, S. and Reggiani, C. (1994a). Unloaded shortening velocity and myosin heavy chain and alkali light chain isoform composition in rat skeletal muscle fibres. *J. Physiol., Lond.* **478**, 341-349.
- Bottinelli, R. S., Canepari, M., Reggiani, C. and Stienen, G. J. M. (1994b). Myofibrillar ATPase activity during isometric contraction and isomyosin composition in rat single skinned muscle fibres. *J. Physiol., Lond.* **481**, 663-675.

- Brandt, N. R. Caswell, A. H., Wen, S. R. and Talvenheimo, J. A. (1990). Molecular interactions of the junctional foot protein and dihydropyridine receptor in skeletal muscle tetrads. *J. Membr. Biol.* **113**, 237-252.
- Brenner, B. (1980). Effects of free sarcoplasmic  $\text{Ca}^{2+}$  concentration on maximum unloaded shortening velocity: measurements on single glycerinated rabbit psoas muscle fibres. *J. Muscle Res. Cell Motil.* **1**, 409-428.
- Brenner, B. (1988). Effect of  $\text{Ca}^{2+}$  on cross-bridge turnover kinetics in single rabbit psoas fibres, implications for the regulation of muscle contraction. *Proc. natn. Acad. Sci. USA* **85**, 3265-3269.
- Brum, G. Stefani, E. and Rios, E. (1987). Simultaneous measurement of Ca current and intracellular Ca concentrations in single skeletal muscle fibres of the frog. *Can. J. Physiol. Pharmacol.* **65**, 681-685.
- Buchthal, F. and Schmalbruch, H. (1980). Motor unit of mammalian muscle. *Physiol. Rev.* **60**, 90-141.
- Burton, F., Dorstelmann, U. and Hutter, O.F. (1988). Single channel activity in sarcolemmal vesicles from human and other mammalian muscle. *Muscle Nerve* **11**, 1029-1038.
- Caldwell, P. C. and Walster, G. E. (1963). Studies on the micro-injection of various substances into crab muscle fibres. *J. Physiol., Lond.* **169**, 353-372
- Callewaert, G. Cleemann, L. and Morad, M. (1988). Epinephrine enhances  $\text{Ca}^{2+}$  current-regulated  $\text{Ca}^{2+}$  release and  $\text{Ca}^{2+}$  reuptake in rat ventricular myocytes. *Proc. natn. Acad. Sci. USA* **85**, 2009-2013.
- Chacko, S. (1981). Effects of phosphorylation, calcium ion, and tropomyosin on actin-activated adenosine 5'-triphosphate activity of mammalian smooth muscle myosin. *Biochemistry* **20**, 702-707.

- Chandler, W. K. Rawowski, R. F. and Schneider, M. F. (1976). Effects of glycerol treatment and maintained depolarisation on charge movement in muscle. *J. Physiol., Lond.* **254**, 285-316.
- Chao, S-H., Zysk, J. R. and Cheung, W. Y. (1984). Activation of calmodulin by various metal cations as a function of ionic radius. *Mol. Pharmacol.* **26**, 75-82.
- Chase, P. B. and Kushmerick, M. J. (1988). Effects of pH on contraction of rabbit fast and slow skeletal muscle fibres. *Biophys. J.* **53**, 935-946.
- Chiarandini, D. J., Reuben, J. P., Brandt, P. W. and Grundfest, H. (1970a). Effects of caffeine on crayfish muscle fibres. I. Activation of contraction and induction of Ca spike electrogenesis. *J. gen. Physiol.* **55**, 640-664.
- Chiarandini, D. J., Reuben, J. P., Brandt, P. W. and Grundfest, H. (1970b). Effects of caffeine on crayfish muscle fibres. II. Refractoriness and factors influencing recovery (repriming) of contractile responses. *J. gen. Physiol.* **55**, 665-687.
- Cohen, P., Holmes, C.F.B., Tsukitani, Y. (1990). Okadaic acid, a new probe for the study of cellular regulation. *Trends Neurosci.* **15**, No 3, 98-103.
- Collins, J. H., Theibert, J. L., Francois, J. M., Ashley, C. C. and Potter, J. D. (1991). Amino acid sequences and  $Ca^{2+}$ -binding properties of two isoforms of barnacle Troponin C. *Biochemistry* **30**, 702-707.
- Cotton, J. L. S. Mykles, D. L. (1993). Cloning of a crustacean mysodin heavy-chain isoform - exclusive expression in fast muscle. *J. exp. Zool.* **267**, 578-586.
- Crowe, L.M. and Baskin, R.J. (1981). Activation of the contractile system in crustacean muscle, ultrastructural evidence for the role of the T system. *Tissue Cell* **13**, 153-164.

- Csemoch, L., Huang, L.H., Szucs, G., Kovacs, L. (1988). Differential effects of tetracaine on charge movements and  $\text{Ca}^{2+}$  signals in frog skeletal muscle. *J. gen. Physiol.* **92**, 601-612.
- Delahaye, G. F. (1975). Depolarisation-induced movement of  $\text{Mn}^{2+}$  across the cell membrane in the guinea-pig myocardium. *Circ. Res.* **36**, 713-718.
- Denhech, M.T. (1992). Central and peripheral actions of the neuropeptide proctolin on the postural neuromuscular muscle system in the Norway lobster, *Nephrops norvegicus* (L). Ph.D. Thesis, University of Glasgow.
- Donaldson, S. K. B. and Kerrick, W. G. L. (1975). Characterisation of the effects of  $\text{Mg}^{2+}$  on  $\text{Ca}^{2+}$ - and  $\text{Sr}^{2+}$ -activated tension generation of skinned skeletal muscle fibres. *J. gen. Physiol.* **66**, 427-444.
- Donaldson, S. K. B., Best, P. M. and Kerrick, W. G. L. (1978). Characterisation of the effects of  $\text{Mg}^{2+}$  on  $\text{Ca}^{2+}$ - and  $\text{Sr}^{2+}$ -activated tension generation of skinned rat cardiac fibres. *J. gen. Physiol.* **71**, 645-655.
- Dudel, J. Finger, W. and Stettmeier, H. (1980). Inhibitory synaptic channels activated by  $\gamma$ -aminobutyric acid (GABA) in crayfish muscle. *Pflügers Arch.* **387**, 143-151.
- Ebashi, S. and Endo, M. (1968). Calcium ion and muscle contraction. *Prog. biophys. Molec. Biol.* 123-183.
- Ebashi, S., Endo, M. and Ohtsuki, I. (1969). Control of muscle contraction. *Q. Rev. Biophys.* **2**, 351-384.
- Eddinger, T. J. and Moss, R. L. (1987). Mechanical properties of skinned single muscle fibres of identified types from rat diaphragm. *Am. J. Physiol.* **253**, C210-C218.
- Edwards, C. and Lorkowic, H. (1967). The role of  $\text{Ca}^{2+}$  in ECC in various muscles of the frog, mouse and barnacle. *Am. Zool.* **7**, 615-622.

- Eisenberg, E., Hill, T. L. and Chen, Y. (1980). Cross-bridge model of muscle contraction. *Biophys. J.* **29**, 195-227.
- Eisenberg, E. and Hill, T. L. (1985). Muscle contraction and free energy transductions in biological systems. *Science* **227**, 999-1006.
- Eisenberg, R. S., McCarthy, R. T. and Milton, R. L. (1983). Paralysis of frog skeletal muscle fibres by the calcium antagonist D-600. *J. Physiol., Lond.* **341**, 495-505.
- El-Saleh, S. C., Warber, K. D. and Potter, J. D. (1986). The role of tropomyosin-troponin in the regulation of skeletal muscle contraction. *J. Muscle Res. Cell Motil.* **7**, 387-404.
- Endo, M., Tanaka, M., Ogawa, Y. (1970).  $Ca^{2+}$ -induced  $Ca^{2+}$  release from the SR of skinned skeletal muscle fibres. *Nature* **228**, 34-36.
- Endo, M. (1977).  $Ca^{2+}$  release from the sarcoplasmic reticulum. *Physiol. Rev.* **57**, 71-108.
- Fadool, D.A. and Ache, B. W. (1992). Plasma-membrane inositol 1,4,5-triphosphate-activated channels. *Neuron* **9**, 907-918.
- Fatt, P. and Katz, B. (1953). The electrical properties of crustacean muscle fibres. *J. Physiol., Lond.* **120**, 171-204.
- Fatt, P and Ginsborg, B. L. (1958). The ionic requirements for the production of action potentials in crustacean muscle. *J. Physiol., Lond.* **142**, 516-543
- Feldmayer, D. Melzer, W. and Pohl, B. (1990). Effects of gallapamil (D600) on calcium release and intramembrane charge movements in frog skeletal muscle fibres. *J. Physiol., Lond.* **421**, 343-362.
- Fleischer, J. and Inui, M. (1989). Biochemistry and biophysics of excitation-contraction coupling. *A. Rev. Biophys. biophys. Chem.* **18**, 333-364.

- Fleischer, J., Ogunbunni, E.M., Dixon, M.C. Fler, E.A. (1985). Localisation of  $Ca^{2+}$  release channels with ryanodine in junctional terminal cisternae of SR in joint skeletal muscle. *Proc. natn. Acad. Sci. USA* **82**, 7256-7259.
- Ford, L. E., Huxley, A. F. and Simmons, R. M. (1977). Tension responses to sudden length change in stimulated frog muscle fibres near slack length. *J. Physiol., Lond.* **269**, 441.
- Ford, L. E., Huxley, A. F. and Simmons, R. M. (1981). The relation between stiffness and filament overlap in stimulated frog fibres. *J. Physiol., Lond.* **311**, 219-249.
- Formelova, J., Humak, O., Novotova, M. and Zachar, J. (1990). Ryanodine receptor purified from crayfish skeletal muscle. *Gen. Physiol. Biophys.* **9**, 445-453.
- Fosset, M., Jaimovich, E., Delpont, E. and Lazdunski, M. (1983). [ $^3H$ ] nitrendipine receptors in skeletal muscle. *J. biol. Chem.* **258**, 6086-6091.
- Fowler, W. S. and Neil, D. M. (1992). Histochemical heterogeneity of fibres in the abdominal superficial flexor muscles of the Norway lobster *Nephrops norvegicus* (L.). *J. exp. Zool.* **264**, 406-418.
- Franzini-Armstrong, C. (1970). Studies of the triad. I. Structure of the junction in frog twitch fibres. *J. Cell Biol.* **47**, 488-499.
- Franzini-Armstrong, C. (1975). Membrane particles and transmission at the triad. *Fed. Proc.* **34**, 1382-1389.
- Franzini-Armstrong, C. (1992). Dispositions of junctional feet in muscles of invertebrates. *J. Muscle Res. Cell Motil.* **13**, 161-173.
- Franzini-Armstrong, C. and Jorgenson, A. O. (1994). Structure and development of EC coupling units in skeletal muscle. *A. Rev. Physiol.* **56**, 509-534.

- Franzini-Armstrong, C. and Nunzi, G. (1983). Junctional feet and particles in the triads of a fast twitch muscle fibre. *J. Muscle Res. Cell Motil.* **4**, 233-252.
- Franzini-Armstrong, C. Peachy, L. D. (1981). Striated muscle- contractile and control mechanisms. *J. Cell Biol.* **91**, 166s-186s.
- Fryer, M. W., Gage, P. W., Neering, I. R., Dulhunty, A. F. and Lamb, G. D. (1988). Paralysis of skeletal muscle by butanedione monoxime, a chemical phosphatase. *Pflügers Arch.* **411**, 76-70.
- Fryer, M. W., Neering, I. R. and Stephenson, D. G. (1988). Effects of 2,3-butanedione monoxime on the contractile activation properties of fast and slow-twitch rat muscle fibres. *J. Physiol., Lond.* **407**, 53-75.
- Fuchs, F. (1974). Chemical properties of the calcium receptor site of troponin as determined from binding studies. In *Calcium binding proteins* (Ed, W. Drabikowski, H. Strzelecka-Golaszewska, E. Carafoli), pp. 1-27. Elsevier Scientific publishing company, Amsterdam.
- Fukunda, J. and Kawa, K. (1977). Permeation of manganese, cadmium, zinc, beryllium through calcium channels of insect muscle membrane. *Science* **196**, 309-311.
- Gainer, H. (1968). The role of calcium in excitation-contraction coupling of lobster muscle. *J. gen. Physiol.* **52**, 88-110.
- Galler, S. (1994). Stretch activation of skeletal muscle fibre types. *Pflügers Arch.* **427**, 384-386.
- Galler, S. and Rathmayer, W. (1992). Shortening velocity and force/pCa relationship in skinned crab muscle fibres of different types. *Pflügers Arch.* **420**, 187-193.
- Galler, S. and Hilber, K. (1994). Unloaded shortening of skinned mammalian skeletal muscle fibres: effects of the experimental approach and passive force. *J. Muscle Res. Cell Motil.* **15**, 400-412.

- Galler, S. and Neil, D.M. (1994). Calcium activated and stretch induced force responses in two biochemically defined muscle fibre types of the Norway lobster. *J. Mus. Res. Cell Motil.* **15**, 390-399.
- Galler, S., Schmitt, T. L. and Pette, D. (1994). Stretch activation, unloaded shortening velocity, and myosin chain isoforms of rat skeletal muscle fibres. *J. Physiol., Lond.* **478**, 513-521.
- Galler, S., Hilber, K., and Pette, D. (1996). Force responses following stepwise length changes of rat skeletal muscle fibre types. *J. Physiol., Lond.* **493**, 219-227.
- Garcia, J. Pizzaro, G. Rios, E. and Stefani, E. (1990). Depletion of the SR reduces the delayed charge movement in frog skeletal muscle. *Biophys. J.* **57**, 341a.
- Garone, L., Theibert, I. L., Miegel, Y., Murphy, C. and Collins, J. H. (1991). Lobster troponin C, amino acid sequences of three isoforms. *Archs. Biochem. Biophys.* **291**, 89-91.
- Gerringa, L. J. A. (1991). Mobility of Cu, Cd, Ni, Pb, Zn, Fe and Mn in marine sediment slurries under anaerobic conditions and at 20-percent air saturation. *Neth. J. Sea Res.* **27**, 145-156.
- Gilly, W. M. F. and Sheuer, T. (1984). Contractile activation in scorpion striated muscle fibres, dependence on voltage and external calcium. *J. gen. Physiol.* **84**, 321-345.
- Goblet, C. and Mournier, Y. (1982). Contractility in relation to excitability in voltage clamped crab muscle fibres, Evidence for two components of tension. *Gen. Physiol. Rev.* **1**, 233-253.
- Goblet, C. and Mournier, Y. (1986).  $Ca^{2+}$ -induced  $Ca^{2+}$  release mechanisms from the sarcoplasmic reticulum in skinned muscle fibres. *Cell Calcium* **7**, 61-72.
- Godt, R. E. and Maughan, D. W. (1977). Swelling of skinned muscle fibres of the frog. *Biophys. J.* **19**, 103-116.

- Godt, R.E., Fogaca, R.T. H., Brotto, M.A.P., Kassouf Silva, I. and Nosek, T.M. (1993). Butanedione monoxime (BDM) induces calcium release from the sarcoplasmic reticulum of crustacean striated muscle fibres. In *Proceedings of the XXXII Congress of the International Union of Physiological Sciences, Glasgow*, p. 2.
- Govind, C. K. (1995). Muscles and their innervation. In *Biology of the lobster*, (ed. J. R. Factor), pp 291-312. London: Academic Press.
- Greaser, M. L., Moss, R. L. and Reiser, P. J. (1988). Variations in contractile properties of rabbit single muscle fibres in relation to troponin T isoforms and myosin light chains. *J. Physiol., Lond.* **406**, 85-98.
- Greene, L. E. and Eisenberg, E. (1980). Co-operative binding of myosin subfragment-1 to the actin-troponin tropomyosin complex. *Proc. natn. Acad. Sci. USA* **77**, 2616-2620.
- Gwathmey, J. K., Hajjar, R. J. and Solaro, R. J. (1991). Contractile deactivation and uncoupling of crossbridges. Effects of 2,3-butanedione monoxime on mammalian myocardium. *Circ. Res.* **69**, 1280-1292.
- Györke, S. and Palade, P. (1992)  $Ca^{2+}$ -induced  $Ca^{2+}$  release in crayfish skeletal muscle. *J. Physiol., Lond.* **457**, 195-210.
- Györke, S., Dettbarn, C., Palade, P. (1993). Potentiation of SR  $Ca^{2+}$  release by 2,3-butanedione monoxime in crustacean muscle. *Pflügers Arch.* **424**, 39-44.
- Hagiwara, S. (1973). Ca Spike. *Adv. Biophys.* **4**, 71-102.
- Hagiwara, S. and Byerly, L. (1981). Calcium channel. *A. Rev. Neurosci.* **4**, 69-125
- Hagiwara, S., Hayashi, H., Takahashi, K. (1969). Calcium and potassium currents of the membrane of a barnacle muscle fibre in relation to the calcium spike. *J. Physiol., Lond.* **205**, 115-129.

- Hagiwara, S and Naka, K. (1964). The initiation of spike potential in barnacle muscle fibres under low intracellular  $Ca^{2+}$ . *J. Gen Physiol.* **48**, 141-162.
- Hagiwara, S. and Miyazaki, S. (1977a). Ca and Na spikes in egg cell membrane. *Prog. Clin. Biol. Res.* **15**, 147-158.
- Hagiwara, S. and Nakajima, S. (1966a). Differences in  $Na^{2+}$  and  $Ca^{2+}$  spikes as examined by application of tetrodotoxin, procaine and manganese ions. *J. gen. Physiol.* **49**, 793-806.
- Hagiwara, S. and Nakayima, S. (1966b). Effects of intracellular ion concentration upon the excitability of the muscle fibre membrane of a barnacle. *J. gen. Physiol.* **49**, 807-818.
- Hagiwara, S. and Takahashi, K. (1967). Surface density of calcium ions and calcium spikes in the barnacle muscle fibre membrane. *J. gen. Physiol.* **50**, 583-601.
- Hall, P. O. J., Anderson, L. G., Vanderloeff, M. M. R., Sundby, B. and Westerlund, S. F. G. Oxygen-uptake kinetics in the benthic boundry layer. *Limn. Ocean.* **34**, 734-746.
- Hartshorne, D. J. (1969). Studies on troponin. *Biochim. biophys. Acta.* **175**, 320-330.
- Hartshorne, D. J. and Boucher, L. J. (1974). Ion binding in troponin. In *Calcium binding proteins*, (Ed. W. Drabikowski, H. Strzelecka-Golaszewska, E. Carafoli), pp. 29-43. Elsevier Scientific publishing company, Amsterdam.
- Hartshorne, D. J. and Sicmankowski, T. F. (1981). Regulation of smooth muscle actomyosin. *A. Rev. Physiol.* **43**, 519-530.
- Haselgrove, J. C. (1973). X-ray evidence for conformational changes in the actin-containing filaments of vertebrate striated muscle. *Cold. Spring. Harb. Symp. Quant. Biol.* **37**, 341-352.

- Heilbrunn, L. V. and Wiercinski, F. J. (1947). The action of various cations on muscle protoplasm. *J. Cell Comp. Physiol.* **29**, 15-29
- Hess, P., Lansman, J. B. Tsien, R. W. (1984). Different modes of Ca-channel gating behaviour favored by dihydropyridine Ca-agonists and antagonists. *Nature* **311**, 538-544.
- Higuchi, H. and Takemori, S. (1989). Butanedione monoxime suppresses contraction and ATPase activity of rabbit skeletal muscle. *J. Biochem.* **105**, 638-643.
- Higuchi, H., Yanagida, T. and Goldman, Y. E. (1995). Compliance of thin filaments in skinned fibres of rabbit skeletal muscle. *Biophys. J.* **69**, 1000-1010.
- Hille, B. (1977). Local anaesthetics: hydrophilic and hydrophobic pathways for the drug receptor reaction. *J. gen. Physiol.* **69**, 497-515.
- Hoar, P. E. and Kerrick, W. G. (1988).  $Mn^{2+}$  activates skinned smooth muscle cells in the absence of myosin light chain phosphorylation. *Pflügers Arch.* **412**, 225-230.
- Hodgkin, A.L. and Horowicz, P. (1960). Potassium contractures in single muscle fibres. *J. Physiol., Lond.* **153**, 386-403.
- Hodgkin, A.L. and Huxley, F. (1952). Currents carried by sodium and potassium ions through the membrane of the giant axon of *Loligo*. *J. Physiol., Lond.* **120**, 171-204.
- Hofmann, P. A., Metzger, J. M., Greaser, M. L. and Moss, R. L. (1990). Effects of partial extraction of light chain 2 on the  $Ca^{2+}$ -sensitivities of isometric tension, stiffness, and the velocity of shortening in skinned skeletal muscle fibres. *J. gen. Physiol.* **95**, 477-498.
- Horiuti, K., Higuchi, H., Umazume, Y., Konishi, M., Okazaki, O. and Kurihara, S. (1988). Mechanisms of action of 2,3-butanedione 2-monoxime on contraction of frog skeletal muscle fibres. *J. Muscle Res. Cell Motil.* **9**, 156-164.

- Hui, C. S., Milton, R. L. and Eisenberg, R. S. (1984). Charge movement in skeletal muscle fibres paralysed by the calcium-entry blocker D600. *Proc. natn. Acad. Sci. USA* **81**, 2582-2585.
- Huxley, A. F. (1980). *Reflections on muscle*. Liverpool University Press, Liverpool.
- Huxley, A. F. and Simmons, R. M. (1970). A quick phase in the series-elastic component of striated muscle, demonstrated in isolated fibres from the frog. *J. Physiol., Lond.* **208**, 52-53P.
- Huxley, A. F. and Simmons, R. M. (1971a). Mechanical properties of crossbridges of frog striated muscle. *J. Physiol., Lond.* **218**, 59-60P.
- Huxley, A. F. and Simmons, R. M. (1971b). Proposed mechanism of force generation in striated muscle. *Nature* **233**, 533-538.
- Huxley, A. F. and Simmons, R. M. (1973). Mechanical transients and the origin of muscular force. *Cold. Spring. Harb. Symp. Quant. Biol.* **37**, 669-680.
- Huxley, A. F. and Straub, R. W. (1958). Local activation and interfibrillar structures in striated muscle. *J. Physiol., Lond.* **143**, 40-41P.
- Huxley, A. F. and Taylor, R. E. (1955). Function of Krause's membrane. *Nature* **176**, 1068.
- Huxley, A.F. and Taylor, R.E. (1958). Local activation of striated muscle fibres. *J. Physiol., Lond.* **144**, 426-441.
- Huxley, H. E. (1973). Structural changes in the actin- and myosin-containing filaments during contraction. *Cold Spring Harbor Symp. Quant. Biol.* **337**, 361-376.
- Huxley, H. E. and Kress, M. (1985). Crossbridge behaviour during muscle contraction. *J. Muscle Res. Cell Motil.* **6**, 153-161.

- Hymel, L., Inui, M., Fleisher, S. and Schindler, H. (1988). Purified ryanodine receptor of skeletal muscle sarcoplasmic reticulum forms  $Ca^{2+}$ -activated oligomeric  $Ca^{2+}$  channels in planar bilayers. *Proc. natn Acad. Sci. USA* **85**, 441-445.
- Hymel, L., Schindler, H., Inui, M. and Fleisher, S. (1988). Reconstitution of purified cardiac muscle calcium release channel (ryanodine receptor) in planar bilayers. *Biochem. Biophys. Res. Commun.* **152**, 308-314.
- Inui, M., Saito, A. and Fleischer, S. (1987). Purification of the ryanodine receptor and identity with feet structures of junctional terminal cisternae of sarcoplasmic reticulum from fast skeletal muscle. *J. biol. Chem.* **262**, 1740-1747.
- Inoue, I., Tsutsui, I., Bone, Q. and Brown, E. R. (1994). Evolution of skeletal muscle excitation-contraction coupling and the appearance of dihydropyridine-sensitive intramembrane charge movement. *Proc. R. Soc. Lond.* **B 255**, 181-187.
- Irving, M., Allen, T. S. C., Sabido-David, C., Craik, J. S., Brandmeier, B., Kendrick-Jones, J., Corrie, J. E. T., Trentham, D. R. and Goldman, Y. E. (1995). Tilting of the light chain region of myosin during step length changes and active force generation in skeletal muscle. *Nature* **375**, 688-691.
- Irving, M., Lombardi, V., Piazzesi, G. and Ferenczi, M. A. (1992). Myosin head movements are synchronous with the elementary force-generating process in muscle. *Nature* **357**, 156-158.
- Itoh, T., Kuriyama, H. and Nanjo, T. (1982). Effects of calcium and manganese ions on mechanical properties of intact and skinned muscles from the guinea-pig stomach. *J. Physiol., Lond.* **333**, 555-576.
- Jahromi, S. S. and Atwood, H. L. (1966). Ultrastructural features of crayfish phasic and tonic muscle fibres. *Can. J. Zool.* **45**, 601-606.
- Jahromi, S. S. and Atwood, H. L. (1971). Structural and contractile properties of lobster leg-muscle fibres. *J. exp. Zool.* **176**, 475-486.

- Jenden, D. J. and Fairhurst, A. S. (1969). The pharmacology of ryanodine. *Pharmacol. Rev.* **21**, 1-25.
- Julian, F. J. and Moss, R. L. (1981). Effects of calcium and ionic strength on shortening velocity and tension development in frog skinned fibres. *J. Physiol., Lond.* **311**, 179-199.
- Julian, F. J., Moss, R. L. and Waller, G. S. (1981). Mechanical properties and myosin light chain composition of skinned muscle fibres from adult and new-born rabbits. *J. Physiol., Lond.* **311**, 201-218.
- Julian, F. L., Rome, L. C., Stephenson, D. G. and Striz, S. (1986). The maximum speed of shortening in living and skinned frog fibres. *J. Physiol., Lond.* **370**, 181-199.
- Kamm, K. E. and Stull, J. T. (1985). The function of myosin and myosin light chain kinase phosphorylation in smooth muscle. *A. Rev. Pharmacol. Toxicol.* **25**, 593-620.
- Katz, B. and Miledi, R. (1969). The effects of divalent cations on transmission in the squid giant synapse. *Publ. Staz. Zool. Napoli.* **37**, 303-307.
- Kennedy, D. and Takeda, K. (1965a). Reflex control of abdominal flexor muscles in the crayfish. I. The twitch system. *J. exp. Biol.* **43**, 211-227.
- Kennedy, D. and Takeda, K. (1965b). Reflex control of abdominal flexor muscles in the crayfish. II. The tonic system. *J. exp. Biol.* **43**, 229-246.
- Kerkut, G. A. and Gardner, D. R. (1967). The role of calcium ions in the action potential of *Helix aspersa* neurones. *Comp. Biochem. Physiol.* **20**, 147-162.
- Kobayashi, T., Takagi, T., Koninshi, K. and Wnuk, W. (1989). Amino acid sequences of the two major isoforms of Troponin C from crayfish. *J. biol. Chem.* **264**, 18247-18259.

- Kojima, H., Ishijima, A. and Yanagida, T. (1994). Direct measurements of stiffness of single actin filaments with and without tropomyosin by in vitro nanomanipulation. *Proc. natn. Acad. Sci. USA* **91**, 12962-12966.
- Kress, M., Huxley, A. F., Farnqi, A. R. and Hendrix, J. (1986). Structural changes during activation of frog muscle studied by time-resolved x-ray diffraction. *J. Molec. Biol.* **188**, 325-342
- Laemmli, U. K. (1970). Cleavage of structural proteins during assembly of the head of bacteriophage T4. *Nature* **227**, 680-685.
- Lai, F.A., Erickson, H.P., Rousseau, E., Liu, Q.Y., Meissner, G. (1988). Purification and reconstitution of the calcium release channel from skeletal muscle. *Nature* **331**, 315-319.
- Lai, F. A. and Meissner, G. (1989). The muscle ryanodine receptor and its intrinsic Ca<sup>2+</sup> channel activity. *J. Bioenerg. Biomembr.* **21**, 227-246.
- Lamb, G. D. (1991). Ca<sup>2+</sup> channels or voltage sensors? *Nature* **352**, 113.
- Lamb, G. D. (1992). DHP receptors and excitation-contraction coupling. *J. Muscle Res. Cell Motil.* **13**, 394-405.
- Lategan, T. W. and Brading, A. F. (1988). Contractile effects of manganese on taenia of guinea pig cecum. *Am. J. Physiol.* **254**, G489-G494.
- Lea, T. J. (1996). Caffeine and micromolar Ca<sup>2+</sup> concentrations can release Ca<sup>2+</sup> from ryanodine-sensitive stores in crab and lobster striated muscle fibres. *J. exp. Biol.* **199**, 2419-2428.
- Lea, T.J. and Ashley, C.C. (1989). CICR from the SR of isolated myofibrillar bundles of barnacle muscle fibres. *Pflügers Arch.* **413**, 401-406.

- Leavis, P. C. and Gergely, J. (1984). Thin filament proteins and thin filament-linked regulation of vertebrate muscle contraction. *Critical Rev. Biochem.* **16**, 235-305.
- Lehman, W. and Szent-Györgyi, A. G. (1975). Regulation of muscular contraction. Distribution of actin control and myosin control in the animal kingdom. *J. gen. Physiol.* **66**, 1-30
- Leung, A. R. Imagawa, T., Block, B. Franzini-Armstrong, C. and Campbell, K. P. (1988). Biochemical and ultrastructural characterisation of the dihydropyridine receptor from rabbit skeletal muscle. *J. biol. Chem.* **263**, 994-1001.
- Li, T., Sperelakis, M. Teneick, R. E. and Solaro, R. J. (1985). Effects of diacetyl monoxime on cardiac excitation-contraction coupling. *J. Pharmacol. Exp. Ther.* **232**, 688-695.
- Li, Y. and Mykles, D. L. (1990). Analysis of myosins from lobster muscles: fast and slow isozymes differ in heavy-chain composition. *J. exp. Zool.* **255**, 163-170.
- Loesser, K. E., Castellini, L. and Franzini-Armstrong, C. (1992). Disposition of junctional feet in muscles of invertebrates. *J. Muscle Res. Cell. Motil.* **13**, 161-173.
- Lombardi, V., Piazzesi, G. and Linari, M. (1992). Rapid regeneration of the actin-myosin power stroke in contracting muscle. *Nature* **355**, 638-641.
- London, B. and Krueger, J. W. (1986). Contraction in voltage-clamped internally perfused single heart cells. *J. gen. Physiol.* **88**, 475-505.
- Lowey, S. (1971). Myosin, molecule and filament. In *Biological macro-molecules subunits in biological systems*, (Ed. S. Timasheff and G. Fasman), **5**, 201-259. Dekker, New York.
- Lüttgau, H. C. and Oetliker, M. (1968). The action of caffeine on the activation of the contractile mechanism in striated muscle fibres. *J. Physiol., Lond.* **194**, 51-57.

- MacLennan, D. H. and Wong, P. T. S. (1971). Isolation of a calcium sequestering protein from the sarcoplasmic reticulum. *Proc. natn. Acad. Sci. USA* **68**, 1231-1235.
- Maier, L. Rathmayer, W. and Pette, D. (1984). pH lability of myosin ATPase permits discrimination of different muscle fibre types in crustaceans. *Histochemistry* **81**, 75-77.
- Marston, S. B. and Smith, S. J. (1984). Purification and properties of  $Ca^{2+}$  regulated thin filaments and f-actin from sheep aorta smooth muscle. *J. Muscle Res. Cell Motil.* **5**, 559-575.
- Matsumura, M. (1978). The rate of action of calcium on the electrical and mechanical responses of the crayfish muscle fibres. *Jap. J. Physiol.* **28**, 75-87.
- McClintock, T. S. and Ache, B. W. (1990). Nonselective cation channels activated by patch excision from lobster olfactory receptor neurons. *J. Membr. Biol.* **113**, 115-122.
- McPherson, S. M., McPherson, P. S., Smathewa, L., Campbell, K.P. and Longo, F. J. (1992). Cortical localization of a calcium release channel in sea-urchin eggs. *J. Cell. Biol.* **116**, 111-1121.
- Meissner, G. (1994). Ryanodine receptor/ $Ca^{2+}$  release channels and their regulation by endogenous effectors. *A. Rev. Physiol.* **56**, 485-508.
- Meyer, T. and Stryer, L. (1991). Calcium spiking. *A. Rev. Biophys. Chem.* **20**, 153-174.
- Miegel, A., Kobayashi, I. and Maeda, Y. (1992). Isolation, purification and partial characterisation of tropomyosin and troponin subunits from the lobster tail muscle. *J. Muscle Res. Cell Motil.* **13**, 608-618.
- Miledi, R. Parker, I. and Zhu, P. H. (1984). Extracellular ions and excitation-contraction coupling in frog twitch muscle fibres. *J. Physiol., Lond.* **351**, 687-710.

- Miyan, A.I. (1984). A methods for the neurophysiological study of reflexes elicited by natural statocyst stimulation in lobsters. *J. exp. Biol.* **108**, 465-469.
- Moiescu, D. G. and Thieleczek, R. (1978a). Calcium and strontium concentration changes within skinned muscle preparations following a change in the external bathing solution. *J. Physiol., Lond.* **275**, 241-262
- Moiescu, D. G. and Thieleczek, R. (1978b). Arthropod skeletal muscles - insensitive to  $Sr^{++}$ . *Proc. Aus. Physiol. Pharmacol. Soc.* **9**, 158P
- Moiescu, D. G. and Thieleczek, R. (1979). Sarcomere length effects on the  $Sr^{2+}$  and  $Ca^{2+}$  activation curves in skinned frog muscle fibres. *Biochim. biophys. Acta.* **546**, 64-76
- Moss, R. L., Lauer, M. R., Giulian, G. G. and Greaser, M. L. (1986). Altered  $Ca^{2+}$  dependence of tension development in skinned skeletal muscle fibres following mechanical modification of troponin by partial substitution with cardiac troponin C. *J. Biol. Chem.* **261**, 6096-6099.
- Mounier, Y. and Vassort, G. (1975). Initial and delayed membrane currents in crab muscle fibre under voltage-clamp conditions. *J. Physiol., Lond.* **251**, 589-608
- Mounier, Y. and Goblet, C. (1987). Role of different Calcium sources in the ECC in crab muscle fibres. *Can. J. Pharmacol.* **65**, 667-671.
- Mulieri, L. A. and Alpert, N. R. (1984). Differential effects of 2,3-butanedione monoxime (BDM) on activation and contraction. *Biophys. J.* **45**, 47a.
- Mykles, D. L. (1985). Multiple variants of myofibrillar proteins in single fibres of lobster claw muscles, Evidence for two types of fibres in the cutter claw. *Biol. Bull.* **169**, 476-483.
- Mykles, D. L. (1988). Histochemical and biochemical characterisation of two slow fibre subtypes in decapod crustacean muscles. *J. exp. Zool.* **245**, 232-243.

- Nasu, T. (1995). Actions of manganese ions in contraction of smooth muscle. *Gen. Pharmac.* **26**, No 5, 945-953.
- Nasu, T. Murase, H. and Shibita, H. (1995a). Manganese ions penetrate via L-type  $\text{Ca}^{2+}$  channels and induce contraction in high- $\text{K}^+$  medium in ileal longitudinal muscle of guinea-pig. *Gen. Pharmac.* **26**, No 2, 381-386.
- Nasu, T. Arakaki, H. and Shibita, H. (1995b). Effects of nifedipine, ryanodine and cyclopiazonic acid on tension of ileal longitudinal muscle by manganese ions in  $\text{Ca}^{2+}$ -free High- $\text{K}^+$  medium. *Gen. Pharmac.* **26**, No 6, 1255-1260.
- Neil, D. M., Fowler, W. S. and Tobasnick, G. (1993). Myofibrillar protein composition correlates with histochemistry in fibres of the abdominal flexor muscles of the Norway lobster *Nephrops norvegicus*. *J. exp. Biol.* **183**, 185-201.
- Nichols, R. A. and Nakajima, Y. (1975). Effects of manganese and cobalt on the inhibitory synapse of the crustacean stretch receptor neuron. *Brain Res.* **86**, 493-498.
- Nistri, A. and Constanti, A. (1979). Pharmacological characterisation of different types of GABA and glutamate receptors in vertebrates and invertebrates. *Prog. Neurobiol.* **13**, 117-235.
- Noyes, R. M. (1962). Thermodynamics of ion hydration as a measure of effective dielectric properties of water. *J. Am. Chem. Soc.* **84**, 513-522
- Ochi, R. (1970). The slow inward current and the action of manganese ions in guinea-pig's myocardium. *Pflügers Arch.* **316**, 81-94.
- Ochi, R. (1975). Manganese action potentials in mammalian cardiac muscle. *Experientia* **31**, 1048-1049.

- Ochi, R. (1976). Manganese-dependent propagated action potentials and their depression by electrical stimulation in guinea-pig myocardium perfused by sodium-free media. *J. Physiol., Lond.* **263**, 139-156.
- Ochiai, E. I. (1977). *Bioinorganic chemistry, An introduction*, pp. 55. Allyn and Bacon Inc., Boston.
- Ohtsuki, I., Maeuyama, K. and Ebashi, S. (1986). Regulatory and cytoskeletal proteins of vertebrate skeletal muscle. *Adv. Protein Chem.* **38**, 1-67.
- Okamoto, H. Takahashi, K. and Yamashita, N. (1977). Ionic currents through the membrane of the mammalian oocyte and their comparison with those in the tunicate and sea urchin. *J. Physiol., Lond.* **267**, 465-495.
- Orkand, R. K. (1962). The relationship between membrane potential and contraction in single crayfish muscle fibres. *J. Physiol., Lond.* **161**, 143-159.
- Österman, Å., Arner, A. and Malmqvist, U. (1993). Effect of 2,3-butanedione monoxime on activation of contraction and crossbridge kinetics in intact and chemically skinned smooth muscle fibres from guinea-pig taenia coli. *J. Muscle Res. Cell Motil.* **14**, 186-194.
- Palade, P. T. and Almers, W. (1978). Slow Na and Ca currents across the membrane of frog skeletal muscle fibres. *Biophys. J.* **21**, 168a
- Palade, P. and Györke, S. (1993). Excitation-contraction coupling in Crustacea: do studies on these primitive creatures offer insights about EC coupling more generally? *J. Muscle Res. Cell Motil.* **14**, 283-287.
- Palade, P. and Vergara, J. (1982). arsenazo III and antipyrylazo III calcium transients in single skeletal muscle fibres. *J. gen. Physiol.* **79**, 679-707.
- Parker, I. and Yao, Y. (1991). Regenerative release of calcium from functionally discrete subcellular stores by inositol triphosphate. *Proc. R. Soc. Lond. B* **246**, No 1317, 269.

- Parnas, I. and Atwood, H.L. (1966). Phasic and tonic neuromuscular systems in the abdominal extensor muscles of the crayfish and rock lobster. *Comp. Biochem. Physiol.* **18**, 701-723.
- Parnas, I., Parnas, H. and Dudel, J. (1982). Neurotransmitter release and its function and its facilitation in crayfish muscle. V. Basis for synapse differentiation of the fast and slow type in one axon. *Pflugers Arch.* **395**, 261-270.
- Parry, D. A. and Squire, J. M. (1973). The structural role of tropomyosin in muscle regulation, analysis of the x-ray diffraction patterns from relaxed and contracting muscles. *J. Molec. Biol.* **75**, 33-55.
- Parys, J.B., Sernett, S. W., Delise, S., Snyder, P. M., Welsh, M. J. and Cambell, K. P. (1992). Isolation, characterisation, and localisation of inositol 1,4,5-triphosphate receptor protein in *Xenopus-laevis* oocytes. *J. biol. Chem.* **267**, No 26, 18776-18782.
- Peachy, L. D. (1965). The sarcoplasmic reticulum and the transverse tubules of the frog's sartorius. *J. Cell Biol.* **25**, part II, 209-231.
- Peachy, L.D. (1973). Electrical events in the T-system of frog skeletal muscle. *Cold Spring Harbor Symp. Quart. Biol.* **37**, 479-487.
- Perry, S. V., Cole, H. A., Head, J. F. and Wilson, F. J. (1973). Localisation and mode of action of the inhibitory protein component of the troponin complex. *Cold. Spring Harbor Symp. Quant. Biol.* **37**, 251-262.
- Pessah, I. N., Stambuk, R. A. Casida, J. E. (1987).  $Ca^{2+}$ -activated ryanodine binding: mechanisms of sensitivity and intensity modulation by  $Mg^{2+}$ , caffeine, and adenine nucleotides. *Mol. Pharmacol.* **31**, 232-238.
- Pette, D. and Staron, R. S. (1990). Cellular and molecular diversities of mammalian skeletal muscle fibres. *Rev. Physiol. Biochem. Pharmacol.* **116**, 1-76.

- Pferrer, S. Kulik, R., Hiller, T. and Kuhn, H. J. (1988). The dependence of isometric tension, isometric ATPase activity, and shortening velocity of limulus muscle on the MgATP concentration. *Biophys. J.* **53**, 127-135.
- Pilgrim, R. L. C. and Wiersma, C. A. G. (1963). Observations on the skeleton and somatic musculature of the abdomen and thorax of *Procambarus clarkii* (Girard), with notes on the thorax of *Pandulirus interruptus* (Randall) and *Astacus*. *J. Morph.* **113**, 453-487.
- Podolsky, R. J. (1968). Membrane systems in muscle cells. In *Aspects of cell motility*, vol XXII. Symposia of the Society for Experimental Biology, (Ed. P. L. Miller), pp. 87-99. University Press, Cambridge.
- Porter, K. R. and Palade, G. E. (1957). Studies on the endoplasmic reticulum. III. Its form and distribution in striated muscle cells. *J. Biophys. Biochem. Cytol.* **3**, 269-300.
- Potter, J. D. and Gergely, J. (1975). The calcium and magnesium binding sites of troponin and their role in the regulation of myofibrillar adenosinetriphosphatase. *J. biol. Chem.* **250**, 4628-4633.
- Rathmayer, W. and Erxelben, C. (1983). Identified muscle fibres in crab. I. Characteristics of excitatory and inhibitory neuromuscular transmission. *J. comp. Physiol. A* **152**, 411-420.
- Rathmayer, W. and Hammelsbeck, M. (1985). Identified muscle fibres in a crab. Differences in facilitation properties. *J. exp. Biol.* **116**, 291-300.
- Rathmayer, W. and Maier, L. (1987). Muscle fibre groups in crabs, studies on single identified muscle fibres. *Am. Zool.* **27**, 1067-1077.
- Reuben, J. P., Brandt, P. W., Garcia, H. and Grundfest, H. (1967). Excitation-contraction coupling in crayfish. *Am. Zool.* **7**, 623-630.

- Reiser, P. J., Moss, R. L., Giullian, G. G. and Greaser, M. L. (1985a). Shortening velocity in single fibres from adult rabbit soleus muscles is correlated with myosin heavy chain composition. *J. biol. Chem.* **260**, 9077-9080.
- Reiser, P. J., Moss, R. L., Giullian, G. G. and Greaser, M. L. (1985b). Shortening velocity and myosin heavy chains of developing rabbit muscle fibres. *J. biol. Chem.* **260**, 14403-14405.
- Reiser, P. J., Greaser, M. L. and Moss, R. L. (1988). Myosin heavy chain composition of single cells from avian slow skeletal muscle is strongly correlated with velocity of shortening during development. *Dev. Biol.* **129**, 400-407.
- Reuter, H. (1973). Divalent cations as charge carriers in excitable membranes. *Prog. Biophys. Molec. Biol.* **26**, 1-43
- Ridge, R. M. A. P. (1989). Motor unit organization in developing muscle. *Comp Biochem. Physiol.* **93A**, 115-123.
- Rios, E. and Brum, G. (1987). Involvement of dihydropyridine receptors in excitation-contraction coupling in skeletal muscle. *Nature* **325**, 717-720.
- Rios, E. and Pizarno, G. (1991). Voltage sensor of ECC in skeletal muscle. *Physiol. Rev.* **71**, 849-908.
- Robertson, J. D. (1956). Some features of the ultrastructure of reptilian skeletal muscle. *J. Biophys. Biochem. Cytol.* **2**, 369-380.
- Rojas, E., Nassar-Gentina, V., Luxoro, M., Pollard, M. and Carrasco, M. A. (1987). Inositol 1,4,5-triphosphate-induced  $Ca^{2+}$  release from the sarcoplasmic reticulum and contraction in crustacean muscle. *Can. J. Physiol. Pharmacol.* **65**, 672-680.
- Ross, W. N. and Stuart, A. E. (1978). Voltage sensitive calcium channels in the presynaptic terminals of a detrimentally conducting photoreceptor. *J. Physiol., Lond.* **274**, 173-191

- Sakai, K. and Uchida, M. (1981). Manganese-induced contraction in  $K^+$  depolarised rat uterine smooth muscle. *Gen. Pharmac.* **12**, 41-45.
- Sanchez, J. A. and Stefani, E. (1983). Kinetic properties of calcium channels of twitch muscle fibres of the frog. *J. Physiol. Lond.* **37**, 1-17.
- Sandow, A. (1952). ECC in muscular response. *J. Biol. Med.* **25**, 176-201.
- Sandow, A. (1965). ECC in skeletal muscle. *Pharmacol. Rev.* **17**, 265-269.
- Sanguinetti, M.C. and Kass, R.S. (1984). Voltage-dependant block of calcium current in the calf purkinje fibres by dihydropyridine calcium channel antagonists. *Circ. Res.* **55**, 336-348.
- Schwartz, L. M., McClesky, E. W. and Almers, W. (1985). Dihydropyridine receptors in muscle are voltage dependent but most are not functional calcium channels. *Nature* **314**, 747-751.
- Seok, J., Xu, L., Kramarcy, N., Sealock, R. and Meissner, G. (1992). The 30S lobster skeletal muscle  $Ca^{2+}$  release (Ryanodine receptor) has functional properties distinct from the mammalian channel properties. *J. Biol. Chem.* **267**, 15893-15901.
- Sherman, R. G. and Atwood, H. L. (1972). Correlated electrophysiological and ultrastructural studies of a crustacean motor unit. *J. gen. Physiol.* **59**, 586-615.
- Silverman, II., Costello, W. J. and Mykles, D. J. (1987). Morphological fibre type correlates of physiological and biochemical properties in crustacean muscle. *Am. Zool.* **27**, 1011-1019.
- Simmons, R. M. (1992). *Muscular contraction*. Cambridge University Press, Cambridge.

- Smith, J. S., Imagawa, T., Ma, J., Fill, M., Campbell, K.P., Coronado, R. (1988). Purified ryanodine receptor from skeletal muscle in the  $\text{Ca}^{2+}$  release channel of the SR. *J. gen. Physiol.* **92**, 176-201.
- Schneider, M. F. and Chandler, W. K. (1973). Voltage dependant charge movement in skeletal muscle. *Nature* **242**, 244-246.
- Somylo, A. V. and Somlyo, A. P. (1968). Electromechanical and pharmacomechanical coupling in vascular smooth muscle. *J. Pharmacol. Exp. Ther.* **159**, 129-145.
- Somlyo, A. P. and Somylo, A. V. (1968). Electrical mechanical and pharmacomechanical coupling in vascular smooth muscle. *J. Pharmacol. Exp. Ther.* **159**, 129-145.
- Squire, J. M. (1981). *The structural basis of muscle contraction*. Plenum Press, New York.
- Staron, R. S. and Pette, D. (1986). Correlation between myofibrillar ATPase activity and myosin heavy chain composition in rabbit muscle fibres. *Histochemistry* **86**, 19-23.
- Steele, D.S. and Smith, G. (1993). Effects of 2,3-butanedione monoxime on sarcoplasmic reticulum of saponin-treated rat cardiac muscle. *Am. J. Physiol.* **93**, H1493-H1500.
- Steiger, G. J. (1977). Stretch activation and tension transients in cardiac, skeletal and insect flight muscle. In *Insect flight muscle* (ed. R. T. Tregear) pp. 221-268. Amsterdam, Elsevier, North Holland, Amsterdam.
- Steiger, G. J. and Abbott, R. H. (1981). Biochemical interpretation of tension transients produced by a four-state mechanical model. *J. Muscle Res. Cell Motil.* **2**, 245-260.
- Stephenson, D. G. and Forest, Q. G. (1980). Different isometric force- $[\text{Ca}^{2+}]$  relationships in slow and fast twitch skinned muscle fibres of the rat. *Biochim. biophys. Acta.* **589**, 358-362.

- Stephenson, D. G. and Thieleczek, R. (1986). Activation of the contractile apparatus of skinned fibres of frog by the divalent cations barium, cadmium and nickel. *J. Physiol., Lond.* **380**, 75-92.
- Stephenson, D. G. and Williams, D. A. (1980). Activation of skinned arthropod muscle fibres by  $Ca^{2+}$  and  $Sr^{2+}$ . *J Muscle Res. Cell Motil.* **1**, 73-87
- Stephenson, D. G. and Williams, D. A. (1981). Calcium-activated force responses in fast- and slow twitch skinned muscle fibres of the rat at different temperatures. *J. Physiol., Lond.* **333**, 637-653.
- Stephenson, D. G. and Williams, D. A. (1981). Slow amphibian fibres become less sensitive to  $Ca^{2+}$  with increasing sarcomere length. *Pflügers Arch.* **397**, 248-250.
- Suarez-Kurtz, G. (1976). A comparison of effects of SKF 525-A and procaine on excitation-contraction coupling in single crayfish muscle fibres. *J. Pharmacol. Exp. Ther.* **198**, No 3, 687-694.
- Suarez-Kurtz, G., Reuben, J. P., Brandt, P. W. and Grundfest, H. (1972). Membrane calcium activation in excitation-contraction coupling. *J. gen. Physiol.* **59**, 676-688.
- Suarez-Kurtz, G. and Sorenson, A. L. (1979). Dissociation of action potentials from contraction in single crab muscle fibres. *Proc. natn. Acad. Sci. USA* **76**, 3029-3030.
- Sweeny, H. L., Kushmerick, M. J., Mabuchi, K., Sreter F. A. and Gergely, J. (1988). Myosin alkali light chain and heavy chain variations correlate with altered shortening velocity of isolated skeletal muscle fibres. *J. biol. Chem.* **263**, 9034-9039.
- Takeda, K. (1967). Permeability changes associated with the action potential in procaine-treated crayfish abdominal muscle fibres. *J gen. Physiol.* **50**, 1049-1074
- Tameyasu, T. (1992). Unloaded shortening after quick release of a contracting, single fibre from crayfish slow muscle. *J. Muscle Res. Cell Motil.* **13**, 619-629.

- Tanabe, T. Beam, K. G. Povel, J. A. and Numa, S. (1987). Restoration of excitation-contraction coupling and slow muscle calcium current in dysgenic muscle by dihydropyridine receptor complementary DNA. *Pflügers Arch.* **410**, 75-82.
- Tang, J. M., Wang, J. and Eisenberg, R. S. (1989).  $K^+$ -selective channels from sarcoplasmic reticulum of split lobster muscle fibres. *J. gen. Physiol.* **94**, 261-278.
- Tallman, J. F. and Gallagher, D. W. (1985). The GABA-ergic system: a locus of benzodiazepine action. *A. Rev. Neurosci.* **8**, 21-44.
- Thompson, C. S. and Page, C. H. (1982). Command fibre activation of superficial flexor motoneurons in the lobster abdomen. *J. comp. Physiol.* **148**, 515-527.
- Tsien, R. W. and Tsien, R. Y. (1990). Calcium channels, stores, and oscillations. *A. Rev. Cell Biol.* **6**, 715-760.
- Van Breemen, C., Farinas, B. R., Casteels, R., Gerba, P., Wuytack, F. and Deth, R. (1973). Factors controlling cytoplasmic  $Ca^{2+}$  concentration. *Prog. R. Soc. London. B* **265**, 57-71
- Vergara, J. and Delay, M. (1986). A transmission delay and the effect of temperature at the triadic junction of skeletal muscle. *Proc. R. Soc. Lond. B* **229**, 97-110.
- Wakabayashi, K., Sugimoto, Y., Tanaka, H., Ueno, Y., Takezawa, Y. and Amemiya, Y. (1994). X-ray diffraction evidence for the extensibility of actin and myosin filaments during muscle contraction. *Biophys. J.* **67**, 2422-2435.
- Walton, P.D., Airey, J. A., Sutko, J. L., Beck, C. F., Mignery, G. A., Sudhof, T. C., Beerink, T. J. and Ellisman, M. H. (1991). Ryanodine and inositol triphosphate receptor coexist in avian cerebellar purkinje neurones. *J. Cell Biol.* **113**, 1145-1157.
- Warren, T. B., Butler, T. M., Seigman, M. J. and Mooers, S. U. (1985). Effects of 2,3-butanedione monoxime (BDM) on force production and myosin light chain

- phosphorylation (MYLCP) in mammalian smooth and skeletal muscle. *Biophys. J.* **47**, 295a.
- Weber, A. (1968). The mechanisms of action of caffeine on the sarcoplasmic reticulum. *J. gen. Physiol.* **52**, 760-772.
- Weber, A. and Herz, R. (1968). The relationship between caffeine contracture of intact muscle and the effect of caffeine on reticulum. *J. gen. Physiol.* **52**, 750.
- Weber, A. and Murray, J. M. (1973). Molecular control mechanisms in muscle contraction. *Physiol Rev.* **53**, 612-673.
- West, J. M., Humphris, D. C. and Stephenson, D. G. (1992). Differences in maximal activation properties of skinned short-and long-sarcomere muscle fibres from the claw of the freshwater crustacean *Cherax destructor*. *J. Muscle Res. Cell Motil.* **13**, 668-684
- Wine, J. J. and Krasne, F. B. (1972). The organisation of escape behaviour in the crayfish. *J. exp. Biol.* **56**, 1-18.
- Wine, J. J. and Krasne, F. B. (1982). The cellular organisation of crayfish escape behaviour. In *The Biology of Crustacea* (ed. D. C. Sandeman and H. L. Atwood), **4**, 241-292. New York: Academic Press.
- Wine, J. J., Mittenthal, J. E. and Kennedy, D. (1974). The structure of tonic flexor motoneurons in the crayfish abdominal ganglia. *J. comp. Physiol.* **93**, 315-335.
- Williams, A. J. and Ashley, R.H. (1989). Reconstitution of cardiac sarcoplasmic reticulum calcium channels. *Ann. N. Y. Acad. Sci.* **560**, 163-173.
- Winter, M. R. C., Head, J. F. and Perry, S. V. (1974). Ion binding in troponin. In *Calcium binding proteins*, (Ed. W. Drabikowski, H. Strzelecka-Golaszewska, E. Carafoli), pp. 109-127. Elsevier Scientific publishing company, Amsterdam.

- Wnuk, W., Schoeclin, M. and Stein, E. A. (1984). Regulation of actomyosin ATPase by a single calcium-binding site on troponin C from crayfish. *J. Biol. Chem.* **259**, 9017-9023.
- Wnuk, W. (1989). Resolution and calcium-binding properties of the two major isoforms of troponin C from crayfish. *J Biol. Chem.* **264**, 18240-18246.
- Woledge, R. C., Curtin, N. A. and Homsher, E. (1985). *Energetic aspects of muscle contraction*. Academic Press, London.
- Wolff, D. J., Poirier, P. G., Brostrom, C. O. and Brostrom, M. A. (1977). Divalent cation binding properties of bovine brain  $Ca^{2+}$ -dependent regulator protein. *J. Biol. Chem.* **252**, 4108-4117.
- Worden, M. K., Rahamimoff, R. and Kravitz, E. A. (1994). A voltage-sensitive cation channels present in lobster skeletal muscle membrane. *J. Membr. Biol.* **141**, 167-175.
- Yagi, S. and Endo, M. (1980). Effects of dibucaine on skinned skeletal muscle fibres. An example of multiple actions of a drug on a single subcellular structure. *Biomed. Res.* **1**, 269-272.
- Yamagishi, S. (1973). Manganese-dependant action potentials in intracellularly perfused squid giant axons. *Proc. Jap. Acad.* **49**, 218-222
- Yoshida, A and Tawada, K. (1976). Temperature-dependence of tension development by glycerinated muscle fibres of rabbit psoas in Mn (II)-ATP and Mg-ATP solutions. *J. Biochem.* **80**, 861-865
- Zacharová, D. and Zachar, J. (1966). Potassium contractures in single fibres of the crayfish. *J. Physiol., Lond.* **186**, 596-618.

- Zachar, J. and Zacharová, D. (1967). The effect of external calcium ions on the excitation-contraction coupling in single muscle fibres of the crayfish. *Physiologia bohemoslov.* **16**, 191-206.
- Zite-Ferency, F. and Rüdel, R. (1978). A diffractometer using a lateral effect photodiode for rapid determination of sarcomere length changes in cross-striated muscle fibres. *Pflügers Arch.* **374**, 97-100.
- Zot, H. G., Iida, S. and Potter, J. D. (1983). Thin filament interactions and  $\text{Ca}^{2+}$  binding to Tn. *Chemica Scripta.* **21**, 133-136.
- Zot, H. G. and Potter, J. D. (1987). Structural aspects of troponin-tropomyosin regulation of skeletal muscle contraction. *A. Rev. Biophys. biophys. Chem.* **16**, 535-559.